USING CATHODIC PROTECTION TO CONTROL CORROSION OF REINFORCED CONCRETE STRUCTURES

HAYDER MAJEED OLEIWI

School of Computing, Science and Engineering
College of Science and Technology
University of Salford, Manchester, UK

Submitted in Partial Fulfilment of the Requirements for the Degree of Doctor of Philosophy, April 2018

Abstract

Cathodic protection (CP) has been increasingly used on reinforced concrete structures to protect steel reinforcement from corrosion. However, due to the complexity of environmental conditions, the specifications in national and international standards are still open to discussion in engineering practices for their accurate suitability. To some extent, the design aspects are still based on practical experience. It implies a great deal of estimations and assumptions. The research conducted in the thesis aims to address some of these challenges.

To obtain reliable experimental results, the present study at first investigated the influence of experimental methods on the measurement of concrete electrical resistivity. It studied the effect of alternative current (AC) frequency, electrode materials and electrode configuration. Based on the results, an optimised method was decided for all the series of the experimental tests in this study.

The CP study consists of two major works. The first one was to investigate the chloride contaminated concrete exposed to atmospheric condition. Impressed constant current method was adopted for the operation of CP. A series of electrical and electrochemical measurements were conducted for concrete resistivity, corrosion potential, corrosion rate, degree of polarization, instant-off potential and four-hour potential decay. An evaluation on the current adopted criterion in standards has been carried out on the experimental results.

The second work was to investigate the corrosion of rebar in concrete specimens submerged (fully and partially) in salty water. For such more corrosive environment, a comparison between the impressed CP operation using constant current and that using constant potential has been conducted. The experiments evaluated the effects of the two major environmental factors, i.e. water and chloride contents, on reinforced concrete durability. The work provided a deep understanding on the electrochemical behaviour of the reinforced concrete system and effectiveness of CP implementation under severe conditions. The research work has an important contribution to fundamental science of corrosion and reinforced concrete deterioration, and the technology and practical application of CP for reinforced concrete structures.

The main results of this work indicate the important influence of the frequency and electrode configuration on the electrical resistance measurement. For the reliability of electrical resistivity measurement, a high frequency of 10,000 Hz and an internal carbon fibre electrode method are recommended.

Regarding the CP for the chloride contaminated reinforced concrete exposed to the atmosphere, it is suggested that adopting an instant-off potential of -500 mV with respect to Ag/AgCl/0.5KCl reference electrode can provide sufficient protection for the reinforced concrete of up to 0.59 % total chloride by weight of concrete, or concrete resistivity is greater than 6.7 kΩ.cm. Furthermore, it was found that the 100 mV depolarization criterion for the evaluation of CP performance gives an overestimated protection. A depolarization of 50 mV is therefore proposed.

In terms of the submerged specimens, the results showed that the water content and chloride content should be explicitly related to the corrosion state rather than through a single parameter of the concrete resistivity for the complicated situations because the water content will affect the oxygen transportation in concrete, and the oxygen availability at the rebar surface will play an important role in the corrosion process, and this is unassessable by concrete resistivity. Moreover, 4 or 24 hours for the 100 mV depolarisation criterion in standards is not applicable for CP assessment where concrete structures are fully submerged due to the low availability of oxygen. On the other hand, the depolarization criterion can be used if the specimens are partially submerged, but different parameters affect the depolarization value such as the magnitude of the applied protection current or potential, chloride concentration, oxygen availability and time of depolarization.

This thesis is dedicated to

My beloved mother, Father in ground,

Wife and lovely kids

Acknowledgements

First, I would like to express my sincere appreciation to my main supervisor Dr. Wayne Yu Wang for his keen supervision, encouragement and continued support throughout this project. This work would not be possible to be produced in its present form without his precious time spent and valuable guidance.

Deep thanks are also due to my co-supervisor Dr. Michele Curioni, Corrosion and Protection Centre, The University of Manchester, for his valuable cooperation, fruitful discussions and suggestions given throughout the study. I am also grateful to him for giving me the opportunity to join his class and access the laboratory sessions related to cathodic protection. Acknowledgment and thanks are extended to Dr. Xianyi Chen, Charter Coating Service (2000) Ltd. in Canada for his critical comments and beneficial suggestions concerning the work. My thanks and gratitude are also to my co-supervisor Prof. Igor Shabalin for his encouragement and assistance at the start of this project.

I am particularly grateful to Dr. Moufaq J. Katwan, my MSc supervisor in Iraq, for his invaluable discussions and advice. I would also like to thank Dr. David Smith, School of Environment and Life Sciences, for his assistance with the chloride analysis. My thanks and appreciation to Dr. Levingshan Augusthus-Nelson for his comments concerning the work, and to all the technical staff of concrete and petroleum laboratories for their assistance. Thanks are also to my friends Adel and Husam for their assistance in the lab.

I am indebted to the Government of the Republic of Iraq, Ministry of Higher Education and Scientific Research for the financial support, and would like to acknowledge the staff of the Iraqi Cultural Attaché in the United Kingdom and the school of Computing, Science and Engineering at the University of Salford for their support.

Finally, a great deal of thanks are deserved to my wife and sons for their endless patience, encouragement and continued support. My mother, brothers and sister for their love and encouragement.

List of Contents

List of Publications

1. Oleiwi, H., Wang, Y., Curioni, M., Augusthus-Nelson, L., Chen, X., and Shabalin, I. *Experimental study of cathodic protection for reinforced concrete submerged in saline water*. Paper presented at the EUROCORR, The annual congress of the European Federation of corrosion, 20th international corrosion congress, 3-7 September 2017, Prague-Czech Republic.

2. Oleiwi, H., Wang, Y., Curioni, M., Augusthus-Nelson, L., Chen, X., and Shabalin, I. *An experimental study of the cathodic polarization of the reinforcement in chloride contaminated concrete.* Paper presented at the EUROCORR, The annual congress of the European Federation of corrosion, 20th international corrosion congress, 3-7 September 2017, Prague-Czech Republic.

3. Oleiwi, H., Wang, Y., Curioni, M., Augusthus-Nelson, L., Chen, X., and Shabalin, I. *An experimental study of concrete resistivity and the effects of electrode configuration and current frequency on measurement.* Paper accepted for the Sixth International Conference on the Durability of Concrete Structures, to be held from 18-20 July 2018, University of Leeds, Leeds, United Kingdom.

4. Oleiwi, H., Wang, Y., Curioni, M., Augusthus-Nelson, L., Chen, X., and Shabalin, I. An experimental study and characterisation of the corrosion state of concrete steel reinforcement under cathodic protection, submitted for Materials and Structures journal.

5. Oleiwi, H., Wang, Y., Xiang, N., Curioni, M., Augusthus-Nelson, L., Chen, X. Electrical resistivity at varied water, chloride contents and porosity – an experimental study, Paper prepared for publication.

List of Figures

List of Tables

Glossary

of Some Terms Related to
Corrosion and Cathodic Protection of Steel in Concrete

The following glossary is presented depending on the information that has been found in Berkeley and Pathmanaban (1990), Broomfield (2007) and Stanish et al. (1997).

Anode: the electrode where oxidation or removal of electrons occurs in an electrochemical cell. It describes the area from which loss of metal occurs.

Cathode: the electrode where reduction or entering of electrons occurs in an electrochemical cell l. It describes the area from which loss of metal has been prevented.

Electrode: an electrical conductor inside an electrical/ electrochemical cell. It is referred to as either an anode or a cathode depending on the direction of current through the cell.

Electrochemical cell: an electrolytic cell comprises three component parts: an electrolyte and two electrodes (a cathode and an anode).

Electrolyte: an electrically conducting medium in which current is carried by the movement of ions. Concrete acts as the electrolyte here.

Potential/ Electrode potential: the difference between the voltage at a metal surface acting as a cathode and a standard electrode (reference electrode) acting as an anode.

Reference electrode: an electrode which always has a stable electrical potential. It is used as a half cell to build an electrochemical cell. This allows the potential of the other half cell to be determined.

Polarization: the change (shift) of electrical potential of an electrode to more positive or negative values by the application of an external current.

IR drop: the voltage drop at the location of the reference electrode due to the current flowing through the concrete resistance.

Galvanic series/ electropotential series: a list of metals and alloys arranged according to their relative potentials in a given environment. The less noble metal which is located at the base of the list is the one with a lower potential (more negative) than the nobler one which is located at the top of the list.

Galvanic cells: a typical cell consists of two dissimilar metals, an electrolyte and a common electrical connection. According to the relative position of the two metals in the galvanic series, the metal having less potential becomes the anode and gives up electrons, while the more potential metal receives electrons and becomes the cathode in the galvanic (corrosion) cell. The anode will corrode, while the cathode does not.

Resistance: a property of a specific material with a specific geometry and composition that describes its ability to withstand the transfer of electrons or ions passing through that material under an electrical field.

Resistivity: a material property describing the difficulty with which electrons or ions travel through a unit length of that material of a unit cross-section under an electrical field

Conductivity: a measure of the ability of a material in which electrons or ions can pass through a unit length of that material of a unit cross-section, the inverse of resistivity.

List of Symbols and Abbreviations

Symbol/ Abbreviations	Definition
CP	Cathodic Protection
CF	Carbon Fibre
GNP	Gross National Product
GDP	Gross Domestic Product
C_3S	Tricalcium Silicate
C_2S	Dicalcium Silicate
E_{corr}	Electrochemical Corrosion Potential
SHE	Standard Hydrogen Electrode
CSE	Copper Sulfate Electrode
SCE	Saturated Calomel Electrode
Ag/AgCl/0.5KCl	Silver Chloride Electrode
BS	British Standard
ASTM	American Society for Testing and Materials
LPR	Linear Polarization Resistance
Rp	Polarization Resistance, in ohms, Ω
I_{corr}	Corrosion Current, mA
i_{corr}	Corrosion Rate, mA/m^2
R	Electrical Resistance, Ω
ρ	Electrical Resistivity, Ω.m
AC	Alternating Current
DC	Direct Current
E_{eq}	Equilibrium Potential
NACE	National Association of Corrosion Engineers
FHWA	Federal Highway Administration
NaCl	Sodium Chloride
RH	Relative Humidity

CHAPTER ONE

INTRODUCTION

CHAPTER 1 INTRODUCTION

1.1 Background

Reinforced concrete is widely used as a major composite material in the construction industry around the world today (Chemrouk, 2015). It is a versatile, economical and durable (Broomfield, 2007). In general, it is thought relatively performing well over its service life because steel rebars embedded in concrete is naturally protected from corrosion by the high alkalinity of concrete pore solution, and the physical barrier effect of the concrete cover itself to limit the access of aggressive species to the steel surface (Hansson et al., 2012; Liu and Shi, 2009a). However, in the recent decades premature deterioration of infrastructure systems has been alarming concerns worldwide (Chemrouk, 2015).

Corrosion of reinforcing steel is the major cause of damage of reinforced concrete structures and can directly affect the sustainability of the infrastructure (Poursaee, 2016). The causes of the corrosion deterioration have been the subject for many studies. The overall conclusion of theses previous researches has confirmed that chloride plays the most significant role in the corrosion caused deterioration of the reinforced concrete (Buenfeld et al., 1998; Kendell, 1995). One of the main sources for the chlorides is the use of de-icing salts (sodium chloride) on highways. In the United States, about 10 million tonnes of salt per year are spread on highways. Onto the UK roads, 1-2 million tonnes are used each year (Broomfield, 2007).

The chloride caused corrosion is a serious problem and can be dangerous, and the repair cost can be extremely costly. Trethewey and Chamberlain (1995) stated that the annual cost of corrosion in the United States was first estimated in 1949 by Uhling to be $5 billion which is equivalent to 2.1% of the Gross National Product (GNP) at that time. The US Federal Highway Administration (FHWA) estimated the annual cost of the maintain of highway bridges in 2002 to be $8.3 billion (Koch et al., 2002). A 1971 study on the cost of corrosion was carried out in the United Kingdom concluded that the total cost to the national economy was a 3.5% of the Gross National Product (GNP). In a recent study in 2009, the Central Intelligence Agency (CIA) reported that the global cost of corrosion was 3-4% of the Gross Domestic Product (GDP) of industrialised countries per year, with $17 billion annual investment is required to address bridge conditions in the USA (Byrne et al., 2016). Considering inflation, this cost is much higher now.

The corrosion problem of steel in concrete induced by chloride is not limited to the United Kingdom and United States, but it is a worldwide serious issue on safety and economy. For instance, in the Middle East, this problem is universal in scope and exacerbated by the environmental conditions in this area (Rasheeduzzafar et al., 1992). Offshore and coastal structures suffer from chloride contamination due to direct immersion, splashing or wind transportation contamination. In addition, In many parts of the Gulf, the high chloride content of the ground water results in severe chloride contamination of foundations and structural elements above the ground (Wyatt, 1995).

In Iraq, particularly in southern parts, a bell of danger on the degree of corrosion of steel reinforcement was rung. Chloride contaminated raw materials, external aggressive agents, mainly from salty ground water, the hot-dry environmental conditions and poor construction practice have been recognized as the main causes for the deterioration of concrete structures and leads to a very short life expectancy (Katwan, 2000).

Given the current situation of the size of corrosion impact, there is a critical need to develop corrosion technology through research and implementation and provide less expensive approaches (Koch et al., 2002; Poursaee, 2016). In the past decades, many potential solutions have been evaluated, including the use of patch repair, high density concrete overlays, corrosion inhibitors, coating of steel reinforcement, electro-chemical chloride removal and cathodic protection (Committee, 1985; Zayed and Sagues, 1990). Each of these repair methods is suitable in certain situations. However, it has been found that most of the non-electrochemical repair techniques are not very effective in reducing the corrosion rate with little or no success in practice (Hong et al., 1993).

Among the various corrosion control methods developed, Cathodic protection (CP) is nowadays recognized as the most effective repair technique so far to control the corrosion of steel embedded in concrete (Martínez and Andrade, 2008). CP is an electrochemical and a major repair technique that has increasingly been used for the maintenance of corrosion damaged reinforced concrete structures in the UK and worldwide (Martínez and Andrade, 2008; Parthiban et al., 2008; Wilson et al., 2013). However, even today the chance of the success of the CP for reinforced concrete structures depends much upon the qualification and technical competence of the repair engineer.

1.2 Problem Statement

Although, cathodic protection has been widely applied to protect steel reinforcement in concrete from corrosion, little amount of information on national or international standards was found until recently to help for the protection design (Chess and Broomfield, 2013). "Cathodic protection of reinforced concrete has been developed by a combination of trial and error" (Wyatt, 1993). The design aspects of such a system are still based on practical consideration, which implies a great deal of uncertainties and assumptions. Important features such as, current density over the protected steel reinforcement, potential distribution, design criteria and others are a matter of contention among experts.

Concrete resistivity plays an important role for the assessment of the condition of reinforced concrete structures and the design of cathodic protection system. Nevertheless, to obtain accurate measurement can be a difficult due to the contact issue between the electrode and the concrete, particularly when doing measurement for unsaturated specimens (Villagrán Zaccardi and Di Maio, 2014). Moreover, different AC frequencies ranging from low to high were suggested recognising that it is hard to define a specific optimal frequency for the variation of the conditions of the concrete.

The present research work is designed to provide new information and to achieve a better understanding on the aforementioned important aspects for the design of CP system for reinforced concrete structures.

1.3 Aims and Research Objectives

The aims of the research project are as follows:

1. To develop a more detailed understanding of the influence of the surrounding environment on the behaviour of the reinforcement in concrete and examine the effect of applied protective currents generated from carbon fibre (CF) sheets anodes on the design of CP system.
2. To evaluate the performance of using internal electrodes of CF for the accuracy of electrical resistivity measurement of saturated and unsaturated concrete specimens.

In order to achieve these two aims, an experimental investigation has been used to study the following objectives:

1. Investigate the effect of chloride contamination and exposure conditions on state of steel reinforcement bars in concrete. The state of steel was evaluated by measuring corrosion rate using linear polarization resistance technique.
2. Study the relationships between concrete chloride content, rebar corrosion rate and the parameters measurable in field, such as concrete resistivity and rebar potential.
3. Examine the influence of applied protective current densities on potential polarisation of the reinforcing steel and evaluate the reliability of CP system in terms of the instant-off potential and potential decay criteria.
4. Investigate the effect of chloride content on cathodically protected reinforced concrete structures. In particular, the relationships between concrete chloride content and concrete resistivity with the CP current requirement that can be used for the guidance of design.
5. Evaluate the electrical performance of the CF as an anode in the impressed CP current method for a relatively long period.
6. Understand if adopting impressed constant current mode is suitable for the CP of submerged reinforced concrete specimens.
7. Investigate the effect of experimental approaches, including the AC frequency, voltage, and electrode material and configuration, on the reliability of electrical resistance measurement.
8. Understand and characterise the influences of the three major influencing factors of the concrete, i.e, chloride content, degree of saturation and porosity, on the electrical resistivity.

1.4 Contribution to Knowledge

The applied protective potential and applied protective current density are the two critical required factors considered by designers to provide adequate CP system. Unfortunately, to date, only limited information is available for optimal design of CP implementation for steel reinforcement in concrete (Chess and Broomfield, 2013; Xu and Yao, 2009). In addition, the contact between electrodes and concrete surfaces is considered complicated to visualise when external electrode method is used for measuring the resistivity of unsaturated concrete specimens as a key parameter for the design of CP system (Villagrán Zaccardi and Di Maio, 2014).

The methodologies adopted by this research has led to significant findings which not only have a direct benefit to technology that using internal electrodes of CF sheets is a more reliable configuration for resistivity measurement, but also have a high interest and direct impact on science, research communities and engineering practice with the improvement of knowledge and understanding of the influence of some important factors on the design of CP for concrete structures. A relationship of practical significance has been obtained between the degree of chloride contamination/concrete resistivity and the CP current demand. Moreover, new design criteria of instant-off potential and depolarization has been suggested for the assessment of protection efficiency.

1.5 Thesis Layout

The thesis is organized into seven chapters as follow:

Chapter 1 presents a brief introduction which covers the size of corrosion problems, possible repair techniques, the main objectives and significance of the investigation.

Chapter 2 is the literature review, which gives an overview of the theoretical background of corrosion process, chloride-induced and carbonation-induced corrosion of reinforcing steel in concrete, techniques for corrosion measurement and evaluation, principle of existing protection methods and performance criteria of CP system.

Chapter 3 describes the research methodology, test specimens and experimental programme undertaken.

Chapter 4 presents the findings obtained and discussion of the electrical resistivity of concrete.

Chapter 5 and 6 deals with the results and discussion of the corrosion and cathodic protection for the air exposed and submerged reinforced concrete specimens, respectively.

Finally, Chapter 7 summarises the conclusions of the present study and provides recommendations for further research.

CHAPTER TWO

LITERATURE REVIEW

CHAPTER 2 LITERATURE REVIEW

2.1 Mechanism of Steel Corrosion in Concrete

2.1.1 Steel in Concrete

Reinforcing steel embedded in concrete that is not contaminated with any influences from the surrounding environment is usually in a passive state, safe from corrosion, due to high alkalinity of concrete typically of pH 12.5-13.5. The high alkalinity of concrete mainly comes from calcium hydroxide which is a result of the hydration of cement compounds (namely C_3S and C_2S) as explained in equations 2.1 and 2.2 (Pithouse, 1986):

$$2(3CaO.SiO_2) + 6H_2O \rightarrow 3H_2O.2SiO_2.3H_2O + 3Ca(OH)_2 \quad (2.1)$$

$$2(2CaO.SiO_2) + 4H_2O \rightarrow 3H_2O.2SiO_2.3H_2O + Ca(OH)_2 \quad (2.2)$$

Many investigators have concluded that passivity is caused due to formation of a very thin protective film (<10 nm) on the steel surface which prevent the steel from corrosion (Ghods et al., 2011; Amir Poursaee, 2016; Solomon et al., 1993; Zakroczymski et al., 1985). The passive film on the surface of steel rebars is complex in chemical composition and controlled by the oxygen availability, pH and chemistry of the surrounding environment (Mundra et al., 2017). It composed of iron oxide, Fe–hydroxides and oxy-hydroxides (Glasser and Sagoe-Crentsil, 1989; Haupt and Strehblow, 1987; Joiret et al., 2002). FeO, Fe_2O_3, Fe_3O_4 and $Fe(OH)_2$ are some of the possible iron oxides formed the protective film according to equations 2.3 to 2.6 (Joiret et al., 2002; Küter, 2009).

$$3Fe + 4H_2O \rightarrow Fe_3O_4 + 8H^+ + 8e^- \quad (2.3)$$

$$2Fe + 3H_2O \rightarrow Fe_2O_3 + 6H^+ + 6e^- \quad (2.4)$$

$$Fe + 3H_2O \rightarrow FeO + 2H_3O^+ + 2e^- \quad (2.5)$$

$$Fe + 4H_2O \rightarrow Fe(OH)_2 + 2H_3O^+ + 2e^- \quad (2.6)$$

Studying the fundamental of the passive film formed on iron in alkaline solutions is common in practice, which makes the exact chemical composition is different in the case of concrete since the chemical composition of the pore solution is more complex (Ghods et al., 2011; Joiret et al., 2002; Saremi and Mahallati, 2002).

It was believed that a good quality of concrete will significantly reduce the permeability of the concrete against penetration of corrosion inducing agents. However, due to inherent porous nature (Chess and Broomfield, 2013), despite the high protective ability of concrete, corrosion of steel reinforcement is unavoidable and has become the most common cause of the deterioration of concrete structures. Particularly, coastal and offshore structures, sewers, structures in aggressive soils, bridge decks and other structures subjected to chloride contaminated water are the most liable to corrosion attack because of the severe environmental conditions (Katwan, 1999).

2.1.2 Principle of Corrosion

Corrosion can be defined as an electrochemical process of a metal in relation to its surrounding environment. Occurring in stages, it can be represented by two electrochemical reactions of the dissolution of iron at anodic sites and the corresponding oxygen reduction at cathodic sites. Both of the anodic and cathodic reactions take place on the surface of the steel. The chemical reactions of corrosion are the same no matter the passive layer around steel breaks down by chloride attack or by carbonation. When depassivation occurs, areas of rust will start appearing on the affected area of the steel surface in the presence of water and oxygen (Gower and Windsor, 2000). The affected steel areas become anodic whilst the passive areas are cathodic (Broomfield, 2007; Gower and Windsor, 2000). At the anode, the steel is oxidized and release electrons to form a ferrous ion which dissolves in electrolyte as in equation 2.7.

$$Fe \rightarrow Fe^{+2} + 2e^{-} \quad \text{(Ferrous ion)} \tag{2.7}$$

To preserve electrical neutrality, the above two electrons need to be consumed elsewhere on the steel surface, thus the electrons pass through the steel and combine with water and oxygen at the cathode surface to produce hydroxyl ions as in equation 2.8. This is also referred to oxygen reduction.

$$\frac{1}{2}O_2 + H_2O + 2e^{-} \rightarrow 2(OH)^{-} \quad \text{(Hydroxyl ions)} \tag{2.8}$$

The above anodic and cathodic reactions are only the first step in the process of creating rust. In the next step, hydroxyl ions (OH^{-}) diffuse in electrolyte (concrete for example) and

react with the ferrous ions (Fe^{+2}) there to produce insoluble ferrous hydroxide ($Fe(OH)_2$) as in equation 2.9.

$$Fe^{+2} + 2(OH)^{-} \rightarrow Fe(OH)_2 \text{ (Ferrous hydroxide)} \quad (2.9)$$

Further oxidations as in equations 2.10 and 2.11 will convert ferrous hydroxide ($Fe(OH)_2$) into hydrated ferric oxide (Fe_2O_3. H_2O) which is commonly known as rust. Figure 2.1 shows the corrosion process of the reinforcing steel in concrete (Zhao et al., 2011).

$$4Fe(OH)_2 + O_2 + 2H_2O \rightarrow 4Fe(OH)_3 \text{ (Ferric Hydroxide)} \quad (2.10)$$

$$2Fe(OH)_3 \rightarrow Fe_2O_3.2H_2O + H_2O \text{ (Hydrated Ferric Oxide, Rust)} \quad (2.11)$$

In the environments poor in oxygen or with low pH, the cathodic reaction is the reduction of hydrogen ion to generate hydrogen gas as in equation 2.12.

$$2H^{+} + 2e^{-} \rightarrow H_2 \quad (2.12)$$

Hydrogen evolution can also occur at low potentials and in neutral to alkaline media, as in equation 2.13.

$$2H_2O + 2e^{-} \rightarrow H_2 + 2OH^{-} \quad (2.13)$$

Steel becomes active to corrode at the anode sites whilst remains passive at the cathode sites. A corrosion cell develops on steel surface as a result of the difference in electrical potential between the anodic and cathodic areas (Nawy, 2008), when a current flows from the anode to the cathode transported by the ions in the electrolyte (Bertolini et al., 2013). The faster the solid iron is converted to ions, the greater the corrosion and the larger is the current flowing in the corrosion cell (Davis, 2000).

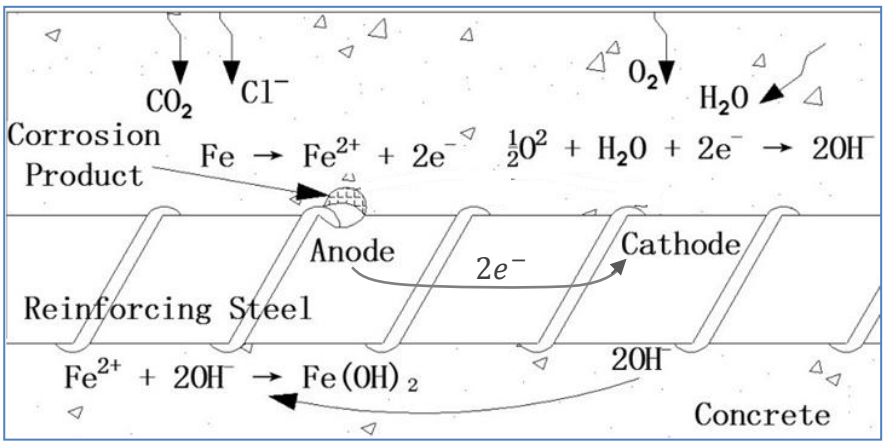

Figure 2.1: Schematic diagram of reinforcing steel corrosion process, adopted from Zhao et al. (2011)

As shown in Figure 2.2, either or both of the microcell and macrocell corrosion mechanisms may occur in reinforced concrete (Evans, 1960). Microcell corrosion takes place when anodic and cathodic reactions take place between adjacent portions of the same rebar. In contrast, macrocell corrosion occurs when anodic or cathodic reactions take place on the surface of different reinforcements or because of different environment. Hansson et al. (2006) confirmed through a monitoring study for more than 3 years that microcell corrosion is the major mechanism of steel corrosion in concrete.

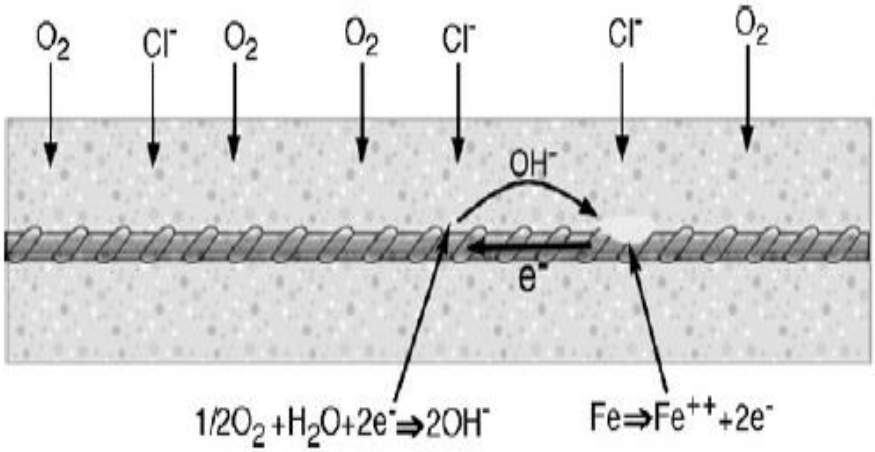

(a) Microcell corrosion

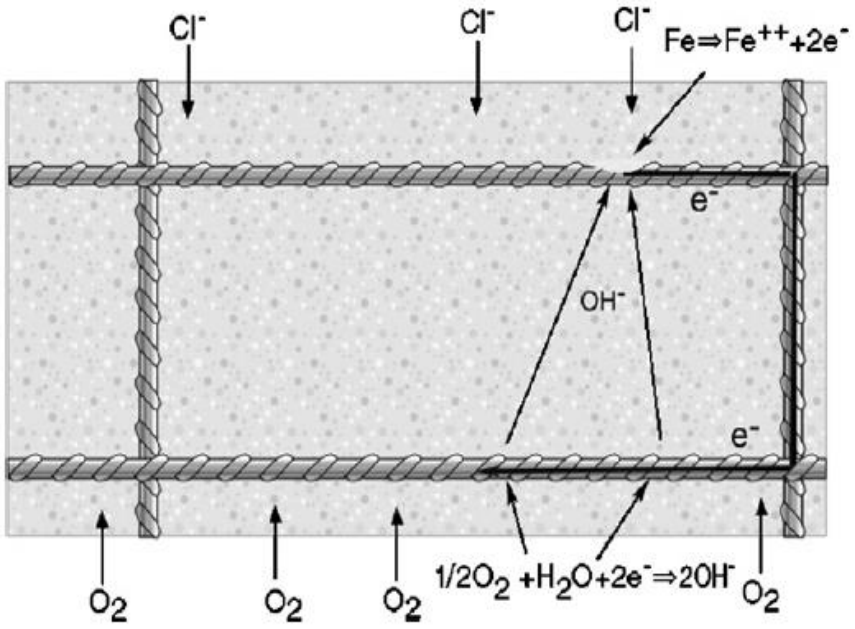

(b) Macrocell corrosion

Figure 2.2: Schematic illustrations of corrosion mechanisms (Hansson et al., 2006)

In concrete structures, corrosion generally starts with the formation of pits on the steel reinforcement which then increase in number depends upon the conditions around the steel, particularly the oxygen availability. When great amount of oxygen is present, general corrosion will tack place as shown in Figure 2.3 (Hansson et al., 2012).

Figure 2.3: General corrosion of steel in concrete (a) underside of bridge deck and (b) Retaining wall of bridge (Hansson et al., 2012)

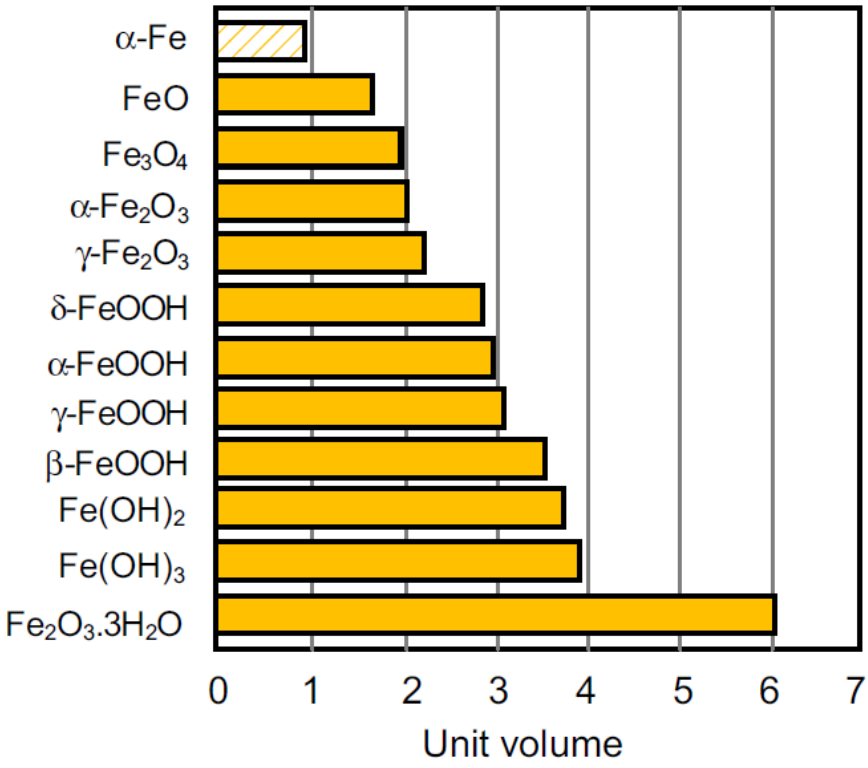

Figure 2.4: Volume of corrosion product from iron (Poursaee, 2016)

Corrosion products usually increase volume several times greater than original metal as shown in Figure 2.4. Different corrosion products of steel in fact occupy different volumes

(Poursaee, 2016). The volume of the corrosion products can reach up to 6 times for the familiar rust (Fe_2O_3. H_2O). Consequently, corrosion products can cause cracking, spalling of concrete cover, and the reduction of the cross-sectional area of rebars, which weaken the bond between reinforcing steel bars and surrounding concrete and threaten the safety of reinforced concrete structures (Al-Sulaimani et al., 1990; Katwan, 1999; Zhou et al., 2014). Figures 2.5 shows the degree of damage to the concrete due to rebars corrosion.

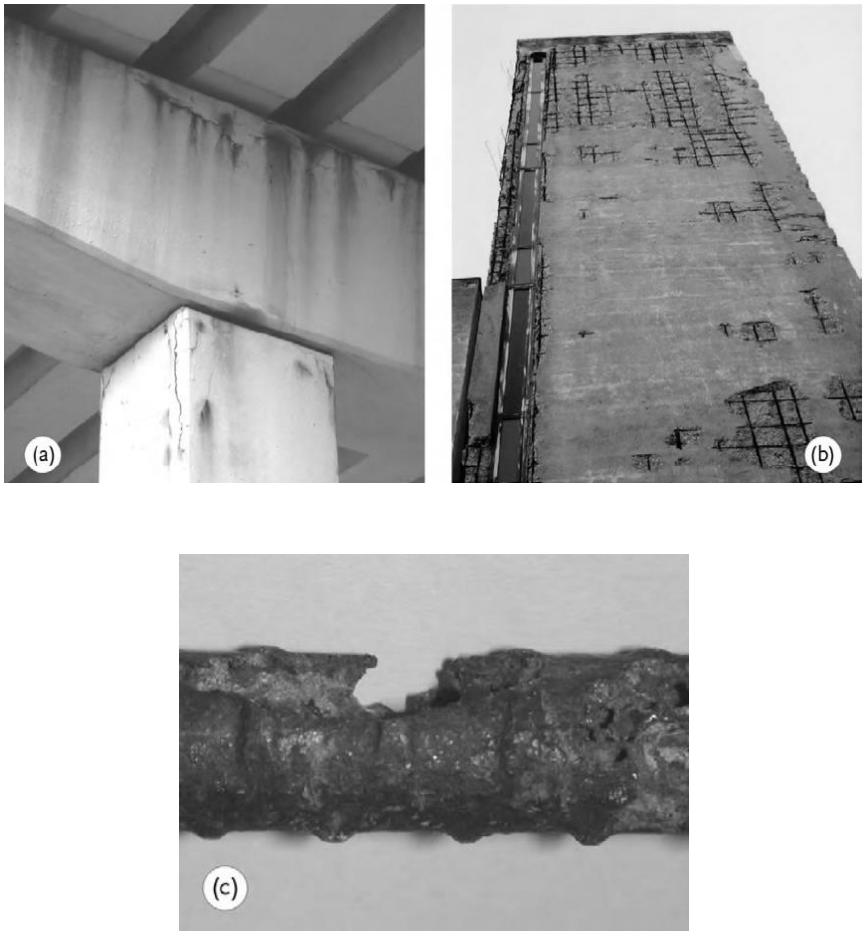

Figure 2.5: Concrete damage due to reinforcement corrosion, (a) surface cracks, (b) spalling and exposure of corroded rebars and (c) reduction in the cross section of reinforcement (Bertolini et al., 2013)

2.1.3 Thermodynamic of Corrosion

To assess whether the corrosion of iron can occur under a given set of conditions, all the possible oxidation reactions for the iron and water (Fe-H_2O) system have been investigated by Pourbaix and presented as a function of the electrochemical potential (E) and pH as

shown in Figure 2.6. This diagram is used to predict the spontaneous direction of reactions for the estimating the composition of corrosion products and evaluating the degree of corrosiveness of the surrounding environment. It shows, generally, the regions in which the metal is immune from corrosion, active to corrode, or passive. These regions are bounded by lines that represent equilibrium conditions between the two adjacent thermodynamically favoured species (Küter, 2009). These lines represent the various possible reactions of the aqueous electrochemical system which are derived from Nernst equation.

The Nernst equation allows calculation of the electrochemical potential (E) for reactions with various concentration in terms of the standard electrode potential (E°) as the latter is only applied to the situation where a metal is immersed in a solution of its own ions at 1 mole concentration (McCafferty, 2010). It is expressed as the following equation (Davis, 2000):

$$E = E^{\circ} - \frac{RT}{nF} \ln \frac{(red)}{(ox)} \tag{2.14}$$

where E is the electrochemical electrode potential, E° is the standard electrode potential, R is the gas constant (8.3143J/mole.K), T is the absolute temperature (in Kelvin), n is the number of electrons involved in the reaction, F is the Faraday constant (96500 C/mole), and (red) and (ox) are the concentrations of reduced and oxidized species, respectively.

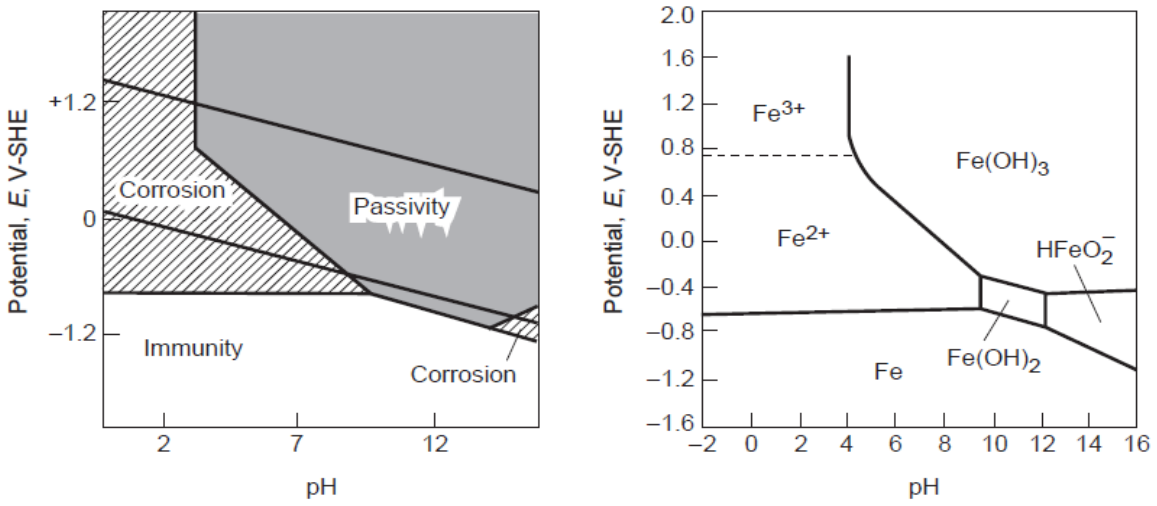

Figure 2.6: Pourbaix diagram for the system of iron in water (Fe-H_2O) at 25°C (a) areas of immunity (no corrosion), passivity, and corrosion, and (b) reaction/corrosion products produced (Davis, 2000)

At the pHs and potentials range found in concrete, solid species of iron oxides (Fe_2O_3 and Fe_3O_4) are stable and thus iron is considered passive. However, if the pH of the pore water is reduced, for example in case of carbonation, the soluble species of Fe^{+2} and Fe^{+3} are stable and can be associated with corrosion (Davis, 2000; Küter, 2009). Corrosion can also occur at high pH in which ($HFeO_2^-$) as in equation 2.15 is the thermodynamically stable reaction, but this is just in corrosion theory with no practical significance (Bremner et al., 2001). At very low potentials, metallic iron (Fe) is thermodynamically stable and the corrosion should not occur (Ohtsuka et al., 2017).

$$Fe + OH^- + H_2O \rightarrow HFeO_2^- + H_2 \quad (2.15)$$

In summary, corrosion prevention can be achieved by lowering the electrode potential down to the zone of immunity, raising the electrode potential up to the region of passivity, or raising the pH or alkalinity of the solution so that a passive film is formed (Schweitzer, 2009). But there are limitations on the use of the diagram. The first limitation is that it cannot be used for predicting the rate of the corrosion reactions. The possibility of precipitation of other ions such as chlorides, sulfates and other impurities has been ignored as such diagrams are only constructed from known reaction between pure metal and pure solution. Finally, the pH at the metal surface may vary drastically because of side reactions, and a prediction of corrosion based on the bulk pH of the solution may be misleading.

2.1.4 The Kinetic of Corrosion

The corrosion behaviour of the reinforcement can be described by means of polarization curves that relate the electrochemical potential (E), and the current density on a logarithmic scale (log I). These polarization curves show the characteristic curves of the anodic and cathodic reactions obtained experimentally starting from the reaction's equilibrium potential. Polarization curves can be used to determine the rate of these reactions that are involved in the corrosion process which relates to corrosion rate (Küter, 2009).

Polarization is defined as an electrochemical process induced by deviation of the potential due to an electric current passing through the electrochemical cell (Perez, 2004). Polarization is said to be anodic, when the anodic reaction on the electrode are accelerated by polarizing the potential in the positive direction or cathodic when cathodic reaction are accelerated by changing the potential in the negative direction.

In noncarbonated and free chloride concrete, steel is passive and its electrochemical behaviour can be represented by the anodic and cathodic polarization curves as shown in Figure 2.7. By looking at the anodic polarization curve, it can be seen it is divided into three potential regions which are active, passive and transpassive with oxygen evolution. At the beginning, as the potential is made more positive, the anodic current increases exponentially according to normal dissolution behaviour and reaches the primary passivation potential (E_{pp}) in which a protective film begins to form and causes a sudden drop in corrosion rate and the metal is said to be passive. As this potential is increased further, there is little change in current flow until the next critical potential which termed as pitting potential (E_{pit}). Beyond this point, at high potentials where a breakdown of the passive film occurs, corrosion current increases again in the transpassive region and oxygen evolution can be occurred at the anode which produces acidity based on the following equation (Pedeferri, 1996; Schweitzer, 2009).

$$2H_2O \rightarrow O_2 + 4H^+ + 4e \tag{2.16}$$

With reference to Figure 2.7, it can be seen the corrosion potential of reinforcement (E_{corr}) exist in the interval of potential range for the passivity region where the corresponding corrosion current (I_{corr}) is negligible. E_{corr} and I_{corr} are the intersection point of the anodic and cathodic polarization curves if the characteristic curves of both the anodic and cathodic reactions are shown on the same diagram. The current at the corrosion potential (E_{corr}) is defined as the corrosion current (I_{corr}). Corrosion potentials between +100 and −200 mV vs SCE (saturated calomel reference electrode) were found for the concrete that is exposed to the atmosphere, while more negative potential at -400 mV vs SCE was reported for the concrete immersed in water (Bertolini et al., 2013).

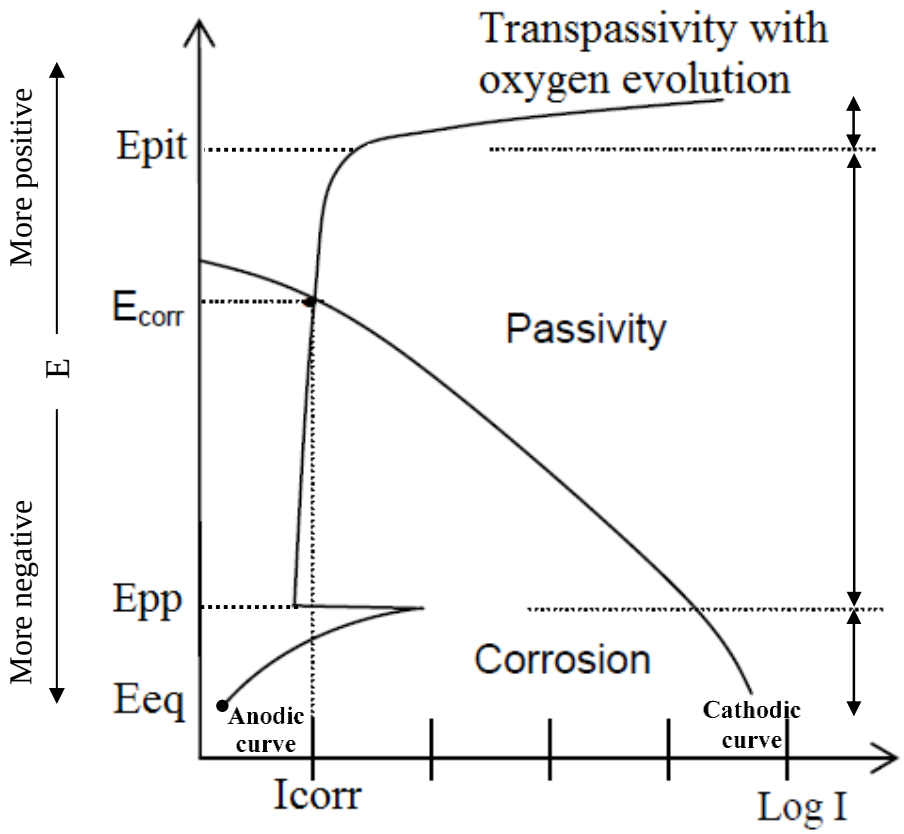

Figure 2.7: Schematic polarization curves of passive steel in concrete, adopted from (Austin et al., 2004; Bertolini et al., 2013)

Chloride ions have a significant effect on the anodic polarization curve (Bentur et al., 1997). It reduces the range of potentials over which the steel is passive. The greater concentration of chlorides, the higher reduction of the passivity interval and hence the E_{pit} is reduced to more negative values, for instance from E_{pit^A} to E_{pit^B} as shown in Figure 2.8. The corrosion current is increased from I_{corr^A} to I_{corr^B}, and pitting corrosion takes place if the corrosion potential (E_{corr}) is more positive than E_{pit} as illustrated in the case B for the high chloride content, otherwise the influence of chloride is negligible as for the case A where little or no chloride is existed (Angst et al., 2009). Typically, steel undergoing pitting corrosion exhibits a potential between -200 to -500 mV with respect to SCE (Katwan, 1988). In general, for the same extent of cathodic polarization curve, the corrosion rate increases with the chloride content while the corrosion potential decreases and becomes more negative. This the base, for the assessment of corrosion risk in the field, that negative corrosion potentials being associated with higher corrosion rates (Bentur et al., 1997).

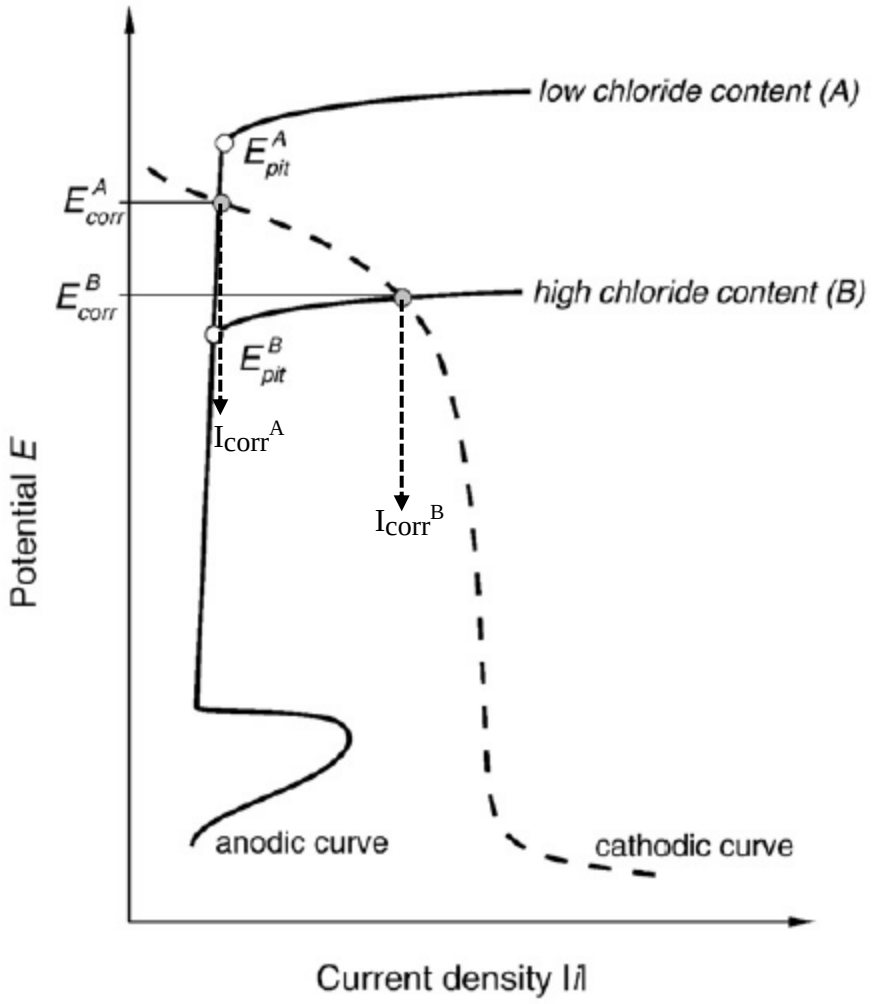

Figure 2.8: Schematic polarization curves for steel in concrete under the influence of chlorides, adopted from Angst et al. (2009).

Wilkins et al., however, indicated that the change in potentials is not necessarily an indication of corrosion activities since change to a more negative potential could be due to increased corrosion or a limiting cathodic reaction which is due to the limited oxygen content in the surrounding environment that can limit the speed of metal corrosion as shown in Figure 2.9 (Katwan, 1988). As the concentration of oxygen decreases, the cathodic reaction current decreases. The net effect is to shift the entire cathodic curve to the left. The intersection of the cathodic polarization curve and the anodic polarization curve moves to the left where the corrosion current density is less (Davis, 2000).

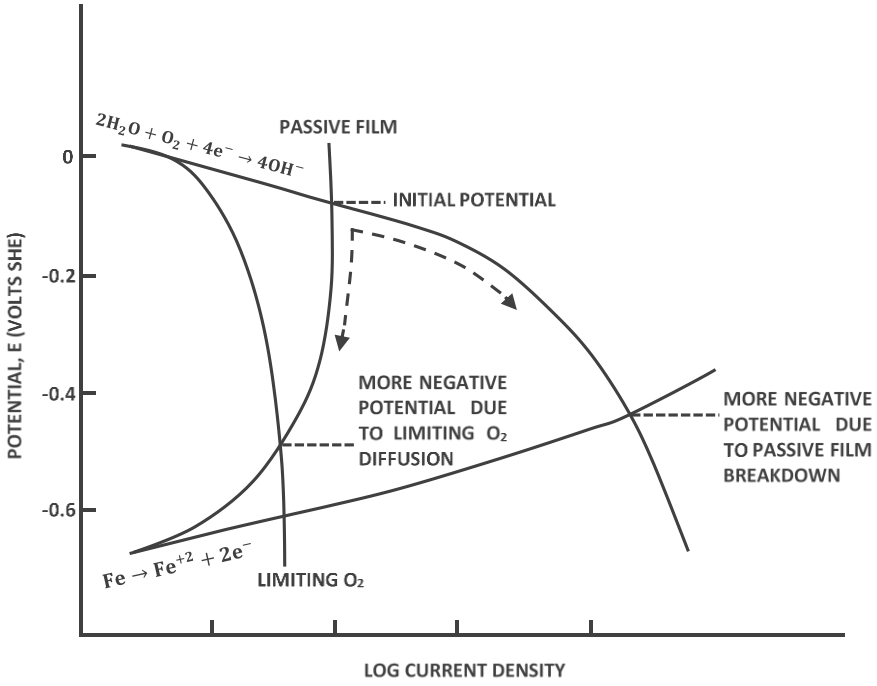

Figure 2.9: Effect of oxygen concentration on the cathodic polarization curve and the corrosion rate of an active metal (Katwan, 1988)

2.2 Depassivation Process

The passive film on the steel surface can be destroyed by the action of a number of agents as below:

2.2.1 Chloride Attack

It is a common knowledge that chloride induced corrosion is the major cause of deterioration of reinforced concrete structures. Chloride can come from several sources. It can diffuse in concrete when structures are subjected to seawater, salty ground water, sea spray or de-icing salts. It may also be cast into concrete when chloride contaminated raw materials are used for concrete, or through admixtures, such as calcium chloride which was used until the mid of 1970's in Europe as an accelerator of cement hydration (Broomfield, 2007; Morris et al., 2004; Page and Page, 2007; Poulsen, 1995). Although chloride ions have only a little influence on the pH of the concrete pore solution, they have the ability to depassivate the steel in concrete even in high alkaline conditions (Bertolini et al., 2013).

Once present in concrete, some chloride ions remain free in the pore solution and others become chemically bound to the hydration products of cement.

The chloride threshold for the initiation of reinforcement corrosion in the concrete is often presented as total chloride content related to the cement weight as its measurement is well documented in standards (ASTM C1152/C1152M, 2012; BS EN 14629, 2007). Furthermore, it was stated that a large part of the bound chloride dissolves as soon as the pH drops to values below 12, and may consequently play a role in the initiation of corrosion (Glass and Buenfeld, 1997).

However, it is generally believed that only the free chlorides are responsible for the corrosion of the reinforcement (Bertolini et al., 2013; Haque and Kayyali, 1993; Neville, 1995) by assuming that the bound chlorides are completely removed from the pore solution and present no risk for corrosion initiation (Angst et al., 2009). The free chloride content is therefore best for expressing the chloride threshold value (Hope et al., 1985). But, the amount of chloride is still quantified in terms of either total or free chloride content (Pargar et al., 2017), and they are sometimes preferred to be expressed relative to the weight of the concrete when binder content in hardened concrete is hard to be quantified.

Another used form to present chloride threshold level is the ratio of chloride to hydroxyl ions. A ratio of 0.6 was suggested by Hausmann (1967). Page and Havdahl (1985), however, thought that this is not a reliable index. A higher Cl^- / OH^- ratio does not necessarily reflects a higher risk of corrosion initiation. For instance, addition of silica fume as pozzolanic material not only reduces the alkalinity of the pore solution, which increases the ratio Cl^- / OH^-, but it also enhances the resistance of concrete and reduces the permeability that lead to slow down the chloride ingress and oxygen diffusion. Consequently it helps corrosion resistance of the steel in concrete.

The concentration of chloride ions required to initiate corrosion in concrete is not a constant but depends on pore solution composition, cement type and w/c ratio. They determine the free chloride available in the pore water and the chemically bound chloride with the cement (Hansson, 1984). Broomfield (2007) observed that the threshold value of chloride is about 0.2% of cement weight for the poor quality concrete and water and oxygen are available.

However, chloride concentration at 1% or higher may not cause corrosion in case of durable concrete. Moreover, chloride threshold to initiate corrosion in mortar specimens were found in the range of 1.24-3.08% and 0.39-1.16%, by weight of cement, in terms of total and free chlorides, respectively, (Alonso et al., 2000).

A wide range of the threshold value was reported. This is mainly due to various influencing factors, which include the method of measurement, method of presenting the threshold value, condition of the steel–concrete interface and the influence of environmental factors (Ann and Song, 2007). However, it is generally in the range of (0.4-1) % as total chloride by cement weight (Bertolini et al., 2009).

For the quality control purposes, but not for the corrosion threshold value, American Concrete Institute (ACI 222R) restricts total acid-soluble chloride ions to 0.20% for the normal reinforced and 0.08% by cement weight for the prestressed concrete respectively (Kerkhoff, 2007). In European countries, total chloride of 0.2~0.4% by cement weight is allowed by the standards for the reinforced concrete structures and 0.1~0.2% for prestressed concrete structures (BS EN 206, 2016). For water soluble chloride, ACI 318 defines 0.15% by cement weight for the normal reinforced concrete and 0.06% of cement weight for the prestressed concrete. The limit of the total chloride content in the concrete in ACI and BS standards is given in Table 2.1.

Table 2.1: Maximum chloride content of concrete (Ann and Song, 2007)

Type	Maximum chloride content (%, cem.)			
	BS 8110	ACI 201	ACI 357	ACI 222
Prestressed concrete	0.10		0.06	0.08
Reinforced concrete exposed to chloride in service	0.20	0.10	0.10	0.20
Reinforced concrete that will be dry or protected from moisture in service	0.40			
Other reinforced concrete		0.15		

2.2.2 Carbonation

Carbonation is another important factor which cause corrosion of rebars in concrete structures. Carbonation is the chemical reaction of the calcium hydroxide in concrete, hydration products in the cement matrix dissolved in the pore water, with carbon dioxide

(CO_2) in the air which produces calcium carbonate ($CaCO_3$) according to the following reactions (Siddiqi, 2012)

$$CO_2 + H_2O \rightarrow H_2CO_3 \quad (2.17)$$

$$H_2CO_3 + Ca(OH)_2 \rightarrow CaCO_3 + 2H_2O \quad (2.18)$$

For simplicity, equations (2.17) and (2.18) can be combined in one reaction as below:

$$Ca(OH)_2 + CO_2 \rightarrow CaCO_3 + H_2O \quad (2.19)$$

The carbon dioxide gas dissolves in water to form carbonic acid (H_2CO_3), which reacts with calcium hydroxide and precipitates calcium carbonate ($CaCO_3$) (Zhou et al., 2014). This reaction consumes the alkalinity of concrete surrounding the reinforcement, which reduces the PH of concrete pore solution from about 13 to less than 9, when the passive film around the steel may be destroyed and corrosion may be accelerated if sufficient oxygen and water are present at the surface of the rebars (Bertolini et al., 1998; Papadakis et al., 1992). Carbonation induced steel corrosion can increase concrete cracking and decrease the durability (Roy et al., 1999).

The depth of carbonation in concrete increases with time. However, Sims (1994) stated that the rate of carbonation in concrete, normally very slow, and it varies depending on many factors such as mix proportion, cement type, compaction, curing, temperature, humidity and ingress of CO_2 into concrete pore system. The rate of diffusion of carbon dioxide is extremely slow in very wet concrete (RH >90%). On the other hand, concrete will not carbonate if it is almost fully dry, RH < 40%, because water is needed for the carbonation (De Schutter, 2012; Siddiqi, 2012). Consequently, carbonation mostly occurs when the concrete is semi-dry. The highest carbonation rate occur at the about 50% RH (Tuutti, 1982), as shown in Figure 2.10, when the moisture content is low enough to permit penetration CO_2 gas but meanwhile high enough to give sufficient water for CO_2 chemical reaction (Küter, 2009). An alternating cycle of wetting and drying provide the most aggressive environment for the carbonation-induced corrosion (Tuutti, 1980).

Carbonation process does not exceed several millimetres in good quality concrete. Virmani and Clemena (1998) indicated that concrete with water cement ratio of 0.45 and concrete cover of 25 mm will need for more than 100 years until carbonation reaches the level of the reinforcement. It was observed that corrosion occurs when the average distance between carbonation front and reinforcement bar surface is less than 5 mm, which means that carbonation-induced corrosion starts slightly before carbonation depth reaches the level of reinforcement (Yoon et al., 2007). This value becomes 20 mm for the concrete structures containing chloride ions.

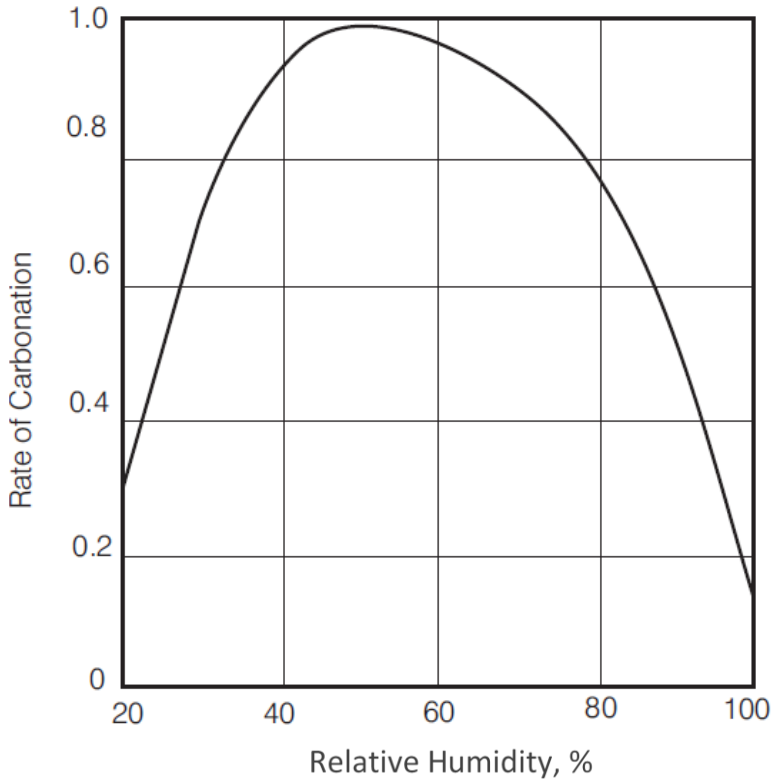

Figure 2.10: The influence of relative humidity on the rate of carbonation on concrete (Tuutti, 1980)

A phenolphthalein indicator is one of the techniques that majority of research works on concrete carbonation can be used for the determination of carbonation depth. This involves spraying concrete broken faces with 1% phenolphthalein in 70% ethyl alcohol (Raj and Muthupriya, 2016). When phenolphthalein is applied, noncarbonated areas turn red or purple, while carbonated areas where pH at 8 remain colorless.

2.3 Corrosion Measurement and Evaluation Techniques

Whilst the possibility of a corrosion reaction occurring can be predicted theoretically, the kinetics of the reaction which is related to the rate of corrosion less predictable and can only be determined empirically (Katwan, 1988).

Various monitoring techniques have been developed to assist in the assessment or prediction of the corrosion. In this section, however, special emphasis will be placed on half-cell potential and linear polarization method as they constitute the main measuring techniques adopted in this study. Tafel extrapolation method is also presented as it provides the basic of Tafel slopes for which the linear polarization method can be used for corrosion rate determination.

2.3.1 Half-cell Potential Method

Among various non-destructive testing techniques for detecting corrosion of reinforcements, half-cell potential measurement prove to be reliable one (Pei et al., 2015; Zhang et al., 2017). It is suitable for in situ evaluation and in the laboratory. In this method potential difference is measured between steel reinforcement and a reference electrode. The principle and measurement of this technique are presented in the next two sub-sections.

2.3.1.1 Principle of Half-cell Potential

The term potential is widely used when considering corrosion. It is a thermodynamic measure of the ability of electron charge transmit between the metal and the surrounding environment and not of the steel itself (Hansson, 1984; Poursaee and Hansson, 2009). Thus, it is not possible to determine the absolute value of the potential and therefore the potential difference between a metal surface and a reference electrode is taken as a measure of the actual potential.

When a metal is immersed in a solution of its ions, there are two possible reactions which may occur. Either the metal ions may leave the surface of the metal and go into solution, resulting in the development of a negative charge on the metal surface as illustrated in Figure (2.6: A) or the metal ions from the solution may be deposited on the metal surface, resulting in the development of a positive charge on the metal surface as shown in Figure (2.6: B).

Both A and B result in a potential deference existing between the metal and the solution (Bird and Chivers, 2014).

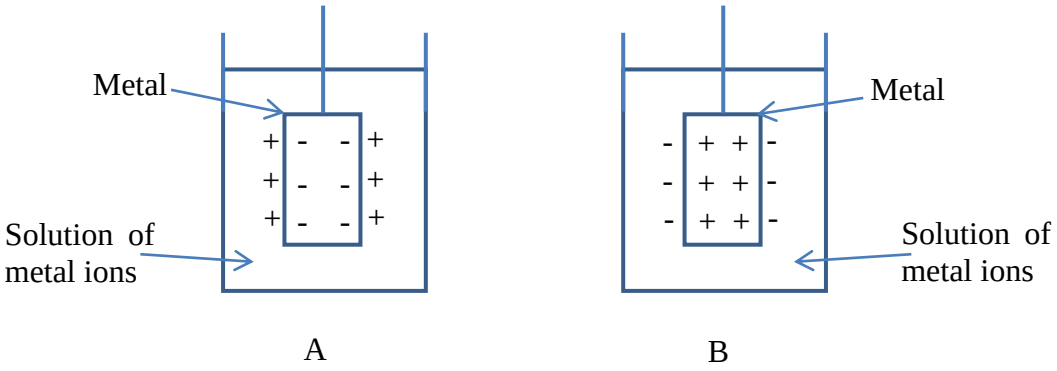

Figure 2.6: (A): A negative charge on the metal surface, e.g. Z (B): A positive charge on the metal surface, e.g. Cu, (Bird and Chivers, 2014)

Any metal in contact with a solution of its ions is called a half-cell, and the potential of the half-cell is called the electrode potential of the half-cell. The potential of a half-cell cannot be determined independently, but is measured by placing it in series with a known potential half-cell (Bird and Chivers, 2014). These are joined together by an electrolyte, and a voltmeter is connected across the complete circuit to measure the potential produced. A standard half-cell electrode has been selected for this purpose. The standard reference electrode is the hydrogen electrode. But, due to limitation of the standard hydrogen electrode, alternative half-cell reference electrodes have been used, such as copper in saturated copper sulphate electrode (CSE), Silver/ Silver chloride in potassium chloride (Ag/AgCl/KCl) and Standard Calomel Electrode (mercury in saturated mercuric chloride) (SCE). Each half-cell consists of a metal rode immersed in a solution of its own ions.

The potential of any reference electrode can be recorded against the Standard Hydrogen Electrode (SHE). Table 2.2 gives the standard half-cell potentials for some metals (Fontana, 2005). Half-cell potentials are a function of concentration of the solution and the metal. A more concentration is more corrosive than a dilute one so a current will flow in a cell made up of a single metal in two different concentrations of the same solution (Broomfield, 2007).

Table 2.2: Half-cell potentials, (Fontana, 2005)

Metal – metal ion equilibrium	Electrode potential against standard hydrogen electrode at 25°C, Volts
Ag-Ag+	+0.799
Cu-Cu^{+2}	+0.337
H_2-H^+	0.000
Fe-Fe^{+2}	-0.440
Zn-Zn^{+2}	-0.763

2.3.1.2 Measurement and Interpretation of Half-cell Potential

Up to the present, the measurement of the half-cell potential, also known as open circuit potential or corrosion potential, E_{corr}, expressed in Volts or millivolts, is the most widely used technique to predict the possibility of corrosion and evaluate the condition of steel in concrete structures (Hansson et al., 2012; Montemor et al., 2003; Poursaee and Hansson, 2009; Song and Saraswathy, 2007a; Zhang et al., 2017). The measurement of E_{corr} is a well-known technique and described in the American Standards (ASTM C876).

An external half-cell (reference electrode) is used to measure the potential of the steel in concrete as shown in Figure 2.11. The reference electrode is placed on the concrete surface and connected via a voltmeter to the steel to create an electrochemical cell which contains of two half cells, the first one is the external half-cell and the second one is the steel in its environment. By agreement, the steel is connected to the positive terminal of the voltmeter and the reference electrode to the negative terminal. This will give a negative reading.

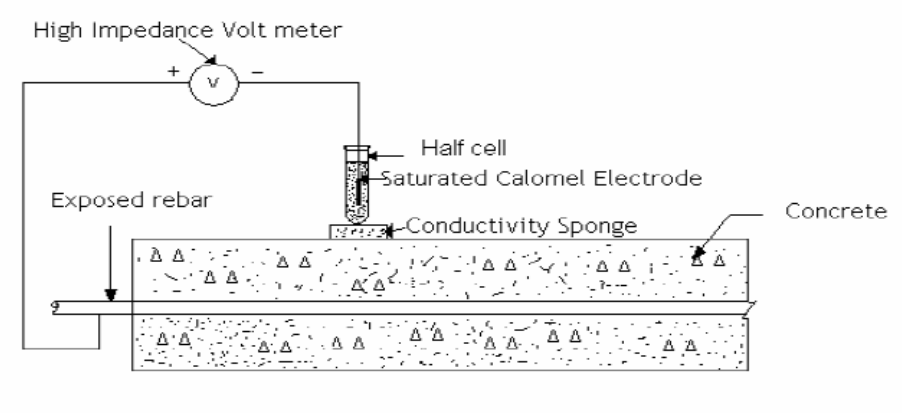

Figure 2.11: Setup of half-cell potential measurement (Song and Saraswathy, 2007b)

The measured electrical potential difference between the two half cells will be a function of the steel in its pore water environment. Different potentials are obtained due to different environment around the steel. Table 2.3 shows the probability of reinforcement corrosion according to ASTM C876 interpretation which is based on empirical observation. The steel is considered passive when the potential measured is small (zero to -200 mV) and active when the potential moves to be more negative.

Table 2.3: Corrosion risk from potential measurement according to ASTM C876 (Verma et al., 2014)

Half-cell potential reading against CSE, mV	Probability of corrosion
more positive than −200	10%
−200 to −350	≈50%
more negative than −350	90%

The most common way of presenting the half-cell potential field data is plotting a potential map of the area surveyed. The advantage of this is that potential gradients can be detected and these generally correspond to a greater risk of corrosion (Broomfield, 2007; Poursaee and Hansson, 2009). It should be emphasized that half-cell potential measurement only gives an indication of the severity of corrosion but not corrosion rate. A simple comparison of the half-cell potential data with the ASTM C876 could cause mistakes in the evaluation of the

structure if other factors are not taken into account (Gu and Beaudoin, 1998; Poursaee and Hansson, 2009). It is generally accepted that a more negative potential readings indicates a higher probability of corrosion. However, this general rule may not always be valid as many influencing factors, such as oxygen availability, chloride concentration, cover thickness, the type of reinforcing bar, whether or not the steel is coated, whether or not inhibitors are used, and concrete resistivity can affect the readings of the potential towards more positive or negative values but these changes may not necessarily be related to the severity of the steel corrosion (Broomfield, 2007; Gu and Beaudoin, 1998). Novokshchenov (1997) and Cairns and Melville (2003) found there is a good correlation between corrosion potential values and corrosion rate measured by polarisation resistance method, however, poor correlation existed in the work of Feliu et al. (1996).

2.3.2 Polarization Measurements for Determining Corrosion Rates

The corrosion rate of reinforcement embedded in concrete can be determined reliably by exposing reinforced specimens to real environments for a period of time and then removing the rebars from concrete to measure the weight-loss of the reinforcement. But this method is considered destructive, costly and time consuming.

In present there are many methods for determination of corrosion rates of metals. The polarization methods, based on electrochemical concepts, are able to determine instantaneous corrosion rate in a few minutes and can be used to predict the service live in years (Badea et al., 2010; Hansson, 1984). However, other methods require multiple measurements over time to provide information of the corrosion rate (Badea et al., 2010). The two most common polarization methods are linear polarization resistance and Tafel extrapolation (Hansson et al., 2012; Lorenz and Mansfeld, 1981; Yang, 2008), which are explained in the following subsections.

2.3.2.1 Tafel Extrapolation Method

In the absence of passivity, for the reinforcing steel in concrete, the typical polarization curves of the anodic and cathodic reactions are presented as in Figure 2.12. Tafel found that a linear relationship between E and log I exists if an electrode potential is polarized to less than -250 mV when acts as cathode and more than 250 mV when acts as anode (Basu, 2016). The regions in which such relationships exist are known as Tafel regions and the slope of

the lines are called the Tafel Constants. Mathematically this relationship is given in equation 2.20 (Yang, 2008).

$$I = I_{corr}\left[\exp\left\{\frac{2.303(E-E_{corr})}{\beta_a}\right\} - \exp\left\{-\frac{2.303(E-E_{corr})}{\beta_c}\right\}\right] \quad (2.20)$$

where I is the measured current under the polarization, I_{corr} is the current at corrosion potential E_{corr}, E is the applied potential, E_{corr} is the corrosion potential, β_a and β_c are Tafel constants which are the slopes of the anodic and cathodic curves in the E-log I plot in the Tafel regions.

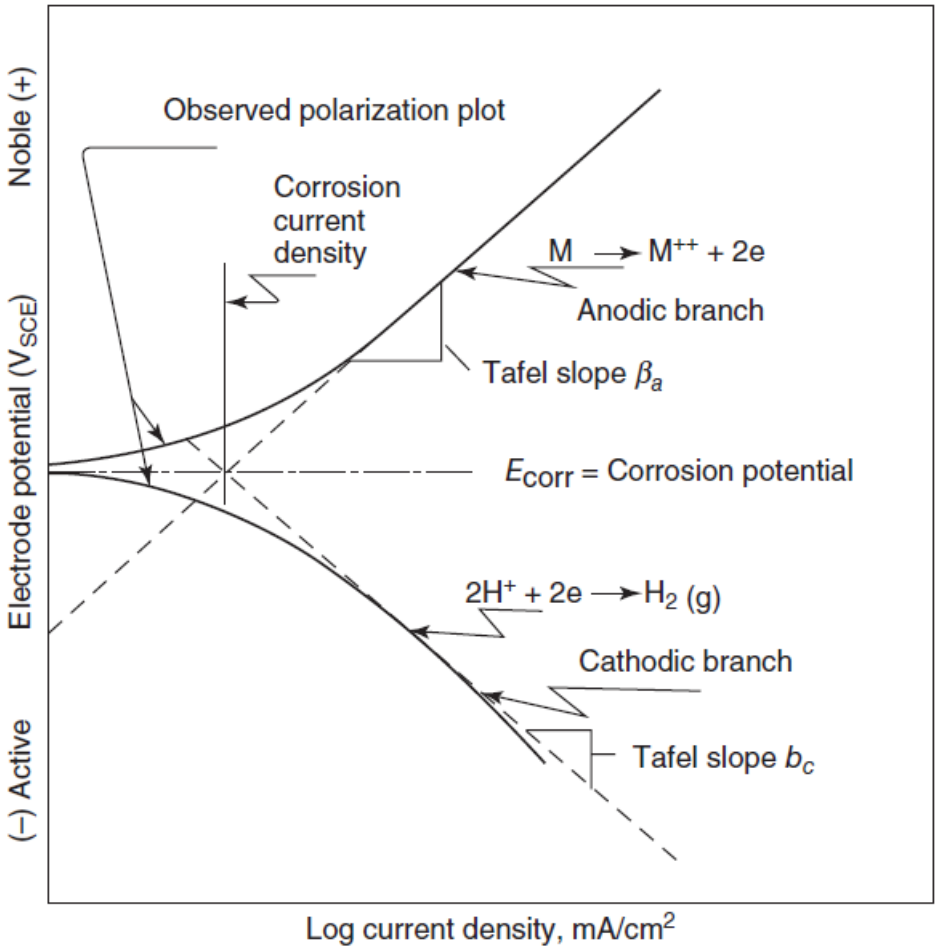

Figure 2.12: Hypothetical cathodic and anodic polarization diagram (ASTM G5, 2014)

The main advantage of this method is that it provides a direct measurement of the corrosion rate and Tafel constants (Yang, 2008). The measurements may be accomplished either

potentio-dynamically with a suitable sweep rate, which is usually used for moderate to high corrosion rate systems or potentio-statically where the potential is applied in steps and the system allowed to come to equilibrium at each step before the current is measured. This technique is more convenient for systems corroding at low rate such as passivated steel in reinforced concrete (Katwan, 1988). However, there are two major disadvantages for the Tafel extrapolation technique. Firstly, in certain systems, the linear Tafel behaviour may not be obtained. Secondly, it is a destructive technique due to a large polarization range required to complete the polarization. A large polarization will disturb the sample electrode and change or damage the surface properties of the electrode. For this reason it is not used as a monitoring technique in the field. On the other hand, continuous polarization on the same sample will yield un-reliable results, so a number of new specimens will be required to complete the corrosion evaluation studies (Moore, 1975; Popov, 2015). Furthermore, for an accurate extrapolation, the slope should extend over a current range of at least one logarithmic decade (Badea et al., 2010).

2.3.2.2 Linear Polarization Resistance (LPR) Method

The disadvantages of the Tafel extrapolation method can be largely overcome by using the polarization resistance technique (Mansfeld, 1981). It is the most accurate technique for corrosion evaluation of the steel in concrete (Angst et al., 2009). It is non-destructive and short experimental duration, which is suitable for the evaluation of the instantaneous corrosion rate in the laboratory and in the field (Ahmad et al., 2014).

Polarization resistance is a charge transfer resistance between the electrodes and the electrolyte which determines the rate of the corrosion reaction and measures the ease of which the electrons transfer across the surface. It developed by Stern and Geary (1957) and has been successfully used by many investigators (Alonso et al., 1988; Kupwade-Patil and Allouche, 2012) to monitor corrosion of steel in concrete. The corrosion current, according to the Stern-Geary equation, is inversely proportional to polarization resistance (Popov, 2015). However, there are some major technical difficulties with this method. One practical difficulty is to know the exact surface area of the reinforcing steel that is actually being polarized by the measurement. In addition, a foreknowledge of the values of the Tafel slopes are necessary for accurate determination of the corrosion rate (Ahmad et al., 2014; Katwan, 1988).

At the E_{corr} , the anodic and the cathodic reactions are in equilibrium. The rate of oxidation is exactly equal to the rate of reduction and there is no net current to be measured. The application of an external current will move the potential away from E_{corr}. This changing of the potential is known as polarization. Cathodic polarization occurs when the electrode is polarized to more negative value and anodic polarization occurs when the electrode is polarized to more positive value. If the polarization is within several mV of E_{corr}, typically ± 10 to 30 mV (Andrade and Gonzalez, 1978; Gowers and Millard, 1999; Popov, 2015; Sadowski and Nikoo, 2014), a linear relationship at the E_{corr} is expected between the potential and the current as shown in Figure 2.13.

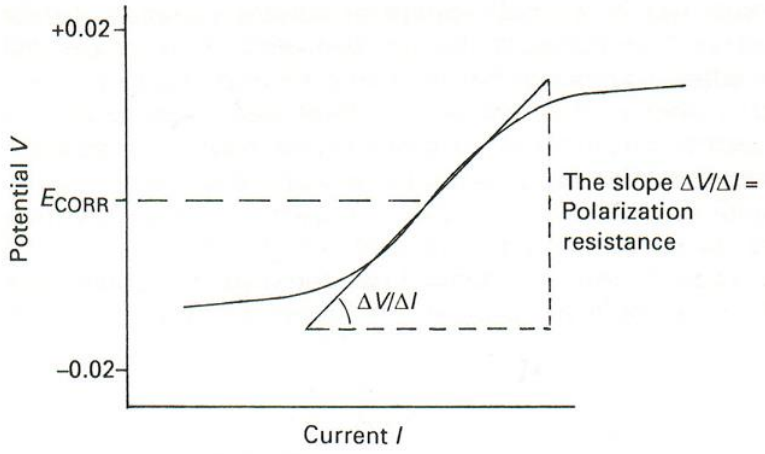

Figure 2.13: polarization curve close to the corrosion potential (Berkeley and Pathmanaban, 1990)

i. Measurement of LPR

A typical experimental setup for the polarisation resistance measurements is shown in Figure 2.14. A power supply known as a potentiostat/galvanostat which controls the out-put voltage/current with three electrodes is used to polarize precisely the potential of the working electrode (WE) whose corrosion rate is being measured. Besides the working electrode, there is a counter electrode (CE), also called the auxiliary electrode, is required to complete the electrical circuit in which the current can be injected from the potentiostat, and a separated reference electrode (RE) to provide the potential readings of the working electrode without passing current through.

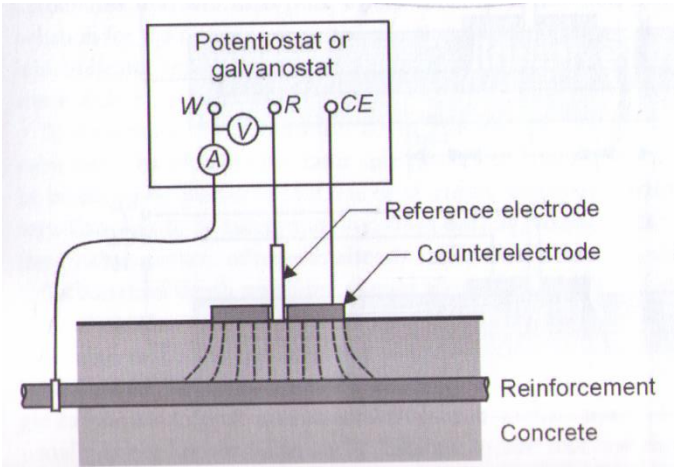

Figure 2.14: Schematic setup for linear polarization technique (Bertolini et al., 2013)

The LPR measurements are performed either in potentiostatic or galvanostatic mode. In the potentiostatic mode, the potential difference between the working and the reference electrodes is kept constant and measuring the current response in the circuit. In the galvanostatic mode, the current flowing in the circuit is kept constant and the potential response of the working electrode is measured (Ahmad et al., 2014; Poursaee, 2016). Potentiodynamic and galvanodynamic modes are also can be used (Poursaee, 2016).

In practice, the potential of reinforcement is initially set to about 20 mV below E_{corr} (Bentur et al., 1997), then swept at a low scan rate of about (0.1 mV/sec) to a potential of about 20 mV above E_{corr}. The current response during the scan is recorded, and the polarization resistance, Rp, is then obtained from the slop of the current - potential plot at the corrosion potential ($\Delta E \rightarrow 0$) using the following equation (Andrade and Alonso, 2004).

$$Rp = \left[\frac{\Delta E}{\Delta I}\right]_{\Delta E \rightarrow 0 (E = E_{corr})} \quad (2.21)$$

The slope of the linear polarisation curve that represents the polarization resistance is related to the corrosion current of the system as in equation 2.22 which was derived by Stern and Geary (1957) for known values of the anodic and cathodic Tafel slopes.

$$I_{corr} = \frac{1}{R_p}\left(\frac{\beta_a.\beta_c}{2.303(\beta_a+\beta_c)}\right) \quad (2.22)$$

then,

$$I_{corr} = \frac{B}{R_p} \quad (2.23)$$

and,

$$B = \frac{\beta a\,.\,\beta c}{2.303(\beta a+\beta c)} \quad (2.24)$$

where ΔE is the changes in potential (i.e. the potential shift from the corrosion potential) in mV, ΔI is the measured flowing current due to the change in potential in mA. $\Delta E/\Delta I$ is the slope of the potential- current curve at the corrosion potential which represents the polarization resistance in Ω, I_{corr} is the corrosion current in mA, B is Stern-Geary constant and β_a and β_c are the anodic and cathodic Tafel slopes in mV, respectively.

The values of the Tafel slopes which are necessary for determination of the corrosion rate could either be determined by the Tafel extrapolation method or could be assumed. In many instances a value of 120 mV is assumed for both β_a and β_c (Popov, 2015; Yang, 2008). Andrade and Gonzalez (1978) showed from their experimental studies that a B value of 26 mV for corroding (I_{corr} > 0.1 - 0.2 μA/cm^2) and 52 mV for non-corroding (I_{corr} < 0.l μA/cm^2) steel in concrete is in a good agreement with gravimetric weight loss results. The validity of this value has also been confirmed by other research workers (Page and Lambert, 1986).

To obtain the corrosion rate i_{corr} in mA/m^2 or μA/cm^2 from the calculated value of corrosion current I_{corr}, the following relationship is used (Zafeiropoulou et al., 2013). Where, I_{corr} is the corrosion current in mA or μA, A is the surface area of the reinforcing steel under test in m^2 or cm^2.

$$i_{corr} = \frac{I_{corr}}{A} \quad (2.25)$$

The amount of section loss after the initiation of corrosion can be estimated using Faraday's law (Smith and Virmani, 2000). It is usually expressed as the penetration rate and measured in mm/year or µm/year using the corrosion rate values. For example, in the case of steel, 1 µA/cm^2 is equivalent to a corrosion rate of 0.0116 mm/year for uniform corrosion as in equation 2.26 (Andrade and Alonso, 2004).

$$\text{Corrosion pentration (mm/year)} = 0.0116\, i_{corr}\ (\mu A/cm^2) \qquad (2.26)$$

Classifications of the severity of rebar corrosion rates based on polarisation resistances are presented in Table 2.4. It is important to realize that a high precision and repeatability for any corrosion rate measurement of steel in concrete in the field cannot normally be expected. Each category in Table 2.4 is an order of magnitude different from the adjacent category. An electrochemical corrosion rate measurement should place the element under study into the appropriate category but small differences in corrosion rates within a particular category should not be deemed to be significant. Corrosion is a dynamic process subject to fluctuations and the interpretation of corrosion rate measurements should focus on the order of magnitude rather than the precise value obtained (Gowers and Millard, 1999).

Table 2.4: Typical corrosion rates for steel in concrete (Andrade and Alonso, 1996; Gowers and Millard, 1999)

Rate of corrosion	Polarization resistance R_p: kΩ cm^2	Corrosion current density i_{corr}: µA/cm^2	Corrosion penetration p: µm/year
Very high	$2{\cdot}5 > R_p > 0{\cdot}25$	$10 < i_{corr} < 100$	$100 < p < 1000$
High	$25 > R_p > 2{\cdot}5$	$1 < i_{corr} < 10$	$10 < p < 100$
Low/moderate	$250 > R_p > 25$	$0{\cdot}1 < i_{corr} < 1$	$1 < p < 10$
Passive	$R_p > 250$	$i_{corr} < 0{\cdot}1$	$p < 1$

As a general figure based on laborotary and field investigation, the corrosion rate can be considered negligible if it is below 0.1 µA/cm^2, low to modertae between 0.1 and 0.5 µA/cm^2, moderate to high between 0.5 and 1 µA/cm^2 and high if it is greater that 1 µA/cm^2 (Broomfield, 2007). In fact, the corrosion rate is the key parameter in order to quantitatively predict residual life of corroding structures, as it may inform about the loss of steel cross-section area over time, the time to cracking of concrete cover or the gradual loss of steel/concrete bond (Andrade and Alonso, 1996). Values below 0.1 µA/cm^2 indicate

lifetimes longer than 100 years. Values giving cross-section losses of 5-25% during 20-50 years are those around 0.5-5 $\mu A/cm^2$, which are precisely those measured onsite.

ii. Influence of IR-drop

The resistance measured by the LPR in fact is the sum of the polarization resistance, Rp, and the concrete resistance, RΩ. If Rp >> RΩ, the resistance which is measured by the LPR is close enough to the polarization resistance that can be used as the actual value (Amir Poursaee, 2016). However, researchers (Andrade and Gonzalez, 1978; Gonzalez and Andrade, 1982; Walter, 1978) indicated that a voltage drop may occur at the location of the reference electrode due to concrete resistance and or any existing surface film and can cause significant errors in the corrosion rates calculated using polarization resistance method.

If an external current I is passing from the working electrode (the reinforcement) through an electrolyte such as the concrete here to the counter electrode, a voltage drop called IR drop develops due to electrical resistance of concrete RΩ, also expressed Re, and causes reducing the actual potential of the working electrode E_p in relation to the applied potential (the measured potential) E_a as in the following equation (Oelssner et al., 2006)

$$E_p = E_a - \text{IR drop} \tag{2.27}$$

As mentioned in the previous section, the polarization resistance is the ratio of the applied potential and the resulting passing current. So, in case of uncompensated IR-drop, the experimentally determined Rp will be the sum of the actual Rp and the resistance of the electrolyte at the rebar surface. Thus, the determined Rp value will be greater than the actual one which makes the calculated corrosion rate lower than the true value.

Montenegro et al. (2012) stated that a part of the IR-drop can be decreased by placing the reference electrode close to the surface of the working electrode. The elimination of the IR drop issue has worried corrosion specialists for more than 50 years and significant effort has been done to solve the problem, which was finally successfully solved using current interruption method or positive feedback method and the result developed in auto IR compensation sophisticated instruments commercially available called potentiostats (Andrade and Alonso, 2004; Oelssner et al., 2006).

2.4 Electrical Resistivity of Concrete

Concrete resistivity is a geometry-independent material property that describes the electrical resistance (Polder, 2001). It is a fundamental property of a particular material and is defined as its capability to withstand the transfer of ions subjected to an electrical field (Azarsa and Gupta, 2017). It is one of the important physical properties of Portland cement concrete that affects a variety of applications (Whiting and Nagi, 2003) and it's measurements are being increasingly used as a non-destructive technique to provide a great deal of information on various aspects of concrete technology (Katwan and Al-Sofi, 1999). It is used to describe, for example, the degree of water saturation, the resistance to chloride penetration or the risk of reinforcement corrosion (Bertolini et al., 2013) and it is essential for the design of cathodic protection system. The resistivity of concrete may have values from tens to thousands of Ω.m as a function of the type of cement used, the w/c, the presence of chloride ion, water content, and concrete carbonation degree (Bertolini et al., 2013; Polder, 2001).

2.4.1 Measurement Techniques

Electrical resistivity can be measured by several ways non-destructively. The most commonly used technique for in situ testing is the Wenner 4-probe technique (Layssi et al., 2015; Morris et al., 1996; Stanish et al., 1997). In this method, the probes are placed on the surface of the test concrete and an alternating current passed between the outer two electrodes while voltage across the inner two is recorded as shown in Figure 2.15.

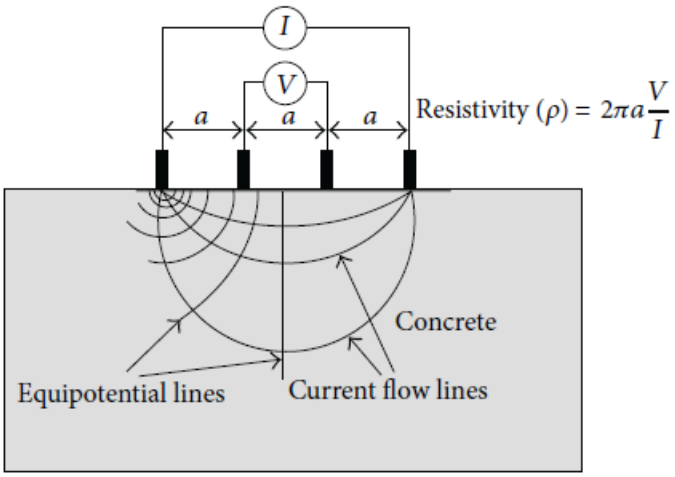

Figure 2.15: Wenner technique (four electrode) for electrical resistivity measurement (Sadowski, 2013)

The operation is simple and the result can be obtained in a short time (Chen et al., 2014). This method was developed by Wenner (1915) to measure soil resistivities, which was then modified for the application to concrete structures by Stratfull (1968) and Naish et al. (1990). Several commercial instruments based on the 4-probe method have been available (Bertolini et al., 2013). However, one of the drawbacks of this technique is that the conduction paths are not accurately known. Additionally, in this technique, the measurement is supposed to be conducted for a semi-infinite homogeneous material (Broomfield, 2007). Therefore, it is to be expected that inhomogeneities will affect electrical resistivity measurements.

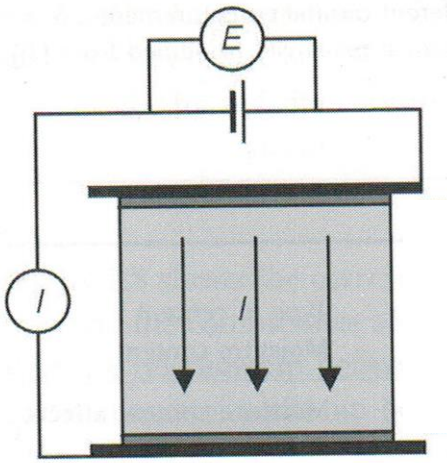

Figure 2.16: Set up of electrical Resistivity testing of concrete by two-electrode method (Bertolini et al., 2013)

More accurate resistivity values can be obtained using bulk resistivity method (also known as uniaxial method), in which external plate electrodes are used enabling the current to traverse the full area of the specimen. However, its application is infeasible for field evaluation because electrodes access to opposite sides of the concrete element is not possible all the time. In this method, steel plates is pressed to two parallel faces of a concrete cube or cylinder, via wetted cloth for good electrical contact, as shown in Figure 2.16 (Bertolini et al., 2013). Sengul (2014) employed a similar arrangement for a very recent study of concrete resistivity and compared the result to those obtained by ASTM C1760 (2012) which is used for the determination of the bulk electrical conductivity of saturated specimens of hardened concrete. There was a very high correlation between the values measured for same environmental conditions. However, there are several technical factors affect such

measurements. These factors are summarized in Table 2.5 based on many different early and recent studies.

Table 2.5: Summary of laboratory test methods for electrical resistivity of concrete, the details of the first ten references were taken from Elkey and Sellevold (1995)

Study	Voltage type (frequency)	Specimen description	Electrode type	Method of contact
Hammond & Robsen, 1955	DC (55-3 kV) AC (0.002-25kHz)	Cubes (4″) Prisms (4 x 4 x 1″)	Brass plates (external	Stiff graphite gel
Monfore, 1968	DC (4-10 V) AC (2-8 V) (0.1-10 kHz)	Cubes (1″ and 4″)	Brass plates (external)	Stiff graphite gel
Bracs, 1970	Not available	Cubes (6″)	Steel wire	Cast in
Bhargava, 1978	AC (0.5-1.5 V) (0.1-50 kHz)	Prisms (40 x 40 x 160 mm)	Hardened cement paste w/Pt black	Cast in
Woelfl, 1979	AC (6 V) (60 Hz)	Prisms (1 x 2 x 6″)	slim rods (material N/A)	Cast in
Hansson, 1983	DC (3-9 V)	Prisms (90 x 70 x 50 mm)	Perforated steel plates (30 x 30 mm)	Cast in
Hughes, 1985	DC (4-8 V) AC (10V)	Cubes (150 mm)	Brass plates (external)	Fluid cement paste (w/c = 0.5)
Hope, 1985	AC (1kHz)	Prisms (25 x 25 x 100 mm)	Brass or steel rods	Cast in
Hauck, 1993	AC	Cylinders (100 mm dia. x 51 mm)	iron mesh (external)	Electrolytic solution
Cabrera, 1994	AC (10V)	Cubes (100 mm)	Brass plates (external)	Fluid cement paste
Principallo et al. (2003)	20 MHz	150x150x200 mm.	Two electrodes method, cylindrical rods (10 mm diameter)	Cast in
Ghods et al. (2005)	AC, 3V, 1.1 kHz	Cylinder, D=150mm, L=100mm	Two electrodes method, Copper plates	External, cement paste
(Chacko et al., 2007)	AC, 10V 60Hz	15 mm ×25 mm ×50 mm & 15 mm × 25 mm × 110 mm	Two electrodes method, copper rods	Cast in
(Polder, 2009)	AC, 120 Hz	Prisms of 100x100x300 mm3	Two electrode method, stainless steel bars	Cast in
Hou et al. (2010)	AC, 36 V	160×130×40 mm & 300×300×60 mm.	Two electrode method, Steel mesh	Cast in

Lübeck et al. (2012)	AC	Prism (100 x 100 x 170 mm)	Four-electrode method (Wenner's)	Cast in
Chang et al. (2013)	DC	Prism (140 x 140 x 280mm)	2-point probe embedded electrodes, metal mesh	Cast in
Sengul (2014)	hand-held resistance meter with a frequency of 1 kHz & ASTM C1760 (DC,60V)	Cylinder (D=100 mm & H =50 mm)	Two electrode method,	External, Wet cloth
Van Noort et al. (2016)	AC, 1 kHz	Cube 15x15x15cm	Two electrode method, Stainless steel plates	External, Wet cloth with a dilute solution of soap

According to the table above, prisms and cubes of different sizes are the most widely employed, though cylinders also are used by some investigators. Use of cubes or prisms provides flat faces to apply the external electrodes. While for cylinders, the measurement is complicated due to the need for smooth surfaces to achieve uniform electrical contacts between the electrodes and the surfaces of the concrete specimens which may require to cut off part of the top surface for placing the electrodes.

As can be seen from Table 2.5, a number of ways can be used to ensure a uniform distribution of current between the external electrodes and the test specimen. Early studies used conductive graphite gels or pastes. These are effective if precautions are taken because they dry with time if not shielded with moisture barriers. Cement paste has also been used, but suffers from the same issues as graphite paste. The most direct and reliable mode of contact is to embed electrodes into the fresh concrete. Then resistivity measurements can be performed on the concrete specimen at various moisture states without disrupting the moisture content of the specimen (Whiting and Nagi, 2003). Electrodes can be of various types. Brass is the most commonly used material, but steel also is used. They can be meshes or plates. In the case of embedded electrodes, wires or thin rods normally are used. In these cases, however, the flow path may not be defined well enough to calculate a true resistivity (Whiting and Nagi, 2003).

As shown in Table 2.5, measurements of electrical resistivity were performed using either direct current (DC) or alternating current (AC) at various frequencies. However, alternating

current is the more frequently used as it is generally acknowledged that measurement of resistivity using direct current produces polarisation of the electrode (Stanish et al., 1997). Application of a DC voltage across a concrete specimen causes current flow, mostly carried by ions in the concrete pore water. Reactions occur at the contact electrodes (Hansson and Hansson, 1983). These reactions produce polarization and cause the actual voltage causing current to be reduced by an unknown amount (Stanish et al., 1997).

Current cannot be accurately measured in the case of DC because of these polarization effects. Thus, the measurement requires alternating current to avoid polarization of the electrodes (Chacko et al., 2007; Layssi et al., 2015; Polder, 2001). The ranges of frequencies used were from 2 to 50,000 Hz and the voltage from 0.5 to 36V. Bhargava and Rehnstrom (1978) examined the resistance of concrete at different voltages and frequencies and they recommended a frequency of at least 1000 Hz to be used for resistivity measurements as they noticed that after 1000 Hz frequency, the difference between the resistance at various voltage disappears. Calleja (1953) showed in his study that the decrease in resistance when frequency increased from 40 to 20,000 Hz was only 10%. To eliminate the polarisation effect, previous researches have suggested the use of both a low frequency, such as 60 Hz (Chacko et al., 2007), 107 Hz (Osterminski et al., 2012), 128 Hz (Newlands et al., 2008) and a high frequency, such as 1000 Hz (Whittington et al., 1981) and 7500 Hz (Banthia et al., 1992). Layssi et al. (2015) suggested that a frequency in the range from 500 to 10,000 Hz could produce an accurate measurement. The work presented by McCarter et al. (2015) shown that using an AC frequency in the range 5 kHz‑10 kHz with a low-resistivity liquid used to saturate the sponges would result in a more accurate assessment in concrete resistivity. Recognising that it is hard to define a specific optimal frequency due to the variation of the conditions of concrete. In term of the applied voltage during resistivity measurements, it should be low to avoid heating of the concrete and usually in the range of 10 V or lower [Streicher and Alexander, 1995], and is only applied for short times.

The electrical resistivity of the concrete using two-electrode method is calculated in terms of the equation 2.28 (Sengul, 2014);

$$\rho = R\frac{A}{L} \tag{2.28}$$

where ρ is electrical resistivity, R is electrical resistance, A is surface area of the electrode and L is distance between the two electrodes. R is measured by applying a specific voltage (V) and measured the resulting current (I) passing through the specimen, then the electrical resistance is obtained according to the Ohm's law as below:

$$R = \frac{V}{I} \tag{2.29}$$

2.4.2 Factors Influencing Electrical Resistivity

The electrical resistivity of concrete is related to the microstructure of the cement matrix, its pore structure, porosity, and pore size distribution. It is also a function of the concentration of ions and their mobility in the pore solution. Therefore, several factors may affect electrical resistivity of concrete, and they can be related to concrete materials and mixture proportions, such as cement type, pozzolanic admixtures, w/c ratio, and pore structure, as well as, environmental factors are affecting the resistivity measurements including moisture content of concrete (i.e. relative humidity) and temperature (Chen et al., 2014; Hunkeler, 1996; Sengul, 2014; Whiting and Nagi, 2003). However, considering all these influencing parameters for on-site resistivity measurements and to make meaningful conclusions is not a simple task (Azarsa and Gupta, 2017). This section will focus on those that have a considerable impact on the electrical resistivity.

Generally, water to cement (w/c) ratio is one of the main controlling factors that strongly influences the performance of the concrete (Van Noort et al., 2016). Not only that it has a significant effect on strength and durability of the concrete, but also that plays an important role in the microstructure of the cement paste as well as the ionic concentration of the pore solution. In general, higher w/c ratio results in a high percentage of porosity and coarser pore structure of the concrete which leads to a lower electrical resistivity value indicating a more permeable concrete (Azarsa and Gupta, 2017; Banea, 2015; Van Noort et al., 2016).

A study made by Monfore (1968) on the electrical resistivity of cement paste showed that an increase in w/c from 0.40 to 0.60 led to a 50% decrease in resistivity. Hughes et al. (1985) examined the effect of w/c ratio on the electrical resistivity of concrete that contains a cement of 400 kg/m^3 and observed a reduction by almost 50% when w/c ratio increased from 0.4 to 0.55. Su et al. (2002) also found similar trend for the saturated specimens, the resistivity

decreases with an increase of w/c ratio. But when w/c ratio is over 0.55 the difference in resistivity is small. However, Gjørv et al. (1977) observed that the influence of w/c ratio on concrete resistivity varies as the degree of saturation changes. The effect of w/c ratio is less significant in highly saturated concrete as compared to dry concrete as shown in Figure 2.17. The decrease in resistivity from a w/c ratio of 0.45 to 0.70 is more pronounced when the degrees of saturations are 40% and 60%, as compared to 100%. Chen et al. (2014) observed that such measurements using four-point Wenner method are inappropriate on concrete specimens with low RH at oven dry or 40% RH as they were too dry to form conductive paths.

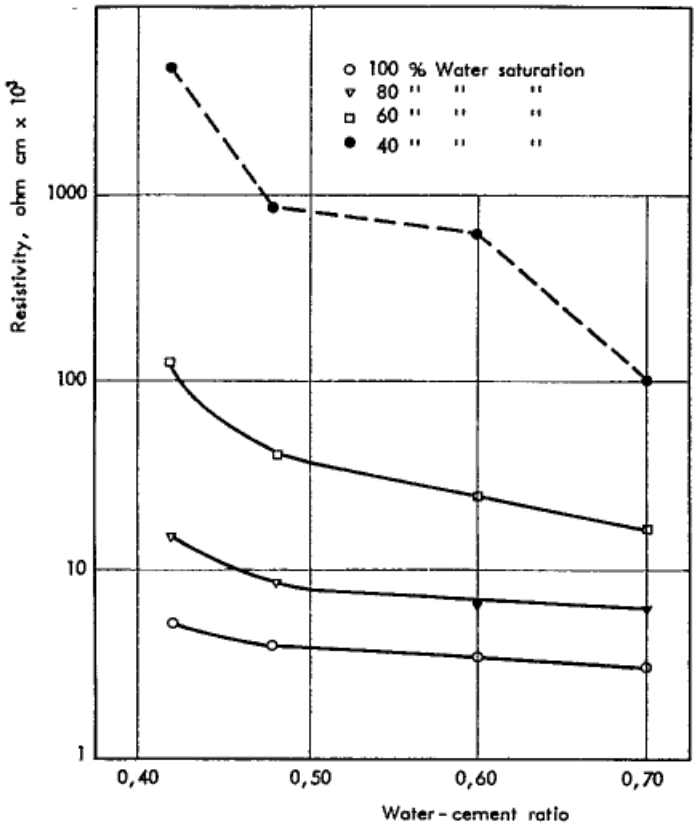

Figure 2.17: Effect of water saturation and w/c on concrete resistivity (Gjørv et al., 1977)

Additionally, concrete containing supplementary cementitious materials such as slag showed an irregular behaviour with the w/c ratio. For instance, an increase in w/c ratio from 0.35 to 0.65 caused an increase in electrical resistivity values, which means a less permeable concrete (Azarsa and Gupta, 2017). Such increased resistivities were attributed to the

densified microstructure by calcium–silicate–hydrate (C–S–H) gel and modified ion species and concentrations. The hydrating products of C–S–H gel fill the micropores, reducing the porosity and pore connectivity. The resistivity was thus increased (Chen et al., 2014).

Chloride concentration in concrete is another parameter that affecting electrical resistivity of concrete. Early study by Henry (1964) on the effect of sodium chloride content on concrete resistivity reported that the concrete with no sodium chloride has the highest electrical resistivity over the testing period. However, the differences in resistivity among four different concentrations ranging from 0 to 31.3 g/kg of the mixing water were not great. Hunkeler (1996) noticed that addition of 0.45% chloride by concrete weight reduced the resistivity by 27%. It should be noted that the influence of chlorides on concrete resistivity is related to cement composition and type of cementitious materials used in concrete. For example, C_3A hydration products have a tendency to bind with chlorides (Rosenberg et al., 1989; Whiting and Nagi, 2003). Therefore, the influence of a given amount of chlorides on electrical resistivity may be reduced when high C_3A cement is used. Using of corrosion inhibiting admixtures also may influence the chloride ion concentration in cement paste and its effect on electrical resistivity (Rosenberg et al., 1989; Whiting and Nagi, 2003).

Among all the influencing factors, the moisture content highly influences the resistivity of concrete (Chen et al., 2014). This is because the overwhelming proportion of electrical current passing through concrete is carried by the ions of pore liquid. As the moisture content of the concrete decreases, there is less pore fluid to carry the current and therefore the resistivity will increase and vice-versa. The effect of moisture content was studied by Gjørv et al. (1977) and the effect of saturation of concrete on resistivity made with different w/c ratios is illustrated in Figure 2.18. Concrete were dried from 100% to 40% saturation and the resistivity determined at intermediate points. At 100% saturation, resistivity ranged from approximately 3,000 to 6,000 Ohm·cm. While at 40% of saturation, resistivities ranged from 100 to 6,000 kohm·cm. For a given level of saturation, the water-cement ratio of the concrete also had an effect on resistivity. As w/c increased, the resistivity decreased. The effect was most pronounced at the lower levels of saturation. In the extreme case of oven-dried concrete, Hammond and Robson (1955) obtained an electrical resistivity of $4x10^4$ Mohm·cm. Sellevold et al. (1997) measured electrical resistivities of samples taken from a post-tensioned concrete highway bridge after 14 years of service. Samples were initially

water saturated, then dried to remove the appropriate amount of water to achieve the desired degree of saturation. Electrical resistivity was determined as a function of degree of capillary saturation, which ranged from 70% to 100%. Resistivity ranged from approximately 10 kohm·cm at 100% saturation to 50 kohm·cm at 70% saturation (Whiting and Nagi, 2003)

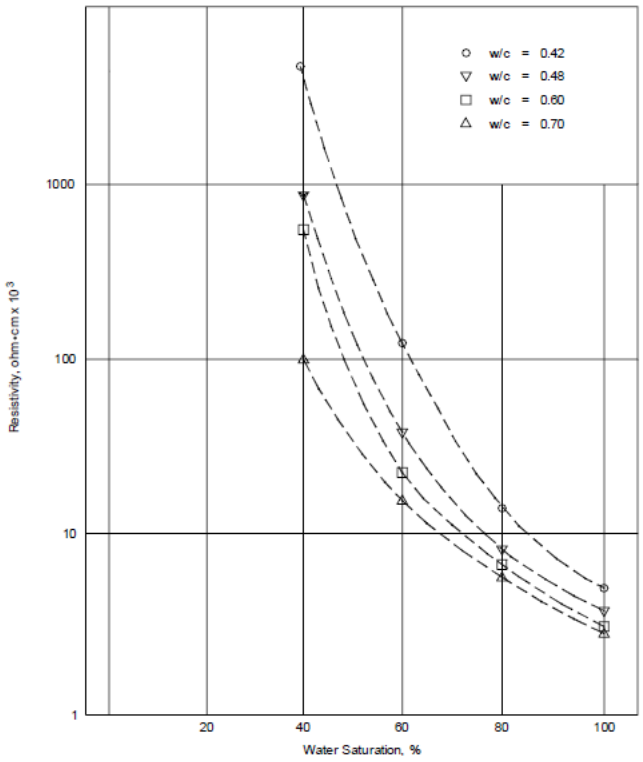

Figure 2.18: Effect of saturation on electrical resistivity of concrete (Gjørv et al., 1977)

Su et al. (2002) also investigated the effect of moisture content on concrete resistivity, by measuring the resistivity using the Wenner technique for air-dried specimens and oven-dried specimens under various w/c ratios (w/c= 0.45, 0.55, and 0.65). The results showed that the resistivity increases as the water loss ratio increases. Under air-dry conditions, the concrete resistivity is 5% ~ 10% higher than that of the saturated concrete. In the second stage, when the entrapped void water is removed, the resistivity abruptly increases.

2.4.3 Concrete Resistivity and Corrosion Rate

Electrical resistivity of concrete is considered as one of the most important parameters that can help to assess corrosion of steel in concrete (Hornbostel et al., 2013). It is fundamentally related to the permeability of fluids and diffusivity of ions through porous materials such as

concrete. Therefore, electrical resistivity can be used as an indirect measure of the ability of concrete to prevent penetration of chloride salt solutions that may cause corrosion of the reinforcing steel (Whiting and Nagi, 2003).

Browner (1982) previously studied the relationship between corrosion rate and electrical resistivity of offshore concrete structures and demonstrated that a concrete resistivity must fall below the range of 5,000 to 10,000 Ohm.cm for the reinforcement corrosion to occur. Hope et al. (1985) showed that reinforcement embedded in concrete with a resistivity higher than 10,000 Ohm.cm is not likely to develop corrosion at a significant rate. Whereas Gonzalez et al. (2004) proposed that the corrosion rate is low when concrete resistivity is higher than 100,000 Ohm.cm and high corrosion rate when resistivity is lower than 20,000 Ohm.cm. Cavalier and Vassie (1981) investigated corrosion damage in a highway bridge and concluded that the probability of corrosion is almost certain when the resistivity is below 5,000 Ohm.cm, it is usually not significant when the resistivity is above 12,000 Ohm.cm and corrosion is probable in the resistivity between 5,000-12,000 Ohm.cm. Tremper et al. (1958) investigated a structure in a marine environment and suggested a value of 60,000 Ohm.cm to prevent accelerated corrosion. However, the accepted critical values are presented in table 2.6 in which it is considered that the risk of corrosion is negligible when resistivity exceed a value of 20,000 Ohm.cm.

Table 2.6: Empirical relationship between concrete resistivity and corrosion rate of embedded steel reinforcement (Gonzalez et al., 2004; Langford and Broomfield, 1987)

Resistivity, ohm-cm	Corrosion rate
< 5,000	Very high
5,000 – 10,000	High
10,000 – 20,000	Moderate to low
>20,000	Low

It is widely accepted that the corrosion rate decreases with increasing concrete resistivity. However, considerable and not fully clarified deviations are found between studies published in the literature (Hornbostel et al., 2013).

2.5 Corrosion Protection and Prevention Methods

The deterioration of reinforced concrete structures caused by steel corrosion is one of the major durability problems (Ahmad, 2003; Orellan et al., 2004). A large number of reinforced concrete structures around the world are deteriorated to varying extents. The size of corrosion problem is horrific. An example of the magnitude of the problem can be seen in the fact that almost half of the greater that 500,000 bridges in the US interstate network are in need of some type of repair due to their damaged state or defective structures. It was estimated that the cost of repair is much higher than that of new construction. It has been reported that rehabilitation costs would amount to about 20 billion dollars, a figure that increases by $500 million every year (Bastidas et al., 2008). The size of the deterioration leads to the need for preventive measures and costly repairs to protect reinforcing steel from corrosion in order to extend the durability and increase the service life of reinforced concrete structures (Bastidas et al., 2008; Verma et al., 2014).

Different chemical, mechanical and electrochemical methods are adopted to protect or prevent concrete structures from corrosion (Popoola et al., 2014; Verma et al., 2014). In some cases, corrosion rate is retarded by careful selection of material and the design of system. In most cases, corrosion can be reduced by the improvement of the concrete properties and environment surrounding the steel, protective systems in the form of coating, using corrosion inhibitors and adopting electrochemical methods such as cathodic protection. The following subsections present more details of some techniques currently used for corrosion protection. They are applied either alone or in combination but each is suitable or feasible in certain physical, economic or operational circumstances.

2.5.1 Patch Repair

This approach is widely used for stopping and subsequently controlling corrosion in reinforced concrete structures by means of replacement of nonprotective concrete with a suitable cementitious material (Dugarte and Sag, 2009; Qian et al., 2006; Tilly and Jacobs, 2007). It is usually undertaken after careful assessment of the condition of the structure and consideration of cost. The repair work involves removal of weak, cracked or damaged concrete of the structure for specific depths, clean back to bars, clean the bars and further strengthen it with extra steel if needed and application of a suitable repair material to provide an adequate cover to the reinforcement.(Chynoweth et al., 1996). In order to prevent further

contamination, the new surface is often coated with a surface coating. Each of these steps must be carried out properly in order to guarantee the effectiveness of the whole repair work (Bertolini et al., 2013).

Protection provided by patch repair can only be guaranteed if the damage is local and all of the affected concrete in contact with the rebars is removed. On the other hand, it is in general desirable to limit concrete removal as much as possible since it is a slow, costly, noisy, and dusty operation (Bertolini et al., 2013), additionally, Cutting out concrete behind the rebar can be a risky operation and a patched structure may have lost considerable load bearing capacity (Broomfield, 2007). In this case, structural support for live and dead loads is required and this will make such repairs completely uneconomic.

Although ordinary Portland cement mortars (or concretes) can be used as materials for conventional repair, different types of additions or admixtures such as microsilica, polymers, water reducing agents, etc. may improve their performance (Mailvaganam and Rixom, 2002; Neville, 1995). The requirements of such repair materials are available in BSEN1504 parts 1-10 (Broomfield, 2007)

However, patch repairing is not usually adequate to stop further deterioration in the presence of chloride attack. If a structure with extensive chloride attack is to be patch repaired then it must be recognized that patching the corroding areas can accelerate corrosion of the surrounding areas (Broomfield, 2007). This is because that the new surrounding anodic zones sacrificially protects the areas which previously protected from corrosion. Once fresh non-contaminated material replaces the contaminated area, this protection is removed and the surrounding areas become the new anodes. This often occurs around the new patch as shown schematically in Figure 2.19. The issue is more prevalent in chloride contaminated structures so corrosion will continue around the patches. However, it can be avoided by applying an electrochemical rehabilitation technique if it is difficult to remove chlorides from all parts of the structure effectively (Broomfield, 2007).

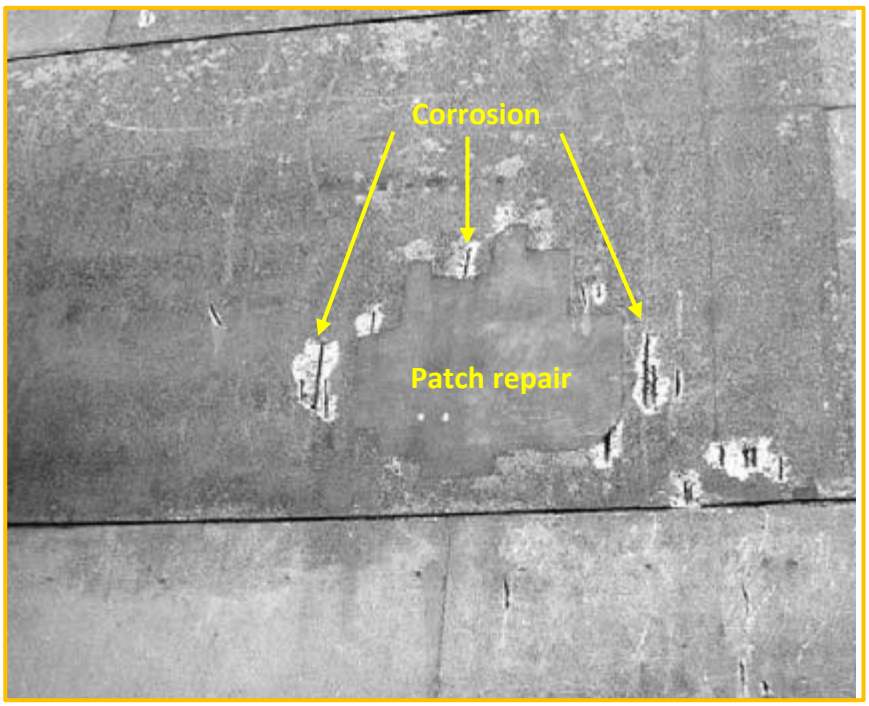

Figure 2.19: Patch repair with surrounding spalling due to incipient anodes on a building (Broomfield, 2007)

2.5.2 Surface Treatment of Concrete

Surface treatment of concrete is usually used as a preventative measure or in combination with patch repair to achieve the required service life of the repair (Byrne et al., 2016). A specific type of treatment, such as coatings, may be used as a physical barriers to delay penetration of carbonation or chlorides or to decrease the moisture content either in the original concrete or in the repair mortar. The effect of this treatment can be taken into consideration in the evaluation of the residual service life of the structure both in the repaired and unrepaired zones. This can lead to a reduction in the extent of the areas to be repaired or in the thickness of the repair material (Bertolini et al., 2013).

2.5.3 Coating of Rebars

Proprietary products are often applied on the surface of the rebars, to promote adhesion to the repair mortar and to improve the corrosion resistance, often inhibiting properties are also claimed and these are called anticorrosion coating (Bertolini et al., 2013; COST Action 521, 2003). The use of surface coatings on the reinforcement should be carefully evaluated. As far as corrosion of steel reinforcement is concerned they should not be recommended, since

the repair mortar is the material intended to protect the reinforcement. Only if it is impossible to provide adequate thickness of repair material cover, so it is locally not possible to provide the required long term protection, may a coating that acts as a physical barrier be useful (Bertolini et al., 2013; COST Action 521, 2003).

2.5.4 Corrosion Inhibitors

Corrosion inhibitors for steel in concrete are of great interest to the concrete repair community. Corrosion inhibitors are defined as a chemical substance that when present in the corrosion system at a suitable concentration decreases the corrosion rate, without significantly changing the concentration of any corrosive agent (BS EN ISO 8044, 2015). This definition excludes other corrosion protection methods such as coatings, pore blockers and other materials, which change the water, oxygen and chloride concentrations. However, some inhibitors also behave as pore blockers, which is a secondary property (Söylev and Richardson, 2008).

Inhibitors can be divided in two groups according to their application methods (Bolzoni et al., 2006; Broomfield, 2007). They are either admixed corrosion inhibitors (ACI) that added directly to the fresh concrete mixture for new structures, or migrating corrosion inhibitors (MCI) that penetrate into the hardened concrete once applied on the concrete surface to react on the reinforcing steel surface to slow down the rate. Based on the mechanism of protection, they can be classified into three groups. The first group is anodic inhibitors which passivate the metal by forming an insoluble protective film on anodic surfaces or by adsorption on the metal such as chromates, nitrites, molybdates, alkali phosphates, silicates, and carbonates. It should be noted that certain anodic inhibitors (e.g., nitrites) can cause accelerated corrosion and pitting attack if used in insufficient concentrations. The second group is cathodic inhibitors such as zinc and the salts of antimony, magnesium, manganese, and nickel. These inhibitors are generally less effective but safer than anodic inhibitors, and function by forming an insoluble or adsorbed film on cathodic surfaces of a metal. And, the last group is mixed inhibitors that use to block both anodic and cathodic reactions by adsorption on the entire surface of the metal. This type of inhibitor includes amines, esters, and sulfonates (Poursaee, 2016; Söylev and Richardson, 2008; Virmani and Clemena, 1998).

Admixed corrosion inhibitors have been studied since the 1950s and they have been commercially available since the 1970s. Calcium nitrite is one of the most inhibitors widely used and is considered to be the most effective inhibitor. A dosage rate of 10–30 litres per cubic metre of concrete is generally specified, depending on the expected maximum chloride level at the rebar (Bertolini et al., 2013; Broomfield, 2007). In fact, to prevent corrosion initiation, a critical concentration ratio of nitrite/ chloride is required (Virmani and Clemena, 1998). The nitrite acts as anodic inhibitors due to its oxidising properties and stabilizes the passive film by oxidising ferrous ions to ferric oxide (Fe_2O_3) (Söylev and Richardson, 2008).

Sodium monofluorophosphate (MFP) that is added to the mix or applied to the surface of concrete is also widely used, but the protection mechanism of MFP is not clear. It may be anodic, cathodic or mixed (Chaussadent et al., 2006; Bernhard Elsener, 2001; Ngala et al., 2003; Söylev and Richardson, 2008).

Inhibitors when compared to the other corrosion protection methods have some advantages such as versatility and cost. Their use in concrete can help to delay the initiation of corrosion of the embedded steel exposed to chloride attack and carbonation (Söylev and Richardson, 2008). However, there are some concerns and uncertainties relating to the effectiveness of corrosion inhibition. Both negative and positive side effects were found in the literature (Söylev and Richardson, 2008). Also, it has not been established whether inhibitors can readily stop or significantly reduce the rate of corrosion and they may only provide additional protection against initial corrosion. They are therefore only adequate in a small number of circumstances (Byrne et al., 2016).

2.5.5 Electrochemical Chloride Extraction (ECE)

This technique has been developed to remove chloride ions from contaminated concrete to overcome the problem of chloride-induced corrosion. It can be applied to structures in which corrosion has not or has already initiated. It aims to modify the environment of the concrete surrounding the steel reinforcement to make it less corrosive by altering the composition of concrete that contains chlorides (Bertolini et al., 2013). The application of the electrochemical chloride extraction treatment along with its associated electrochemical reactions is shown schematically in Figure 2.20. ECE is similar to cathodic protection, but it is only applied for a few weeks (Liu and Shi, 2009b) or few months (Luca Bertolini et al.,

2013) and involves the application of a large direct current density reaches to 1000–2000 mA/m^2 between a temporary anode placed on the external surface of the structure and the reinforcement. Under the action of the electrical field, the negatively charged chloride ions repel from the steel surface and move towards the external anode where they are collected.

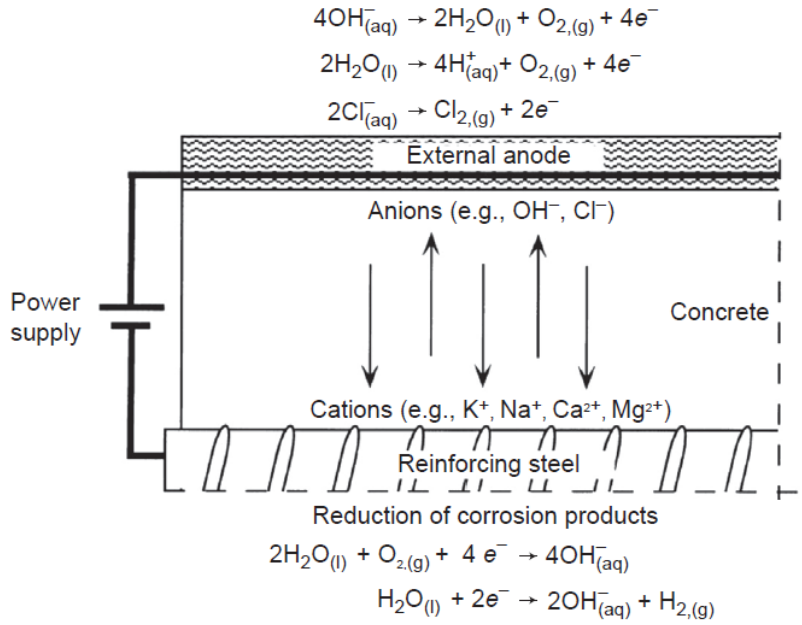

Figure 2.20: Principle of electrochemical chloride extraction (Marcotte et al., 1999)

ECE was first studied in the USA in the 1970s (Bertolini et al., 2013) and, as yet there is no standard for electrochemical chloride extraction, but a technical specification was published in 2011 (DD CEN/TS 14038-2). This technique has been used successfully in many countries of the world with applications varying from quays, office buildings, road bridges, car parks, housing and industrial plants (MILLER, 1994).

Orellan et al. (2004) investigated the efficiency and side effects of ECE, and their experimental results showed that about 40% of the total chloride was removed near the steel within 7 weeks. However, the electrochemical chloride extraction also could lead to some problems after the treatment. For example, it may be possible that the ECE accumulates locally high amounts of alkali ions that stimulate the alkali–silica reaction even though the concrete contained nominally inert siliceous aggregates. Additionally, in laboratory tests on steel in mortar, it has also been shown that the applied current during ECE can significantly

alter the composition and morphology of the mortar at the steel/mortar interface, and decline the bond strength between the concrete and steel (Marcotte et al., 1999)

2.5.6 Electrochemical Realkalization (ER)

This system is used for reinstalling the passivation of steel in carbonated structures and to stop carbonation-induced damage (González et al., 2011; Redaelli and Bertolini, 2011). ER was introduced by Noteby in the late 1980s (Luca Bertolini et al., 2013; Redaelli and Bertolini, 2011). A state of the art document on realkalization (and chloride extraction) was published by the European Federation of Corrosion (Mietz, 1998) and technical information was provided from two European COST Actions (COST Action 509, 1997; COST Action 521, 2003). A technical specification was published in 2004 before an European standard is published in 2016 (BS EN 14038-1).

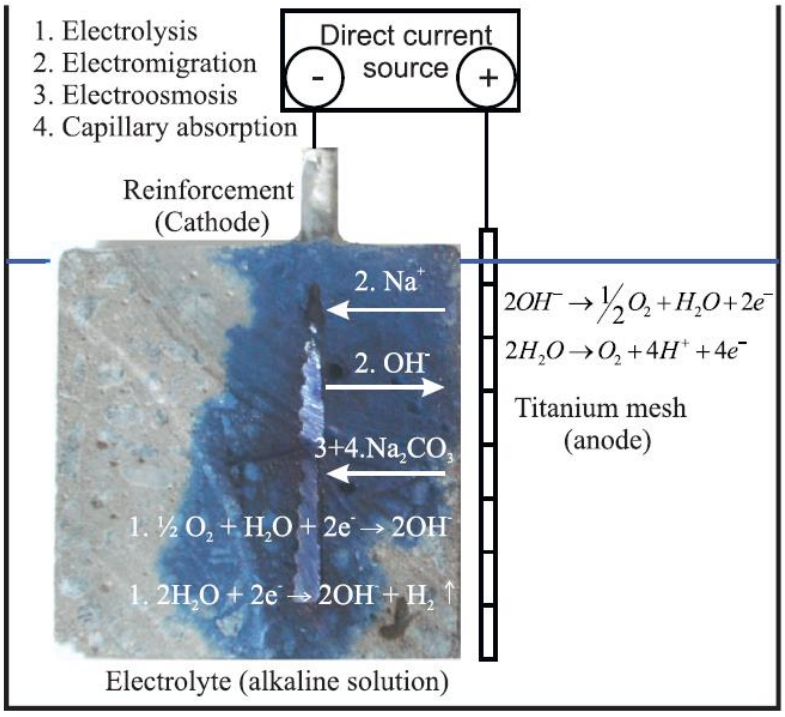

Figure 2.21: Illustration for the electrochemical realkalization method (Ribeiro et al., 2013)

The principles of the electrochemical realkalisation are shown in Figure 2.21. It is similar to ECE. The technique drives a current through the concrete to the reinforcement by means of

an externally applied anode attached to the concrete surface. Sodium carbonate is generally used as electrolyte covering the concrete surface (Yeih and Chang, 2005). During the operation, hydroxyl ions are produced at the rebar surface re-alkalise the concrete from the reinforcement outwards the concrete surface and, at the same time, the electrolyte at the concrete surface moves under electro-osmotic pressure and re-alkalises the concrete from the surface towards the reinforcement (Bertolini et al., 2008; Redaelli and Bertolini, 2011; Yeih and Chang, 2005).

Several laboratory experimental works suggested that the application of a current of 1000–2000 mA/m^2 for few weeks can induce the complete realkalisation of concrete covers of 20–30 mm (Redaelli and Bertolini, 2011). However, despite of these suggestions, the choice of current density and polarization time is still difficult (Yeih and Chang, 2005).

Electrochemical realkalisation has been introduced at the end of the 1980s and a significant number of structures have been treated with this technique (Ribeiro et al., 2013). Some documents report these experiences (Bertolini et al., 2008) and show the ability of the technique in recovering protective pH levels. These studies also show that, even after some years, the alkalinity remains at high levels, which would be enough to protect the reinforcement (Ribeiro et al., 2013). On the other hand, the effectiveness of the treatment in repassivating the reinforcement has been questioned (Bastidas et al., 2008; González et al., 2011; Miranda et al., 2006) and, although some work is being carried out on this specific topic (Redaelli and Bertolini, 2011), there is still not a consensus.

2.5.7 Cathodic Protection

Most of the non-electrochemical repair techniques are not very effective in reducing the corrosion rate, since they may arrest the problem with little or no success (Hong et al., 1993).

Cathodic protection is an electrochemical technique that has increasingly been used for the repair and maintenance of corrosion damaged reinforced concrete structures around the world (Martínez and Andrade, 2008; Parthiban et al., 2008; Wilson et al., 2013). Federal Highway Administration, USA has stated that CP is the most effective repair technique and it is the only way to stop the corrosion of steel embedded in concrete (Barnhart, 1982).

To illustrate the principle of CP, consider the system in Figure 2.22 which shows the potential of the metal (E) against the logarithm of the anodic and cathodic reaction rates expressed as current densities Log (I). As explained before, the corrosion current, Icorr, and the corrosion potential, Ecorr, occur at the point of intersection of the anodic and cathodic curves where anodic and cathodic reactions rates are equal, i.e. the rate of electron release equals the rate of electron consumption and there is no net current flow although metal is consumed at a rate equivalent to Icorr.

In CP an external current is applied to the corroding metal by an auxiliary in which electrons are supplied to the metal surface and so that the potential of the metal is lowered. For example, to E^{-}. At E^{-}, the corrosion rate will have been reduced from Icorr to Ia- and thus the metal will be partially protected. $|I_c^-|$ - I_a^- is the amount of current that needs to be applied to provide the shortfall electrons. At Ea, the net anodic reaction rate is zero and the anodic dissolution will be stopped. As a result, the metal will be fully protected if $|I_c^=|$ is applied. Excessive negative potentials to provide further protection are insignificant as the metal is then said to be over-protected and problems related to hydrogen evolution at the metal surface can be developed (Ashworth, 2010).

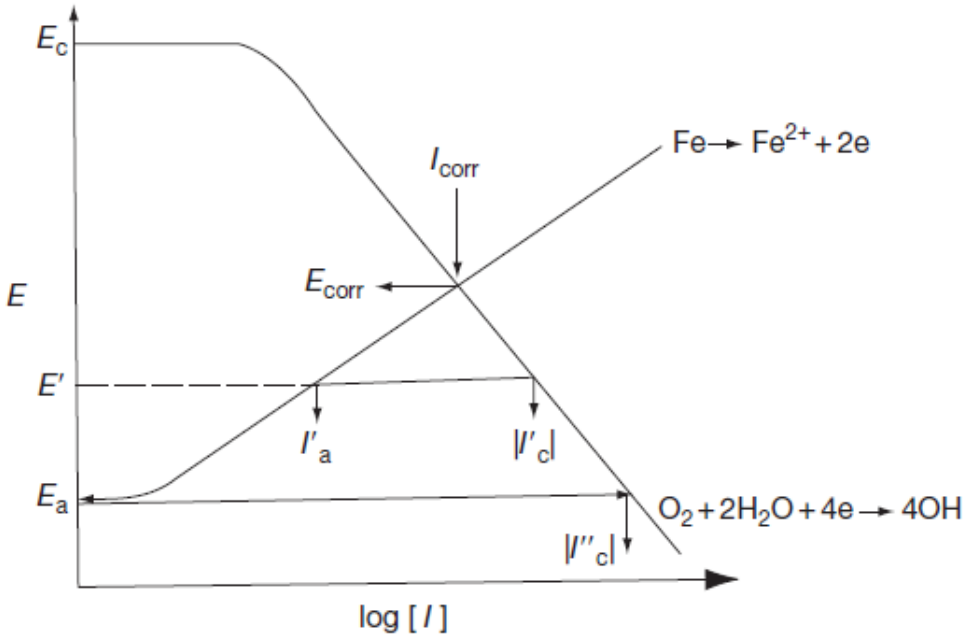

Figure 2.22: Principle of cathodic protection illustrated on a potential-current diagram (Ashworth, 2010)

2.6 Cathodic Protection of Steel in Concrete

Theoretically, the amount of required current to achieve cathodic protection must be enough to lower the potential of the reinforcing steel towards the immunity zone, the region where the potential become below the equilibrium potential (E_{eq}) given by Nernst law and electrochemical attach cannot occur, so that all the reinforcement become cathodic and corrosion will be stopped (Pedeferri, 1996).

However, To achieve cathodic protection of steel reinforcement embedded in chloride contaminated concrete it is not necessary to establish immunity conditions, that is, lowering the potential below the equilibrium potential Eeq given by Nernst's law. These immunity conditions are normally required on steel in active condition as on steel structures in soil or immersed in seawater, where potentials more negative than −850 mV CSE should be imposed. Conversely, the target of cathodic protection in concrete structures is to reduce the corrosion rate by taking the steel into the passivity range or by reducing the macrocell activity on its surface, and this can be done with a small reduction in potential and a small current (Bertolini et al., 2013).

For new reinforced concrete structures in which steel is passive and corrosion has not initiated yet, the application of CP technique is called 'cathodic prevention' where expected corrosion initiation is prevented during the service life, whereas for existing structures which are already corroding, the application of CP is termed 'cathodic protection' where further corrosion of steel is stopped.

The behaviour of reinforcing steel of different potentials and in the environment of varied chloride contents, where pitting can initiate, propagate or protected against, has been presented by Pedeferri (1996), as shown in Figure 2.23. Based on the Figure, to achieve the aim of CP, the potential of the steel shall be kept either at the perfect passive zone, zone C, where corrosion does not initiate or propagate or at the zone B, imperfect passivity zone, where pitting does not initiate but can propagate for pre-existing pits.

The initial condition is represented by location 1 where the chloride content is nil and the steel is passive. Location 2 represents the potential after the application of cathodic prevention. It is more than 200 mV of polarization. If this level of polarization in maintained,

pitting initiation will be prevented even when relatively high chlorides ingress into the concrete and reach the reinforcement as in location 3. If there is no protection and with the increase of chloride content, the location 1 leads to 4 in the corrosion zone where pitting can initiate and propagate. Using the cathodic protection, this is shifted to 5 in the passivity zone (C), where pitting cannot further propagate nor initiate, or to 6 into the imperfect passivity zone (B) without fully restoring passivity so that existing corrosion sites will continue to corrode at a reduced rate but new sites of pitting can 4 not initiate. In all cases the corrosion rate is reduced. In summary, (1→2→3) represents a typical evolution path for cathodic prevention, (4→5) represents cathodic protection where the steel is fully protected and (4→6) represents cathodic protection to reduce corrosion rate.

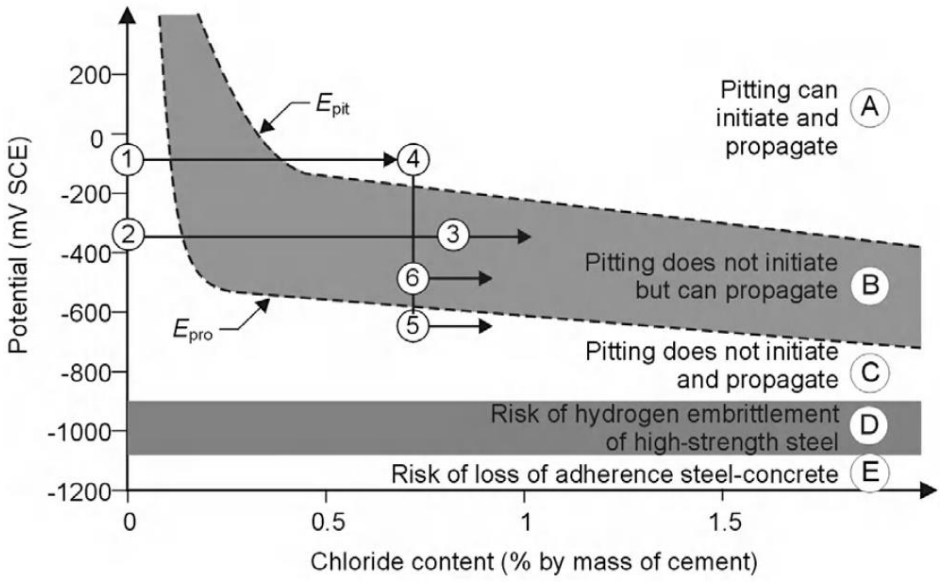

Figure 2.23: Schematic illustration of steel behaviour in concrete for different potential and chloride contents, (Bertolini et al., 2013)

2.6.1 Methods of Applying Cathodic Protection

Cathodic protection can be applied by either the impressed current technique or by the use of sacrificial anodes.

2.6.1.1 Impressed Current Method

In this method, a small amount of direct electric current from a permanent anode, as auxiliary electrode usually applied on the concrete surface and connected to the positive terminal of

DC power source, is impressed through the concrete to the reinforcement which is electrically connected to the negative terminal of a power source, as illustrated in Figure 2.24. In CP, the steel to be protected is forced to become cathodic and prevented from corrosion (Gower and Windsor, 2000; Pedeferri, 1996). Oxygen and moisture availability in the concrete is essential for the CP system to work.

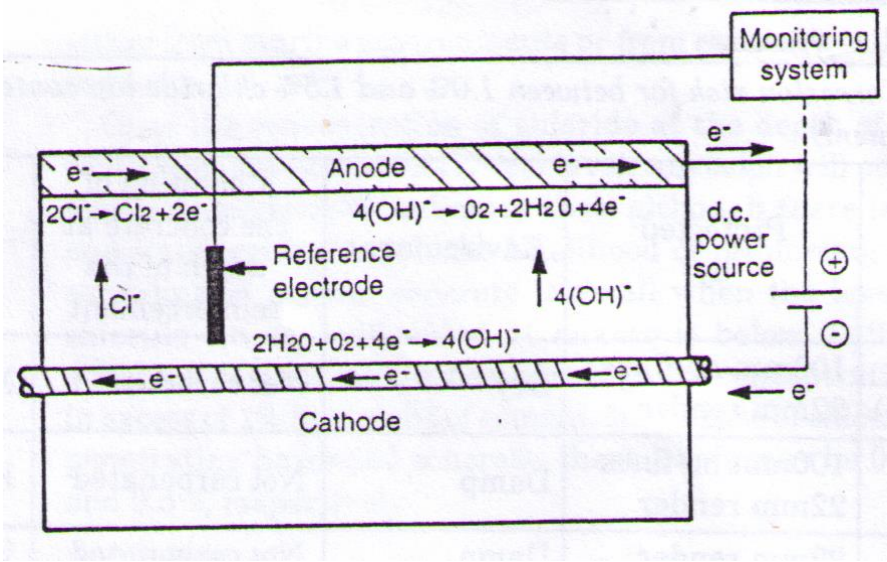

Figure 2.24: Schematic illustration of impressed current cathodic protection system (Gower and Windsor, 2000)

Due to the electrochemical process at the cathode (the steel), hydroxyl ions are produced as in equation 2.30, alkali ions (sodium, potassium) are attracted and chloride ions are repelled.

$$\frac{1}{2}O_2 + H_2O + 2e^- \rightarrow 2(OH)^- \quad (2.30)$$

The generation of hydroxyl ions will increase the alkalinity and help to rebuild the passive layer where it has been broken down by chlorides. At the anode, negatively charged ions such as hydroxide and chlorides are consumed.

However, when the potential becomes too negative, the following cathodic reaction can occur at the surface of the steel and lead to hydrogen gas evolution. This hydrogen evolution can cause hydrogen embrittlement of the steel reinforcement.

$$H_2O + e^- \rightarrow H + OH^- \quad (2.31)$$

Hydrogen atoms generated can diffuse into the steel and develop defects in the crystalline matrix of the steel (Broomfield, 2007), thereby leading to weak the steel, reduction in ductility of rebar and cause failure even in the absence of external load (Shi et al., 2011). This problem is known as hydrogen embrittlement. However, the problems of hydrogen evolution and embrittlement are usually controlled by controlling the potential of the steel to be below the hydrogen evolution limit.

The essential components of an impressed current cathodic protection system are an external DC source, an electrode (anode), wiring and monitoring system (reference electrode and voltmeter) to monitor the potential of steel, in addition to the reinforcement to be protected and concrete surrounding the steel (Gower and Windsor, 2000; Polder et al., 2014). The service life of the anode is very important and must be taken into account to provide the required current, resist deterioration and achieve protection to the reinforcement (Kepler et al., 2000; Pedeferri, 1996). Titanium mesh sheet coated with noble metal oxides (iridium, ruthenium, cobalt, etc.) is the most common type of anode (Pedeferri, 1996). The anode is normally pinned to the prepared concrete surface and a suitable cementations overlay is applied as shown in Figure 2.25. However, other materials offering ease of installation and cost efficiency have also been employed (Zhu et al., 2014). In recent years, due to its good chemical stability, carbon fibre has been successfully used as anode material in CP implementation for concrete structures (Lambert et al., 2015; Van Nguyen et al., 2012; Zhu et al., 2014).

Figure 2.25: A. Fixation of titanium mesh on the concrete surface with plastic fasteners, B. Applying of mortar overlay by projection after securing the anode (Araujo et al., 2013)

As with the electrochemical treatments, CP can cause certain problems if it is uncontrolled or appropriate preventive measures are not taken. It may lead to an accumulation of alkali ions in the region of the steel reinforcement. It is therefore possible that increase alkalinity in concrete containing potentially reactive aggregates may be sufficient to aggravate or initiate alkali-silica reaction if the applied current densities are much higher than those typically used in practice (Sergi et al., 1991). However, this may occur with electrochemical chloride removal or electrochemical realkalization, but not cathodic protection (Bertolini et al., 2013). In addition, it has been suggested that the current density at the anode should be kept less than 100 mA/m^2 to prevent the formation of chlorine gas /or acid at the anode

which can consume the anode and lead to deterioration of concrete around it (Bertolini et al., 1996). Moreover, Chang et al. (1999) have shown that bond-strength decreases with higher current density and polarization time. The reduction in bond-strength is attributed to the softening effects of concrete caused by the formation of soluble silicates near the steel resulting from the interaction of alkali hydroxides formed by cations (such as K+ and Na+) with calcium silicate hydrate in cement (Ali and Alsulaimani, 1993). However, these influences become considerable only in the long-run if the potential falls below -1100 mV vs SCE (Bertolini et al., 2013). In general, three factors must be taken into account when controlling CP system. Firstly, there must be sufficient current to overwhelm the anodic reactions and stop or severely reduce the corrosion rate. Secondly, the current must stay as low as possible to minimise the acidification around the anode and the attack of the anode for those that are consumed by the anodic reactions. Lastly, the steel should not exceed the hydrogen evolution potential, especially for pre-stressed steel to avoid hydrogen embrittlement (Chess and Broomfield, 2013).

2.6.1.2 Sacrificial Anode System

Using the impressed current technique, the driving voltage for the protective current comes from a DC power source. While, in the sacrificial anodic system, external power is not required to supply the current to stop corrosion, but instead the protected metal is made to be the cathode by connecting it to a more active metal, having a lower potential than the protected one. For instance, zinc with potential of -1100 mV versus (CSE) can be electrically connected to corroding steel with potential of -400 mV versus CSE (Torres-Acosta et al., 2004). Because of their relative position in the electrochemical series of metals, a potential difference exists between them which cause a small electrical current to flow from the zinc through the concrete to the reinforcing steel, as explained in Figure 2.26, forcing a cathodic reaction to occur at the steel surface and creating hydroxyl ions that increases the pH, and its charge encourages the migration of chloride ions away from the reinforcement (Polder, 1998). The zinc will corrode during the process while the reinforcing steel will be protected from corrosion. In this method, the sacrificial anode must be spontaneously anodic to the structure, that is, be more negative in the galvanic series for the given environment, while the impressed current anode may be more noble or more base than the protected structure because the power source forces it to act as an anode (Ashworth, 2010).

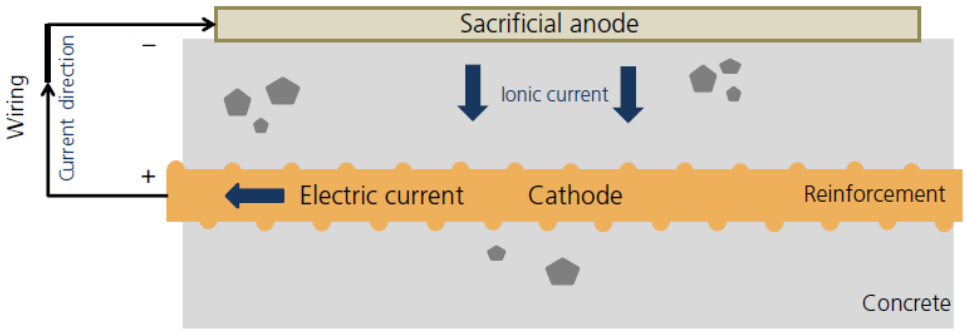

Figure 2.26: Schematic illustration of sacrificial anode system for reinforced concrete, Byrne et al., 2016

Thus, zinc, aluminium and magnesium or aluminum-zinc-indium (Al-Zn-In) are typical anode materials used to protect the steel (Byrne et al., 2016; Daily, 1999; Kepler et al., 2000). Zinc and its alloys is the most common anode used in galvanic anode cathodic protection systems for concrete structures. Aluminium and magnesium and their alloys are also used but less attractive for concrete applications as their oxides and corrosion products can attack the concrete.

The main restriction of this method is that the driving voltage is low. It is only a few hundred millivolts, and gets smaller with actively corroding steel and may be inadequate to provide full cathodic protection in very high chloride conditions (Broomfield, 2000, 2007). Furthrmore, applying this techniqe in concrete requires a continuous humidity condition in order to keep the electric current flowing between the anode and the cathode (Araujo et al., 2013). However, the low driving voltage may make it a safe option for protecting prestressed structures without the risk of hydrogen embrittlement.

This system is often used on oil platforms for both concrete and steel structures below water (Broomfield, 2000), but the level of protection and current provided cannot be controlled. Thus, changes in the structure that can cause an increase in protection current demand may necessitate the installation of further anodes (Byrne et al., 2016).

The anodes of this system can be installed in different ways. Figure 2.27 Shows the application of using thermal sprayed aluminium/zinc/indium for atmospherically exposed

reinforced concrete that has low concrete resistivity. While Figure 2.28 shows a galvanic zinc strip was applied for a building and can be also used for bridges.

Figure 2.27: A sacrificial coating of Al-Zn-In to a reinforced concrete bridge pier, (Daily, 1999).

Figure 2.28: Zinc sheet anode applied to a concrete balcony, prior to overpainting, (Broomfield, 2000)

2.6.2 Cathodic Protection Criteria

One of the most advantages using CP method to stop corrosion is that its effectiveness can be measured by a simple non-destructive measurement of the potential of the protected steel. Various criteria have been suggested to evaluate protection status against corrosion, and a combination of criteria may be used for a single structure. However, there are two acceptable criteria in CP performance appraisal. One relates to the instant-off potential (the absolute potential measured immediately when the CP system is switched off) of the reinforcement. The other one relates to the potential decay (depolarization) of the reinforcement (Chess and Broomfield, 2013; Cheung and Cao, 2013). The specifications in national and international standards for the criteria were principally established on the empirical evaluation of the data obtained from successfully operated CP cases (NACE SP0290, 2007). For example, Takewaka (1993) suggested that the corrosion of reinforced concrete structures can be stopped when the potential of rebar is set to be less than -600 mV with respect to Ag/AgCl/0.5KCl. More negative potentials in the range of -645 mV to -705 mV with respect to Ag/AgCl/0.5KCl have been also reported for chloride contaminated concrete (Shi et al., 2011). Several authors pointed out that a more negative potential is required for immunity from corrosion, a value of -900 mV CSE is reported to be adequate (Robinson, 1975). While, the British standard (BS EN ISO 12696, 2012) specifies that the instant-off potential should be more negative than -720 vs Ag/AgCl/0.5KCl for any structure under CP. However, achievement of this level of potential over an entire structure is only practical if the entire structure suffers from active corrosion prior to the application of cathodic protection. Application of this criterion to areas of a structure which are not previously corroding may be unrealistic and may lead to excessive current provisions and significant overprotection due to the severe variation of the corrosion environment in concrete (Broomfield, 2007).

A further requirement related to the instant-off potential for CP system operation is that to avoid hydrogen evolution at the steel surface, the potential should be kept at a low limit value of -1100 mV Ag/AgCl/0.5KCl for normal reinforcing steel and -900 mV with respect to Ag/AgCl/0.5KCl for high strength steel reinforcement which is used for pre-stressed structures (BS EN ISO 12696, 2012).

Another most widely adopted performance criteria based on potential decay is the 100 mV depolarization criterion. The field evaluation have shown that the 100 mV negative shift in

structures potential stops all further signs of corrosion damage in catholically protected structures. In order to ensure that the protection is achieved and overprotection is avoided, and more generally to determine the performance of the CP system, this potential should decay (become less negative) by at least 100 mV from the instant-off potential over a period between 4 and 24 hours after the CP system is switched off (BS EN ISO 12696, 2012; NACE SP0290, 2007; Page and Sergi, 2000). Depolarization tests are often performed over 4 hours, and the current to the system is adjusted until the polarization drops 100 mV in that period. Figure 2.29 describes the concept of depolarization or potential decay. The potential decay measurement should be determined by switching off the CP system and monitoring the potential of reinforcing steel measured relative to a reference electrode. When the current is switched off, an immediate voltage drop that is the result of eliminating the IR-drop occurs. The true fully polarized potential of steel, termed the instant-off potential, is then obtained. The instant-off potential must be measured within a very short time, typically between 0.1 and 1.0 second after interrupting the current. Then, the reinforcement is allowed to depolarize and the potential decay is measured after a period of time.

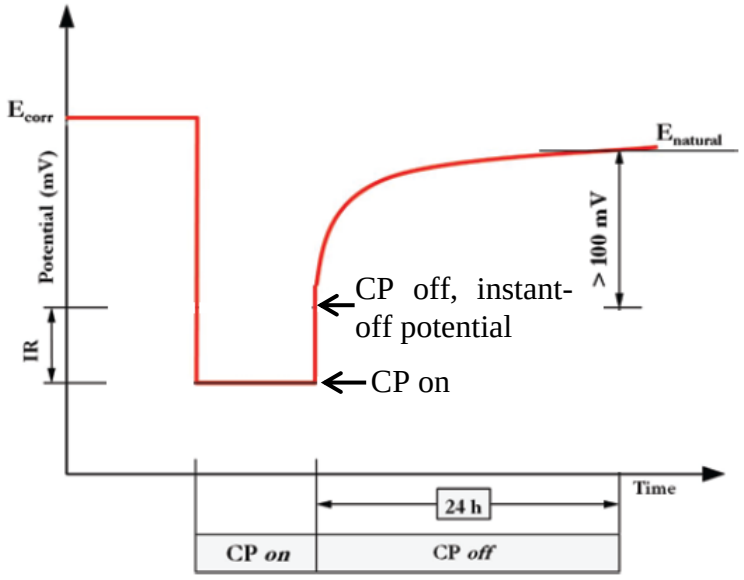

Figure 2.29: Potential decay curve, (Araujo et al., 2013)

2.6.3 Current Density for Cathodic Protection

The amount of CP current density or potential of the reinforcement steel are the important factors that need to be designed to provide protection for the corroded reinforcement and to

ensure that the anode has the ability to supply a current across the affected structure at a reasonable DC output voltage (Kepler et al., 2000). The aim of the protection will not be achieved if the delivered current density to the protected reinforcing steel is not enough. Unfortunately, little information was available until some recent efforts (Chess and Broomfield, 2013; Xu and Yao, 2009).

Adequate protection to the reinforcing steel in different conditions cannot be achieved by applying a fixed current density as stated in some early publications (Chess and Broomfield, 2013). Due to a number of factors affecting corrosion rates, there is no fixed value of either the potential or the current density to be applied under CP system. Each case must be designed separately (Kepler et al., 2000).

The current density required to maintain a metal surface cathodically protected must be not only high enough but also stay as low as possible to reduce the adverse effects at the cathode or on the anode. A previous work suggested that, for newly built concrete structures, a current density in the range of 1-2 mA/m^2 on the rebars is sufficient for protection, while for the structures that have already suffered from reinforcement corrosion, a current density in the range of 5-20 mA/m^2 is recommended (Bertolini et al., 2013). Higher practical CP current densities in the range of 30-50 mA/m^2 were also suggested when severe environmental condition exists around the reinforcing bars (Carmona et al., 2016; Chess and Broomfield, 2013). Due to the complexity of environmental conditions, the specifications in national and international standards are still open to discussion in engineering practices for their accurate suitability. Moreover, little amount of information was found to help for the protection design.

Some theoretical studies has been undertaken to describe the distribution of current in reinforced concrete CP system (Hassanein et al., 2002). However, they have been regarded insufficient because of the large variations, such as the resistivity of concrete and effect of orientation and density of reinforcing steel (Chess and Broomfield, 2013).

Pastore et al. (1991) studied the current distribution in concrete structures using uncontaminated and chloride contaminated concrete slabs. The results showed that the use of the anodes distributed all over the surface of the structure and multi-layer net anodes on

zones with high concentration of rebars helps in solving to reasonable extent the problem of non-uniform protection. However, current distribution can remarkably vary due to the resistivity of concrete, which relates to the anode to reinforcing bar distance, relative humidity, chloride content in concrete, etc.

Bertolini et al. (1993) used experimental test and modelling to study the current and potential distribution in uncontaminated and chloride contaminated concrete slabs using mixed metal oxide activated titanium mesh as anode. Considerable polarization was noticed in the study on the rebars of uncontaminated slabs, whereas the polarization was observed only on the bars close to the anode in the chloride contaminated slabs. In terms of current, the study demonstrates that the rebars closed to the anode got more than 90% of the total current both in absence and in presence of chlorides. They concluded that the penetration of cathodic protection over the depth of new concrete structures is greater than in already corroding ones. There is a wide range of potentials in which the cathodic protection of uncorroding structures can safely operate and its high throwing power permit rebars to be considerably polarized relatively far from the anode without overprotection those close to it.

Kranc et al. (1997) investigated the CP distribution in partially submerged reinforced concrete columns by a combination of sacrificial anodes, Zinc alloy, placed below water and Zinc mesh above water up half-length. Computational and experimental program were used in the study. The columns were partially submerged, to quarter of its length, in 5% NaCl solution. The measurements indicate that the greater polarization has been associated with both of submerged portion and the surrounded with surface anode of the column. The rebars in concrete area surrounded by the surface anode received most of the protective current, followed by the submerged zone and then the areas above the level of surface anode. The model predictions showed reasonable agreement with these results.

Hassanein et al. (2002) modelled the current distribution from a surface mounted anode to reinforcing steel in atmospherically exposed concrete using finite element method. The programme considers the effects of concrete resistivity, current density, geometry of an anode applied to the surface of concrete containing multiple layers of steel bars and vibration in the condition of bars. This research is only limited to the theoretical study.

Xu and Yao (2009) investigated by experimental investigation the current distribution in reinforced concrete CP system with and without chloride contaminated with a specific rebar arrangement, using carbon fibre reinforced cement (CFRC) composite material as the conductive overlay anode, activated titanium strip was embedded in the conductive mortar as primary anode. One mix was used in the investigation. The influences of initial corrosion state of steel, concrete resistivity and magnitude of impressed current density on the protection current distribution have been discussed. The uniformity of current worsens as the corrosion rate increases. The authors' concluded that the current distribution in reinforced concrete with more than one layer of reinforcement placed at different cover depths is markedly influenced by concrete resistivity and magnitude of impressed current density has little effect on the current distribution when the corrosion rate of steel is relatively low.

2.7 Summary

Steel reinforcement corrosion has been recognised as the major cause for the premature deterioration of reinforced concrete structures worldwide (Ahmad, 2003). Previous extensive researches on the deterioration mechanisms have concluded that chloride plays the most significant role in the corrosion of the reinforcement in concrete (Buenfeld et al., 1998; Kendell, 1995). Although, in recent decades, different technologies using chemical, mechanical and electrochemical methods have been developed to address the corrosion problem (Popoola et al., 2014; Verma et al., 2014), cathodic protection (CP) as an electrochemical method has been proved to be the most effective and widely applied to protect steel reinforcement in concrete from corrosion in aggressive environment. However, so far, quantitative specific information in national and international standards is still very limited, making the design and operation practice are primarily based on empirical assumptions and qualitative assessment.

This research has setup two tasks:

I. The CP performance appraisal is in general based on two criteria, they are the instant-off potential and potential decay. For example, the British standard (BS EN ISO 12696, 2012) specifies that the instant-off potential should be more negative than -720 vs Ag/AgCl/0.5KCl for any structure under CP. However, achievement of this level of

potential over an entire structure is only practical if the entire structure suffers from active corrosion prior to the application of cathodic protection. Application of this criterion to the reinforcement which are not yet in active corrosion states may unrealistically lead to excessive current giving and significant overprotection due to the severe variation of the corrosion environment in concrete (Broomfield, 2007).

Another popular assessment for CP performance is based on potential decay, given the 100 mV depolarization criterion, e.g., in order to ensure that the protection is achieved and overprotection is avoided, this potential should decay (become less negative) by at least 100 mV from the instant-off potential over a period between 4 and 24 hours after the CP system is switched off (BS EN ISO 12696, 2012; NACE SP0290, 2007; Page and Sergi, 2000).

The amount of CP current density or potential of the reinforcement steel are the two important conditions needed to be controlled to provide required protection for the corroded reinforcement. The aim of the protection will not be achieved if the delivered current density to the protected reinforcing steel is not enough. Unfortunately, little information was available until some recent efforts (Chess and Broomfield, 2013; Xu and Yao, 2009). It has been concluded that adequate CP cannot be achieved by applying a fixed current density throughout the life span of concrete structures. Previous researches have suggested that for new built concrete structures a current density in the range of 1-2 mA/m^2 on the total surface area of the protected rebars can be applied, while for structures already suffered from reinforcement corrosion a current density in the range of 5-20 mA/m^2 were recommended (Bertolini et al., 2013). However, these definitions are still felt a bit loose for applications.

In order to obtain further more detailed specific information for the CP design for chloride contaminated reinforced concrete structures, this study reports an experimental work on the effect of concrete chloride contamination degree on the corrosion evaluation parameters that are employed for reinforcement cathodic protection assessment. Specifically, the correlation between the chloride content and concrete resistivity with corrosion rate, and the effect of the applied CP current density on the parameters taken as the traditional CP criteria are investigated. It aims to identify more precise characteristic

relationships of the chloride content and concrete resistivity with the CP current and the instant-off potential requirements to provide sufficient protection. Ultimately, these experimental results can provide a direct guidance for the specification of the CP current density requirements for atmospherically exposed reinforced concrete structures at different levels of chloride contamination.

Using constant current for CP is the most popular approach in practice, particularly for the structures exposed to atmospheric conditions. However, for submerged structures, the situation of the reinforcement is quite different, for which, constant current approach is efficient to provide adequate protection is still not very clear. To have a deep understanding for the question, an experimental investigation has also been conducted for reinforced concrete specimens protected by impressed electrical current of both constant current density and constant potentiostatically controlled potential, respectively.

II. Concrete resistivity has been proved to be one of the most effective parameters that can be utilized to estimate and control the corrosion of reinforcing steel in concrete (Hornbostel et al., 2013), particularly when steel corrosion is caused by chloride attack (Morris et al., 2004).

The most commonly used technique for in situ site testing is the Wenner 4-probe technique (Layssi et al., 2015; Morris et al., 1996; Stanish et al., 1997). One of the drawbacks of this technique is that the conduction paths are not accurately known. More accurate resistivity values are obtained using external plate electrodes enabling the current to traverse the full area of the specimen (Bertolini et al., 2013; Newlands et al., 2008; Polder, 2001; Sengul, 2014; Spragg et al., 2011; Van Noort et al., 2016). Nevertheless, an accurate reading can be a difficult due to the contact between the electrode and the concrete, particularly when measurements are employed on unsaturated specimens (Villagrán Zaccardi and Di Maio, 2014). The most direct and reliable mode of contact is to embed electrodes into the fresh concrete. Then resistivity measurements can be performed on the concrete specimen at various moisture states without disrupting the moisture content of the specimen (Villagrán Zaccardi and Di Maio, 2014; Whiting and Nagi, 2003). Electrodes can be of various types. Brass is the most commonly used material, but steel is also used. They can be meshes or plates. In the case of embedded

electrodes, wires or thin rods normally are used. In these cases, however, the flow path may not be defined well enough to calculate a true resistivity (Whiting and Nagi, 2003).

Previous researches have suggested the use of both a low frequency, such as 60 Hz (Chacko et al., 2007), 107 Hz (Osterminski et al., 2012), 128 Hz (Newlands et al., 2008) and a high frequency, such as 1000 Hz (Whittington et al., 1981) and 7500 Hz (Banthia et al., 1992). Thus, it is hard to define a specific optimal frequency due to the variation of the conditions of concrete.

In this study, internal and external electrodes were compared in order to understand effect of the electrodes configuration. Carbon fibre (CF) sheets were employed as the internal electrodes and CF and copper sheets were used as external electrodes. Furthermore, frequency of applied current was varied from low to high, to identify the most suitable frequency that can be utilized for stable and reliable results. Optimised electrodes configuration and the current frequency were then used for all the series of the experimental tests in the present study.

CHAPTER THREE

RESEARCH METHODOLGY AND PROGRAMME

CHAPTER 3 RESEARCH METHODOLOGY AND PROGRAMME

3.1 Research Methodology

A series of electrical and electrochemical measurements on plain and reinforced concrete specimens were performed to achieve the purpose of the research work.

The present experimental work was carried out in two parts. The first part investigates the influence of the experimental methods on electrical resistivity measurement. It also studies some of major influencing factors on concrete electrical resistivity that haven't been fully investigated before. The second part reports an experimental study to investigate the effect of chloride content on cathodically protected reinforced concrete structures exposed to various exposure conditions and identify the most convenient criteria for the evaluation of CP performance under such environments.

The following sections outline the research programme and describe the details of the material, test specimens, experimental setup and measurements for both parts.

3.2 Materials

Locally produced Portland limestone cement was supplied by Travis Perkins Trading Co. Ltd, CEM II/A-LL conforming to the British standard BS EN 197-1: 2011 was used in this study. The chemical composition and some characteristics of the cement are given in Table 3.1. Concrete specimens were prepared following the method recommended by the British Building Research Establishment (BRE) (Teychenné et al., 1997) to give a minimum 28 days compressive strength of 35 N/mm^2 for the standard mix in this work (water to cement ratio of 0.4). The concrete mixture used had a cement content of 390 kg/m^3. Natural sand of the maximum size of 4.75 mm and a relative density of 2.47 was used for the fine aggregate at 580 kg/m^3. Crushed limestone of maximum size of 10 mm and a specific gravity of 2.49 was used at 1125 kg/m^3 as coarse aggregate. The mix quantities for the solid materials used were kept constant for all batches in the study.

Table 3.1: Chemical composition of the cement

Element	Percentage (%)	Element	Percentage (%)
SiO_2	16.19	SO_3	3.19
Al_2O_3	4.19	MgO	0.86
Fe_2O_3	2.75	Na_2O	0.14
CaO	65.0	K_2O	0.51
Loss on ignition (%)	7.23		
Specific surface area (m^2/kg)	447		
Limestone (%)	15		
Alkali content (%)	0.72		

3.3 Part I - Concrete Resistivity

In this part, at first the difference of the resistivity measurements using internal and external electrodes was conducted, respectively. It also investigated the effect of the applied current of different frequencies from low to high to identify the most suitable frequency that can be utilized for stable and reliable results. Thereafter, with the determined optimised electrode configuration and the current frequency, a series of resistivity measurements were conducted on all concrete specimens for the effects of the major influencing factors affecting concrete resistivity. Compressive strength, porosity and free & total chloride were also measured in this part of study.

3.3.1 Concrete Specimens

Concrete cubes of the size of 100mm x 100mm x 100mm with two embedded electrodes made of carbon fibre (CF) sheets were cast as shown in Figure 3.1. CF sheets are flexible materials, so they are glued on flat surface of a perforated plastic mesh plate to keep it straight. Thereafter, the two of the CF electrodes were placed upright with a certain parallel distance to each other in concrete mould in casting. For comparison, external electrodes test method using both CF sheets and copper plates electrodes were also conducted on other

plain concrete cubes made of the same mixture and of the same size, 100mm x 100mm x 100mm.

The concrete mixes were prepared to have four different chloride contents by adding NaCl in the mix water. The added chloride contents were 0, 1.5, 3 and 4.5 % of the cement mass, respectively. Three water to cement ratios were used for each chloride content mix, they were 0.4, 0.5 and 0.6, respectively.

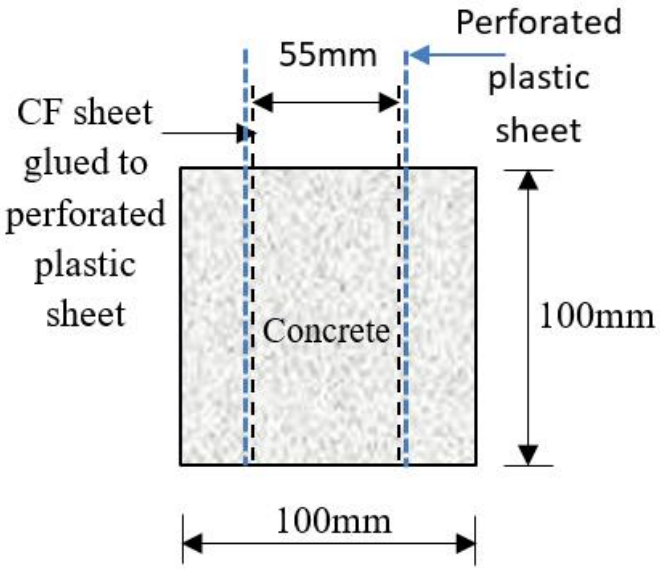

(a) Sample dimension

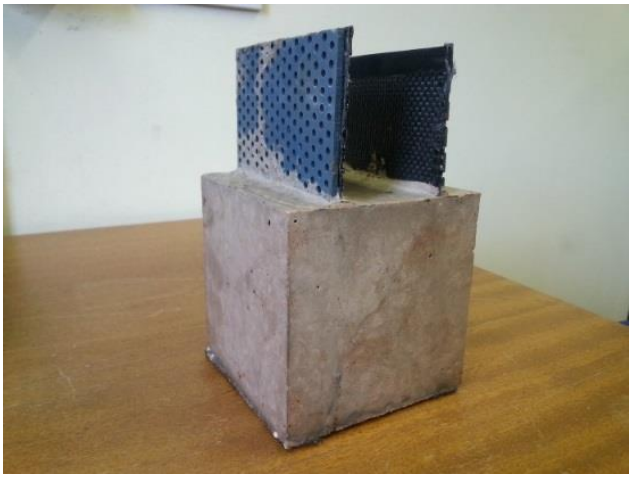

(b) Experimental sample

Figure 3.1: Concrete specimens with internal electrodes of CF sheets for resistivity measurement

The components of concrete were mixed together followed the British standard, BS 1881-125:2013. Prior to mixing, all the required constituents were prepared. The saturated surface dry coarse and fine aggregates and the cement of each mix were placed in a plastic container and manually mixed for approximately two minutes. Thereafter, the tap water with a specified chloride content was added and the mixture was continuously mixed manually again for other three minutes until a uniform consistency was achieved. Prior to casting, all moulds inner surfaces were oiled. Fresh concrete was then poured in by two layers, 5 cm each, and the concrete was compacted using a vibrating table for a duration of 15-30 seconds. After then, all the casted specimens were left to set in their moulds and covered by plastic sheet for two days at lab temperature and then de-moulded.

In the next, all the casted concrete samples were cured by submerging in the water of the same chloride content as that used for their mixes for 28 days before starting tests. For each mix, three specimens were prepared for each property measured, and the final result took the average of the three specimens.

A total of 117 cubic specimens of the size of 100mm x 100mm x 100 mm were prepared at this stage were divided into three groups, one group of 72 specimens was for resistivity measurements, the other group of 9 chloride free specimens was used to test the compressive strength of different water to cement ratios, and last group of 36 specimens was for the measurement of porosity and the free & total chloride analysis. Figure 3.2 shows a summary of the plan for this part.

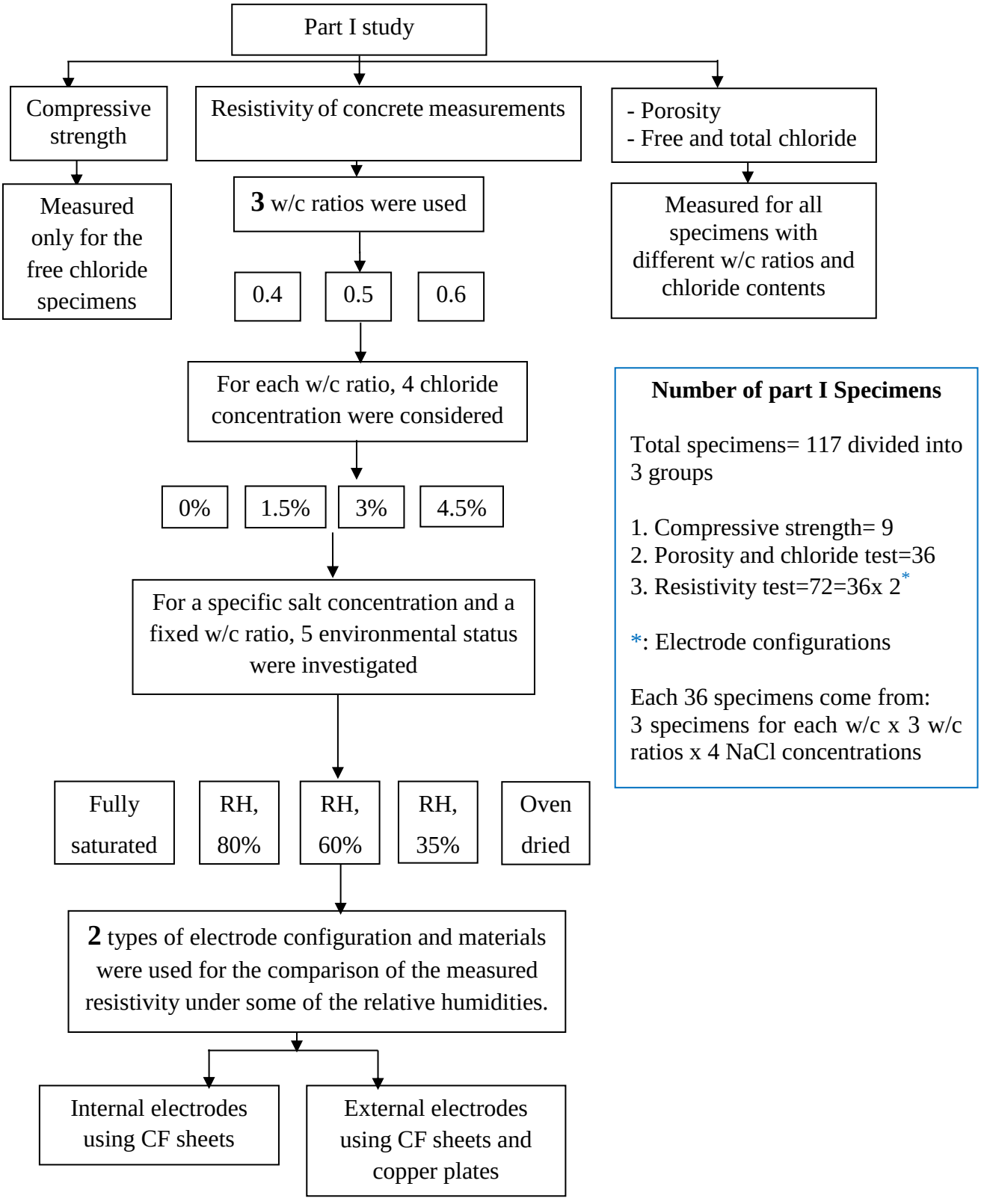

Figure 3.2: Research programme chart of part I

3.3.2 Experimental Tests

3.3.3 Compressive Strength

To confirm the quality of the made concrete, compressive strength was tested using triplicate chloride free concrete cubes according to BS EN 12390-3:2009.

3.3.4 Absolute Porosity

The absolute porosity of concrete specimens was worked out in terms of the saturated surface-dry mass at the end of curing and the mass of the oven-dried at 100±5°C until achieving a constant weight. The absolute porosity was calculated using the equation below (Arya et al., 2014):

$$\text{Absolut porosity} = \frac{(\text{Ws}-\text{Wd})/\rho}{\text{V}} \times 100 \quad (3.1)$$

where, ρ is density of water, V is the volume of sample, Wd is the oven-dry mass of the specimen and Ws is the saturated surface-dry mass of the specimen.

3.3.5 Chloride Analysis

In this work, the actual chloride content in the specimens after wet curing has been measured in terms of the water and acid-soluble chlorides following American Society for Testing and Materials (ASTM) standards. The results provide information of the free and total chloride contents.

There is no standardized test method in the UK for determining the water-soluble chlorides in concrete, although BS EN 1744-1 describes a method for testing aggregates and BS EN 14629 for the determination of the acid-soluble chlorides content of hardened concrete.

Contrary to UK practice, American practice places limits on the water soluble chlorides in concrete, for both the constituent materials and the hardened concrete, as it is considered that only these chlorides can contribute, under normal circumstances, to reinforcement corrosion (Dhir et al., 1990; Xi and Bažant, 1999) and bound chlorides have limited contributions to corrosion initiation (Shakouri et al., 2017).

Water-soluble chlorides are commonly referred to the free chlorides in the cementitious systems, while acid-soluble chlorides associates to both the free and bound chlorides and defined as the total chloride (Angst et al., 2011; Ann and Song, 2007; Mohammed and Hamada, 2003; Shakouri et al., 2017).

The procedure typically involves the extraction of chlorides from a sample of powdered concrete using dilute with deionized water for the free chloride and nitric acid for the total chloride followed by quantification using potentiometric titration as summarized below in accordance to ASTM C1218/C1218M (2015) and ASTM C1152/C1152M (2012).

Dry drilling method was used to collect the concrete powder from boreholes on the concrete surface using a rotary power drill. Three cylindrical holes of the size 12 x100 mm (diameter x length) evenly distributed along the central line of a cubic specimens (100x100x100) mm^3 were drilled. The concrete sample obtained from the three cylindrical holes was at least 45g, and mixed together to represent each mixture. Porcelain mortar and pestle were used to crush any particles that greater than 850 μm (ASTM C1152/C1152M, 2012). The collected powder was then transferred to a small sealed plastic bag and labelled for the analytical chemistry procedure to measure free and total chloride

3.3.5.1 Total Chloride Test Procedure

There were three steps in the process to measure the concrete chloride content: they are Digestion, filtration and titration. Digestion generally includes mixing of 10±0.01 g of concrete powder with 75 ml deionized water and 25 ml of dilute (1+1) nitric acid in a 250 ml beaker to dissolve the solid sample. Magnetic stirring bar was added in the beaker for mixing the solution over a stirrer during this step to break up any lumps of sample. 3 drops of methyl orange indicator was added to the beaker to insure the acidity of solution. Pink colored must be observed during adding the indicator, otherwise, more nitric acid is required. After then, a watch glass was placed to cover the beaker, and the covered beaker was heated rapidly to boiling and removed from hot plate. Figure 3.3 shows the solution after digestion process, but it has not been heated yet. This process was performed inside fume cupboard for safety.

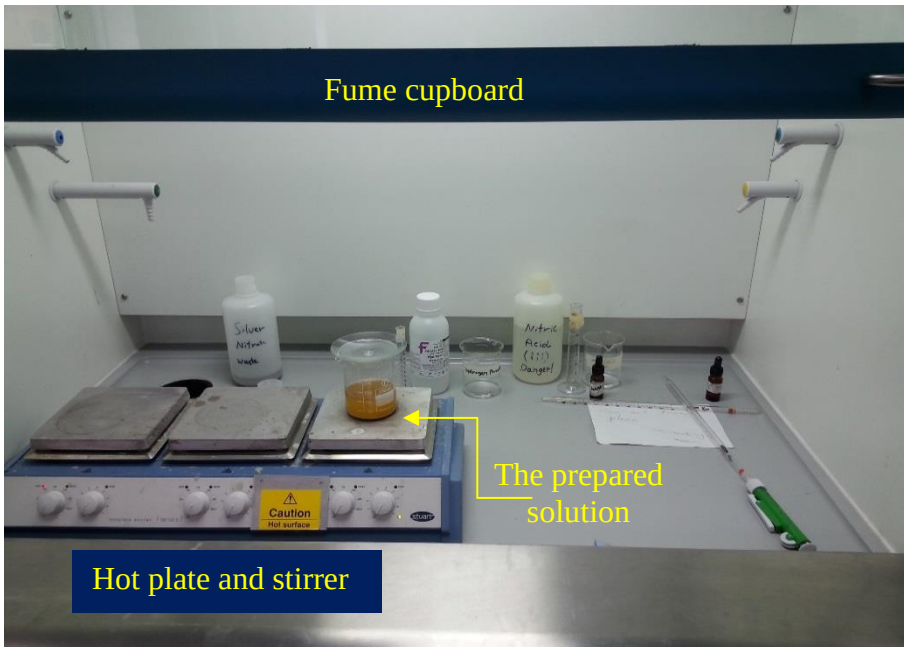

Figure 3.3: The prepared solution for the total chloride analysis after digestion process

The second step is filtration to remove any undissolved solids. In this process, the boiled solution was filtered through coarse-textured filter paper using suction as shown in Figure 3.4. The beaker and the filter paper were rinsed twice with small portions of water. The filtrate was transferred to a 250 ml beaker and rinsed the flask once with water. The filtrate was left to cool to room temperature before using it for the next final stage.

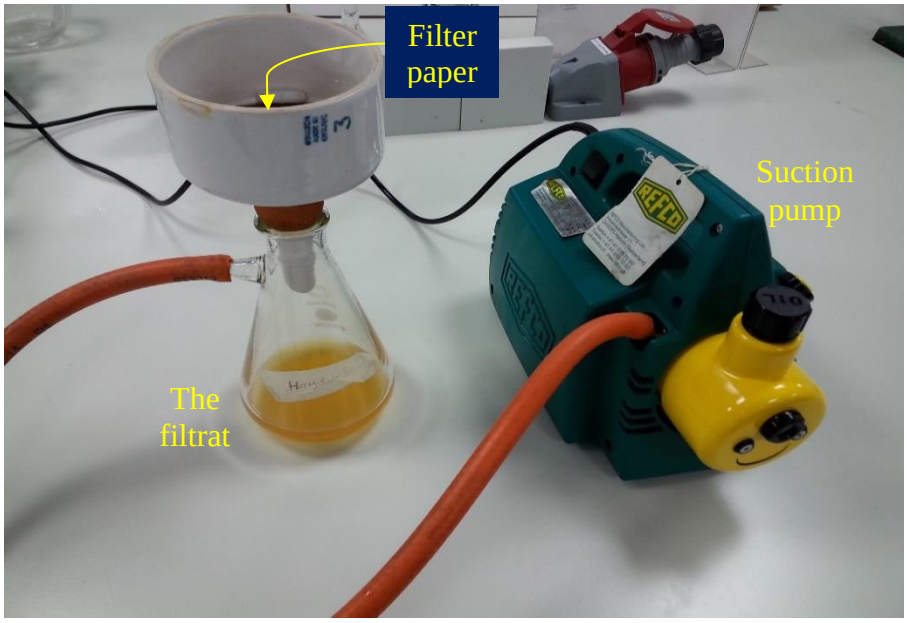

Figure 3.4: Filtration process

Finally, potentiometric titration is to use a standard solution of silver nitrate (0.05 N AgNO3) as titrant to determine chloride content. Potentiometric titrations involves the measurement of the potential of an indicator electrode with respect to a reference electrode as a function of titrant volume. A chloride combination electrode model HI-4107 which has the reference built in, and potentiometer model HI-5522 made by HANNA instruments were used for the potential reading of the solution during titration. Figure 3.5 shows the apparatus for potentiometric titration, it illustrates a beaker containing solution was placed on a magnetic stirrer and a magnetic stirring bar was added in the beaker for mixing during titration. The electrodes were immersed into the solution and connected to the potential meter. The delivery tip of the burette filled to the zero mark with standardized 0.05 N AgNO3 was placed above the sample solution.

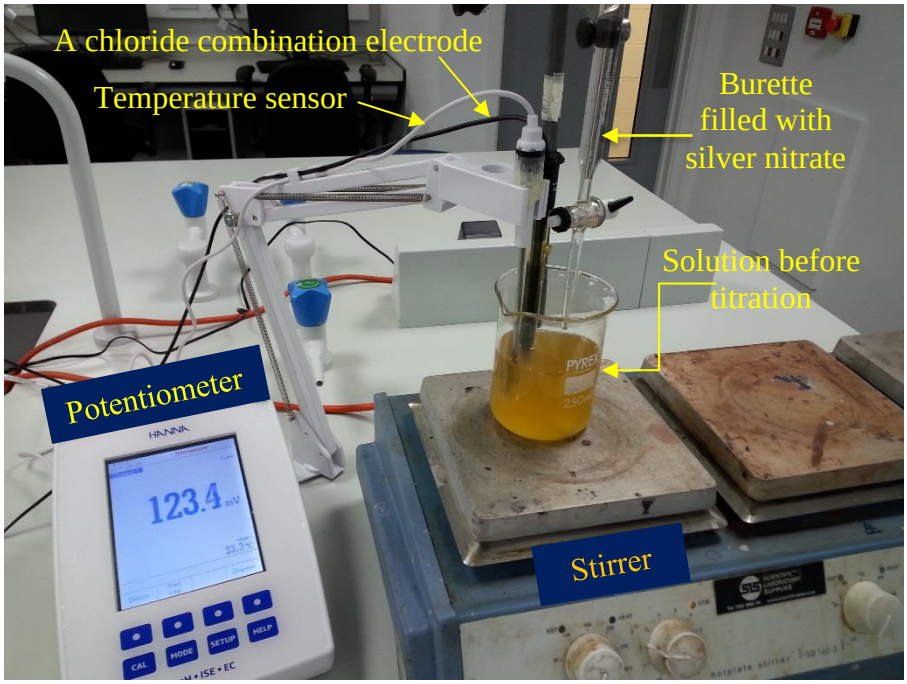

Figure 3.5: Titration test setup

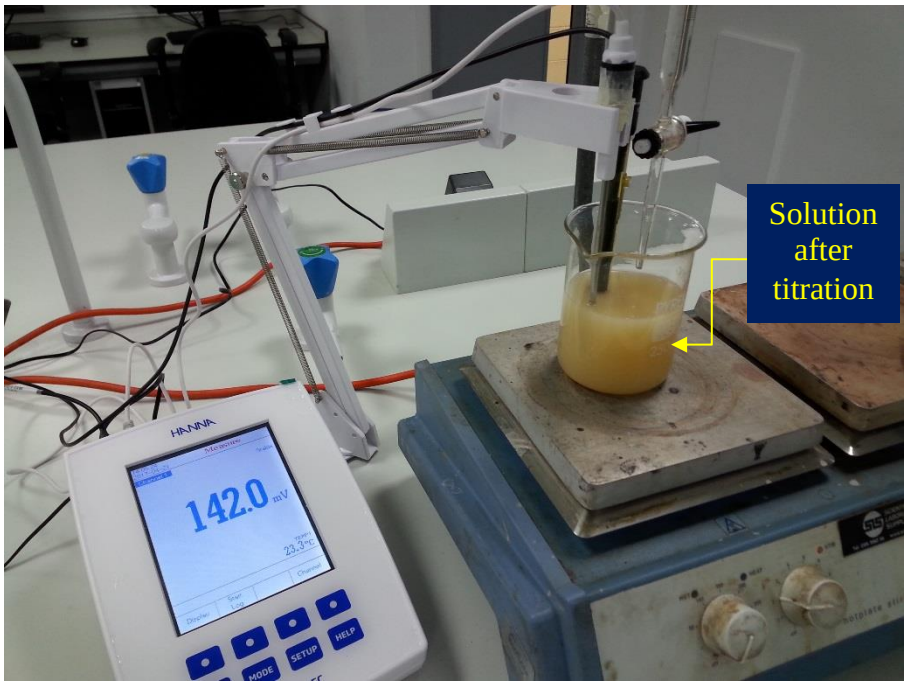

Figure 3.6: The analysed solution for the total chloride after titration

To start with the titration, silver nitrate (0.05 N AgNO3) was gradually added to the solution and the burette readings in ml with the corresponding measured electrodes potential readings in mV were recorded. The silver nitrate was added generally in big increments at the outset. Later the increment became smaller and smaller in the way approaching to the equivalent point for a steady small observable change in the potential reading. Once beyond the equivalence point, potential change will decrease. At least three readings beyond the equivalent point were determined to obtain the titration curve. Figure 3.6 shows the analysed solution after titration. The equivalent point can be determined directly from the titration curve, a direct plot of potential against the added silver nitrate volume as shown in Figure 3.7. The equivalent point is the inflection point of the curve. To obtain the accurate equivalence point, second derivative curves, as shown in Figure 3.8, were plotted for the change of potential-change $(\Delta E)^2$ at per volume change of the silver nitrate $(\Delta V)^2$, i.e. the slope of the first derivative curve (Checchetti and Lanzo, 2015). The slope was plotted against the corresponding volume of the silver nitrate. The data changes sign from + to − at the equivalence point.

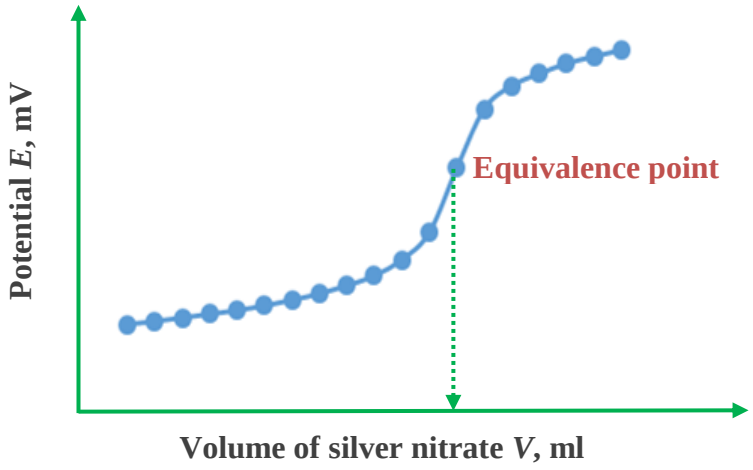

Figure 3.7: Typical titration curve

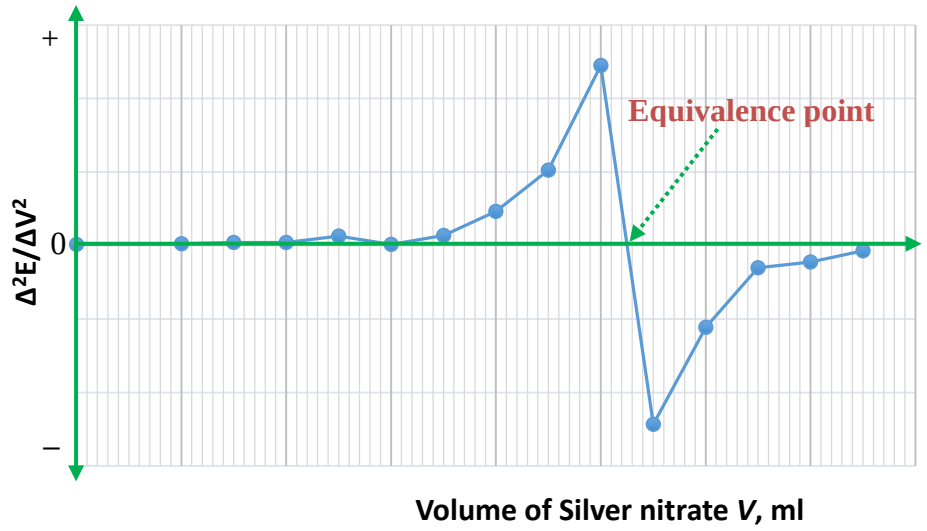

Figure 3.8: Second derivative curve

At last, the percent of chloride by dry mass of concrete to the nearest 0.001 % was calculated according to the standard (ASTM C1152/C1152M, 2012):

$$\% \text{ C1, by mass of concrete} = \frac{3.545 \times V \times N}{W} \quad (3.2)$$

where,

V = volume of silver nitrate at the equivalence point, ml

N = normality of silver nitrate, 0.05.

W = mass of concrete sample, 10 g.

For calculating chloride as percentage of the cement mass, the following equation was used.

$$\% \text{ Cl, by mass of cement} = \frac{\% \, C1, by \; mass \; of \; concrete \times 100}{P} \quad (3.3)$$

where P is the cement percentage by mass of concrete samples.

3.3.5.2 Free Chloride Test Procedure

Same procedure of the total chloride analysis was conducted for the free chloride with the exception of digestion. The digestion step for the free chloride was slightly different and involved mixing the concrete powder with 50 ml of deionized water and boiled for 5 minutes. Then after, covered with a watch glass, samples were let to stand for 24 hours before filtered by suction through a fine-texture filter paper. Later, the filtrate was transferred to a 250 ml beaker and added in 3 ml of (1:1) nitric acid and hydrogen peroxide (30 % solution). The beaker was covered using a watch glass and allowed to stand for 1 to 2 minutes. The covered beaker was heated rapidly to boiling and removed from the hot plate. At last, followed the proceeded for the total chloride test described before to determine the free chloride. Figure 3.9 shows some photographs for the free chloride solution during the process of analysis

(a) Powdered concrete sample mixed with water

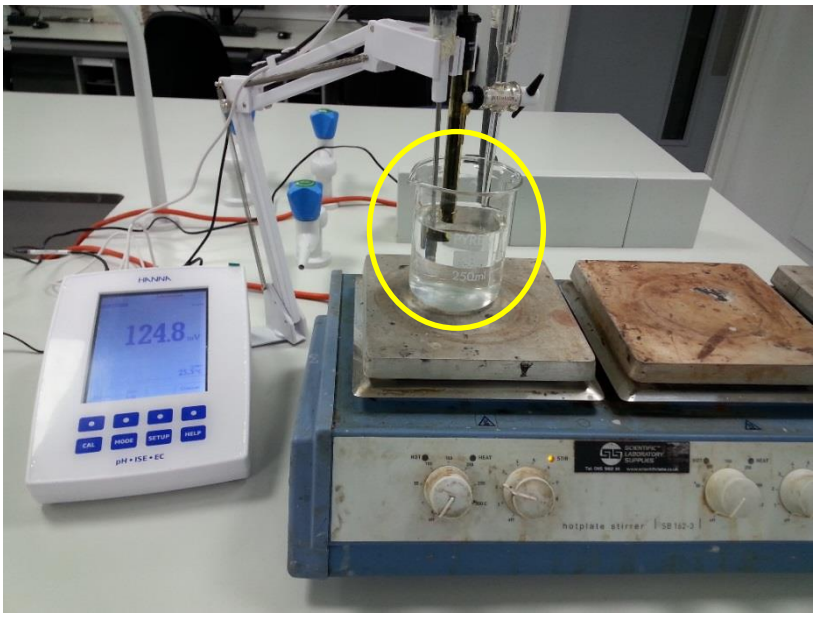

(b) The prepared solution after filtration and ready for titration

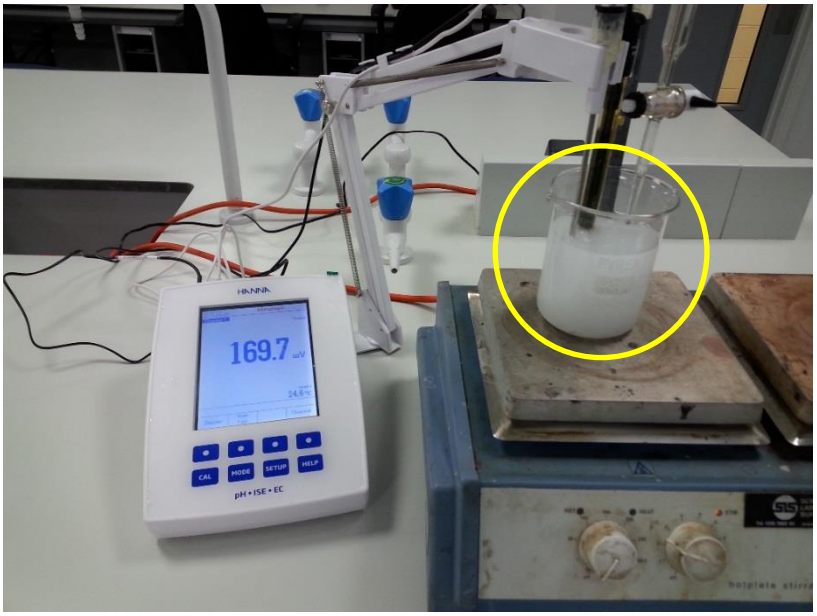

(c) The free chloride sample after titration

Figure 3.9: Photographs of some of the steps during the analysis of free chloride

3.3.6 Electrical Resistivity of Concrete

Concrete electrical resistivity can be obtained by applying a voltage on concrete using two electrodes attached to the ends of a uniform cross-section specimen and measuring the response current.

Both internal and external electrode methods were used to study the effect of configuration, respectively. CF sheets were employed as the internal electrodes and CF and copper sheets were used as external electrodes. Figures 3.10 and 3.11 illustrate the test setup for the two methods. A function generator model TG210 supplied by Thurlby Thandar Instruments (TTI) in the UK was employed to generate a sine wave at desired frequency and amplitude. The two terminals of the function generator were connected to the electrodes. A voltmeter was connected in parallel with the function generator to measure the applied voltage or amplitude, while an ammeter was connected in series with the tested specimen to measure the passing current. For the external method, two pieces of wet sponge soaked with 1M sodium sulfate were put between the concrete surfaces and the copper plate electrodes for full contact to lower the potential of extra electrical resistivity at the interfaces (Newlands et al., 2008). A G-clamp was applied on two pieces of 100mm×100mm×24mm plywood to produce a uniform holding pressure.

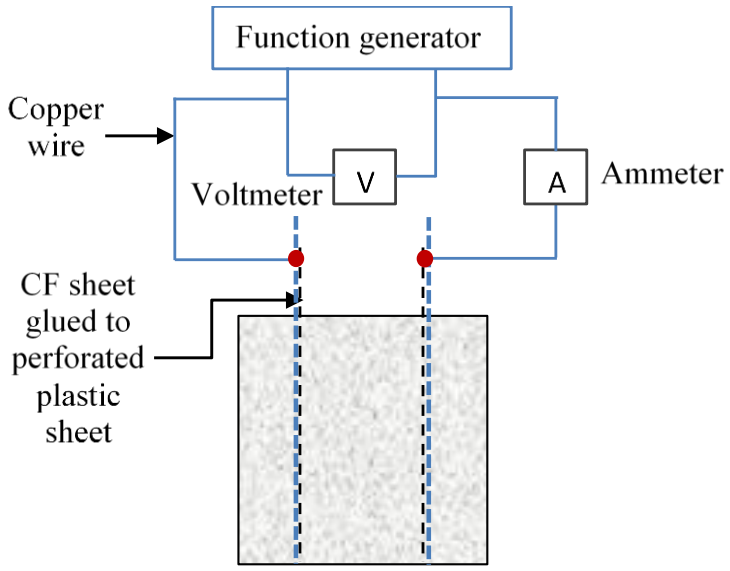

(a) Schematic diagram of experimental setup

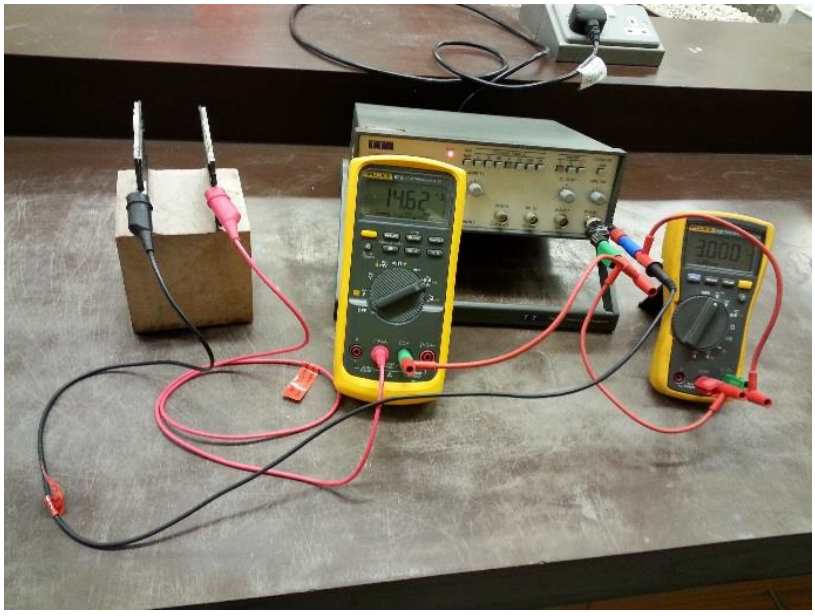

(b) Photograph of testing setup

Figure 3.10: Electrical resistivity testing setup for concrete specimens with internal electrodes

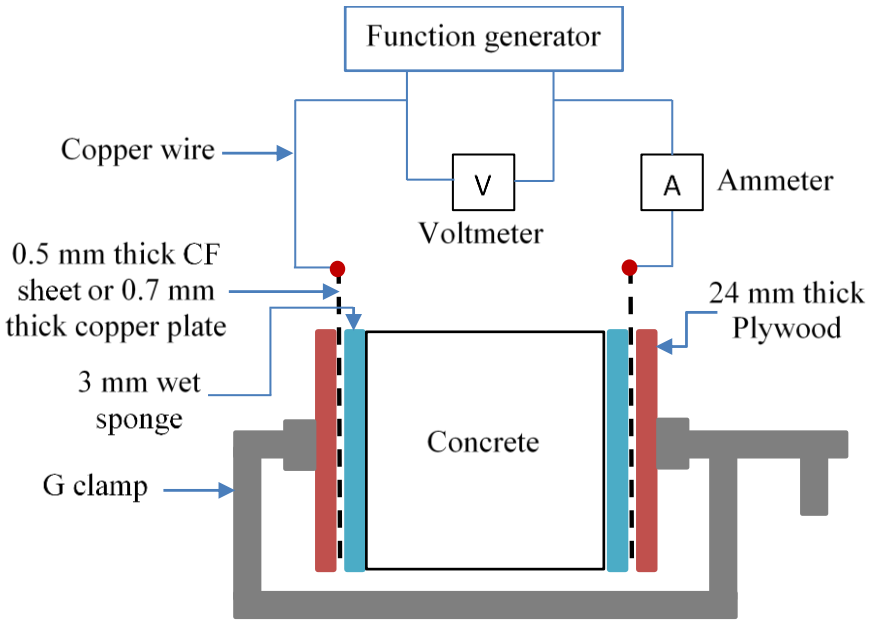

(a) Schematic diagram of experimental setup

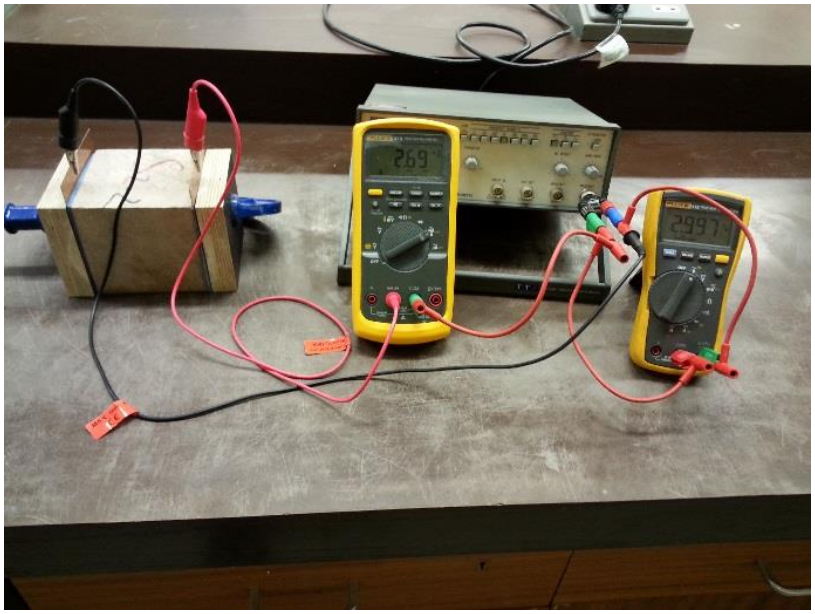

(b) Photograph of experimental setup using external electrodes of copper sheets

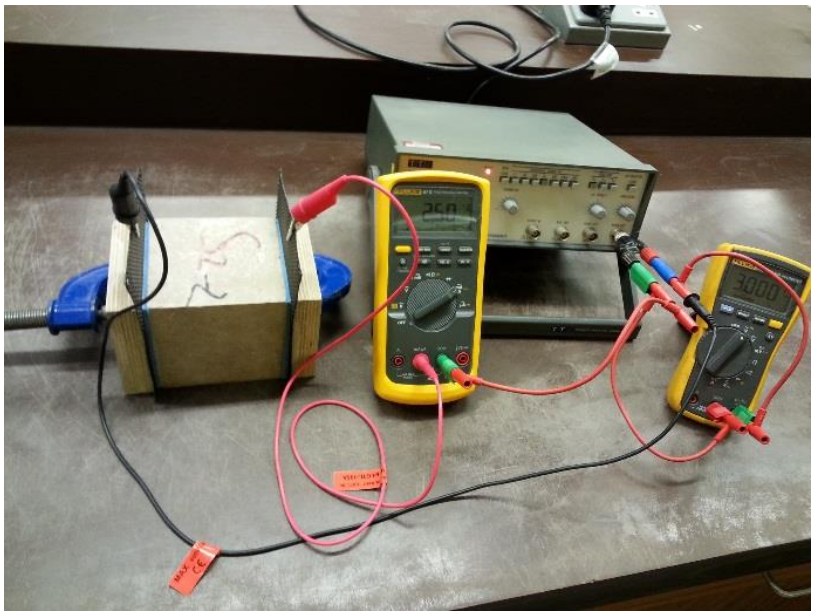

(c) Photograph of experimental setup using external electrodes of CF sheets

Figure 3.11: Electrical resistivity measurement setup for concrete specimens with external electrodes

Based on the measurement, the electrical resistivity of the concrete specimens can be worked out in terms of the Ohm's law below (Hornbostel et al., 2013),

$$R = \frac{\text{V amplitude}}{\text{I amplitude}} \quad (3.4)$$

and

$$\rho = R\frac{A}{L} \quad (3.5),$$

where R is electrical resistance, V is the applied voltage, I is the measured current, ρ is electrical resistivity, A is the cross-sectional area of the electrode perpendicular to the current flow and L is the distance between the two electrodes.

In the test, fully saturated samples were measured at first. Later, to obtain the condition of different and uniformly distributed water contents, the 100 mm cubes of different chloride contents were cut into small cubes of 50 mm nominal dimension using cutting machine with a diamond saw. The downsized samples, which will shorten the time required to achieve the equilibrium when the specimens have uniform moisture distribution under a certain

environmental condition, were placed in an environmental chamber of three controlled relative humidities, which were 35%, 60% and 80%, respectively under a constant temperature of 21°C for sufficient time until a stable weight observed. Figure 3.12 shows the environmental chamber used.

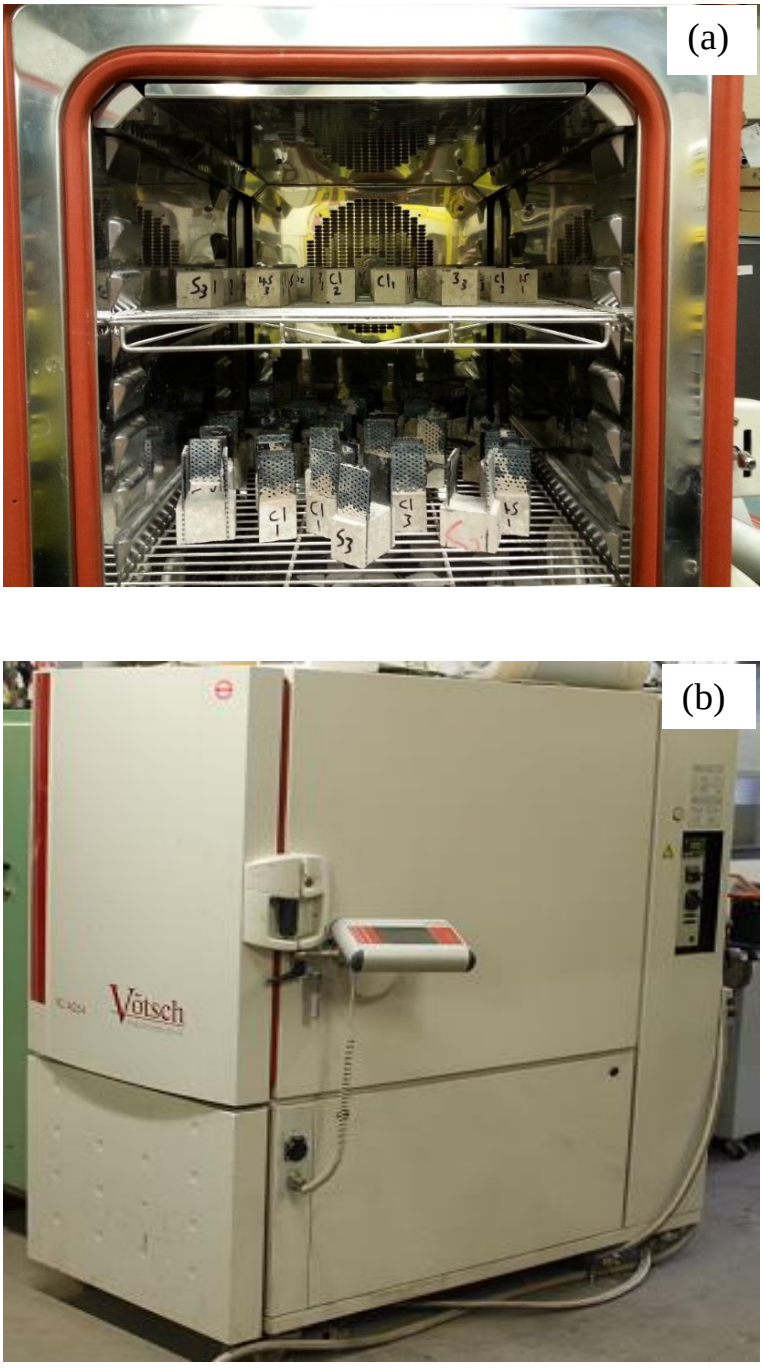

Figure 3.12: Photographs of (a) the resistivity specimens in a humidity chamber (b) the humidity chamber used to control the humidity and temperature

The water content of specimens was evaluated by weighing them. A uniform water content distribution was assumed achieved when 24 h variations in mass is less than 0.01g (Villagrán Zaccardi & Di Maio, 2014).

After the measurement of their electrical resistivity at different water contents, all these samples at last were put in an oven (100±5°C) until reached a stable dry condition. Then they were measured again for their electrical resistivity. The actual water content for each condition was measured using the weighing method.

The influence of applied AC Frequency on electrical resistivity measurement was evaluated in the range of 1 Hz to 10000 Hz. In theory, the most suitable frequency should produce the lowest resistance (Katwan, 1988). The influence of the magnitude of the applied voltage has also been investigated in a range of 1~6 V in an interval of 1 V. based on the study, the identified optimum frequency, voltage, electrode material and configuration were used for all the tests in this study.

3.4 Part II - Cathodic Protection

In this part, the experimental work was designed to investigate the effect of CP application on corrosion state of the steel reinforcement in the concrete exposed to different water and chloride conditions. Important parameters in the design of CP system such as the exposure conditions, state of the steel, concrete resistivity and design criteria were evaluated in order to provide an optimal protection of reinforced concrete structures.

3.4.1 Specimens Design

Reinforced concrete specimens of 150x90x93 mm^3 illustrated in Figure 3.13 were prepared to investigate the cathodic protection system. These specimens were cast using wooden moulds specially prepared. Three rebars of 10 mm in diameter with a net exposed surface area of $3\times\pi\times10$ mm$\times$73 mm = 6880 mm^2 were used as reinforcing steel. The reinforcing bars were fixed in their designated position by mean of making holes in the moulds as shown in Figure 3.14.

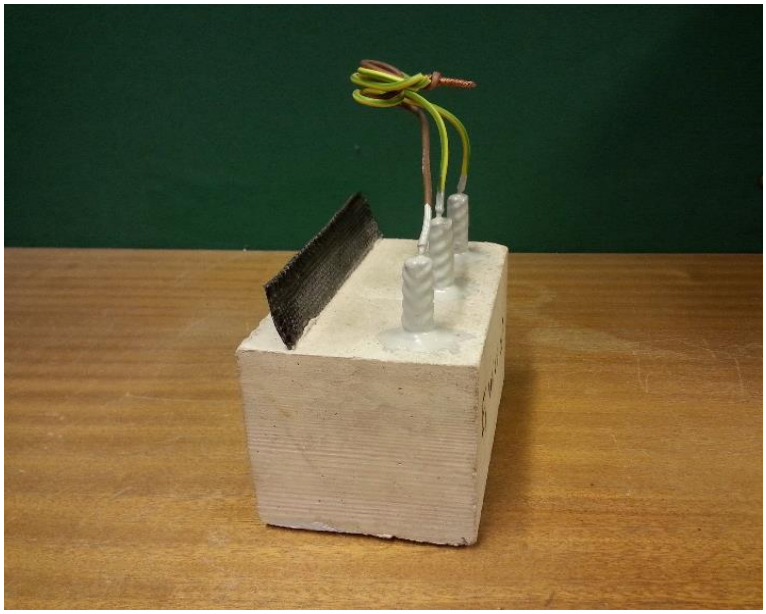

(a) The casted reinforced specimen

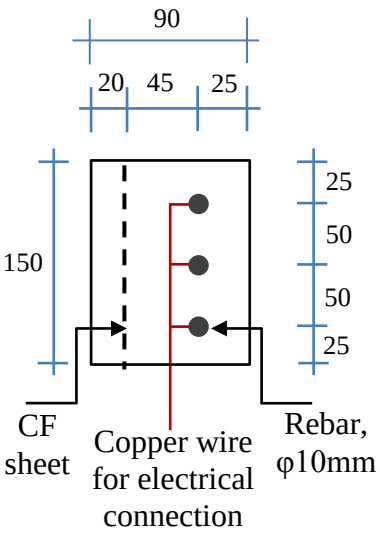

(b) Top view

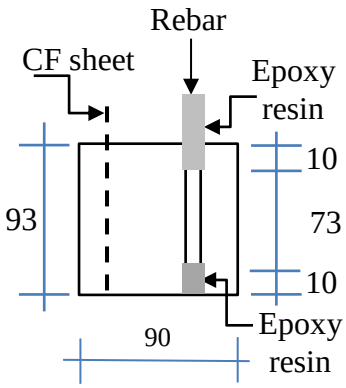

(c) Front view

Figure 3.13: The specimen used for the measurement of the electrochemical behaviour of the rebar under CP, size unit is in mm

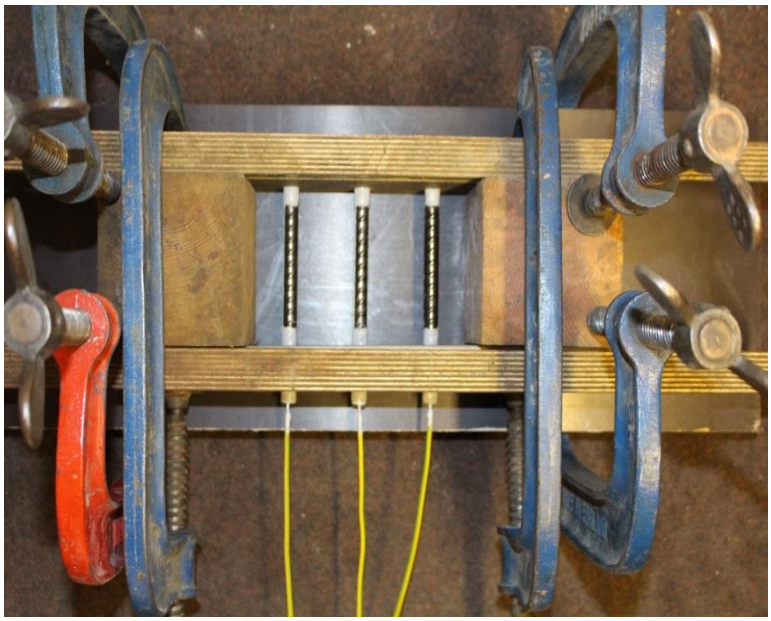

Figure 3.14: Wooden mould for casting CP specimens

3.4.2 Reinforcing Bars

All the surfaces of the reinforcing steel bars were cleaned at first using wire brush and power drill to remove rust on surfaces. Later, a hole of 3 mm in diameter and 5 mm in length was drilled at one end of each steel bar. After then the drilled end was heated prior to soldering an external copper wires to ensure a strong bond between the solder and the bar for better electrical connection. Before casting, both ends of all steel bars were coated using epoxy resin to reduce edge effect and avoid corrosion, so that only an effective length of 73 mm in the middle was exposed to the concrete environment. Figure 3.15 shows a typical steel bar used in the corrosion electrochemical measurements and the equipment used for cleaning and soldering.

After casting, all the parts of steel bars, which were exposed to atmosphere, were coated again using epoxy resin to increase the protection from corrosion. The three bars of each individual concrete specimen were electrically isolated from each other during casting the concrete, after casting they are connected together using external copper wire to make all bars electrically in contact.

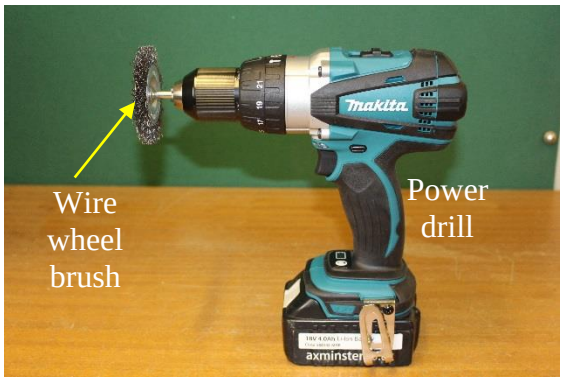

(a) Cleaning tools

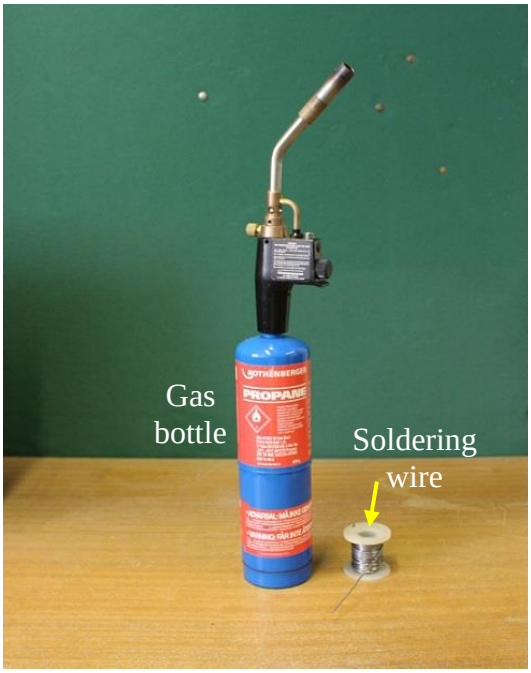

(b) Soldering tools

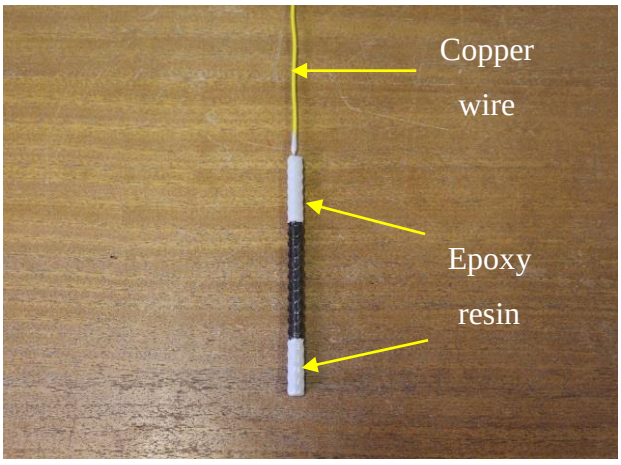

(c) Typical steel rebar used in the study

Figure 3.15: Photographs of the steel bar prepared for corrosion measurements and equipment used

3.4.3 Anode Material

A plain woven carbon fibre (CF) fabric sheet of specific area weight 375 g/m^2 as shown in Figure 3.16, supplied by the East Coast Fibreglass Supplies in the UK, was used for the anode.

Figure 3.16: Carbon fibre sheet anode

3.4.4 Reinforced Concrete Specimens

Applied mineral oil on all the internal faces of the moulds using a brush. Put the moulds on a vibration table. Filled the concrete mix into the moulds by two layers. Each layer of approximate 35mm in depth was given sufficient vibration time for a duration of 30 seconds to reach full compaction. After that, a layer of CF sheet was embedded in each specimen to represent the anode. The layer of the anode was then covered by 20mm thick of concrete and compacted on the vibrating table. The area of the embedded anode was 144x93 mm^2. About 30 mm of the CF sheet extends out of the specimens for electrical connection. Upon completion of compaction, the specimens were covered with nylon sheet to minimize evaporation during 48 hrs. After 48hrs of casting, the specimens were demoulded and moved in water of the same chloride concentration as their respective mix water for wet curing up to 28 days from the time of the completion of casting. The specimens prepared are shown in Figure 3.17.

Figure 3.17: Photograph of the specimens used in the study of part II

3.4.5 Experimental Procedure

Figure 3.18 illustrates the planned experimental programme in this part. Similar as that for the mixtures used for electrical resistivity test in part I, different concentrations of chloride as pure NaCl salt of 0, 1, 2, 3.5 and 5% of the cement mass, respectively, were added into the mix water to prepare the specimens with different chloride contents and create various environment around the rebars. All the concrete mixes in this part of research had a constant water to cement ratio of 0.4 to meet the strength requirement for most of the normal concrete structures. The achieved 28 days compressive strength was 38 N/mm^2.

For the planned experimental programme, 40 reinforced concrete specimens were made, they were divided into different groups and subjected to various environment. Three different environmental conditions, namely air exposed, fully and partially submerged in salty water, were studied for the weather conditional influences on the design of CP system

and its performance. These conditions are proposed to simulate the weather in the practice for different constructions which may have a various effect on the design of CP system.

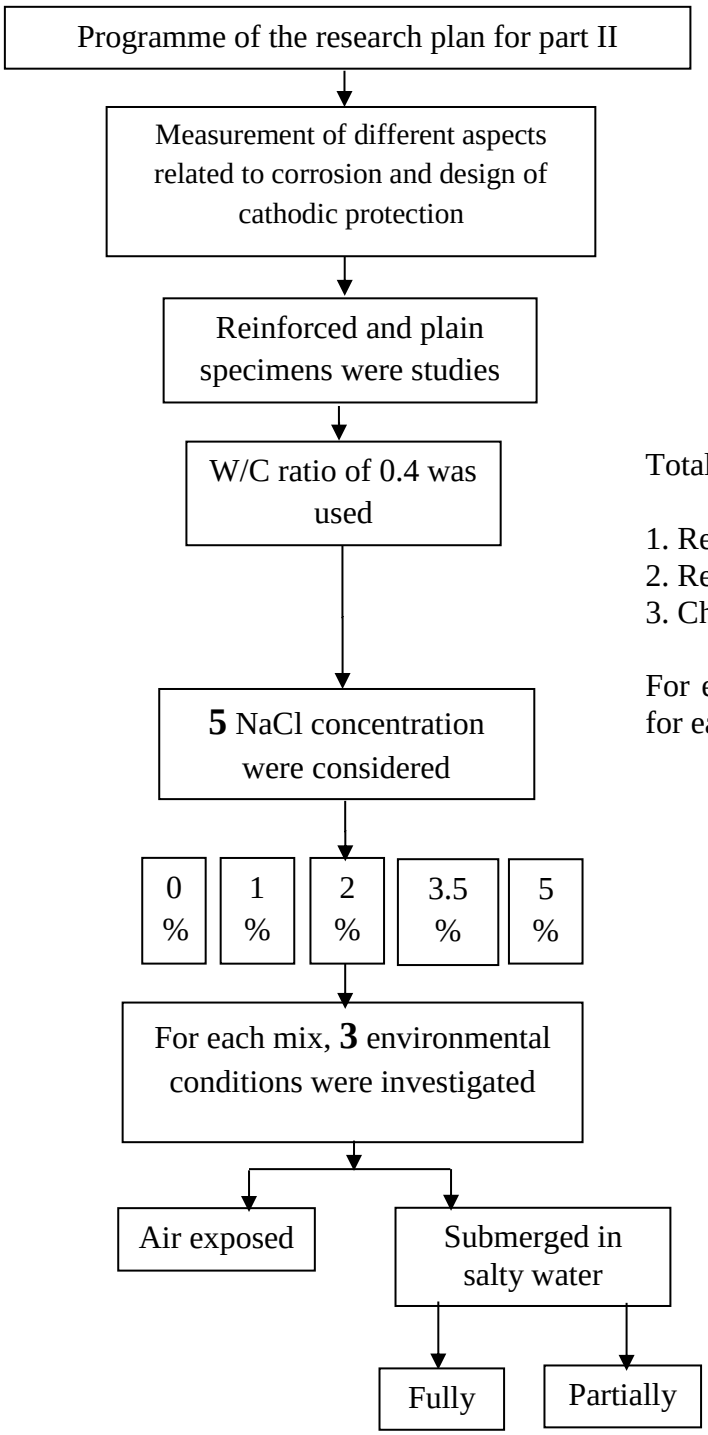

Number of part II Specimens

Total specimens= 90, divided into 3 groups:

1. Reinforced specimens for CP= 40
2. Resistivity specimens=40
3. Chloride test specimens = 10

For each mix, 2 specimens were prepared for each property measuring.

Figure 3.18: Research programme chart of part II

After 28 days of curing, a group of ten specimens (two for each chloride content) were exposed to the atmosphere in the lab of relative humidity of 50±5% and a temperature of 20±3°C until they reached a stable weight before conducting the electrochemical measurement to represent the air exposed concrete specimens.

A second group of 20 specimens were fully submerged in salty water of the same percentages of NaCl as that added in the concrete mix water for two weeks to ensure full saturation before performing the desired tests. The specimens of this group were divided into two groups. Each group was tested using a different technique for the operation of CP, constant CP current and constant CP potential.

The last group of another 10 specimens were partially submerged in salty water of the same percentages of NaCl as that added in the concrete mix water for two weeks before conducting the planned measurements to represent the exposure condition of partially submerged concrete specimens.

In addition to the reinforced concrete specimens, 40 non-reinforced concrete cubes with two embedded CF sheets, which have the size of 100 mm×100 mm×70 mm in Height x width x Depth as shown in Figure 3.19, were cut to the size from the casted cubes prepared for concrete resistivity measurement using the same mixtures and the curing procedure as that of the reinforced concrete specimens described above. The distance between the two electrodes was 55 mm, which were held in the upright position using two perforated plastic plates.

To obtain the accurate free and total chloride contents in the specimens after the used fully wet curing approach, other ten concrete specimens of all the same mixtures (two specimens for each designed chloride content) with the size of 100×100×100 mm^3 and cured under the same conditions were analysed using potentiometric titration method described in section 3.3.5.

(a) Sample prepared

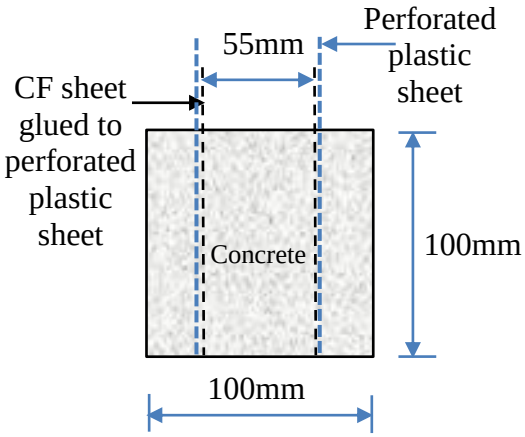

(b) Sample illustration

Figure 3.19: Concrete specimens details used for electrical resistivity measurement of Part II

3.4.6 Measurements

3.4.6.1 Corrosion Potential

The corrosion potential of the rebars in the reinforced concrete specimens after the designed exposure was measured at first following the ASTM C876 (2015) before CP implementation for assessing the probability of corrosion. The experimental setup for the reinforced concrete specimens of the air exposed is shown in Figure 3.20. A silver/silver chloride (Ag/AgCl/0.5M KCl) half-cell made by SILVION Ltd in the UK was used as the reference electrode. According to the manufacturer, the reading of this reference electrode is approximately equal to +65 mV vs saturated copper sulphate electrode (CSE). A wet sponge soaked by sodium sulphate ($NaSO_4$) solution was placed between the reference electrode and the top surface of the concrete to provide ionic conduction (Montemor et al., 2000) and to improve the electric conductivity between the reference electrode and concrete (Medeiros et al., 2017). The potential difference between the rebars and the reference electrode was measured using a high impedance digital voltmeter manufactured by FLUKE Corporation in the USA and was of a 0.1 mV resolution. The reinforcing steel was connected to the positive terminal of the voltmeter, while the reference electrode to the positive terminal. Based on the measured values of corrosion potential, the severity of corrosion was determined.

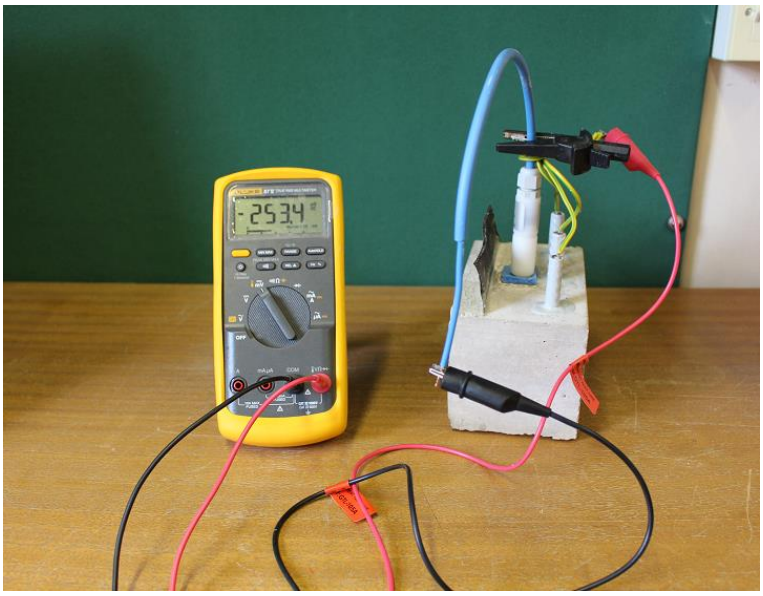

(a) Test setup

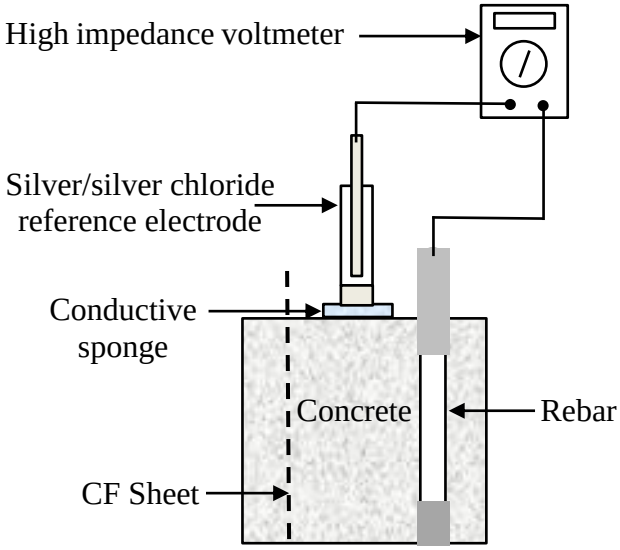

(b) Schematic drawing

Figure 3.20: Experimental setup for determination of reinforcement corrosion potential for the concrete specimens of the air exposed condition

For the fully and partially submerged exposure experiments, the porous part of the reference electrode was immerged in water during the measurement of corrosion potential as shown in Figure 3.21 (a and b).

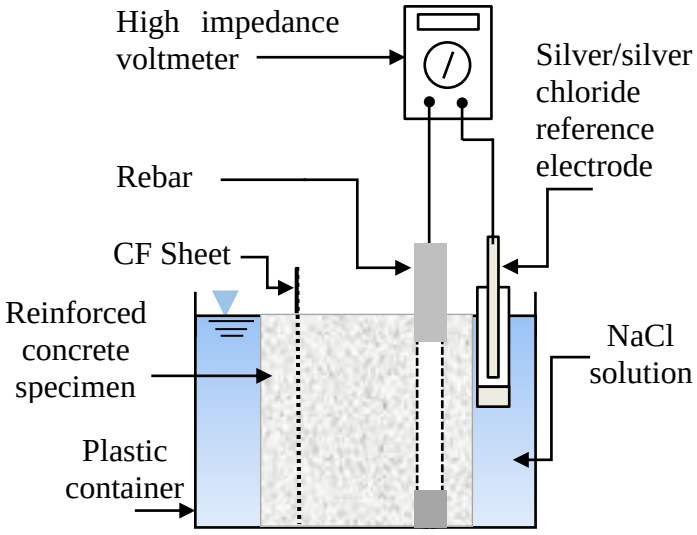

(a) Submerged exposure condition

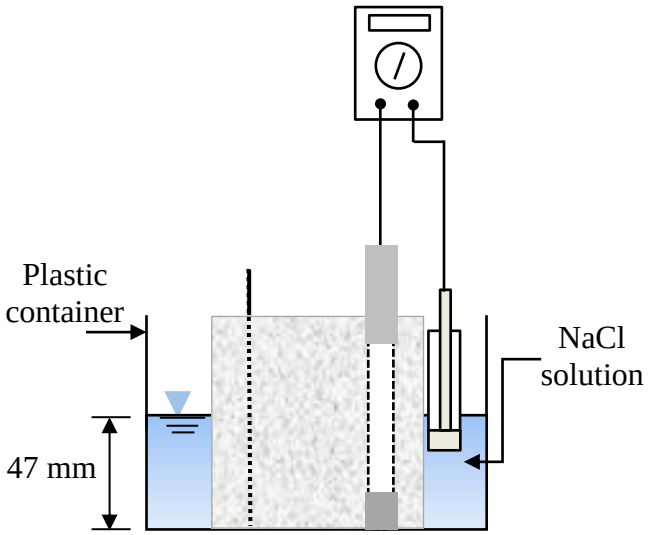

(b) Partially submerged exposure condition

Figure 3.21: Experimental setup for determination of reinforcement corrosion potential for the concrete specimens of the submerged and partially submerged exposure conditions

3.4.6.2 Corrosion Rate

The corrosion rates of rebars in the reinforced concrete specimens under various exposure conditions were assessed before the implementation of CP using the linear polarization method described by Stern and Geary (1957). This method is a non-destructive and the most popular technique used to monitor the corrosion of rebars in concrete (Hornbostel et al.,

2013). The linear polarization method implemented, as shown in Figures 3.22-3.24, is a three-electrode technique, where the potential of the three reinforcing bars being collected together through the soldered wires, and the corrosion rate of the three rebars was measured in terms of the average current density, icorr, on their surfaces. The corrosion cell setup consists of a silver/silver chloride (Ag/AgCl/0.5M KCl) electrode placed on the concrete surface which was connected to the reference electrode terminal of the potentiostat for potential monitoring, the rebars were connected to the working electrode terminal, and the CF sheet was connected to the counter electrode terminal. The setup forms an electrical circuit. The potentiostat works as a DC power supplier, which controls the potential of the rebars in concrete at a fixed value in spite of environmental condition change during the test period and provides a voltage between the rebars and CF sheet.

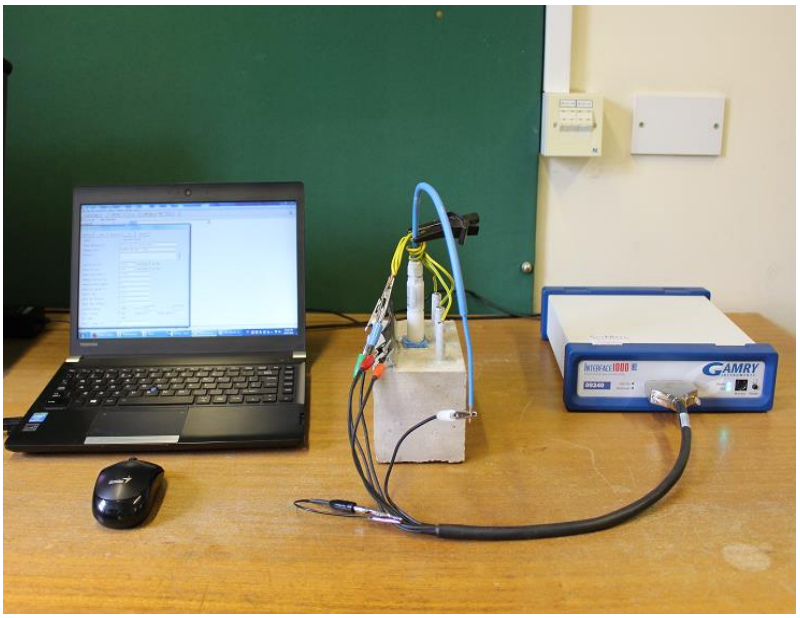

(a) Photograph of polarization resistance testing setup

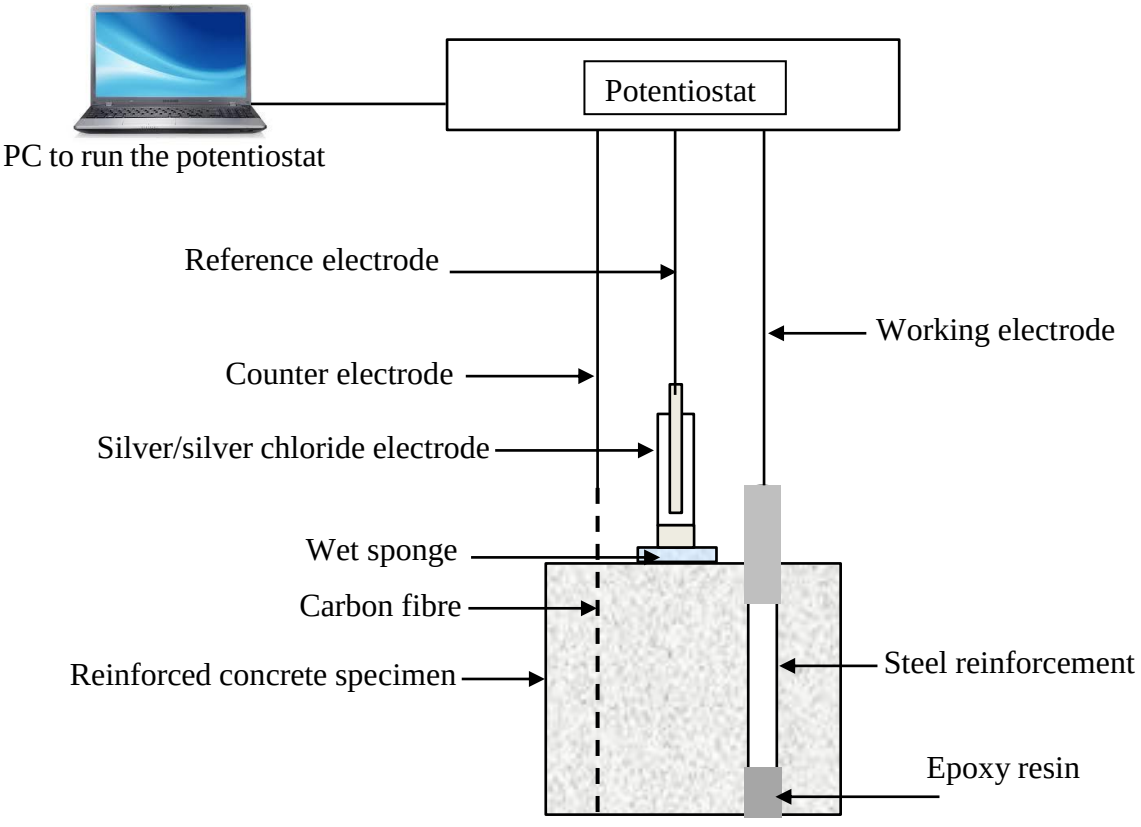

(b) Schematic drawing of polarization resistance test setup

Figure 3.22: Polarization resistance test setup for the air exposed reinforced concrete specimens

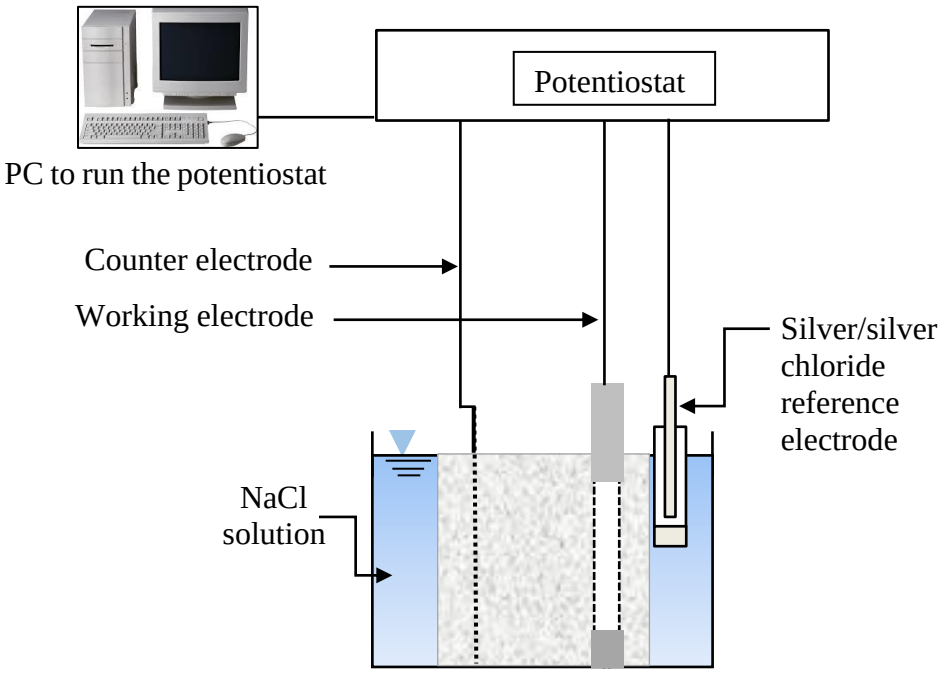

Figure 3.23: Polarization resistance test setup for the submerged reinforced concrete specimens

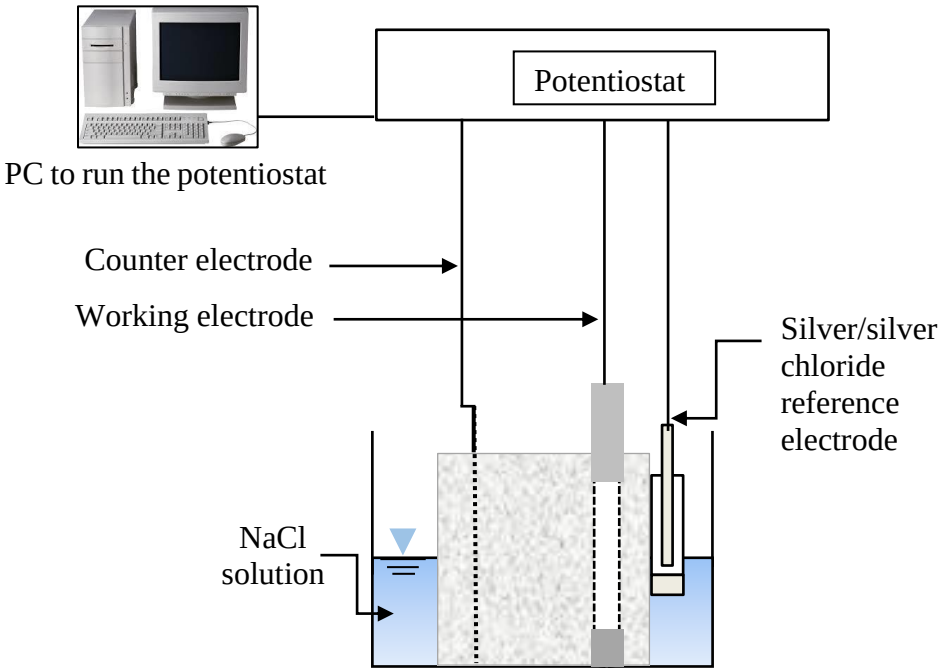

Figure 3.24: Polarization resistance test setup for the partially submerged reinforced concrete specimens

A small potential shift, ΔE, was applied on the existing open circuit potential, E_{corr}, of rebars from -20 mV to +20 mV (Kupwade-Patil and Allouche, 2012; Sathiyanarayanan et al., 2006) at a scan rate of 0.125 mV/s using a computer controlled Gamry potentiostat (Model 1000E). The IR drop was automatically compensated by the programmed potentiostat.

The passing current between the rebars and the CF sheet was monitored. For a small perturbation on the open-circuit potential, there is a linear relationship between the potential variation and corresponding current change. The change of applied voltage ΔE was plotted against the corresponding change of the measured current Δi per unit area of electrode. The polarization resistance, Rp, was then determined according to the slope of the plot the curve plotted at the point of zero current as shown in Figure 3.25 (Pradhan, 2014) .

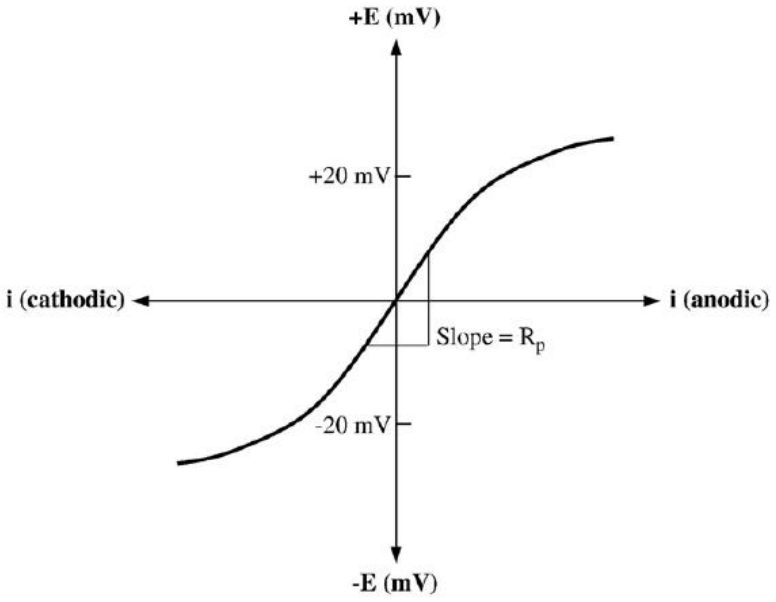

Figure 3.25: Schematic illustration of linear polarization curve for the measurement of polarization resistance, Rp (Pradhan, 2014).

This method was applied for all the specimens for the sake of comparison (Huang et al., 1996; Pradhan, 2014). The corrosion current was then determined using the Stern-Geary equation which shows there is an inverse relation between the corrosion current and the polarization resistance, as shown below.

$$Icorr = \frac{\beta a * \beta c}{2.3(\beta a + \beta c)} \frac{\Delta i}{\Delta E} \quad (3.6)$$

Then,

$$Icorr = \frac{B}{Rp} \quad (3.7),$$

where,

βa and βc are the anodic and cathodic Tafel constants

B: a constant in mV which equals to (βa*βc / 2.3 (βa+βc))

Rp: the polarization resistance in Ω (ΔE / Δi) at i=0

I corr: is the corrosion current in mA

A value of 26 mV was used for the constant *B* for the chloride contaminated specimens, while 52 mV was used for the chloride free specimens (Martínez and Andrade, 2008; Morris et al., 2002; Qiao et al., 2016).

The corrosion rate, i_{corr} , in (mA/m^2) was determined in terms of the Eq. (3.8) (Zafeiropoulou et al., 2013), where *A* was the total exposure surface area of all the three rebars in a specimen.

$$i_{corr} = \frac{I_{corr}}{A} \quad (3.8)$$

3.4.6.3 Concrete Resistivity

Concrete electrical resistivity was measured using the two-electrode specimens (Figure 3.10). A sinewave alternating current of 3000 mV amplitude and a frequency of 10 kHz was applied across the two parallel electrodes. The electrical resistivity of the concrete was then calculated as described in section 3.3.6.

Internal configuration for the electrodes and a frequency of 10 kHz have been chosen based on the obtained results during the experiments of part I as low values of resistance were achieved indicating the suitable frequency and configuration that can be used in this part of study.

3.4.6.4 Operating Period of CP

In order to decide the proper operation time for the CP test, at first, the variation of the instant-off potential of reinforcements with different protection time was measured for the reinforcement in the air exposed specimens. Three different current densities of 10, 20 and 30 mA/m^2 were adopted for different activation periods of 10 minutes, 30 minutes, 1 hour, 3 hours, 6 hours, 12 hours and 24 hours. Additionally, the current density of 20 mA/m^2 was applied for a longer period of 5 days. The instant-off potential values were recorded at these activation periods. The suitable operation period time was identified when a steady state of instant-off potential achieved.

3.4.6.5 Cathodic Protection Test

As stated in the experimental programme, three exposure conditions were designed for the implementation of CP in the study. Details of the experimental setup and procedure for each of the exposue conditions are presented below.

i. Air Exposed Condition

Galvanostatic polarization technique was addopted to apply ten different CP current densities on the rebars of each specimen. They were 5, 10, 15, 20, 25, 35, 45, 55, 65, and 75 mA/m^2, respectively, in terms of the total surface area of rebars. Ten specimens (two for each chloride content) were connected in series in each test at the same time as shown in Figure 3.26. Silver/silver chloride (Ag/AgCl/0.5KCl) half cells were used for the reference electrodes. Multi-channel data logger with 10 Megaohm input impedance and 0.1 mV resolution was used for the collection of all potential readings.

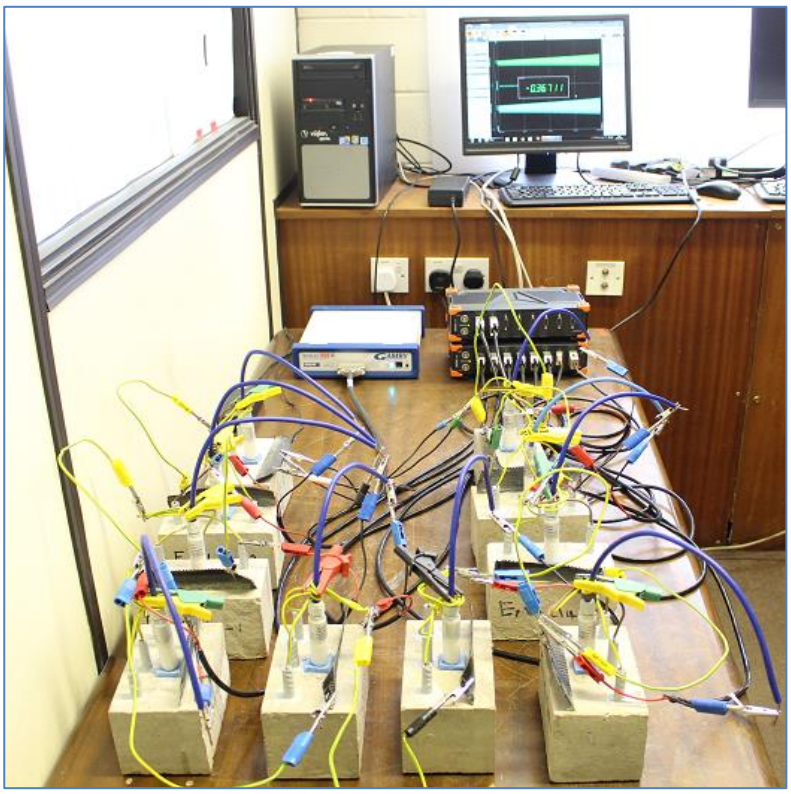

(a) Photograph of CP experimental arrangement

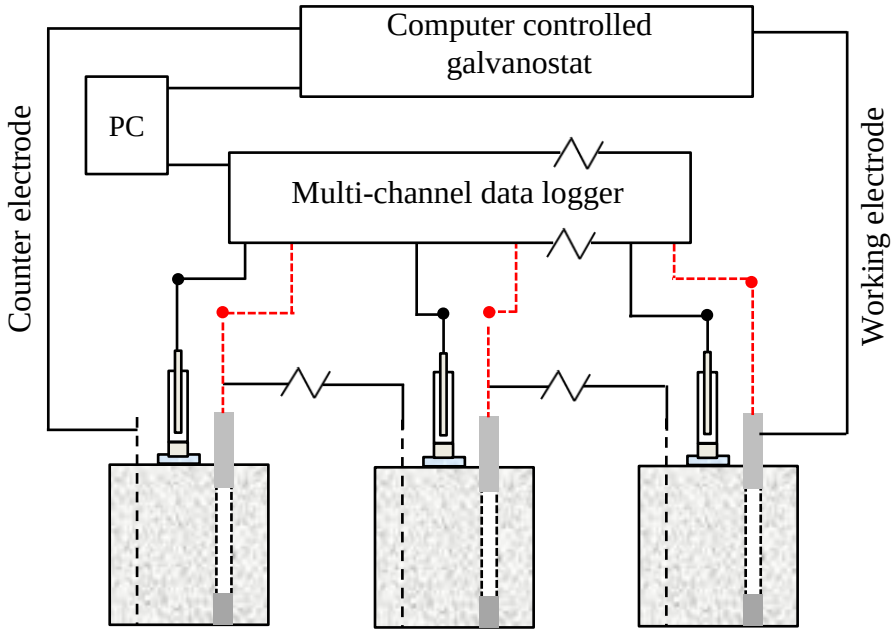

(b) Electrical schematic of wiring arrangement

Figure 3.26: Experimental arrangement for air exposed CP test

Before applying CP current, the free potential of the rebars was measured. Each test had a certain CP current density applied for 24 hours, which was believed and confirmed long enough to achieve a steady state for the polarization of rebars, and afterward the current was switched off for more than one day to ensure a sufficient depolarization of the rebars. The potential of rebars was continuously recorded from the start of CP implementation and until 4 hours after the interruption of the CP current (4 hours depolarization). Based on the recorded data, the instant-off potential, IR drop, and four-hour potential decay were obtained. Figure 3.27 shows the cycle of the application of the CP current densities.

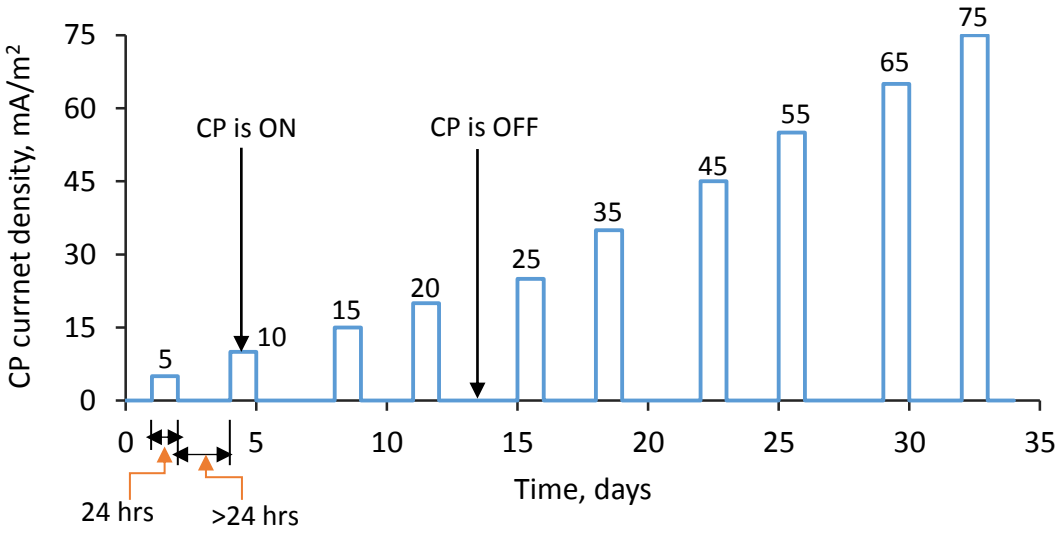

Figure 3.27: Illustration for the CP current implementation for the air exposed specimens

ii. Fully Submerged Exposure Condition

Three different levels of constant current densities using galvanostatic polarization technique were applied to produce a cathodic polarization at the rebars of the specimens. These levels were chosen based on the obtained results of corroion rates of each chloride group. They were equal or less than the measured corrosion rate. The setup of the experiment used is illustrated in Figure 3.28. The rebars were connected to the working electrode of the galvanostat whereas the anode to the counter electrode. The tip of the reference electrode was dipped in the solution and connected to the reference electrode lead of the galvanostat. Each level of CP current densities was applied for 5 days and the potential of rebars was recorded during the operation using data logger. After the day 5 of operation, the system

was switched-off and the depolarization was monitored using data logger for 24 hours to evaluate the performance of CP. Instant-off potential was measured at 1 minute after the CP was switched off.

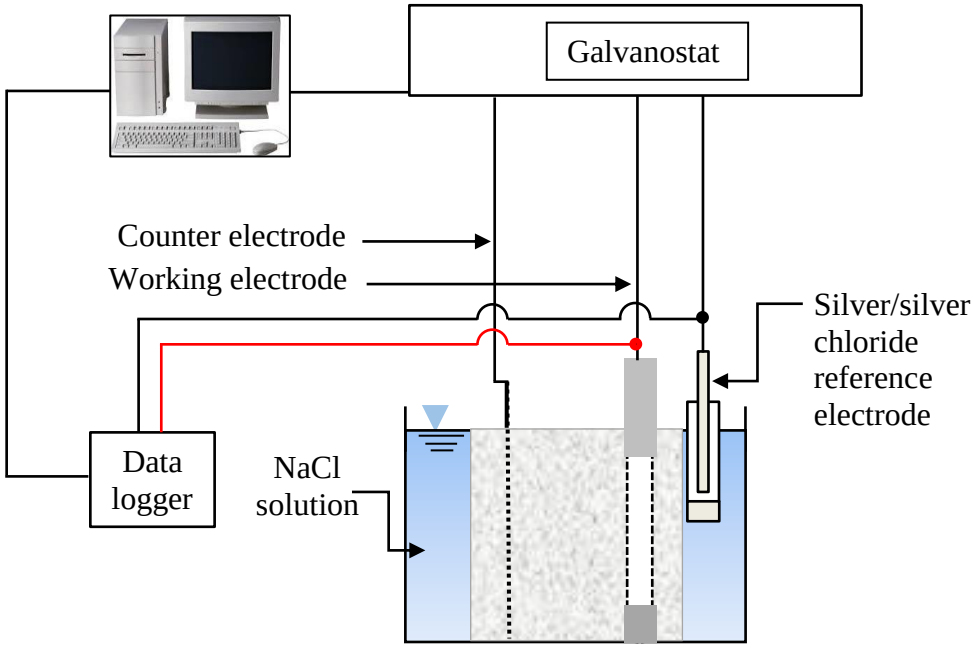

Figure 3.28: Expernintal setup for the fully submerged exposure CP test

The potential differences between the instant-off potential and the potential measured at 4 and 24 hours after switching off the CP current were also measured to be used to evaluate the efficiency of PC protection (Carmona et al., 2015; Jeong et al., 2012).

A constant potential CP test was also performed for the comparison with the constant current method technique. In this test, the potential of the reinforcement was polarized to be -800 and -900 mV, respectively with respect to Ag/AgCl/0.5KCl reference electrode. These levels of potentials represent the recommended potential for the normal protection in practice. Same experimental setup shown in Figure 3.28 was used in this test. The test of each level of the desired potentials was operated for 5 days and then switched-off for 24 hrs. The variation of the passing current was recorded during the operation, and the potential variation after switching off the system was also monitored using data logger to evaluate the technique for protection.

iii. Partially Submerged Exposure Condition

Based on the result from the fully submerged exposure test, only constant potential method was investigated for this case. Figure 3.29 shows the test setup. In this test, the potential of the reinforcement was polarised to -800 and -900 mV vs Ag/AgCl/0.5KCl, respectively. Similar as the CP test for the fully submerged specimens, 5 days were considered for the operating time of each level of the specified potentials, and then switched off for 24 hrs. The variation of the passing current was recorded during the operation, and the potential variation after switching off the system was also monitored using data logger for the evaluation of protection.

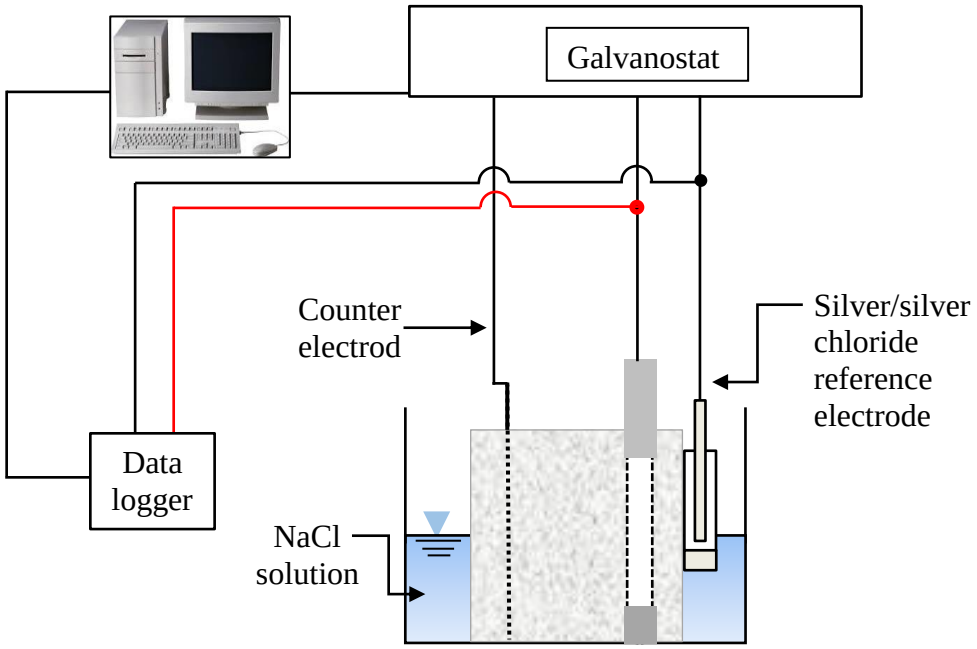

Figure 3.29: Expernintal setup for the CP test of the partially submerged specimes

3.4.6.6 Protective Potential (On Potential)

Protective potential is the potential of the embedded rebars under cathodic protection. Figure 3.30 shows a typical potential variation form of rebars under CP operation between t = 0 to t = t1. The applied CP current produces an immediate polarization, a shift from the initial corrosion potential, E_{corr}, to a new more negative value. After an initial sharp shift, the potential of the rebars presents a continuing drop in a very slow rate until reaching a stabe value called the on-potential. The on-potential equals to the true polarized potential of the

rebars plus the voltage (IR) drop due to the concrete resistance between the rebars and the reference electrode (Sathiyanarayanan et al., 2006). Silver/silver chloride (Ag/AgCl/0.5M KCl) reference electrodes and multi channels data logger of 10 Megaohm input impedance were used for the collection of all potential readings. The rebars of each specimen were connected to the negative terminal of a channel in the data logger, while the reference electrode of each specimen was connected to the positive terminal of the channel.

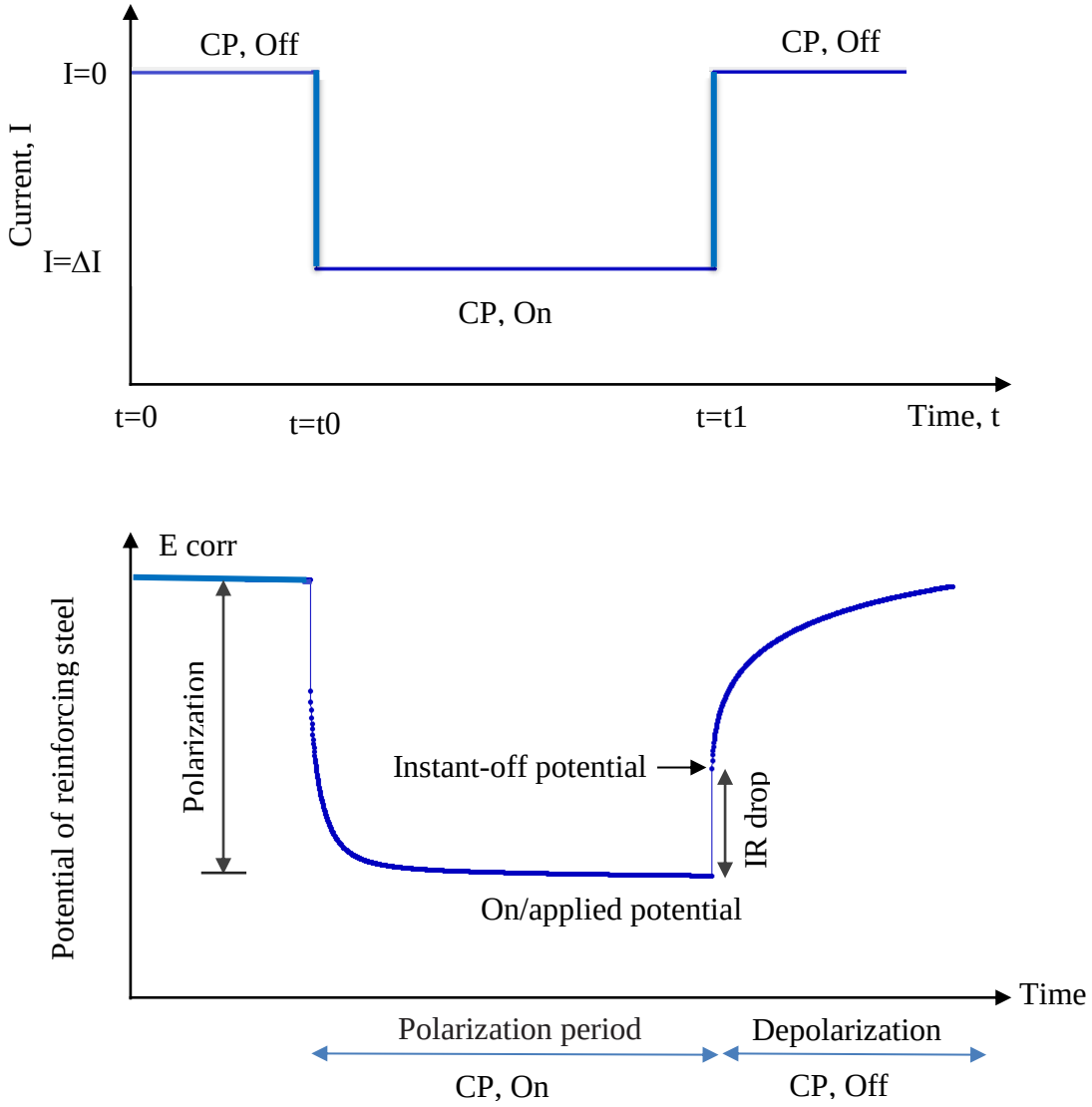

Figure 3.30: Typical potential variation under CP

3.4.6.7 Instant-off Potential

Referring to Figure 3.30 above, at time t1, when the applied CP current is switched off, the IR drop disappears and the measured potential immediately drops to a new value. Subsequently, it continues to decrease gradually until reaches to a value very close to the initial potential, Ecorr. The potential measured instantly after the switch-off of CP current is called the instant-off potential. In the present study, this was measured 1 seconds after the CP was switched off.

3.4.6.8 Four-hour Potential Decay

The four-hour potential decay criteria was adopted to evaluate the efficiency of CP. It is the potential difference between the instant-off potential and the potential measured at 4 hours after switching off the CP current. The BS EN ISO 12696 (2012) states that an at least 100mV potential decay over a maximum of 24 h after 'Instantaneous OFF' is required for an adequate CP for reinforcing steels. This criterion is consistent with that of NACE SP0290, which considers that a 4-hours CP depolarization greater than 100mV effective to protect the steels in concrete (Jeong et al., 2012). The 4-hours decay polarization criterion was adopted in the study for its popularity (Jeong et al., 2012)

3.4.6.9 Performance of Carbon Fibre as CP System Anode

The effectiveness of impressed current CP depends greatly on the correct operation of the anodes, their electrical conductivity for electrochemical process, and their service life or rate of consumption due to a number of environmental and operational factors. The anode system is required to deliver sufficient current in order to provide adequate protection for the structures. Therefore selecting the appropriate value of current contributes significantly to the minimisation or avoidance of damage to the anodes due to excessive consumption, passivation or loss of bond with the concrete (Van Nguyen et al., 2012).

The performance of CF anode was evaluated by monitoring the feeding voltage of the CP system with time (Zhu et al., 2015). Feeding voltage represents the electrical output potential from a DC source necessary to maintain a constant current density along the CP operation. It was measured as the voltage difference between the rebars cathode and the CF anode (Carmona et al., 2016; Zhu et al., 2015).

Air exposed specimens in a laboratory environment, in which the resistivity of the concrete is relatively high, incorporated with 3.5% sodium chloride concentrations were selected for this investigation. A constant current density of 20 mA/m^2 referring to the surface area of reinforcement was applied for the two specimens. To accelerate possible damage at the CF anode, higher current density of 200 mA/m^2 was also applied for two specimens of 3.5% NaCl.

Galvanostatic polarization technique as explained in section 3.4.6.5 was carried out to investigate the behaviour of the CF anode. The applied currents were maintained for 28 days, while the feeding voltage between the rebars cathode and the CF sheet anode was measured with a high impedance data logger. The increase of feeding voltage indicates a deterioration of the electrical connection in the system, since the current remained constant during the test period (Zhu et al., 2015).

Another parameter called CP circuit resistance was monitored for the seek of the performance of the CF anode (Covino Jr et al., 2002; Van Nguyen et al., 2012). It was calculated using equation (3.9) in $\Omega.m^2$. CP circuit resistance at time (t) equals to the voltage between the anode and the cathode V(t) in mV divided by the passing current density I(t) in mA/m^2. The increase of CP circuit resistance reflects a dissolution of the CF anode.

$$CR(t) = \frac{V(t)}{I(t)} \tag{3.9}$$

CHAPTER FOUR

RESULTS OF CONCRETE

RESISTIVITY AND DISCUSSION

CHAPTER 4 RESULTS OF CONCRETE RESISTIVITY AND DISCUSSION

4.1 Compressive Strength

To confirm the quality of the made concrete specimens, all the chloride free mixes using different water to cement (w/c) ratios were tested for the compressive strength at the age 28 days. Figure 4.1 shows the effect of w/c ratio on the compressive strength. As expected, the result shows that the compressive strength decreases as the w/c ratio increases. Compressive strength of concrete having w/c ratio of 0.6 is about half of that concrete having a w/c ratio of 0.4. This can be related to the increase of the amount of pores. Evidence for that is provided in Figure 4.2, which shows an increase in absolute porosity with increasing w/c ratio, and increasing w/c from 0.4 to 0.6 gave an increase of 12.5 % in the porosity. Lian et al. (2011) concluded that the strength of concrete is significantly influenced by the porosity of its pore structure. Moreover, Whiting and Nagi (2003) also reported that the w/c ratio has a significant influence on the structure of the hydrated cement paste. A low w/c ratio generally leads to a reduction in the pore volume and the total amount of pores (Sulapha et al., 2003).

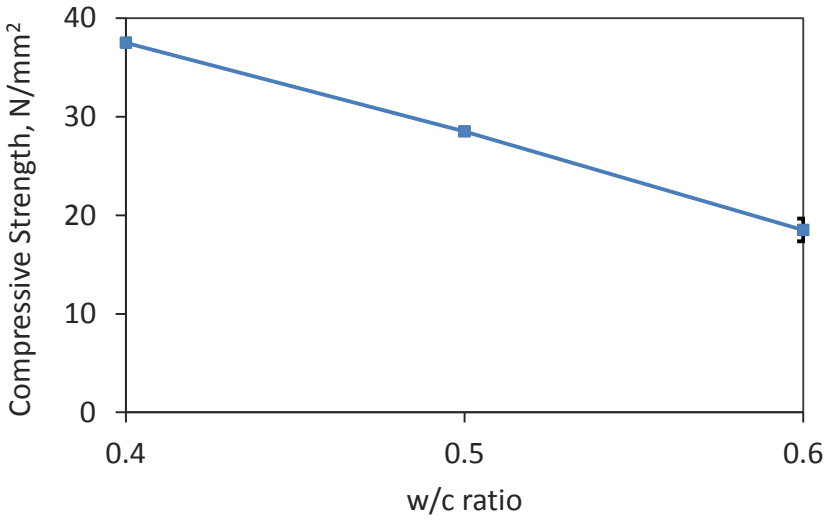

Figure 4.1: Effect of w/c ratio on compressive strength of the investigated mixture for chloride free concrete specimens

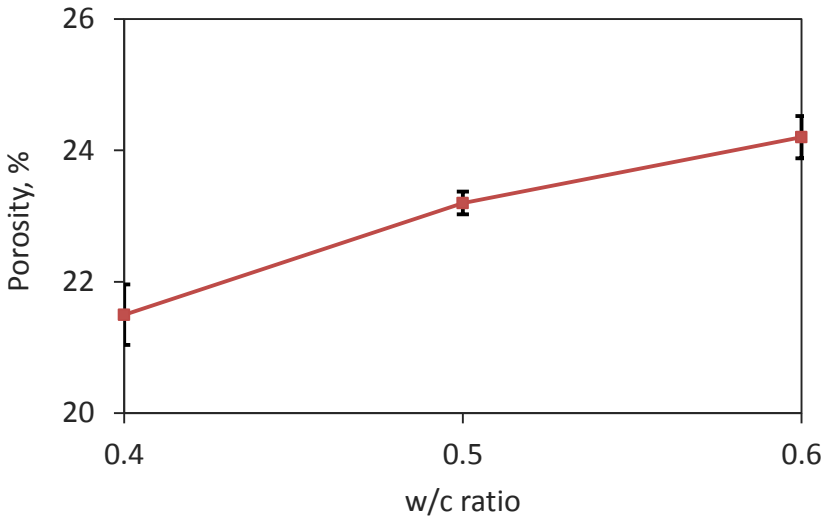

Figure 4.2: Effect of w/c ratio on absolute porosity of chloride free concrete specimens

4.2 Influence of Frequency

Figure 4.3 shows the influence of the AC frequency on the electrical resistance measurements when external electrodes of copper, a commonly used electrode material for measuring electrical resistivity of concrete, were employed. Concrete specimens produced using w/c ratio of 0.5 at two chloride contents (free chloride and 3% NaCl) in saturated state were examined in this test. Most of the time, the saturated condition is chosen as the standard moisture state (Chen et al., 2014). It can be seen that frequency has a significant influence on the measured resistivity. The use of a high frequency of 10,000 Hz reduced the measured resistivity of the two mixes by about 58% on average, compared to a frequency of 1 Hz. These obtained results indicate that the measurement at low frequencies leads to a significant increase in the measured resistivity causing overestimated values. In terms of Farnam et al. (2015), at a low frequency of less than 500 Hz, the measurement is primarily influenced by the condition at the electrode-concrete interface.

The influence of electrode-contact interface was eliminated or reduced to be minimum when internal electrodes made of CF were used as shown in Figure 4.4, where the variation of the measurements in the range of the AC frequencies becomes so small and the measured electrical resistance is almost unchanged particularly for the mix that having chloride.

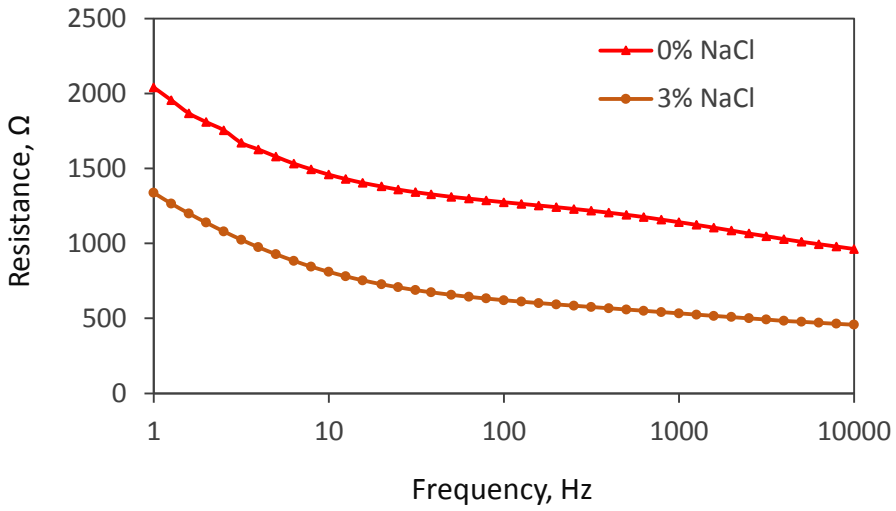

Figure 4.3: Influence of AC frequency on the electrical resistance measurement when using external electrodes of copper plates

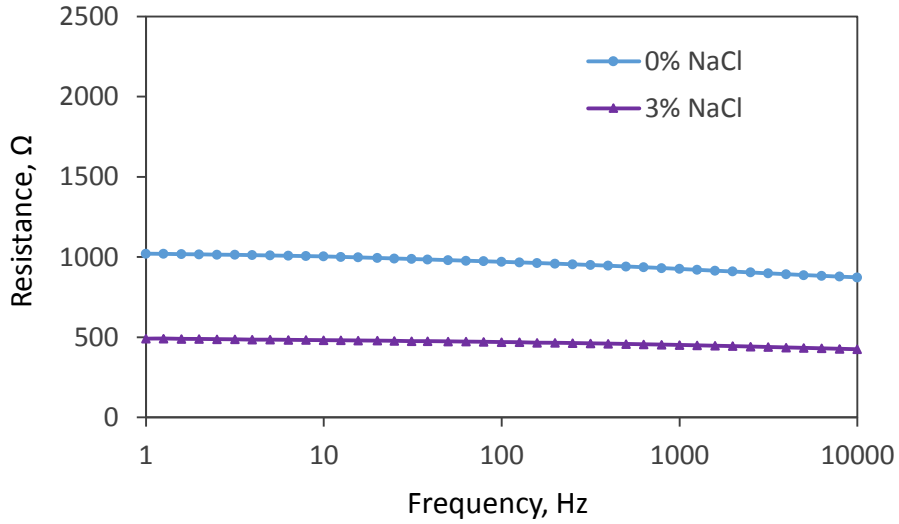

Figure 4.4: Influence of AC frequency on the electrical resistance measured using internal electrodes of CF sheet

Figures 4.5 and 4.6 compare the values of electrical resistance of the two mixture samples measured using the internal electrodes and two different external electrodes at different frequencies. It can be easily found that using carbon fibre external electrodes shows a significant improvement on the variation of the measurement compared to copper at low frequencies. This is mainly due to the flexibility of CF which can provide improvement of the contact between the electrodes and the concrete surface. However, using internal

electrode method is much lesser than external electrodes method. For instance, at low frequency of 1 Hz, using internal electrodes of carbon fibre reduced the measured resistance by 55 and 43.5% on average compared to the external electrodes of copper and CF, respectively.

It is also clear that the differences between the measured resistance decreases as the applied frequency increases. All the measurements using different approaches tend to become very close at high frequencies of 10,000 Hz. However, using CF improves the accuracy of the measurement in a wide range of AC frequencies for the internal electrode method. This is mainly due to the high stability of the contact between the electrodes and the concrete sample. Katwan (1988) concluded that the most acceptable frequency is the one that causes minimum electrode perturbation, lesser polarization effect and gives lower resistance value. Accordingly, a frequency of 10,000 Hz was adopted for all the tests in this study as the most appropriate frequency and was used for the comparison between the resistivity of different mixes under different conditions.

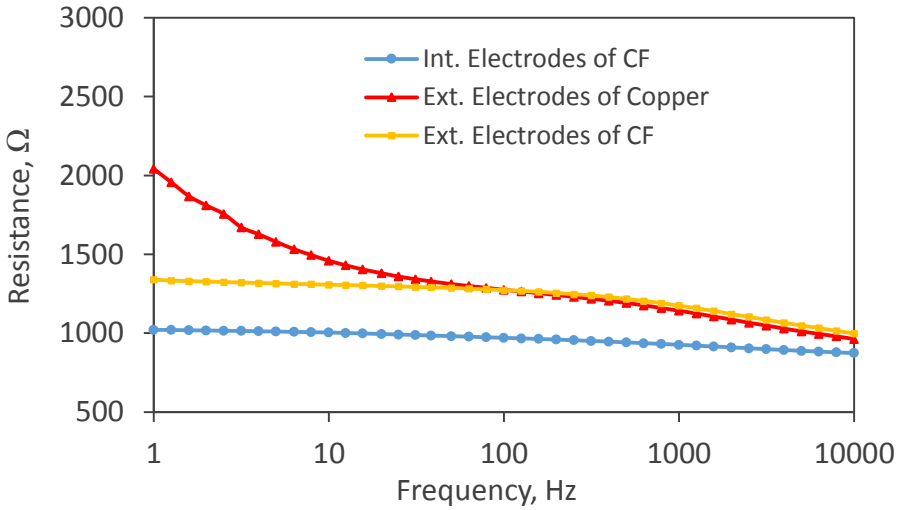

Figure 4.5: Influence of applied frequency on the electrical resistance of free chloride concrete specimens measured using internal and external electrodes

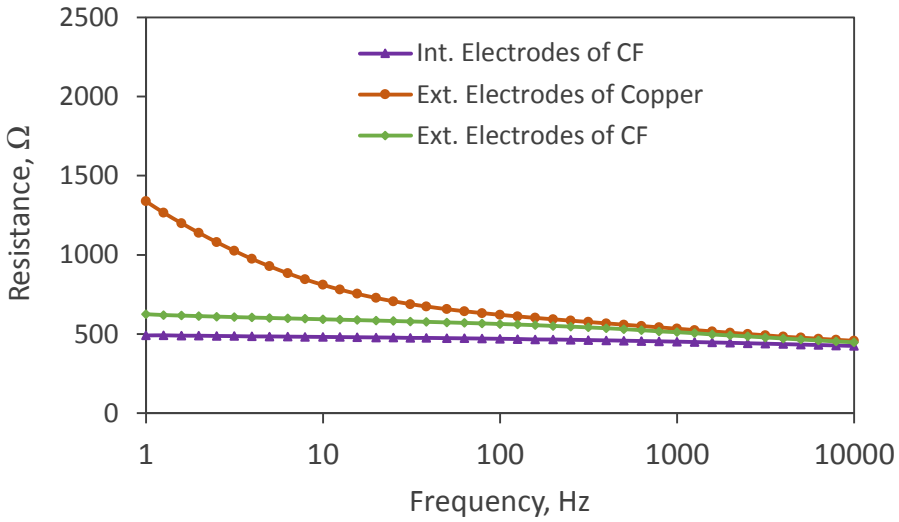

Figure 4.6: Influence of applied frequency on the electrical resistance of concrete specimens having 3% NaCl measured using internal and external electrodes

4.3 Effect of Applied Voltage

Figure 4.7 shows the relationship between the applied voltages in the range of 1 to 6 Volts and the measured currents on two mix concrete samples at saturated state using internal electrodes method. The results demonstrate a perfect linear relationship which confirms the Ohm's law. As a result, it can be concluded that the voltage value applied will not affect the resistivity measurement, and any value in this range can be used for resistance measurements. The voltage magnitude of 3V was used for the saturated specimens and 6V for unsaturated specimens due to the increased resistivity for the second case.

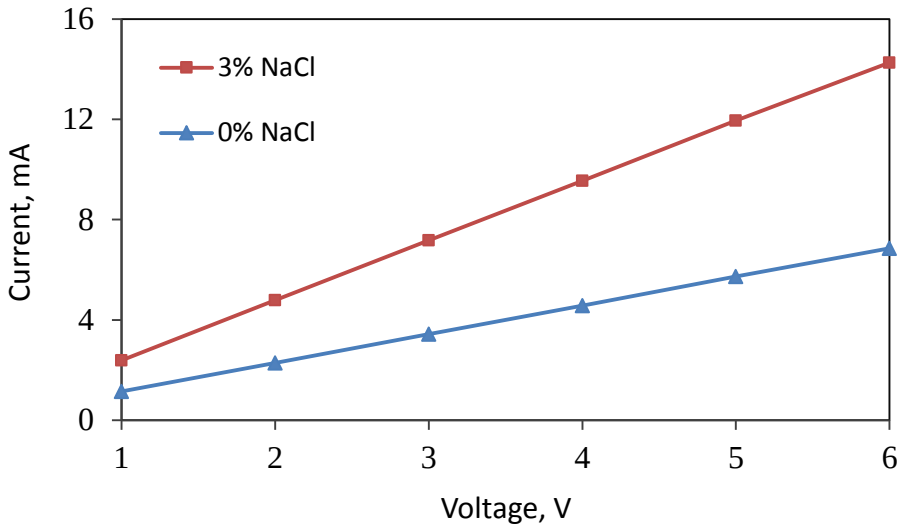

Figure 4.7: Relationship between the applied voltage and the measured current during electrical resistance measurement of concrete specimens

4.4 Effect of Electrode Configuration at Different Concrete Conditions

In order to have more information about the influence of electrode configuration on the measured resistivity when the most appropriate frequency (10,000 Hz) that concluded in section 4.2 is applied, saturated and unsaturated concrete specimens were investigated. Relative humidity of 60% has been chosen for the unsaturated specimens at this test as it represent the average humidity in site environment (Lambert et al., 2015). Concrete specimens with different amounts of added sodium chloride (NaCl) and w/c ratios were studied.

Figures 4.8 illustrates the influence of using different types of electrodes and configurations on the resistivity measurement of concrete specimens at saturated condition. It clearly shows that results obtained here confirms what observed in a previous section related to the accuracy of the internal electrode method. Using internal CF electrodes, for all of the investigated mixes, showed in general the lowest value compared to using external CF electrodes and copper electrodes. It was observed that the resistivity values of internal electrodes reached up to 10% lower than those obtained using external electrodes. These differences becomes less and less with the increase of NaCl content but there no particular influence for the change of w/c ratio.

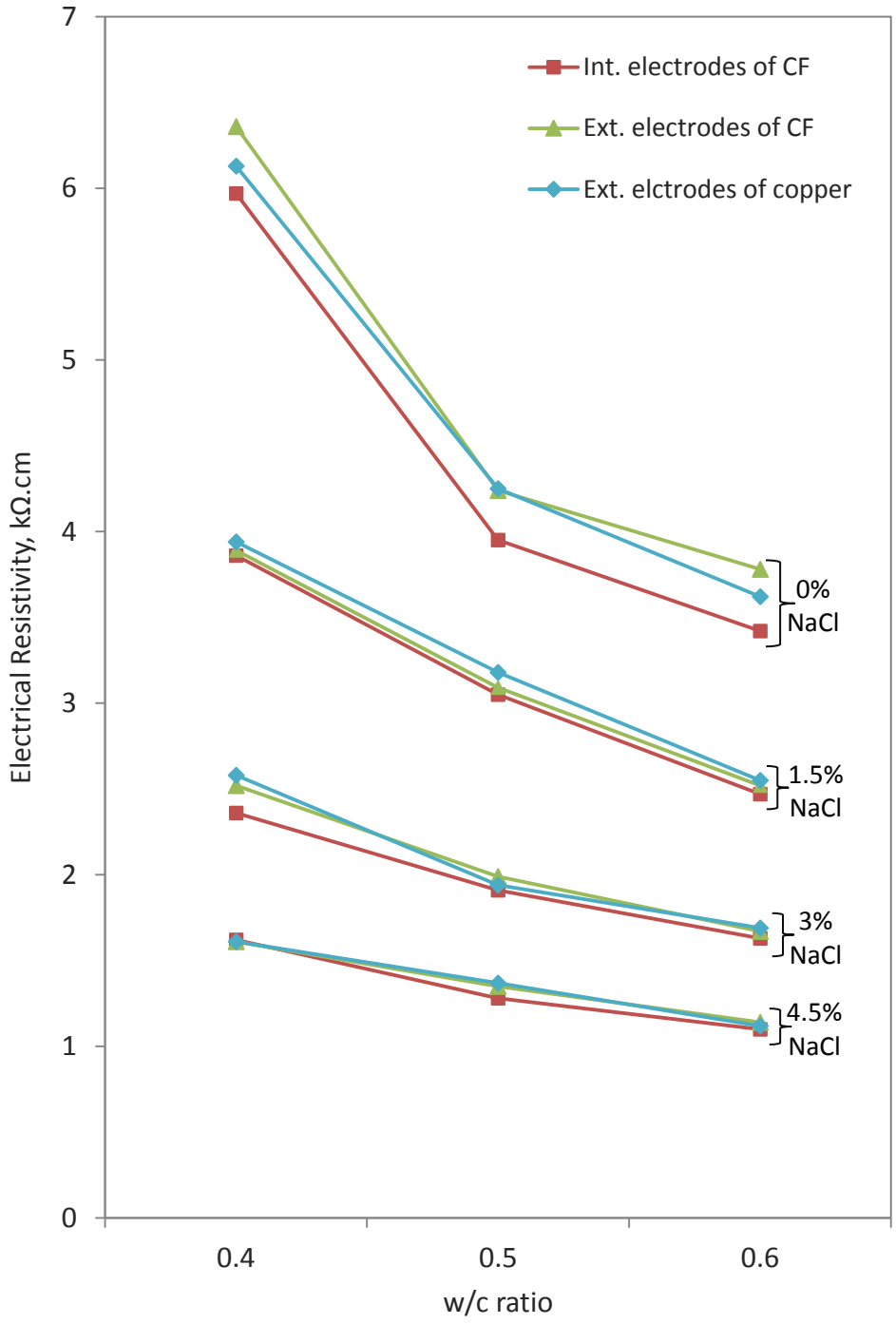

Figure 4.8: Influence of electrode type on the electrical resistivity of saturated specimens mixed with different w/c ratios and sodium chloride contents.

However, the measured resistivity for the unsaturated specimens at 60% relative humidity displays different results as shown in Figure 4.9. The use of external electrodes reduced the measured resistivity by a value up to 22% (decreases with the increase of NaCl content) compared to the use of internal electrodes. The reason for that is explained due to the water absorbed from the wet sponge, which was used in between the electrodes and the concrete for electrical contact, and thus increasing the amount of water available in the pores leading to lower resistivity than that measured using internal electrodes. As with the specimens at saturation state, the values obtained at the unsaturated condition using external CF sheets or copper plate electrodes are very close when a frequency of 10,000 Hz is considered.

In conclusion, using internal CF sheet electrode is a more reliable method which significantly improves the accuracy in all situations and can provide the following advantages. Firstly, it can be used to measure the resistivity of unsaturated specimens without affecting the internal water content that lead to underestimating values. Secondly, it eliminates any potential extra resistance due to the use of conductive medium even at fully saturated specimens. Finally, a wide range of frequency can be used with a little influence on the measured resistivity as discussed in section 4.2 above. All of these benefits are attributed to the stable contact zone between the internal electrodes and the concrete.

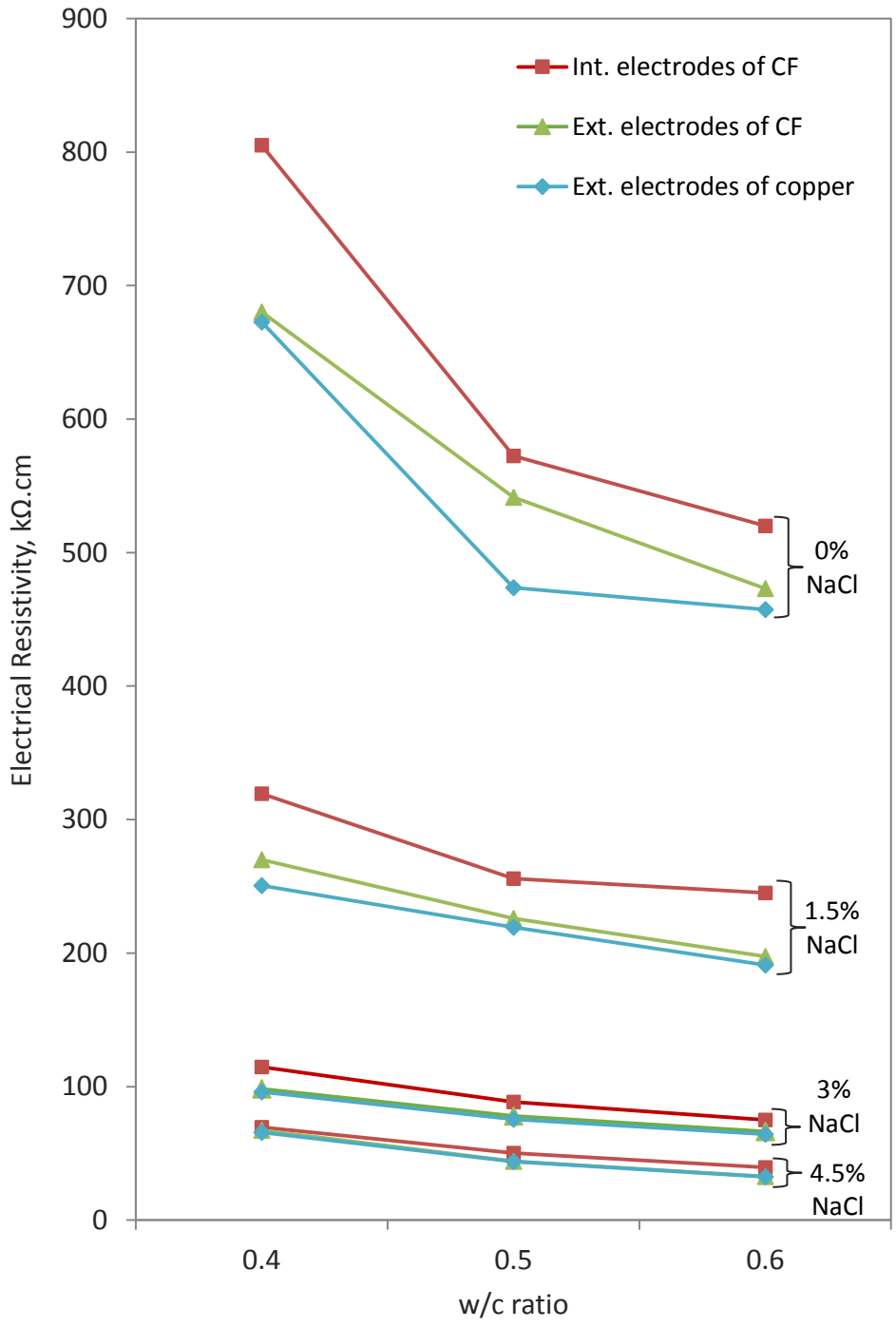

Figure 4.9: Influence of electrode type on the electrical resistivity of unsaturated specimens at 60% RH mixed with different w/c ratios and sodium chloride contents.

4.5 Effect of Chloride

In order to obtain an accurate chloride contents for quantitative approach after wet curing, free and total chlorides measurements were conducted for all the concrete specimens with different amounts of added sodium chloride and water to cement ratios. Appendix A presents the titration curves for the data obtained during the potentiometric titration method used for the determination of free and total chlorides. Figure 4.10 shows the measured free and total chloride contents in terms of both the concrete and cement weights of the samples made using different w/c ratios. The free and total chlorides in the samples of the same w/c ratio present a linear relationship. In the rest of the results, all the chloride contents are expressed in terms of the dry weight of concrete (using concrete weight rather than cement weight is considered to be more convenience for in-situ practice). Figure 4.11 replots this data, which shows that both total and free chloride contents increase slightly when w/c ratio increases. The result was reasonably related to the curing method, since when the casted concrete samples were submerged in the same salty water containing the same NaCl contents as that used for mixing, the high w/c ratio resulting in a high porosity would leave more chloride ingress into the concrete during the curing process.

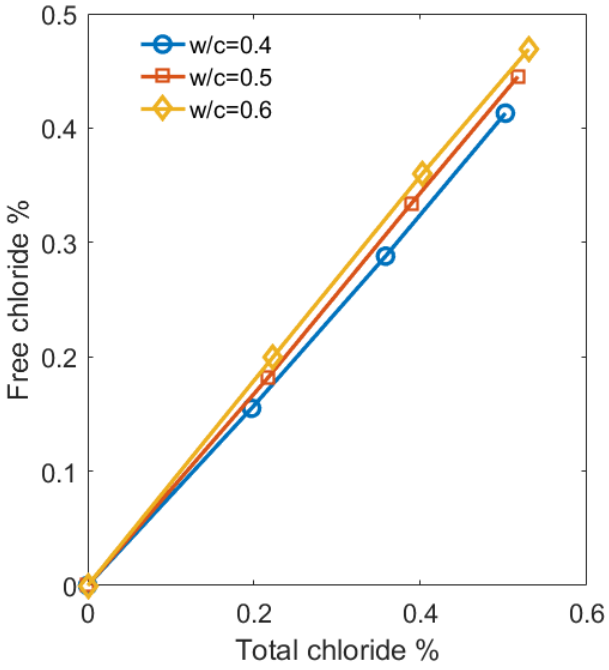

(a) Chloride in terms of concrete weight

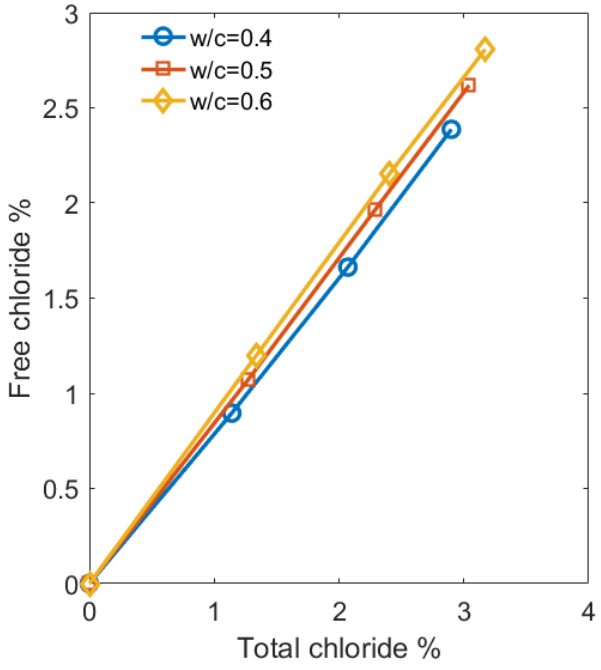

(b) Chloride in terms of cement weight

Figure 4.10: The relation between the free and total chloride content

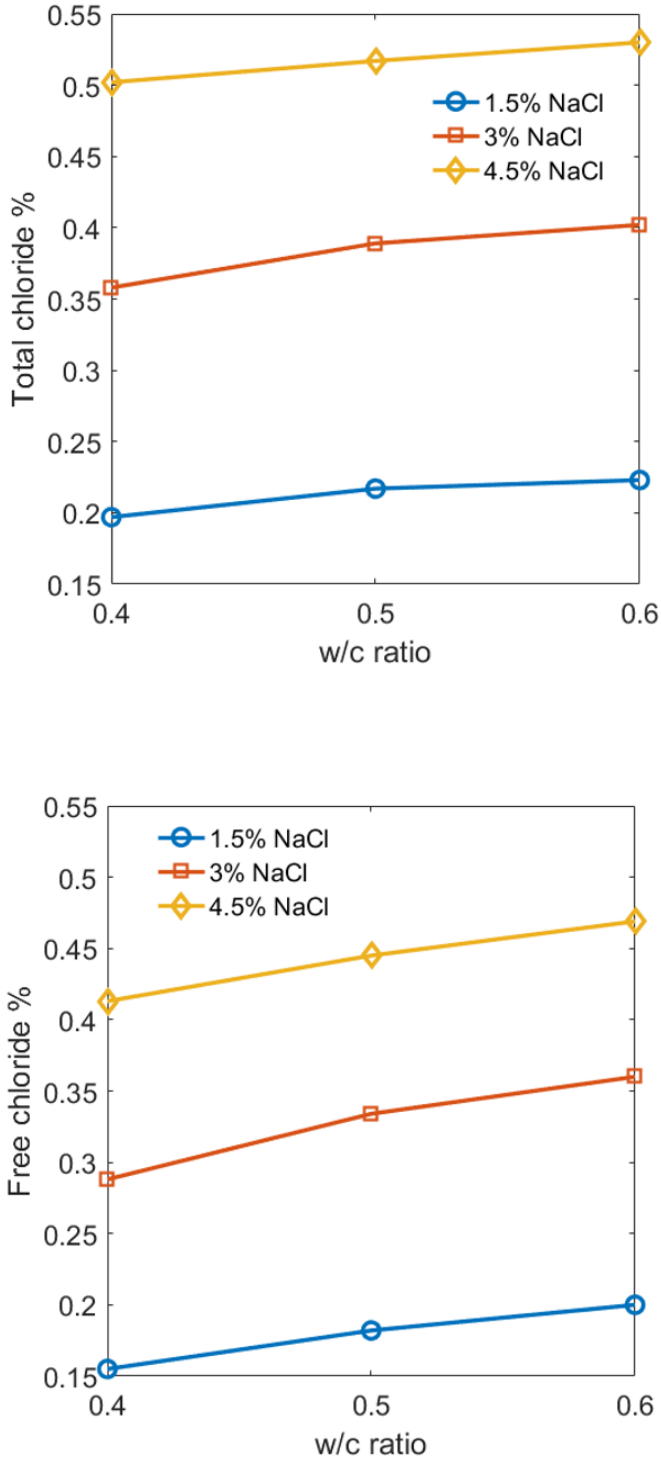

Figure 4.11: The total and free chloride content in the cured concrete samples with different added NaCl and w/c ratio

Figure 4.12 shows the effect of total chloride on the measured electrical resistivity of all the concrete specimens at different relative humidities (RH) and w/c ratios. It can be seen that, at all the w/c's, the electrical resistivity of the concrete decreases as the chloride concentration increases. In the log scaled electrical resistivity plot, the relationship between the electrical resistivity and the chloride content exhibits an approximate linear trend.

The results show there is a noticeable decrease at high concentration of chloride, particularly with those having high levels of RH. For instance, at a w/c ratio of 0.4 and 100% RH, the resistivity values of the concrete specimens which are incorporated with 0.2, 0.35 and 0.5% total chloride dropped approximately to 63, 42 and 27% respectively of those are free of chloride. Similar tendency of reduction in the resistivity due to increasing of chloride has been observed under different values of w/c and RH. The fact that electrical resistivity becomes lower as the total chloride increases is attributed to that high amount of chloride in the pore solution decreases the resistivity of pore solution (Farnam et al., 2015). The influence of chloride on concrete resistivity was studied by Hunkeler (1996) and reported that adding of 0.45% chloride by concrete mass reduced the resistivity by only 27%. Whiting and Nagi (2003) stated that the risk of a specific amount of chlorides on concrete resistivity is dependent on the type of cement and additives used in concrete. Cements blended with pozzolanic materials have higher resistivity than ordinary Portland cement (Medeiros-Junior and Lima, 2016).

From figure 4.12, it is also can conclude that for a fixed w/c, reducing the RH decreases the effect of chloride on resistivity. However, at a certain chloride content and w/c, the lower the RH (moisture content), the higher the concrete electrical resistivity. For example, at a w/c ratio of 0.4 and 0.2% chloride, reduced the RH from 100 to 80, 60 and 35% increased the resistivity from 3.8 to 54.6, 319.4 and 1315 kΩ.cm respectively which indicates that RH has a significant impact on the resistivity more than the influence of chloride.

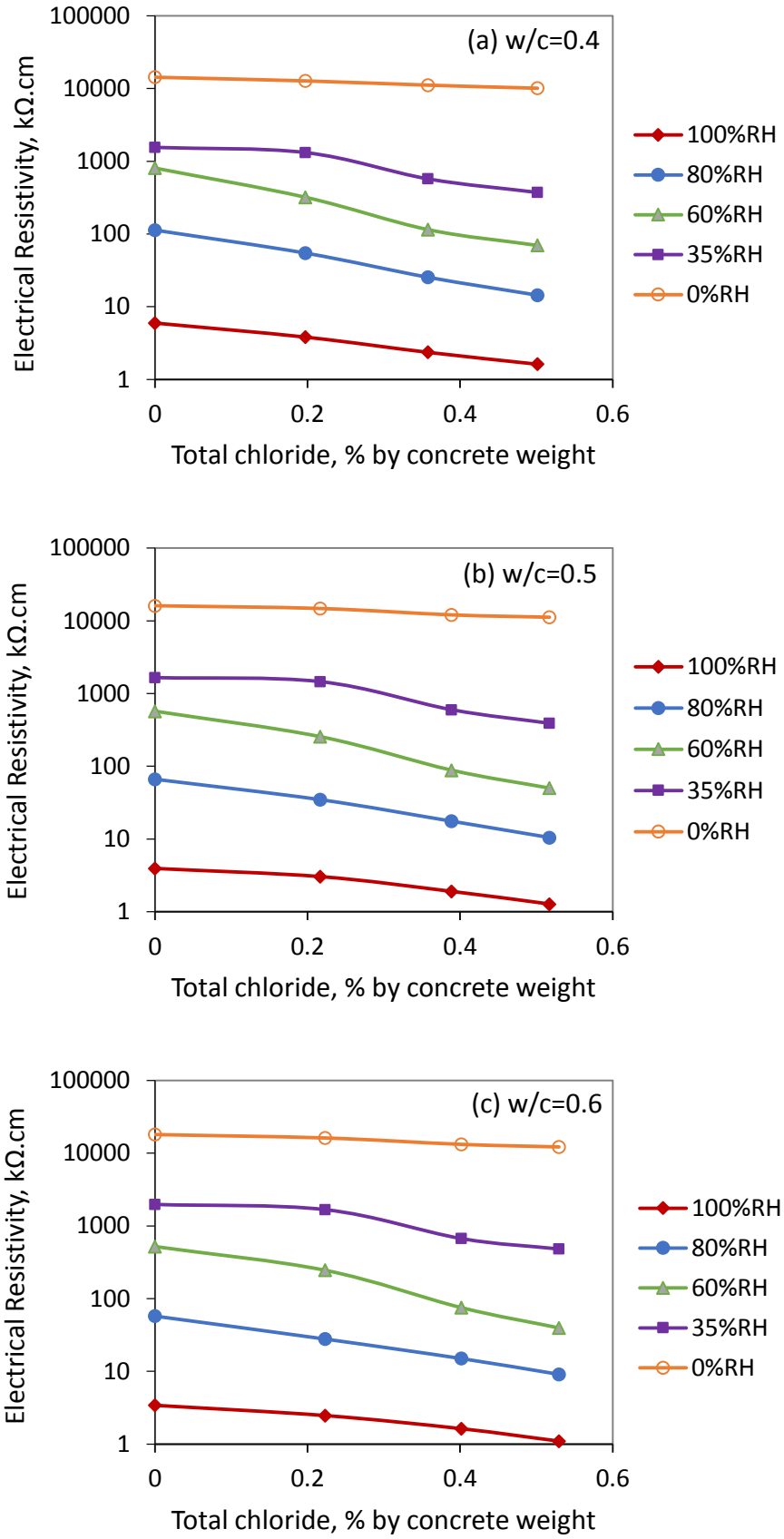

Figure 4.12: Chloride effect on the electrical resistivity measured using internal electrodes of CF sheets at varied RH and w/c.

4.6 Effect of Water to Cement (w/c) Ratio

As stated in the previous section, for a single amount of added NaCl, total chloride is changing with w/c ratio, but for comparison, a single chloride content is required to study the influence of w/c ratio on the measured resistivity in details for the mixes of different chloride contents and relative humidities as shown in Figure 4.13. It is worth noting that the values of this Figure were derived from the data of Figure 4.12 in previous section using polynomial fitting with an R^2 of greater than 0.99.

It can be noticed, there is a general tendency towards lower resistivities with the increase of w/c ratio for all the mixes of different chloride contents at high RH of 100, 80 and 60%. For specimens with 0% chloride (Cl), increasing w/c from 0.4 to 0.5 and 0.6, about 35 and 43 % reduction on average was observed for specimens at RH of 100, 80 and 60%. This is due to that water to cement ratio is a major parameter in determining the pore structure of concrete. Increasing the water to cement ratio will increase the pore size and the connectivity of pore network, and decrease the electrical resistivity of concrete at high water content (Van Noort et al., 2016).

It is also evident that for a chosen w/c, decreasing RH increased the resistivity by tens to hundreds of kΩ.cm. For instance, at w/c of 0.4 and 0% chloride specimens, decreasing RH from 100 to 80 and 60%, increased the electrical resistivity from 6 to 113 and 805 kΩ.cm respectively. At w/c of 0.5, those differences are 4, 66.4 and 572.4 kΩ.cm. The same trend has been obtained with w/c of 0.6 and all other mixes with various amount of chlorides indicating that moisture content is the main controlling factors and seems to be much important than the influence of w/c.

The trend of reduction in resistivity when w/c increased is in agreement with previous observation reported by Monfore (1968), Gjørv et al. (1977), Lübeck et al. (2012), Chen et al. (2014) and Van Noort et al. (2016), but different values of reduction were found due to variation in the experimental setup and the technique used for the resistivity measurement and some studies were just limited to free chloride and wet exposure conditions. Another study has noted no significant influence on the electrical resistivity of unsaturated specimens at 65% RH when w/s ratio changed from 0.4 to 0.6 (Medeiros-Junior and Lima, 2016).

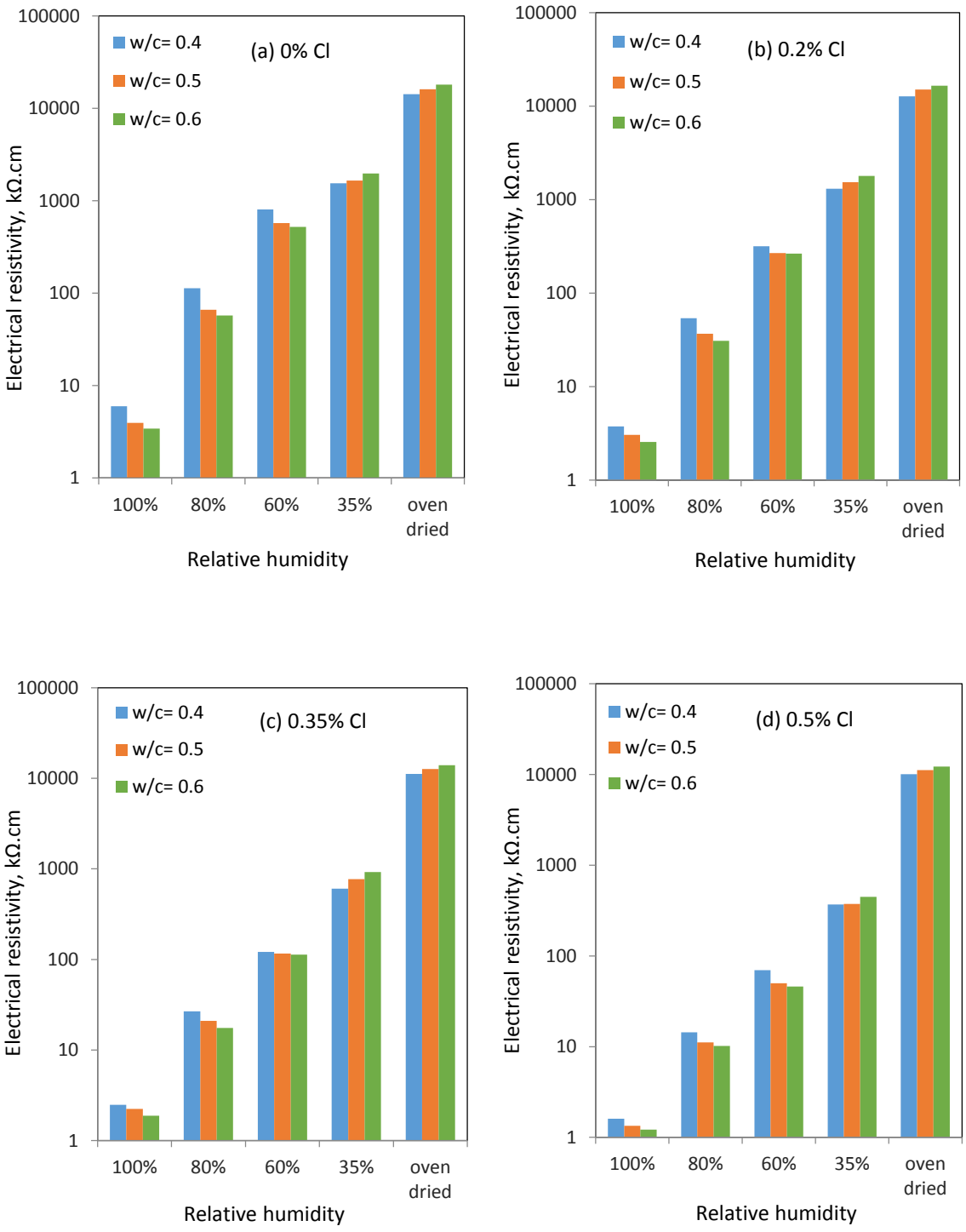

Figure 4.13: Effect of w/c ratio on electrical resistivity of concrete specimens at various relative humidities and chloride contents

However, at a low RH, at 35% RH or oven-dried as illustrated in Figure 4.13, resistivity increases with the increase of w/c ratio which is the opposite of the relationship presented for the high levels of RH, which means the resistivity of concrete is affected directly by the degree of saturation not w/c ratio. Interestingly, the resistivity of specimens mixed with w/c ratio of 0.6 is approximatly 29% on average higher than that of the specimens mixed with w/c ratio of 0.4. This is due to that at low water contents, most pores, particularly of big sizes, are empty and occupied by air, and air is electrically inconductive. So the lower the water content and the higher the w/c ratio, the higher the electrical resistivity. A 40% of RH has been identified by Hunkeler (1996) for capillary water to be avialable and any water below this level is concidered not conductive and the resistivity tends to be very high. Howevor, A study by Gjørv et al. (1977) showed that resistivity decreases with w/c correspondingly even at low RH of 40% and it is more pronounced compared to wet exposure and high RH conditions. Another study by Chen et al. (2014) on concrete specimens with low RH at oven dry or 40% RH using four-point Wenner method and observed such measurements are inappropriate as they were too dry to form conductive paths. Such results suggest that a correlation between electrical resistivity of concrete with amount of water is very important for a clear vision and to provide quantitative approach for practical application.

4.7 Effect of Water Content

Moisture content is an environmental factor that can significantly influence the values of concrete resistivity and can be considered the most controlling factor as most of electric charge passes through the concrete microstructure is carried by ions of the pore solution. The values presented here are the result of water amount for five relative humidities of 100%, 80%, 60%, 35% and 0%. The water content were determined using the following equation (Saleem et al., 1996):

$$m\% = \frac{(W - Wd)}{Wd} \times 100 \qquad (4.1)$$

where, m is the moisture content %, W is the weight of sample in each RH (gm) and Wd is the oven dry weight (gm)

To determine the amount of water accurately for each RH, specimens were placed in humidity chamber at the designated humidity and a uniform moisture content was reached when the variation of weight in 24 hours was less than 0.01g (Villagrán Zaccardi and Di Maio, 2014).

Figure 4.14 shows the measured electrical resistivity of chloride free concrete at different water contents and their corresponding pore water saturation degrees (the ratio of the water content at a certain RH to the water content at saturated state), respectively. A significant influence of water content on the concrete electrical resistivity can be observed. The electrical resistivity decreases sharply and nonlinearly with the increase of the water content or water saturation degree. It also can be seen that at a certain absolute water content, the porosity change in the three w/c range has almost negligible influence on the concrete resistivity. However, porosity effect has to be taken into account independently when the water effect is quantified using water saturation degree.

Figure 4.15 shows the measured water contents in all samples when reaching the equilibrium with the controlling RH. It presents a very important characteristic of the concrete, the water vapour sorption isotherm. Interestingly, the water content in the concrete depends not only on the environmental relative humidity but also on the chloride content. This result verified a previous research which stated that the water vapour sorption isotherm and the underlying capillary water condensation mechanism are intrinsically linked to the interfacial physiochemical interaction at pore surfaces in concrete (Wang et al., 2012), which is influenced by both free and bound chloride contents in this case. Under the same RH conditions, the higher the chloride content, the more the water condensed in pores.

Figure 4.16 compares porosity expressed as w/c ratio influences on the electrical resistivity of the concrete samples at different water contents and at a near constant chloride content (the difference of total chloride content for each comparison is no more than 0.05%). It can be seen that when water content is small, saying less than 5%, the influence of porosity on the electrical resistivity is negligibly. The results are in good agreement with those shown in Figure 4.14.

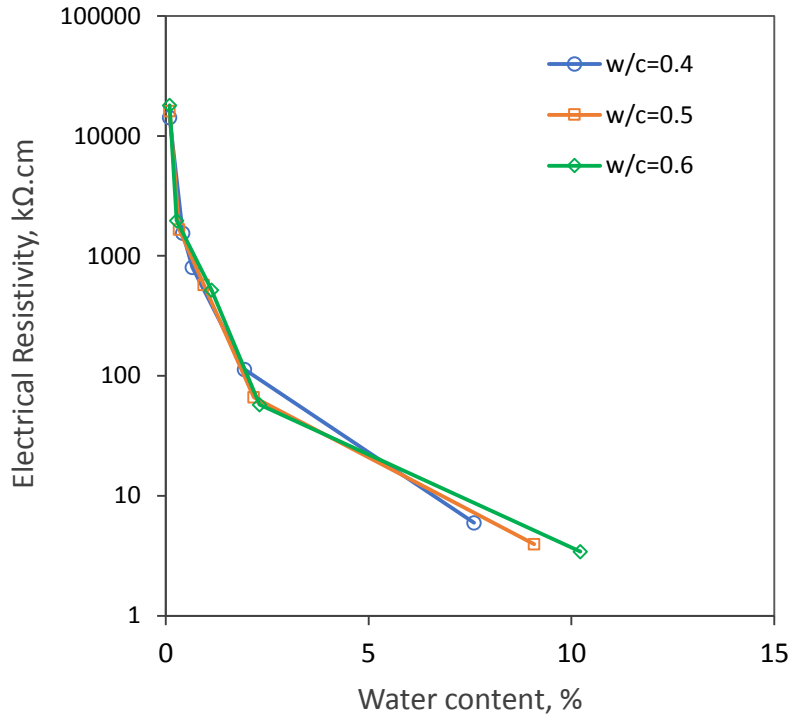

(a) Electrical resistivity vs water content

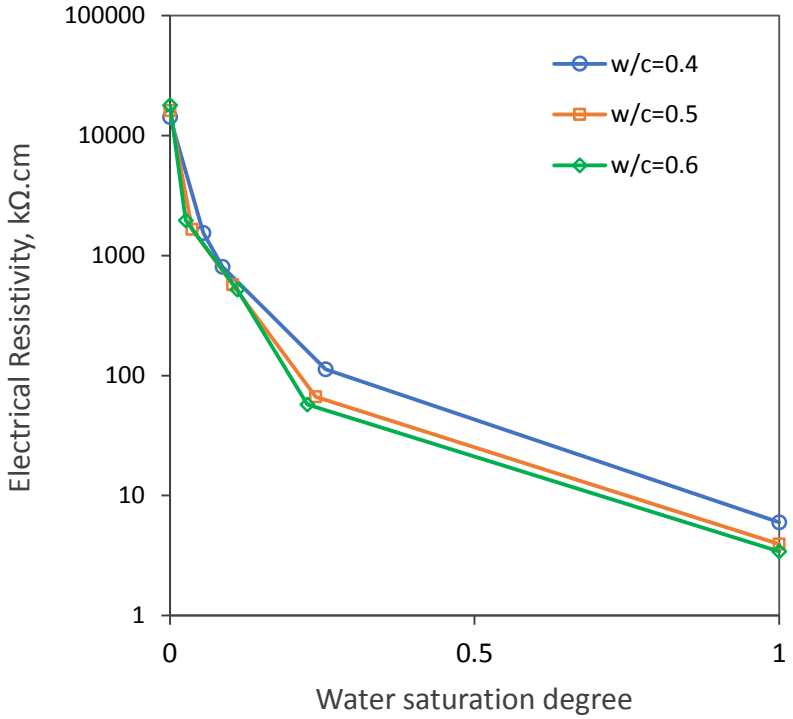

(b) Electrical resistivity vs water saturation degree

Figure 4.14: Water effect on the electrical resistivity of the chloride free concrete

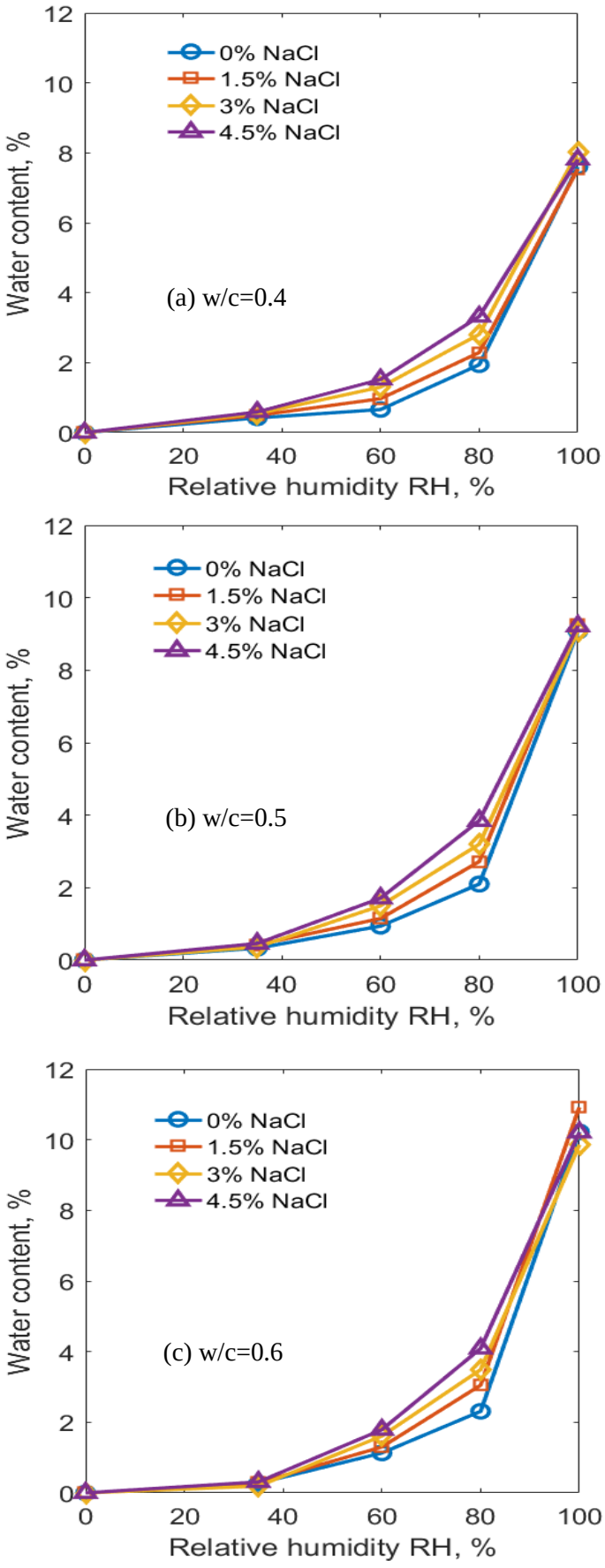

Figure 4.15: Equilibrium water content of the concrete under controlled relative humidity

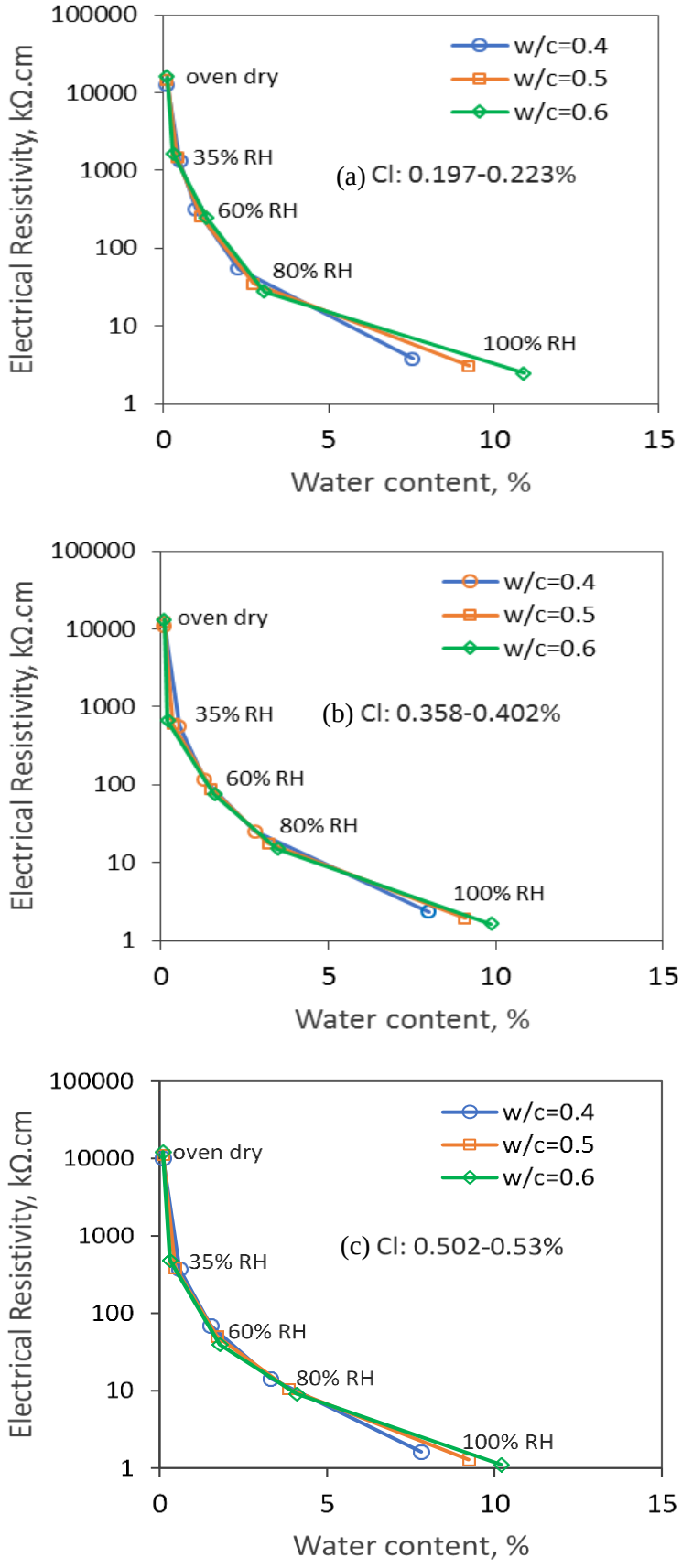

Figure 4.16: Water effect on concrete electrical resistivity at different chloride contents

Also, it can be seen that the change in the resistivity is very sensitive to the amount of water in the pores of concrete even at the highest chloride used in the study, the resistivity of the concrete specimens is very high at low water contents. This is due to that, as explained before, at low water contents large pores are empty and less liquid is available in pores, which significantly reduce the passing current and therefore increasing the electrical resistivity of concrete.

Using the obtained results by this study, and the threshold limit of 10 kΩ.cm (Hope et al., 1985; Morris et al., 2004; Morris et al., 2002) for the resistivity of reinforced concrete to be considered at high risk form corrosion, all the specimens at 100%RH independent of chloride contents fall below the threshold level. However, specimens at such high level of moisture content are unlikely to corrode due to the limited availability of oxygen (Poursaee and Hansson, 2009; Soleymani and Ismail, 2004). It can also be observed that increasing total chloride to 0.5% by concrete weight decreased the threshold moisture content by 45% compared to 0% chloride specimens (Figure 4.14). According to previous recommended interpretation (Andrade and Alonso, 1996), low to high corrosion rate is considered when concrete resistivity is between 10-100 kΩ.cm. Based on this interpretation and the obtained results, it can be conclude that water content in the range of (1.9-5.8)%, (1.3-4.7)% and (1.2-3.8)% are enough to produce these classifications of corrosion rate for the specimens that having total chloride of (0.197-0.223)%, (0.358-0.402)% and (0.502-0.530)% , respectively. In other words, reinforced concrete specimens with high salt concentration can sustain corrosion even at RH less than 60%, while unlikely for specimens with chlorides less than 0.2%.

CHAPTER FIVE

CP FOR AIR EXPOSED

CONCRETE SPECIMENS

CHAPTER 5 CP FOR AIR EXPOSED CONCRETE SPECIMENS

5.1 Chloride Contents, Corrosion Potential and Concrete Resistivity

The free and total chloride contents in the cured specimens of each mixes with different added NaCl were measured as with the previous chapter which are listed in the Table 1, where chloride contents are expressed in terms of the percentage of the concrete weight of specimens. It is clear that both free and total chloride increases with the increase of added sodium chloride, and a linear relationship was observed between free and total chloride contents as presented in Figure 5.1. Figures A.10 to A.13 in Appendix A show the titration data obtained for the determination of total and free chloride contents.

Table 5.1: Total and free chloride content in cured specimens for different added NaCl

Added NaCl % cement weight	0	1	2	3.5	5
Measured total Cl^- % concrete weight	0	0.141	0.246	0.391	0.571
Measured free Cl^- % concrete weight	0	0.115	0.183	0.324	0.475

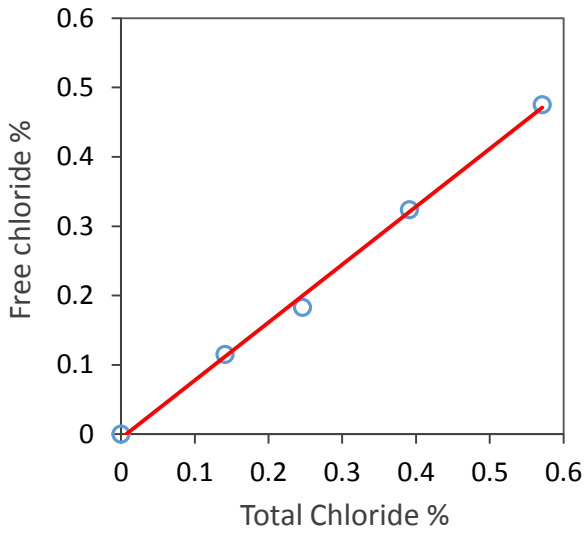

Figure 5.1: Relation between free and total chloride content for specimens of w/c of 0.4 and different added NaCl

Figure 5.2 shows the chloride effects on the corrosion potential of reinforcement in terms of the total chloride contents, where the potential was measured against the Ag/AgCl/0.5KCl reference electrode. It can be seen there was a strong correlation between corrosion reinforcement potential and the chloride contamination degree. The reinforcement in the chloride free specimens have a potential just above -135 mV (equivalent to -200 mV with respect to the reference CSE), which indicates of a low risk of corrosion according to the ASTM standard C876. When the chloride content increased, the potential of reinforcement significantly reduced to a more negative value. According to the same standard, the probability of reinforcement to corrode is 90% if potential is below -285 mV, a value corresponding to a chloride content of 0.141%, which may indicate a criterion for the start of active corrosion due to breakdown of the passive layer of rebars. The result that the potential value becomes more negative with the increase of chloride content is in agreement with that found by Oh et al. (2003) and Yodsudjai and Pattarakittam (2017), and is also consistent with the role of chlorides in the corrosion process. The relationship between the corrosion potential and the chloride content presents a non-linear trend which is in agreement with the study of Yodsudjai and Pattarakittam (2017). However, Oh et al. (2003), reported a linear correlation between the corrosion potential and chloride content.

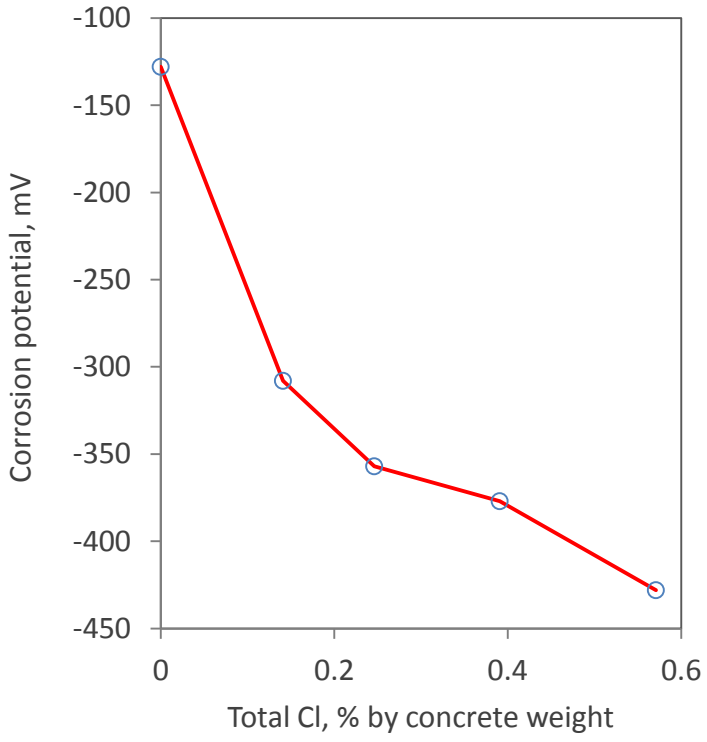

Figure 5.2: Influence of chloride concentration on steel corrosion potential in concrete

Due to convenience of measuring, electrical resistivity of concrete has been popularly employed to evaluate the risk of corrosion of rebars in the design of cathodic protection system. Figure 5.3 shows that the concrete resistivity decreases linearly with the increase of chloride content. An earlier study (Morris et al., 2004) concluded that very high corrosion occurred when resistivity was less than 10 kΩ.cm, and the corrosion became low to moderate if resistivity was more than 30 kΩ.cm. Another study (Sadowski, 2013) showed a very high probability of reinforcement corrosion in concrete when concrete resistivity was lower than 5kΩ.cm measured using the four-point Wenner method, and the probability was moderate when concrete resistivity was higher than 5 kΩ.cm. Figure 5.4 shows relation between the corrosion potential and the concrete resistivity in terms of the result in Figures 5.2 and 5.3. It can be seen that under the chloride contaminated condition, a passive region (corrosion potential is more positive than -135 mV) approximately has a resistivity greater than 18 kΩ.cm. The reinforcement may suffer a severe corrosion when concrete resistivity is less than 16 kΩ.cm with a corrosion potential of -300 mV.

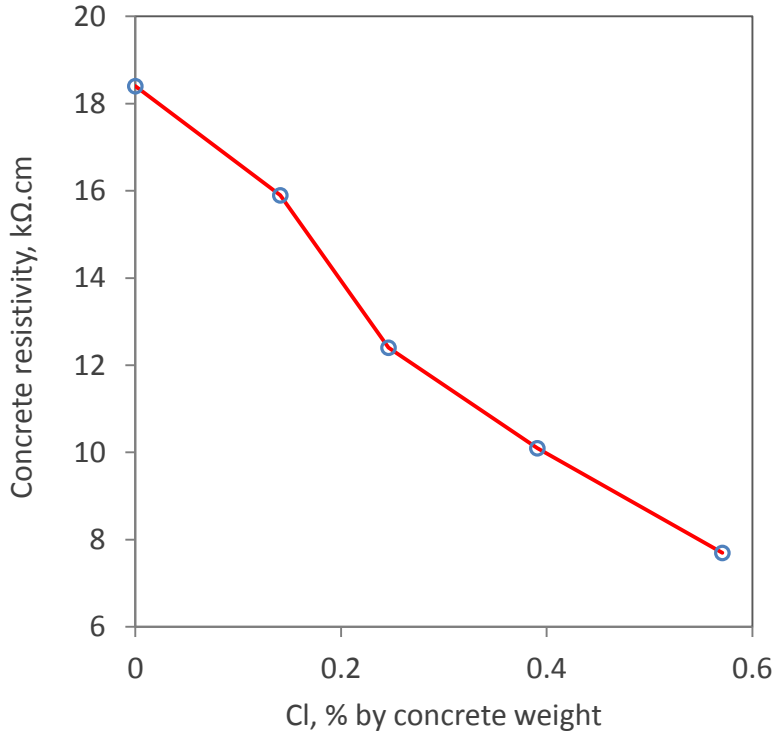

Figure 5.3: Influence of chloride content on concrete resistivity

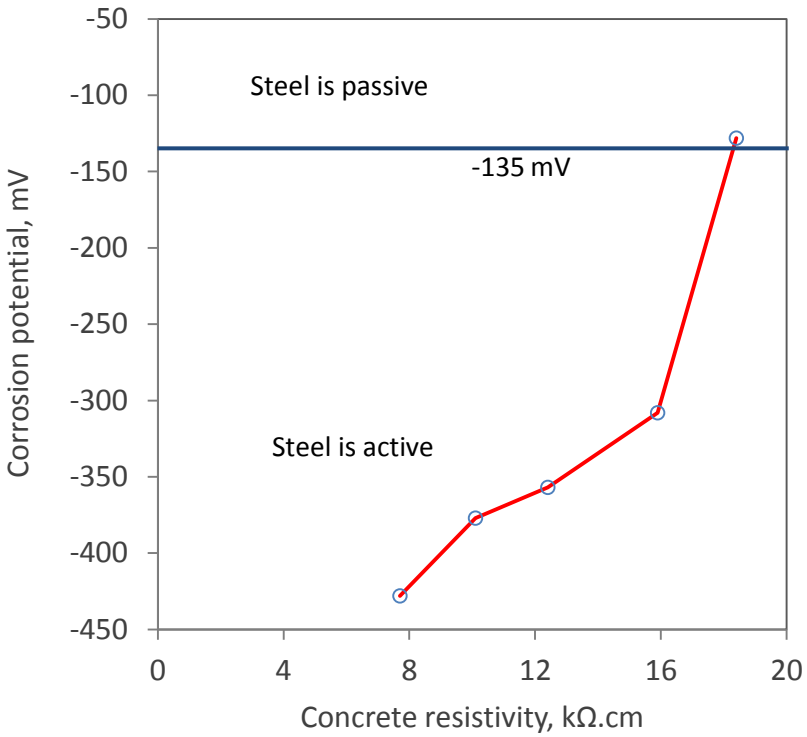

Figure 5.4: Corrosion potential vs concrete resistivity

5.2 Corrosion Rate

As explained in Chapter 3, polarization resistance (Rp) method was adopted to measure the instant corrosion rate of rebars embedded into concrete specimens of varied chloride contents. The data of Rp measurement for all specimens of five different chloride contents are presented in Figure 5.5. Most of the specimens present an obvious linear relationship between the applied potential and the measured current at zero current except the chloride free ones which present a sharp slope at the point of zero current.

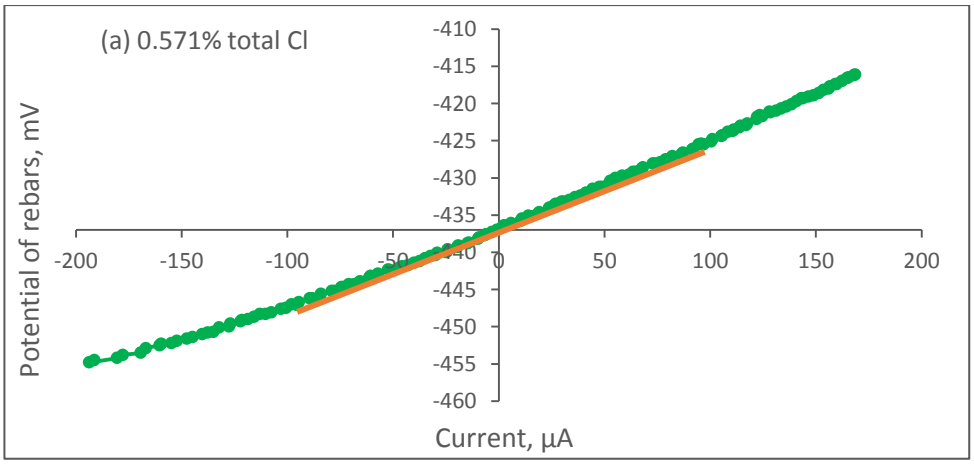

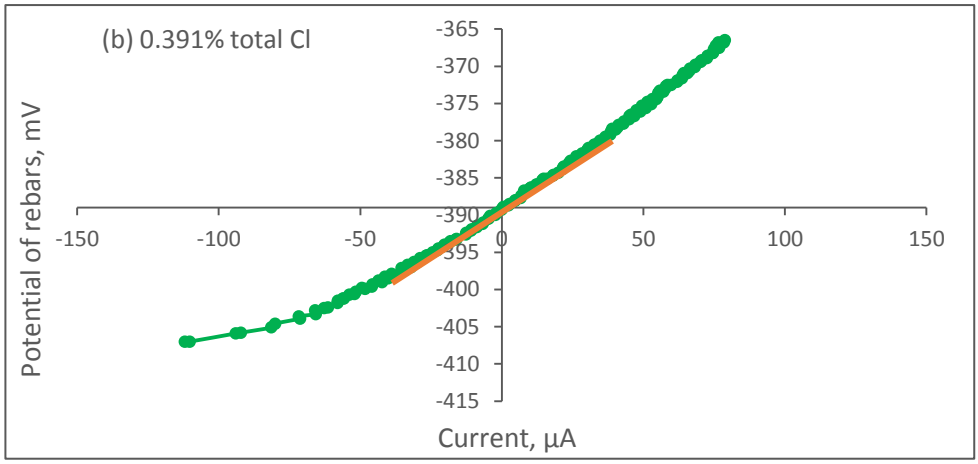
(b) 0.391% total Cl
Potential of rebars, mV
-365
-370
-375
-380
-385
-390
-395
-400
-405
-410
-415
-150
-100
-50
0
50
100
150
Current, µA

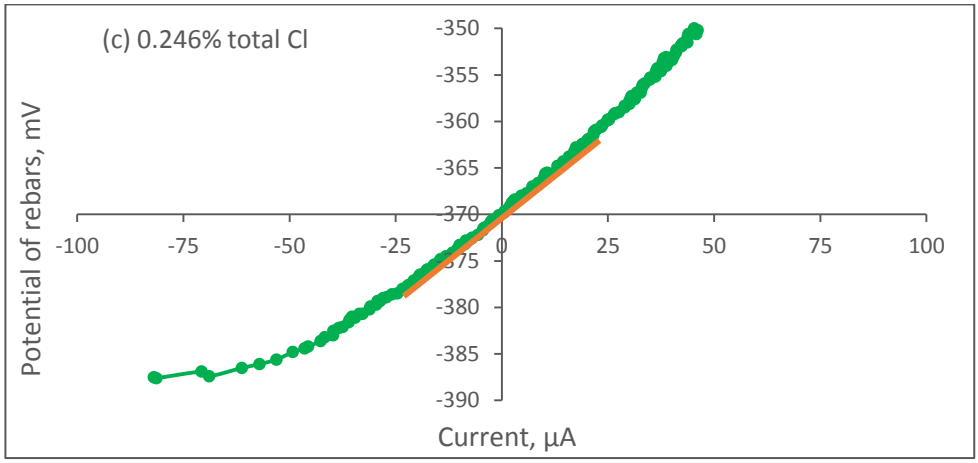
(c) 0.246% total Cl
Potential of rebars, mV
-350
-355
-360
-365
-370
-375
-380
-385
-390
-100
-75
-50
-25
0
25
50
75
100
Current, µA

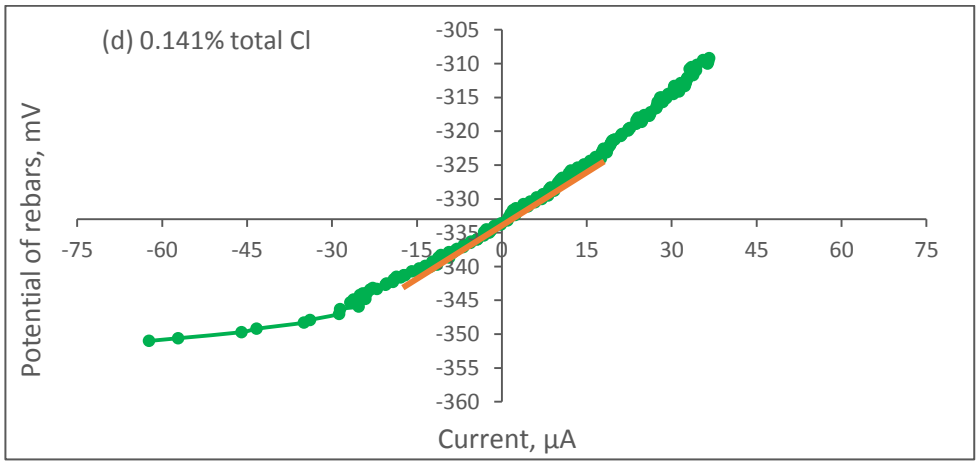
(d) 0.141% total Cl
Potential of rebars, mV
-305
-310
-315
-320
-325
-330
-335
-340
-345
-350
-355
-360
-75
-60
-45
-30
-15
0
15
30
45
60
75
Current, µA

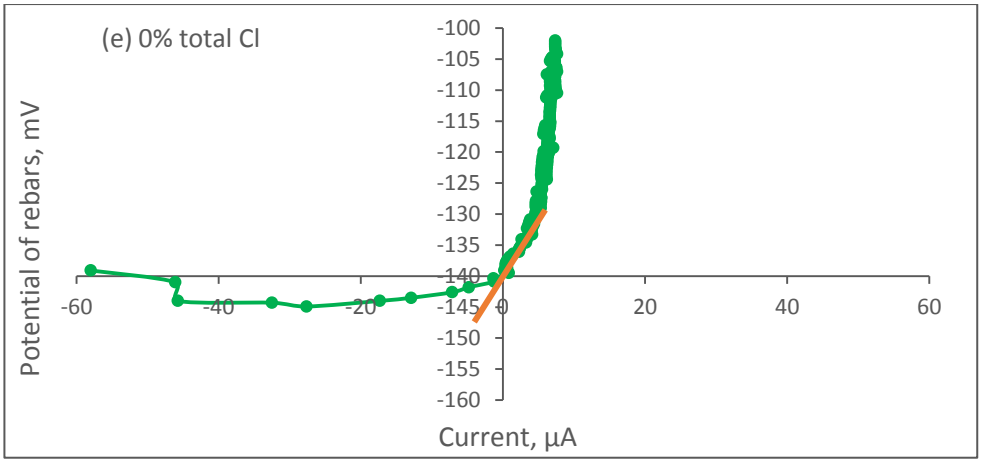

Figure 5.5: Polarization resistance data for specimens mixed with different chloride contents

Figure 5.6 shows the corrosion rates worked out on the obtained values of Rp at different chloride concentration. It can be seen that the reinforcement in the chloride free specimens presents a very low corrosion rate, and the corrosion rate increases with the increase of chloride content.

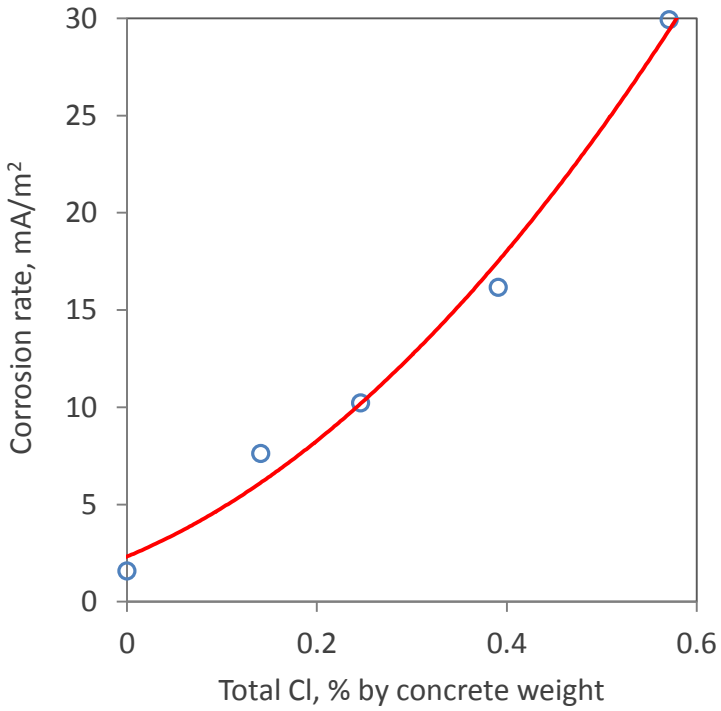

Figure 5.6: Influence of chloride concentration on steel corrosion rate in concrete

Figure 5.7 plots the relationship between concrete resistivity and corrosion rate in term of the data in Figures 5.3 and 5.6. It shows that reinforcement corrosion rate decreases with the increase of the electrical resistivity of the concrete.

Previous research (Broomfield, 2007) suggested that corrosion risk is considered to be low when corrosion rate is in the range of 1~5 mA/m^2, moderate when in the range of 5~10 mA/m^2, and high when greater than 10 mA/m^2. In terms of the classification, reinforcements will have a low corrosion rate if the total chloride content is less than 0.1% by concrete weight (equivalent to 0.58% by the mass of cement) and this chloride content may be taken as a threshold for the risk posed by reinforcement corrossion. The threshold value is in agreement with that recommened in literature (Bertolini et al., 2009), in which the critical chloride content is in the range of 0.4 to 1% by weight of cement. If chloride content is over 1.2% by weight of cement (equivalent to 0.208% by concrete weight), reinforcements present a high corrosion rate. In terms of the concrete electrical resistivity, reinforcements will have a low corrosion rate if the concrete electrical resistivity is higher than 17 kΩ.cm, or a high corrosion rate if the concrete resistivity is less than 15 kΩ.cm. These results are quite close to that obtained above based on the potential evaluation.

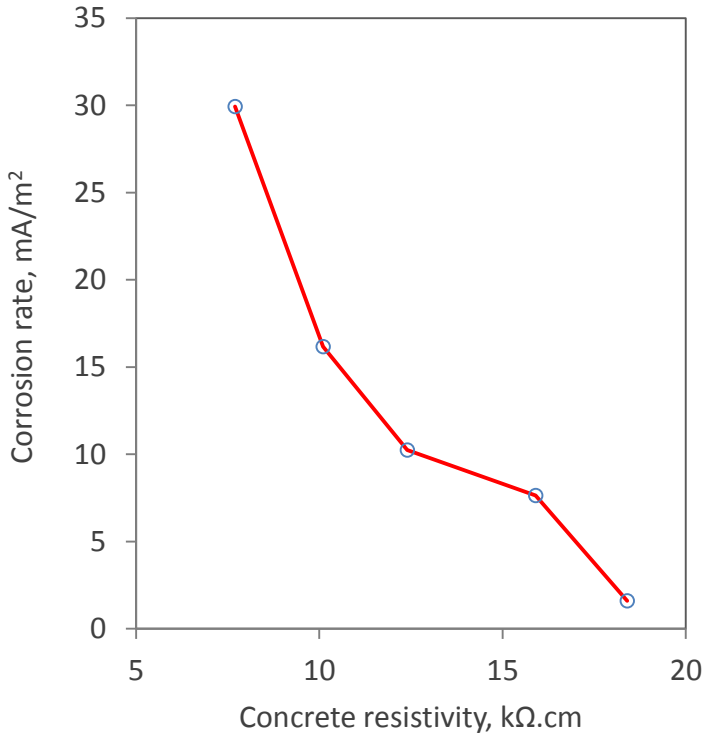

Figure 5.7: Correlation between corrosion rate and concrete resistivity

Table 5.2 shows a summary of the chloride effect on the parameters of corrosion rate, corrosion potential and electrical resistivity of concrete.

Table 5.2: The influence of chloride content on corrosion rate, corrosion potential and electrical resistivity of concrete

Total chloride content,% by concrete weight	Concrete resistivity, kΩ.cm	Corrosion rate, mA/m^2	Risk of corrosion according to corrosion rate, Broomfield (2007)	Corrosion potential, mV	Probability of corrosion, ASTM C876
0	18.4	1.59	low	-128	10% (passive)
0.141	15.9	7.62	moderate	-308	90%
0.246	12.4	10.23	high	-357	90%
0.391	10.1	16.17	high	-377	90%
0.571	7.7	29.93	very high	-428	90%

5.3 Effect of CP Operating Time on Instant-off Potential

Figure 5.8 shows the variation of the instant-off potential of the reinforcements with the time of CP operation under three different protection current densities for the specimens of 1% added NaCl. It can been seen that the instant-off potential display a significant change in the first three hours of CP operation under all the applied current densities. After 3 hours, all the curves become stable and flat, showing a very slight variation up to 24 hours. Figure 5.9 shows the curve of the applied current density of 20 mA/m^2 up to 120 hours (5 days), which confirms the small variation in a long time. According to the results in the Figures 5.8 and 5.9, in this study, all the parameters used for CP performance assessment were taken after 24 hours of CP implementation. The values of the instant-off potential in Figure 5.8 have been obtained based on the results in appendix B. The Figures in appendix B shows the variation of rebars potential with time under the application of three different CP current densities. They also show the potentials just after the switch-off the CP current for the instant-off potential determination as explained in section 3.4.6.7.

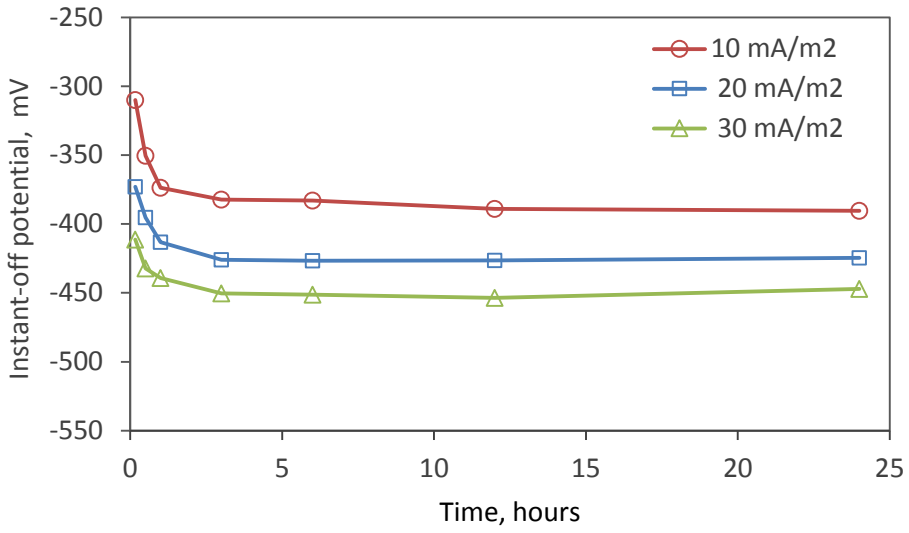

Figure 5.8: Reinforcement instant-off potential vs CP operation time under different CP current densities up to 24 hours

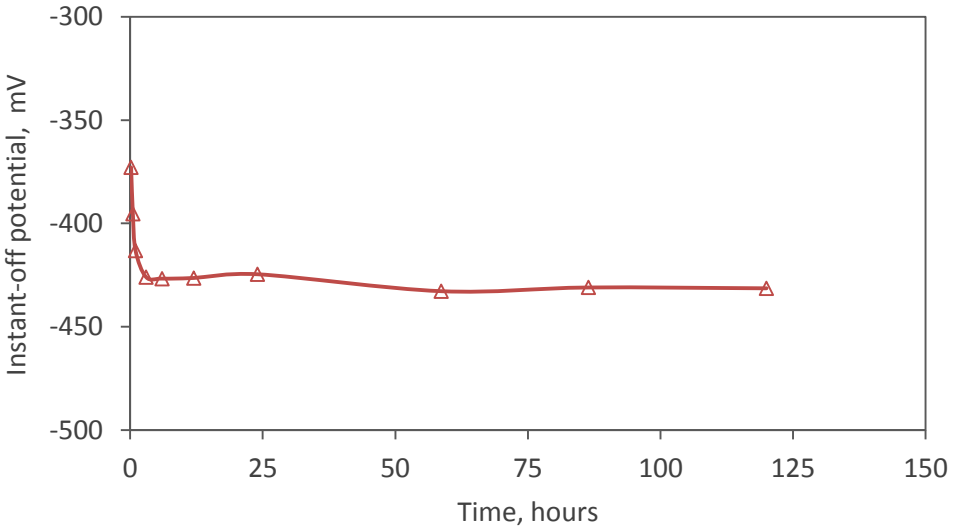

Figure 5.9: Variation of instant-off potential with time under 20 mA/m^2 CP current density up to 120 hours

5.4 Applied Potential Shift

Figure 5.10 represents the variation of the applied potential shift (also known as polarization) for the specimens of different chloride contents and under different applied CP current densities. It can be seen that the potential shift is strongly dependent on the environment around the reinforcement and the applied current density. The amount of potential shift decreases as chloride content increases, and it is directly proportional to the applied current

at any chloride content. However, the current becomes less influential at high amounts of chloride. A steep increase in the potential shift particularly happened at the initial chloride content increase starting from 0%. Specimens of a low chloride content show a higher potential shift than those of a high amount of chloride. For instance, the potential shift of the concrete specimens that contain 0.571% Cl was 9.2 mV compared to 204.2 mV for the chloride free specimens under the application of CP current density of 5 mA/m^2. Increasing the applied current density from 5 to 25 mA/m^2 the potential shift increases from 204.2 to 382.5 mV and from 9.2 to 59.2 mV for the chloride free specimens and those having 0.571% Cl, respectively. This reflects that a small amount of current will effectively provide the required potential for the cathodic protection of specimens with low chloride contents.

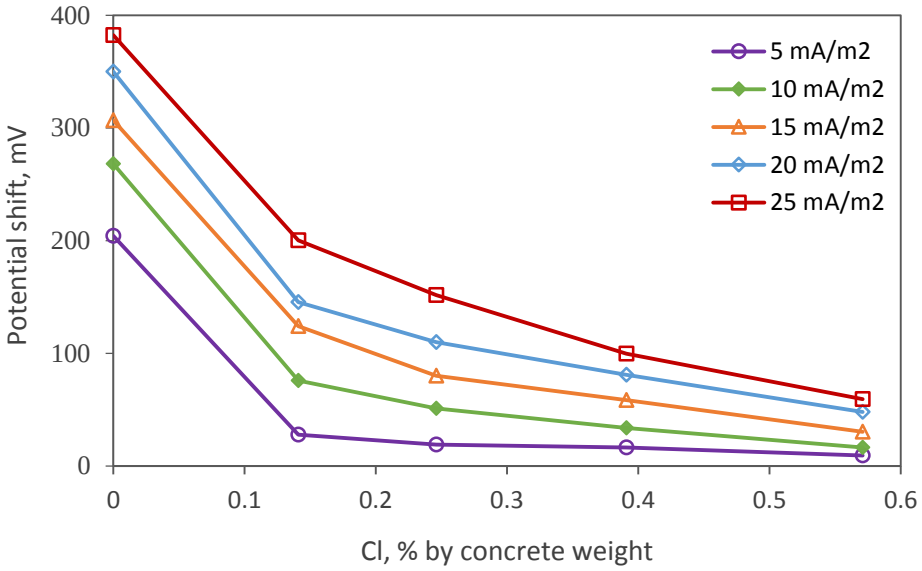

Figure 5.10: Potential shift of rebars under different chloride contents and applied CP current densities

Figure 5.11 shows the potential shift variation of reinforcement in terms of the concrete resistivity. It can be seen clearly that potential shift increases with the increase of concrete resistivity, and the correlation is highly pronounced at high resistivity and applied current density. It should be pointed out that the observation here is opposite to a previous finding (Elsener et al., 2003), which suggested that reinforcement in low resistivity concrete had a high polarization. A reasonable explanation for the difference is that this work only considered the chloride effect. Although high chloride content will decrease the concrete

resistivity, it will increase both the corrosion potential and corrosion rate, and, as a result, reduces the polarization effect under a certain CP current.

At last, Figure 5.12 shows the correlation between potential shift and polarization resistance of reinforcement for the specimens that only have chloride. The chloride free specimens gave a very high polarization resistivity (4961 Ω) indicating that reinforcement in passive state, and its existence in this plot affects the output of the results. From Figure 5.12, potential shift increases linearly with the increase of polarization resistance, and the degree of the increase is highly pronounced with both of the reinforcement polarization resistance and applied current density.

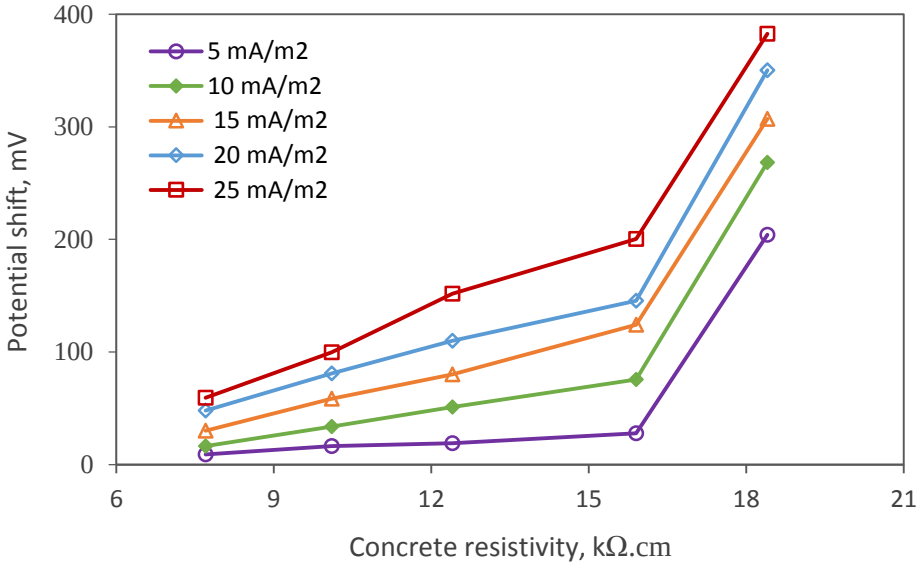

Figure 5.11: Dependence of potential shift on resistivity of concrete

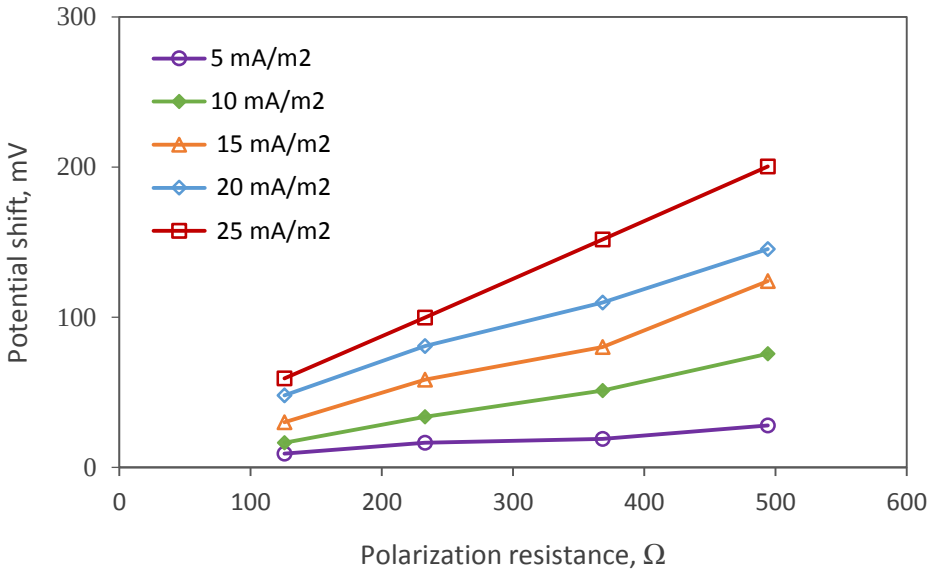

Figure 5.12: Dependence of potential shift on polarization resistance Rp of reinforcement

5.5 Effect of CP Current Density and Chloride Content on Instant-off Potential

The instant-off potential is one of the important criteria used to evaluate CP performance, which is measured immediately after interrupting the cathodic protection current to eliminate the influence of IR drop according to NACE International standard SP0290 (2007). The measurement is independent of the position of the reference electrodes. The IR drop is the difference between the applied protecting potential magnitude and the instant-off potential magnitude due to concrete resistance, which depends both on the applied CP current and the concrete resistivity as shown in Figure 5.13. It can be seen that IR drop increases when concrete resistivity and the applied CP current increases. Under a certain CP current, the variation of IR drop against concrete resistivity may be characterised approximately using a linear trend.

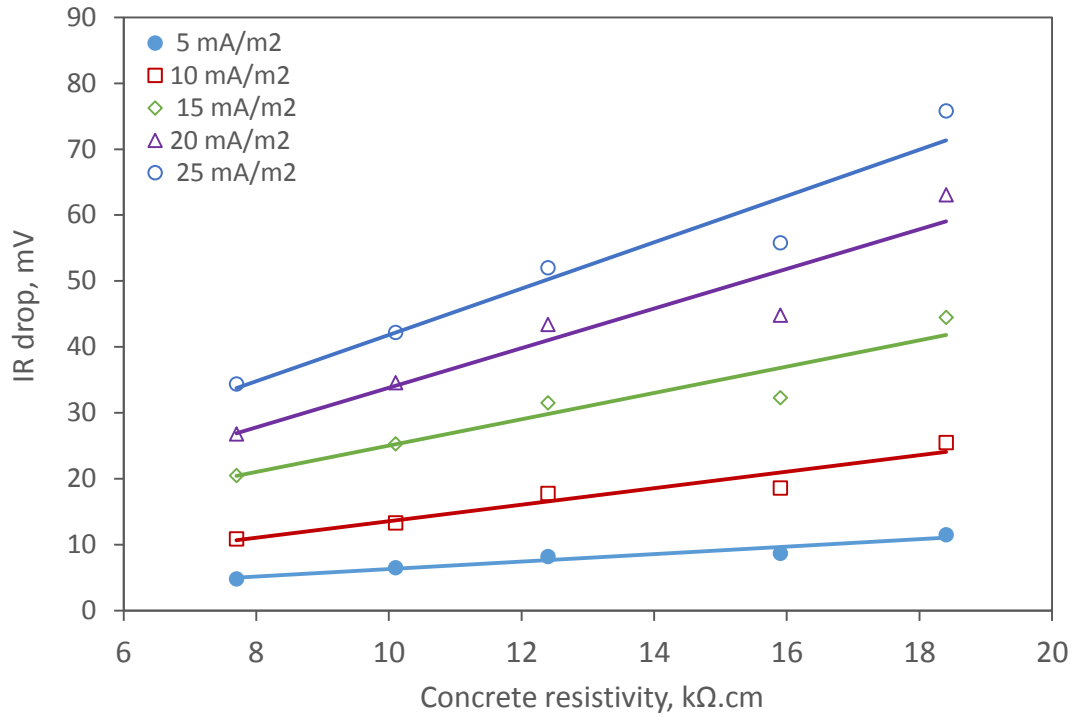

Figure 5.13: IR drop variation with concrete resistivity under different applied CP current densities

The accuracy of instant-off potential measurement is very sensitive to the time of measuring because the IR drop occurs in just less than a second. Katwan (1988) stated that the time to take measurement should be at least 0.6 seconds after switching off the protection current in order to obtain an accurate IR drop for cracked reinforced concrete elements subjected to salty water. Gummow (1993), however, found that the reading was unstable in the first portion of a second due to a positive spike influence the instantaneous voltage drop. The British standard 12696:2012 and NACE International standard SP0290:2007 recommend a time between 0.1-1.0 second after the switch-off of CP current to measure the instant-off potential.

Figure 5.14 shows the variation of the instant-off potential of the reinforcements in the specimens of different chloride contents under different CP current densities. It can be seen that the instant-off potential absolute value increases with the increase of the applied CP current density, the slope of the curve become flat when the concrete chloride content increases. The results in Figure 5.14 show that at the highest current density (75 mA/m^2)

applied to the different chloride contaminated specimens the -720 mV criterion hasn't been achieved.

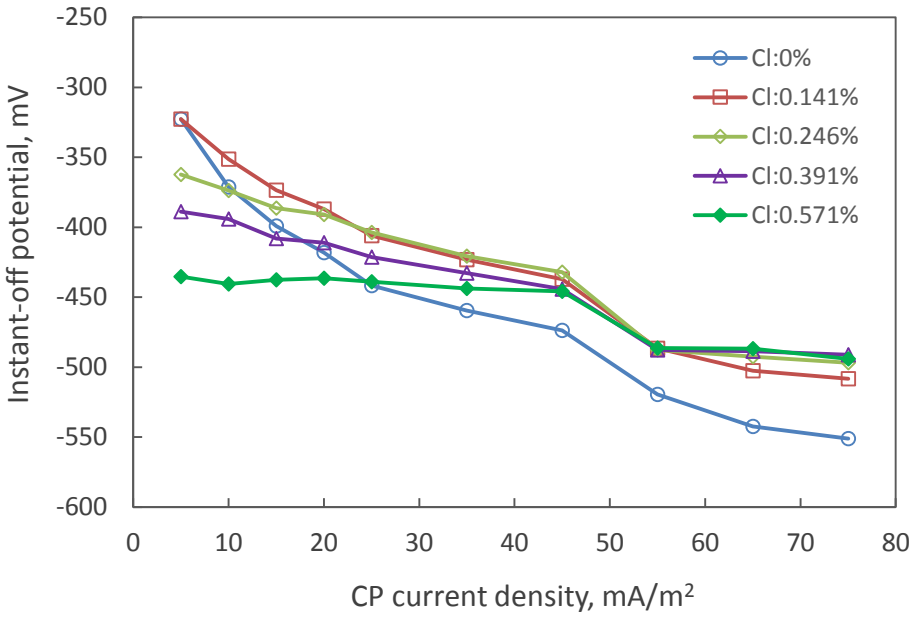

Figure 5.14: Variation the instant-off potential with the applied current and chloride content

In order to produce applicable information, Figure 5.15 replots the data in Figure 5.14. It shows that the relationship between the instant-off potential and the applied current density for concrete under a certain chloride contamination can be characterised using a linear function y=a+bx, where the two parameters, a and b, depend on chloride content. Figure 5.16 shows the variation of the two parameters against the chloride content in terms of the total chloride contents. It can be seen that the two parameters present a linear trend with the chloride content. For the data fitting of parameter b, the point of the chloride free specimens was ignored, because it looks like an out layer of the trend.

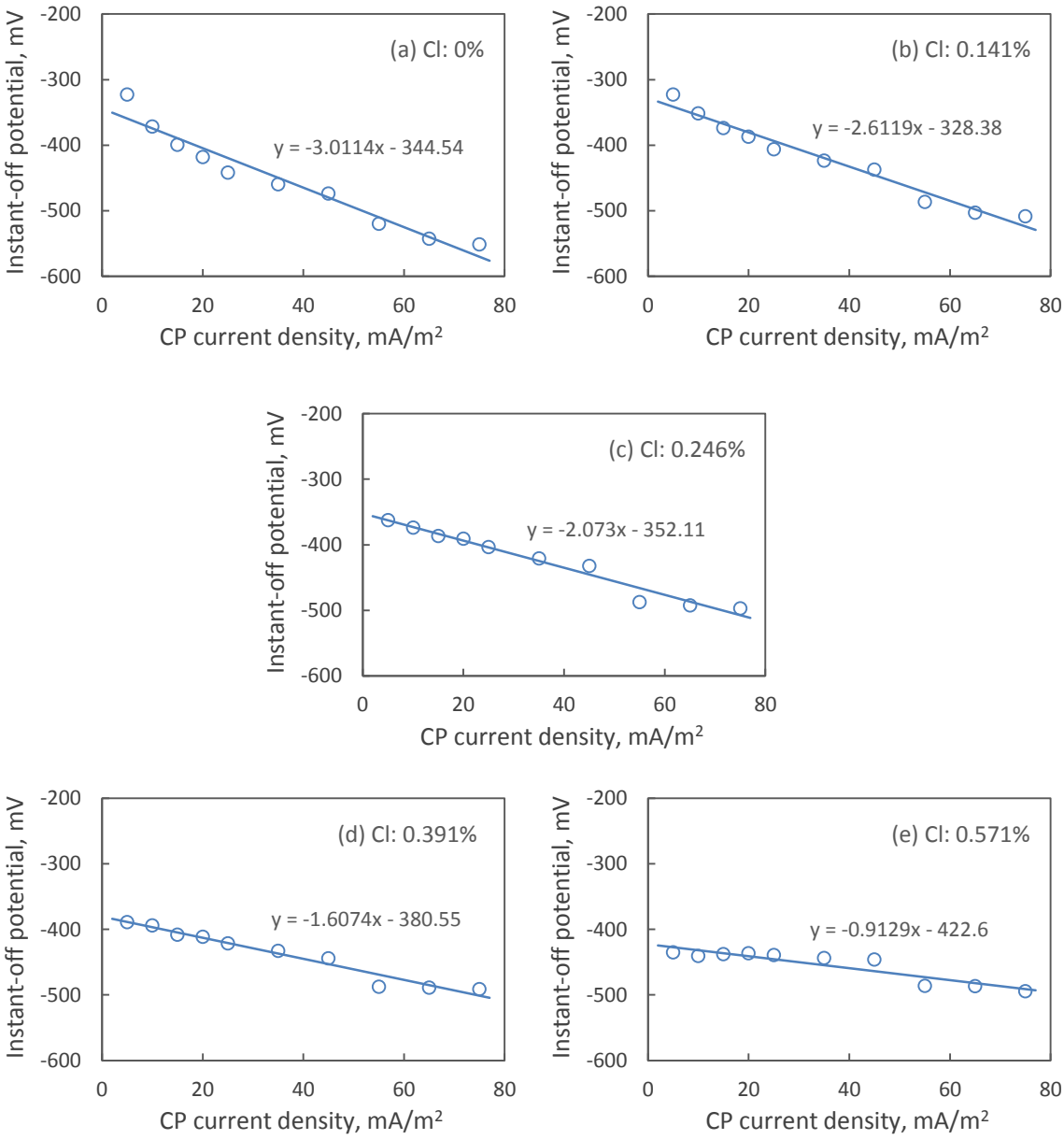

Figure 5.15: Instant-off potential vs CP current density at different chloride contents

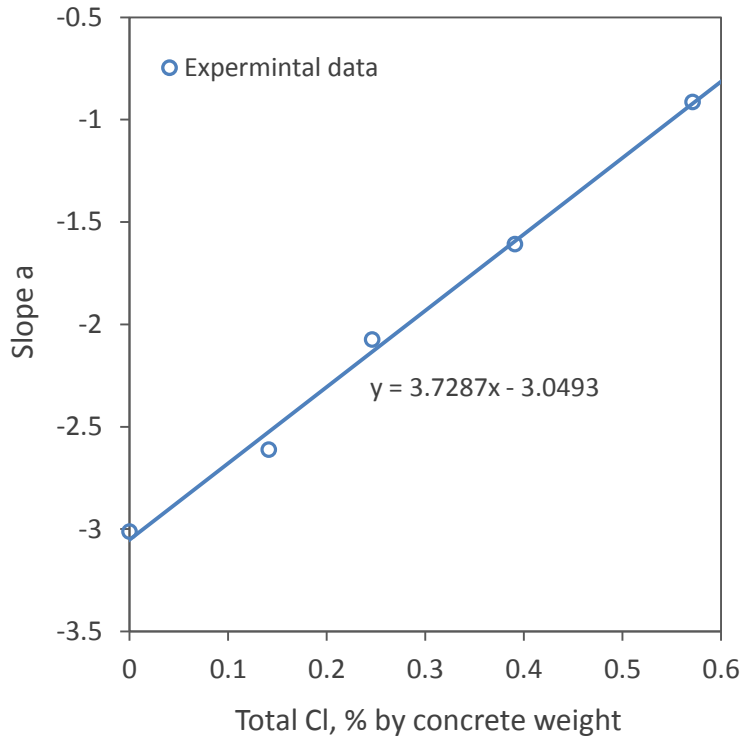

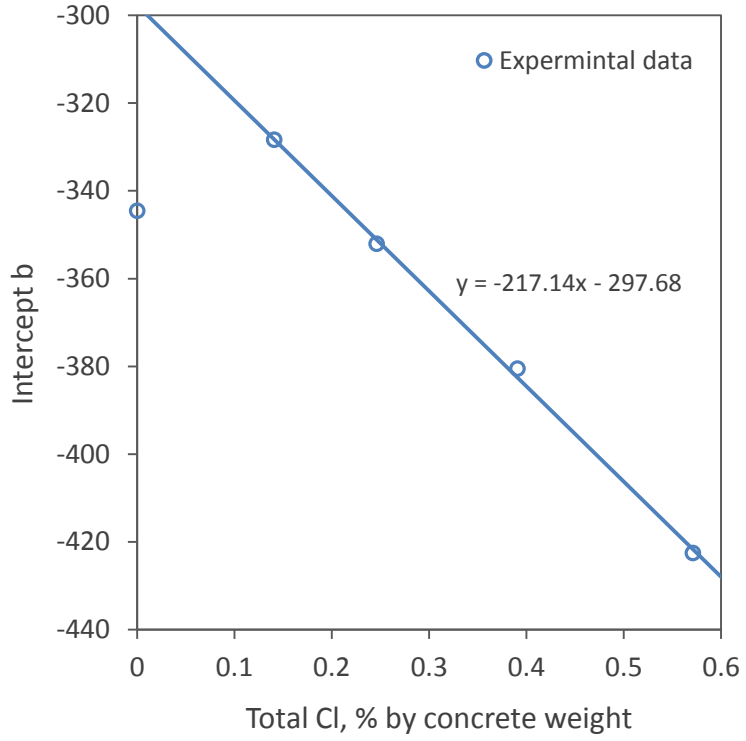

Figure 5.16: Parameter fitting for instant-off potential characterisation

5.6 Four-hour Decay Potential

The potential decay after switching off the CP current is another important parameter used to evaluate CP performance. Generally, 100 mV depolarization in a four hour period of time is the most accepted criterion.

Figures 5.17 and 5.18 show the potential decay curves obtained for specimens with different chloride contents after application CP current densities of 15 and 75 mA/m^2. The potential decay curves obtained for the same specimens after application various CP current densities are available in appendix C. It can be seen there is an immediate elimination of the IR drop after switching-off the protective CP current. This is practically clear after the application of high CP current densities or for chloride free specimens when small CP current densities was applied. After that, the potential goes back, at a slow rate, towards the original potential before the application of CP. These figures demonstrate that the most of the depolarization occurs during the initial hours after switching off the protection current.

Figure 5.19 shows a summary for the obtained values of the reinforcement depolarization (4-hours potential decay) against the applied CP current density and the instant-off potential at different chloride contamination. It can be seen that for a certain chloride content, the depolarization of the reinforcements increases with the increase of the applied current density. For chloride free specimens, the 4-hours potential decay curve is in the region above 100 mV (the horizontal solid line). It indicates that the reinforcements in a chloride free concrete environment are safe from corrosion even without CP (I = 0). Comparing the Figure 5.14 and Figure 5.19, it can be clearly noticed that a current density about 15 mA/m^2 is sufficient to provide the required protection for the reinforcement in the concrete of 0.141% chloride in terms of the 100 mV potential decay criterion. However, current density of 75 mA/m^2 is not enough to protect the reinforcement even in chloride free concrete in terms of the -720 mV instant-off potential criterion.

Figure 5.20 plots out the correlation between the instant-off potential and 4-hours potential decay at different CP current density in terms of the results in Figures 5.14 &5.19. It shows that in terms of the 100 mV depolarization criterion, -500 mV instant-off potential is sufficient to protect the reinforcements in all the investigated contaminated concretes.

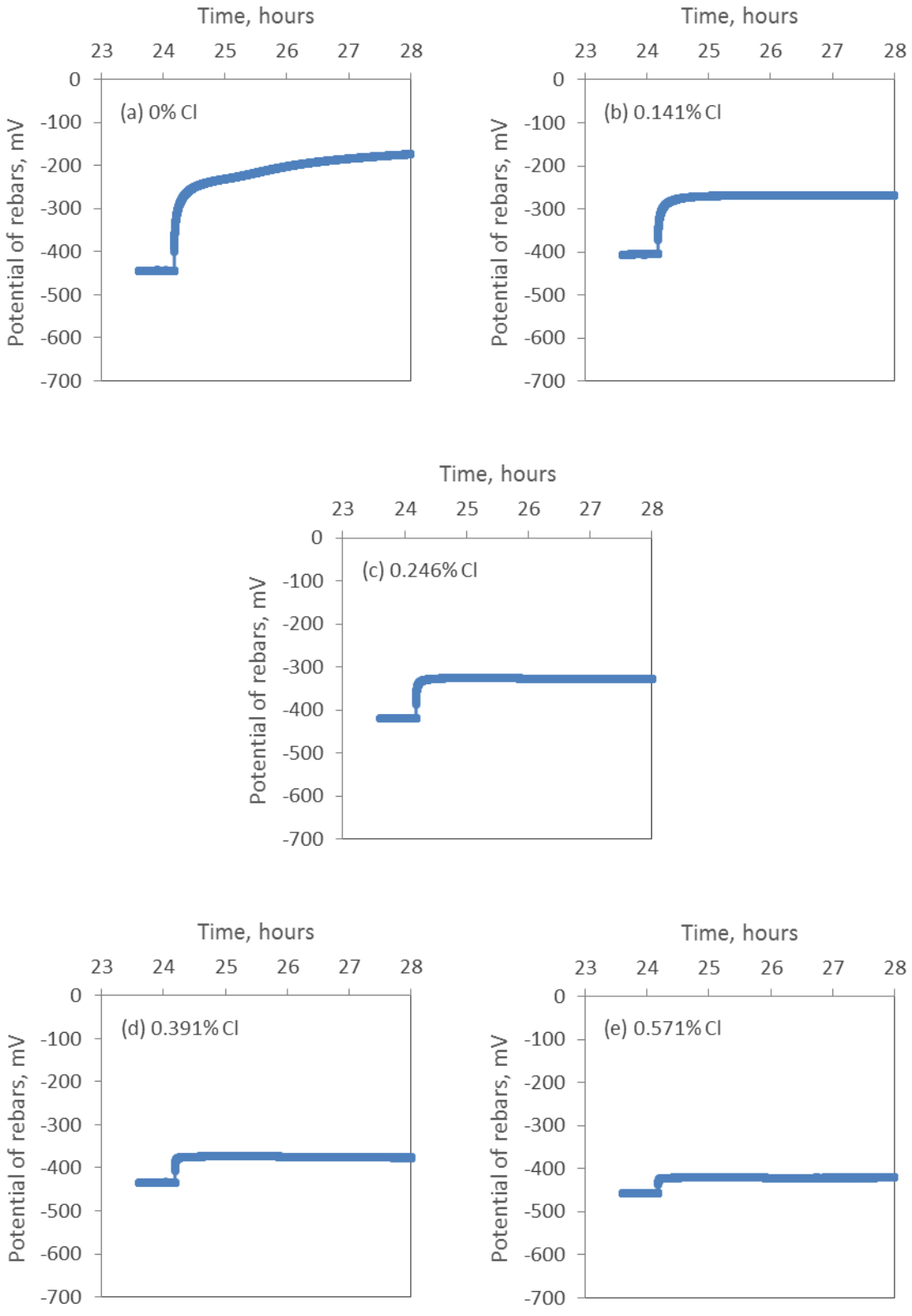

Figure 5.17: Potential decay curves for specimens at various chloride contents after application of CP current density of 15 mA/m^2

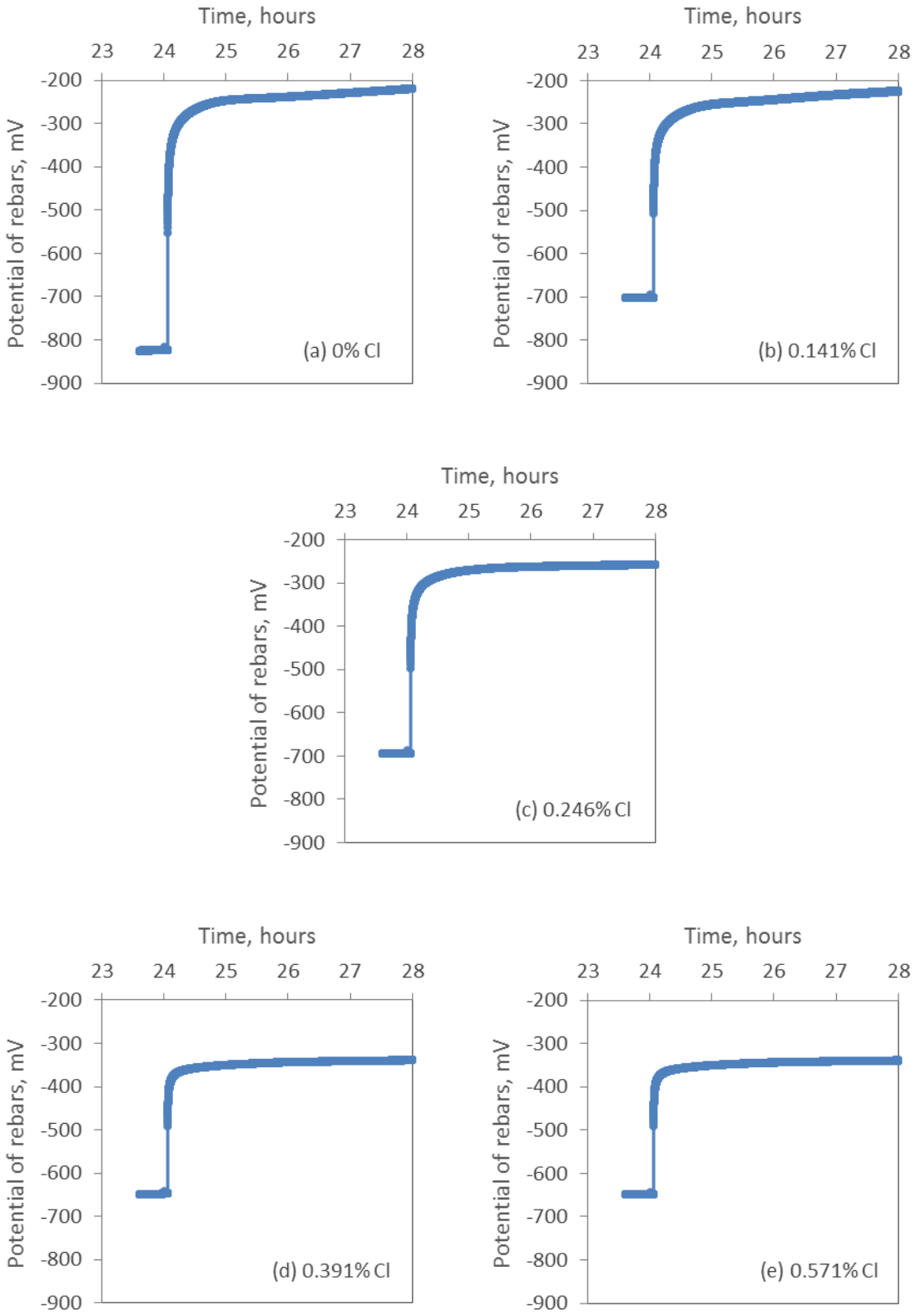

Figure 5.18: Potential decay curves for specimens at various chloride contents after application of CP current density of 75 mA/m^2

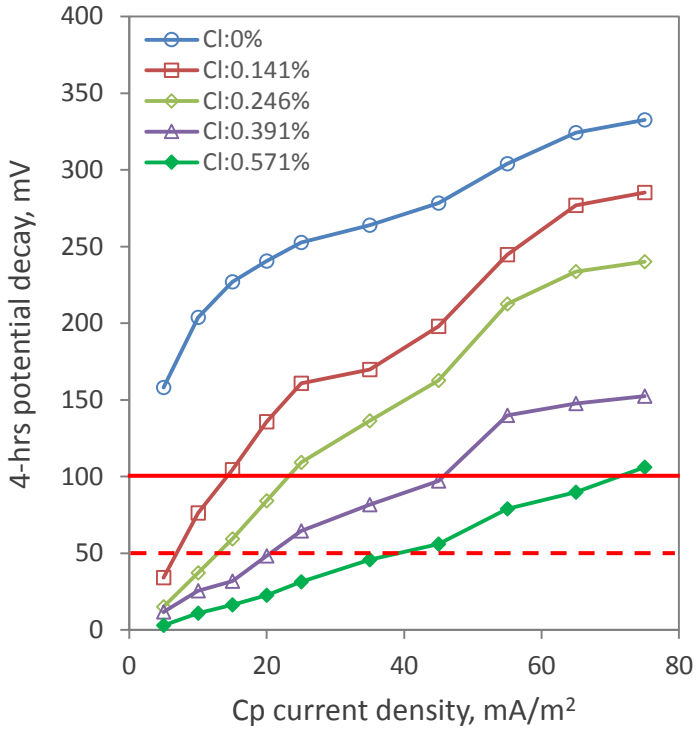

Figure 5.19: Reinforcement depolarization vs CP current density, (The horizontal solid line for the criterion of 100 mV while the dash line for 50 mV)

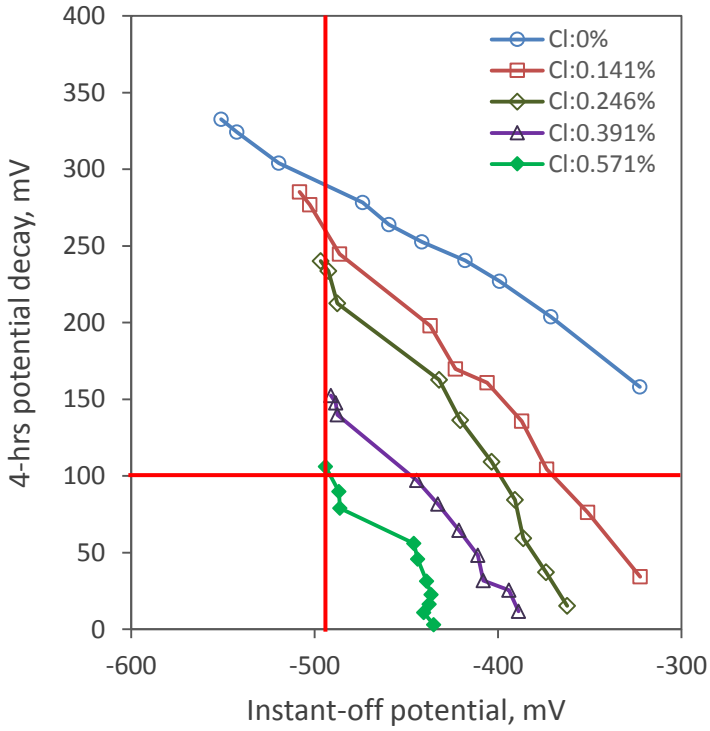

Figure 5.20: Reinforcement depolarization vs instant-off potential.
(The horizontal solid line for the criterion of 100 mV while the dash line for 50 mV)

Figure 5.21 shows the CP current densities and the corresponding instant-off potential after 24 hours CP application on the specimens of different chloride contents, which give the 100 mV depolarization (the 4-hours potential decays). The experimental data are the interception points of all the curves in the Figures 5.19 & 5.20 on the horizontal line at 100 mV 4-hrs potential decay. It is be seen that the required CP current density and the 24-hours CP instant-off potential for the 100 mV depolarization criterion present an approximately linear correlation to chloride content. According to the results, there is no CP needed when chloride content is less than 0.055% (this data is about half of the 0.1% that was discussed before according to the classification of Broomfield (Broomfield, 2007). Considering the instant-off potential plot, it can be seen that an instant-off potential of -500 mV can provide adequate protection for the reinforced concrete of up to 0.59% chloride content, and the effectiveness of the CP system depends on the chloride content if the instant-off potential is less negative than -500 mV.

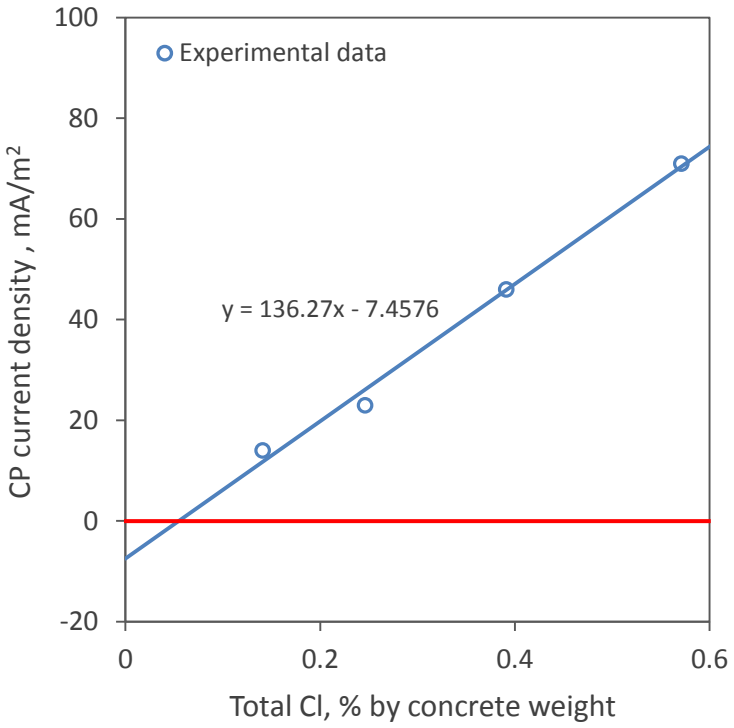

(a) CP current density for 100 mV 4-hours potential decay vs chloride contents

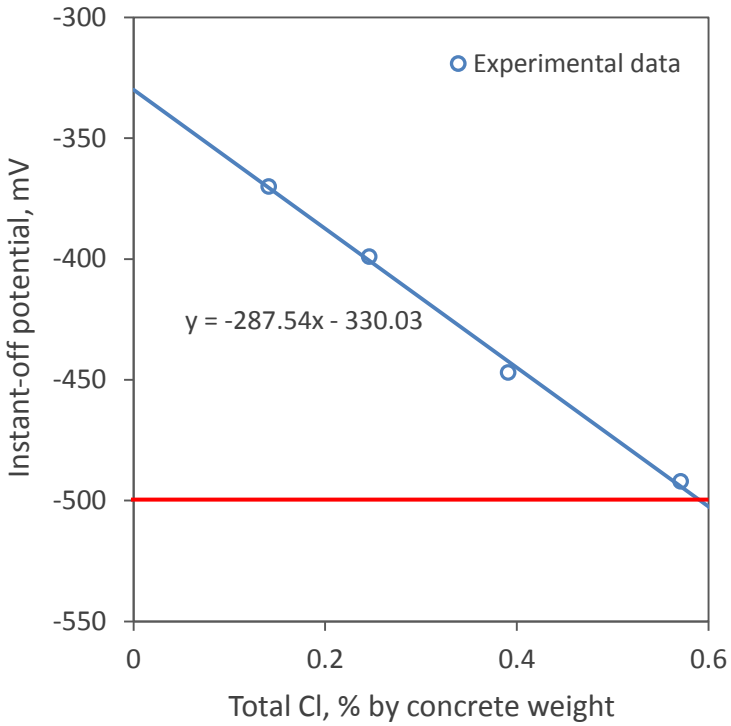

(b) Instant-off potential for 100 mV 4-hours potential decay vs chloride contents

Figure 5.21: The required CP current density and the corresponding instant-off potential for the protection criterion 100mV depolarization (4-hour decay potential) at different chloride contents.
(The horizontal lines indicate no CP current and -500 mV instant-off potential, respectively)

Figure 5.22 replots the data in Figure 5.21, in reference to that in Figure 5.3, to show the interception points at the corresponding concrete resistivity. Simply using a linear trend to approximate these interception points enables suggesting that there is no need of CP if concrete resistivity is more than 17 kΩ.cm, and -500 mV instant-off potential is adequate to protect the reinforcements in the concrete of no less than 6.7 kΩ.cm resistivity.

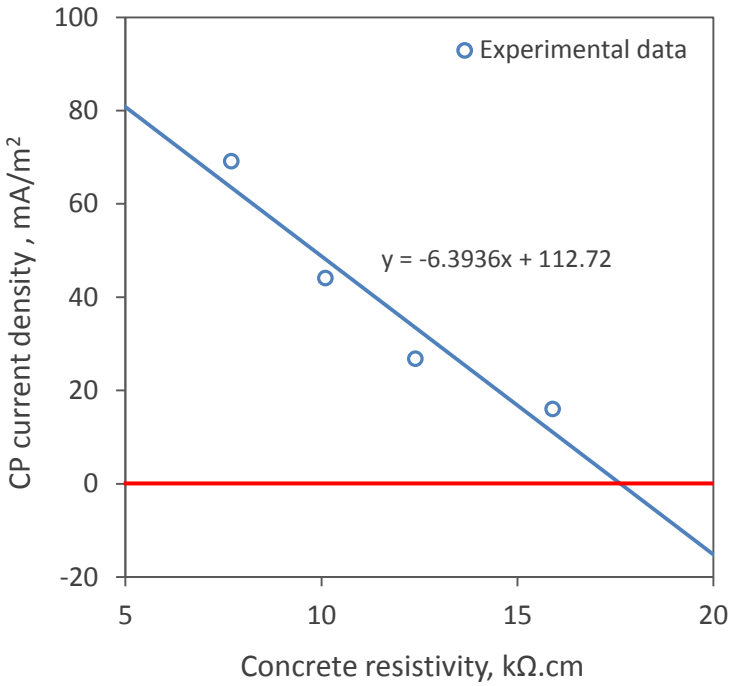

(a) CP current density vs concrete resistivity

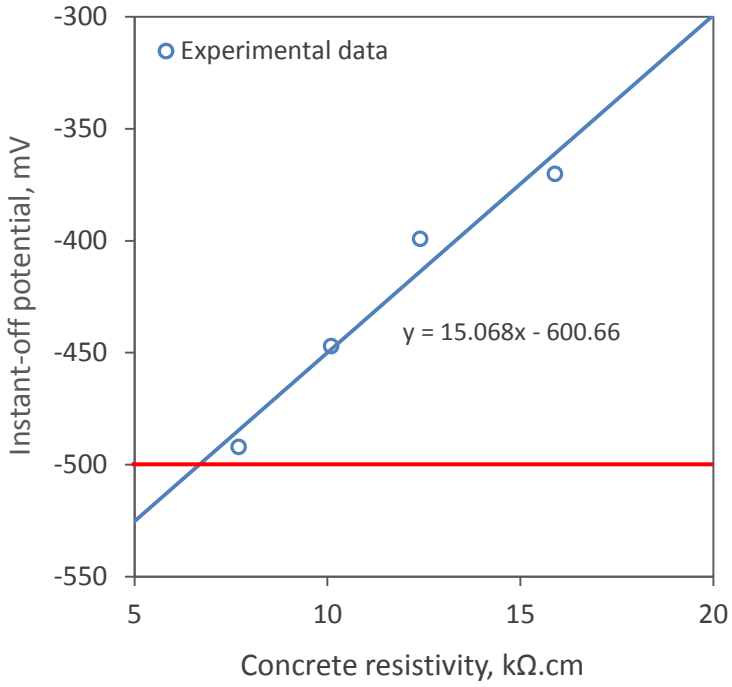

(b) CP current density vs concrete resistivity

Figure 5.22: The required CP current density and the corresponding 24-hour CP instant-off potential for the protection criterion 100mV depolarization (4-hour decay potential) at different concrete resistivity

(The horizontal lines indicate no CP current and -500 mV instant-off potential, respectively)

Figure 5.23 shows the required current densities for 100 mV and 50 mV depolarization (the 4-hours decays potential) for the reinforcements at different initial corrosion rates before CP operation, where the dash-dot line indicates the condition when the applied CP current density equals to the initial corrosion rate of the reinforcements. It can be seen that the suggested protection current density in terms of the 100 mV depolarization criterion is much higher than the corrosion rate of reinforcements. Particularly, the extra protection current density is projected at a high CP current density when reinforcement exposes to high chloride contamination or has a high corrosion rate. However, the CP current density in terms of the 50 mV depolarization condition (the interception points on the horizontal dash line in Figure 5.19) is very close to the dash-dot line at all reinforcement initial corrosion rates. Figure 5.24 shows the required current density at different chloride content and the corresponding concrete resistivity for the 50 mV depolarization threshold.

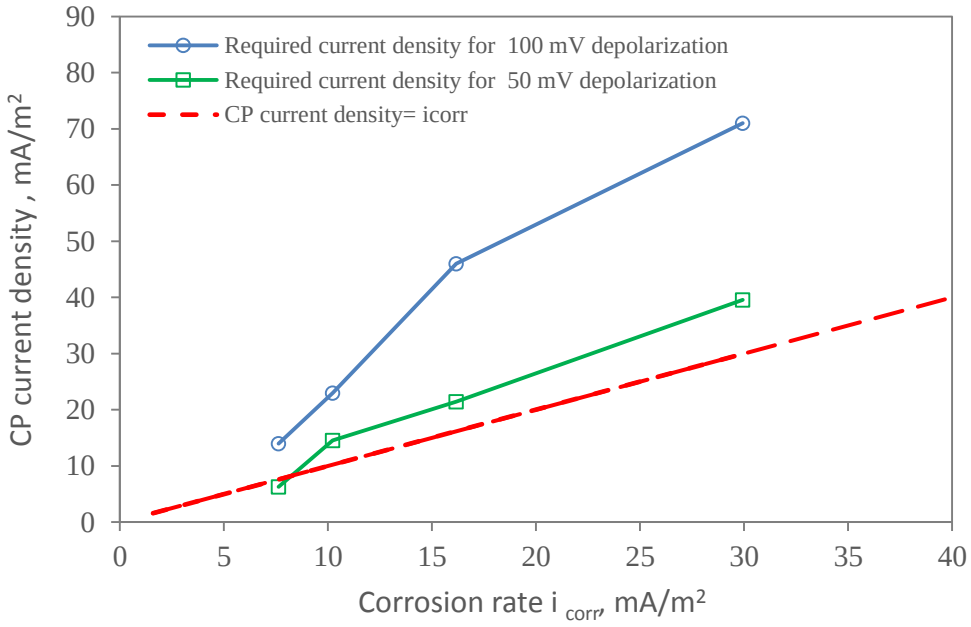

Figure 5.23: The required CP current density for different depolarization vs the initial corrosion rate of reinforcements

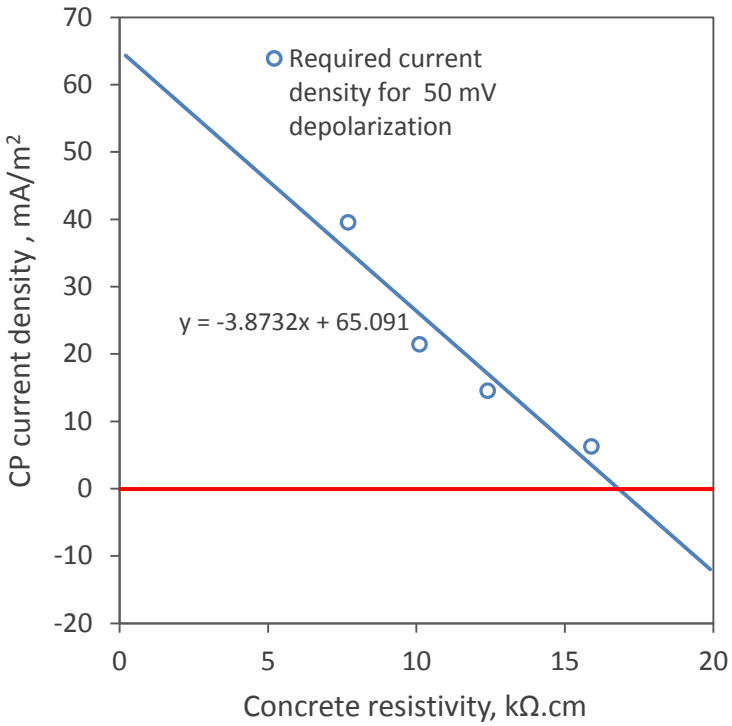

(a) CP current density vs concrete resistivity

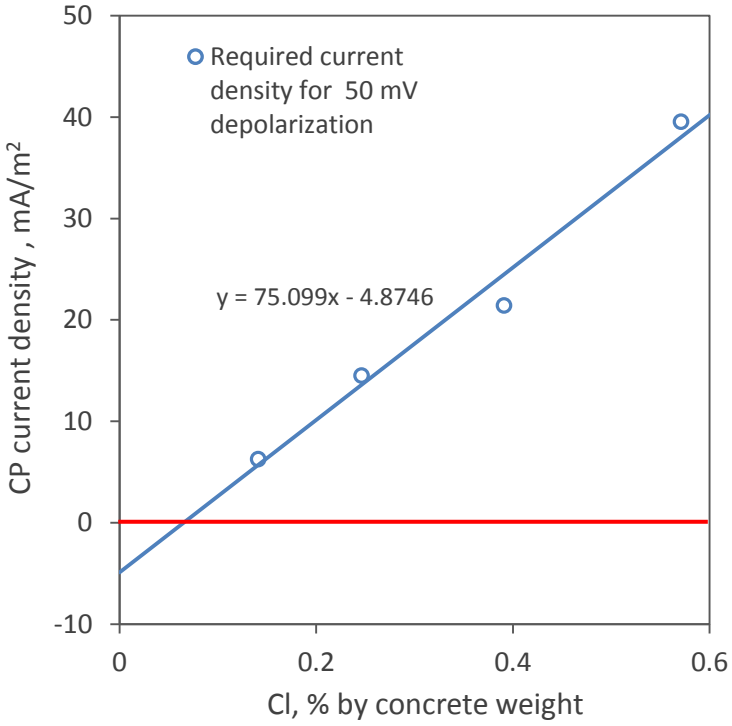

(b) CP current density vs chloride contents

Figure 5.24: The required CP current density for 50 mV depolarization

(The horizontal lines indicate no CP current)

5.7 Performance of Carbon Fibre as CP System Anode

The electrical performance of the CF anode is represented by the feeding voltage between the anode and the cathode when external CP current is impressed for a relatively long period (Van Nguyen et al., 2012; Zhu et al., 2014).

Figure 5.25 shows the feeding voltage measured between the rebars cathode and CF anode when CP current density of 20 and 200 mA/m^2 (on steel area) was applied for 28 days on the specimens of 3.5% NaCl. Although the increase of the applied current density from 20 to 200 mA/m^2 increases the magnitude of feeding voltage, the variation of feeding voltage under a certain current density is not significant as time goes by. The recorded voltages for the specimens under 20 mA/m^2 CP current density was about 2000 mV during the first 5 days. After then, the voltage was almost equal or less than 2000 mV except at the periods between 17.5-19 days and after 25 days. The biggest difference between the highest recorded voltage and the highest voltage reading during the first five days was 8%.

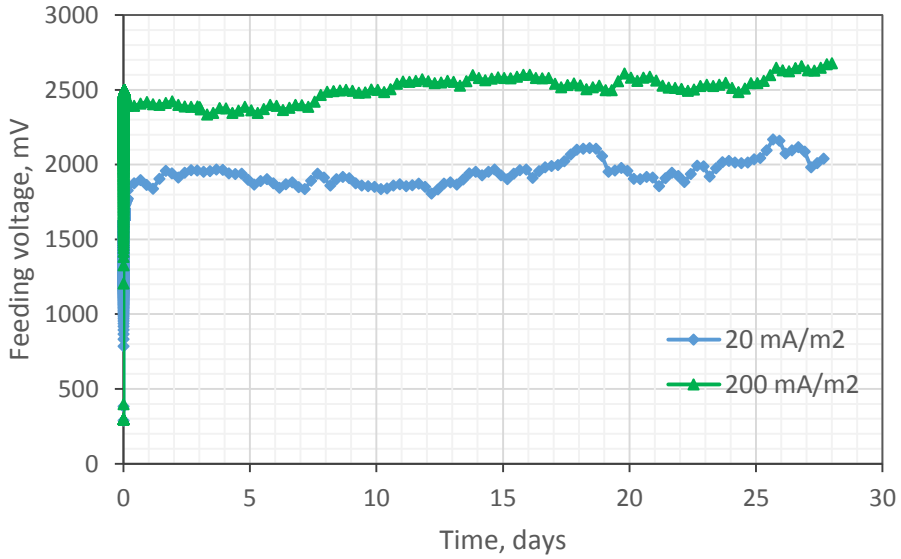

Figure 5.25: Variation of feeding voltage between rebars cathode and CF anode with time.

The voltage reading during the first few days of operation can be considered as a reference for comparison with the readings at other times of operation. Assuming no damage or debonding during the early days of CP operation, the increase of voltage thereafter indicates the change of the situation assumed around the anode system.

In case of the application 200 mA/m^2 CP current density, the highest recorded potential during the first 7 days was 2400 mV. The difference between the average potential values for the period after the seventh day and the highest value during the first 7 days was 6%.

Figure 5.26 presents the effect of current density on the electrical conductivity of CP circuit. It can be seen that the highest resistance obtained corresponded to the highest recorded voltage in Figure 5.24. The electrical conductivity was evaluated by resistance over a test period. The resistances were calculated by using Ohm's law from the passing current and the measured voltages. It should be noted that the circuit resistance between carbon fibre anodes and steel cathodes in concrete consist of the anode resistance at the anode-concrete interface, the electrolyte at the steel/concrete interface, and the steel bar resistance (Van Nguyen et al., 2012). For the purpose of analysis and simplicity, The CP circuit resistance was assumed to the measured voltage divided by the applied current density. From Figures 5.25 and 5.26, it can be seen that under both of the applied CP current densities, the results are very similar, i.e., the voltage and the CP circuit resistance are fluctuated and shows a very slow increasing trend. The fluctuation could be attributed to the change of the weather conditions during testing, and electrical connections (Zhu et al., 2014), while the increase in the measured voltage could be attributed to debonding issues or damage at the concrete-CF interface (Van Nguyen et al., 2012) that leads to an increase in the resistance of the CP circuit. But in this test there were no signs of damage or debonding problems observed at the concrete-CF interface.

Van Nguyen et al. (2012) investigated the performance of using external CF, glued to the concrete surface using carbon reinforced epoxy, as anode. Their results showed that there was a significant increase in the resistivity of CP circuit due to the deterioration occurred at the concrete-CF interface. The resistivity increased from 36.5 to 420 $\Omega.m^2$ after 24 days of application of 10 V. Zhu et al. (2015) used commercial conductive carbon aluminosilicate paste and carbon fibre reinforced mortar as contact materials between the CF anode and the concrete surface. They found that the voltage increased from 2 to 10 V after 25 days of application a current density of 1244 mA/m^2, and in some cases the voltage increased from 5 to 27.5 V.

From the results of the current study, it can be concluded that using embedded CF as anode improved the problems due to the debonding at concrete-CF interface as no signs of cracks or deterioration was observed at the concrete-embedded CF interface.

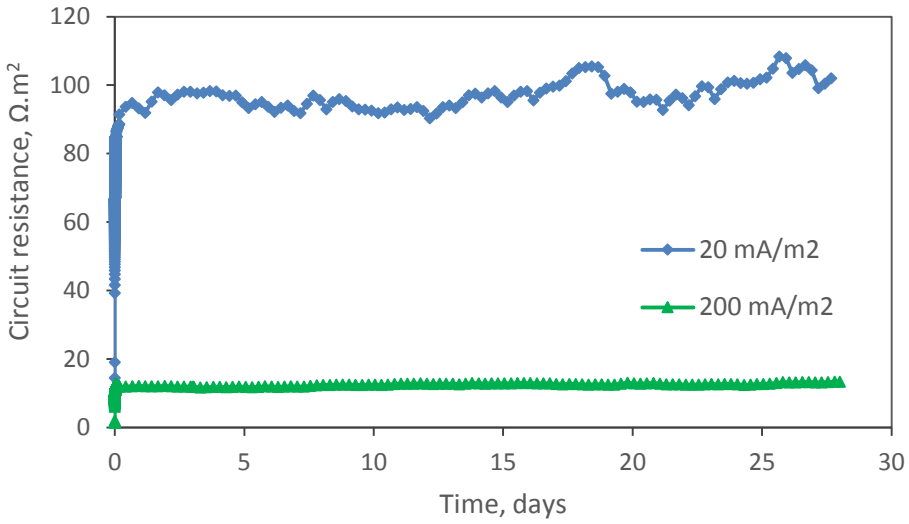

Figure 5.26: The CP circuit resistance with operating time

CHAPTER SIX

CP FOR SUBMERGED

CONCRETE SPECIMENS

CHAPTER 6 CP FOR SUBMERGED CONCRETE SPECIMENS

6.1 Corrosion Potential, Corrosion Rate and Electrical Resistivity

Figure 6.1 shows a plot of corrosion potential of reinforcement against total chloride content for fully and partially submerged concrete specimens. It can be seen that potential readings of the fully submerged specimens are less (more negative) than partially submerged specimens. So the fully submerged specimens have more risk of corrosion. However, it can be clearly seen that the values of the reinforcement potential of all the specimens in the two cases are much lower than -300 mV vs Ag/AgCl/ 0.5KCl (-350 vs CSE), which indicate high risk of corrosion according to the ASTM standard C876.

Comparing the two curves, we can see that the reinforcement in the fully saturated specimens has a less much potential variation in the range of chloride variation from about 0.1 to 0.6% comparing with the potential variation of the reinforcement in the partially saturated specimens. The results indicates that the water content variation plays a more important role in corrosion than chloride, because it affects the availability of oxygen. In fully saturated concrete, the limitation of oxygen dwarfed the effect of the chloride contents.

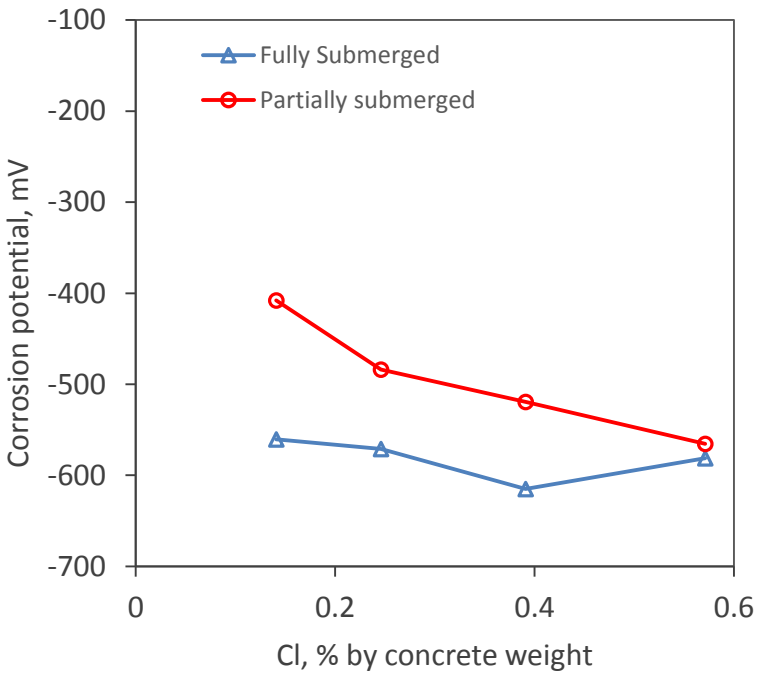

Figure 6.1: Corrosion potential of rebars with chloride concentration in fully and partially submerged concrete specimens

Chess and Broomfield (2013) reported that ASTM standard C876 may not be applicable to saturated concrete because they assume that saturated concrete reinforcement has little corrosion rate because of the limited amount of the oxygen available at the rebar interface under water. In terms of their reasoning, in the case of the Fig. 6.1, the low corrosion potential of the rebar in the fully saturated specimens doesn't mean a high corrosion rate. However, Broomfield (2007) had a different opinion, who stated that the reinforcement in highly water saturated concrete structures could experience a severe corrosion.

Figure 6.2 shows the corrosion rates of the reinforcements in the fully and partially submerged specimens at different chloride concentration. The result is in agreement with what stated by Broomfield (2007) who found that significant corrosion can develop in the concrete structures of high moisture content. It is evident that corrosion rate increases when chloride content increases in specimens. In addition, for a certain chloride content, corrosion rate of the reinforcement in fully submerged specimens is higher than that in partially submerged specimens. This confirms that water content in concrete plays an important role in the reinforcement corrosion as previously discussed.

Unlike corrosion potential, corrosion rate for the fully and partially submerged specimens presents a clear similar correlation with the chloride content. For example, when total chloride increased from 0.141% to 0.571% for the fully submerged specimens, corrosion rate increased from 40 to 140 mA/m^2. For the partially submerged specimens, corrosion rate increased from 10 to 110 mA/m^2.

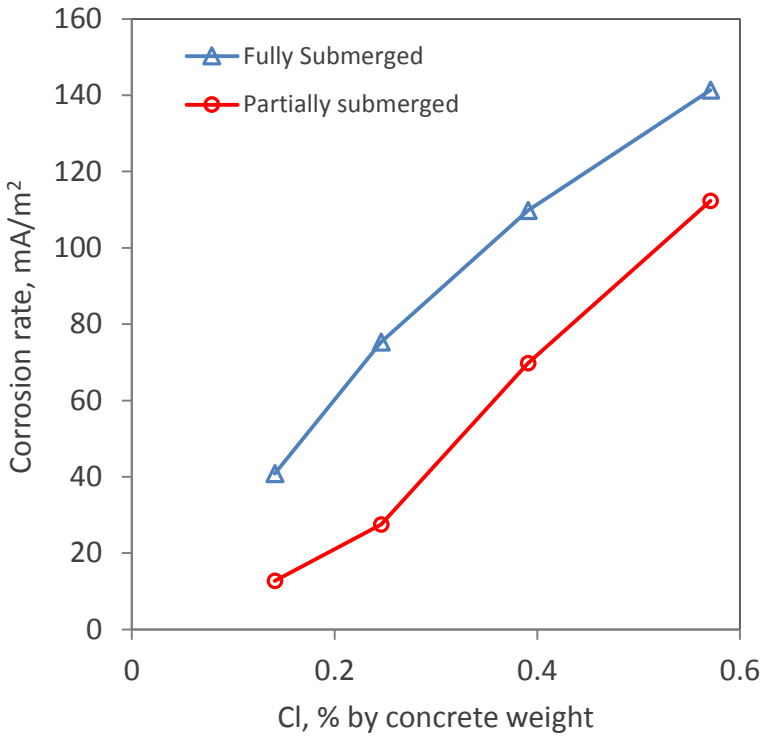

Figure 6.2: Influence of chloride concentration on steel corrosion rate in fully and partially submerged concrete specimens

Figure 6.3 shows the values of electrical resistivity obtained for both fully and partially submerged specimens at different chloride contents. As previously observed in this study, concrete resistivity decreases linearly with the increase of chloride.

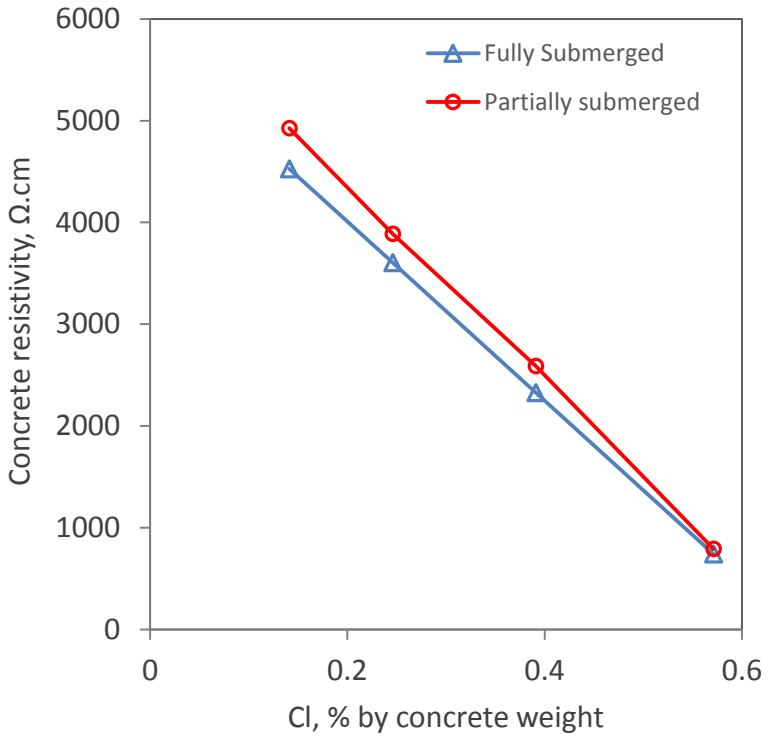

Figure 6.3: Concrete resistivity vs total chloride content for fully and partially submerged concrete specimens

Based on the data in Figures 6.2 and 6.3, a correlation between rebars corrosion rate and resistivity of concrete is presented in Figure 6.4, which shows that severity of corrosion increases as concrete resistivity decreases. High corrosion rates in the range of (40-140) and (10-110) mA/m^2 were observed for the fully and partially submerged specimens, respectively with a corresponding resistivities of less than 5,000 Ω.cm. It can be seen that for a certain concrete resistivity, the corrosion rate of the reinforcement in fully submerged specimens is higher than that in partially submerged specimens.

Together with the finding in the previous chapter for the air-exposed specimens, the water content and chloride content should be explicitly related to the corrosion state rather than through a single parameter of the concrete resistivity for the complicated situations because the water content will affect the oxygen transportation in concrete, and the oxygen availability at the rebar surface will play an important role in the corrosion process, and this is unassessable by concrete resistivity.

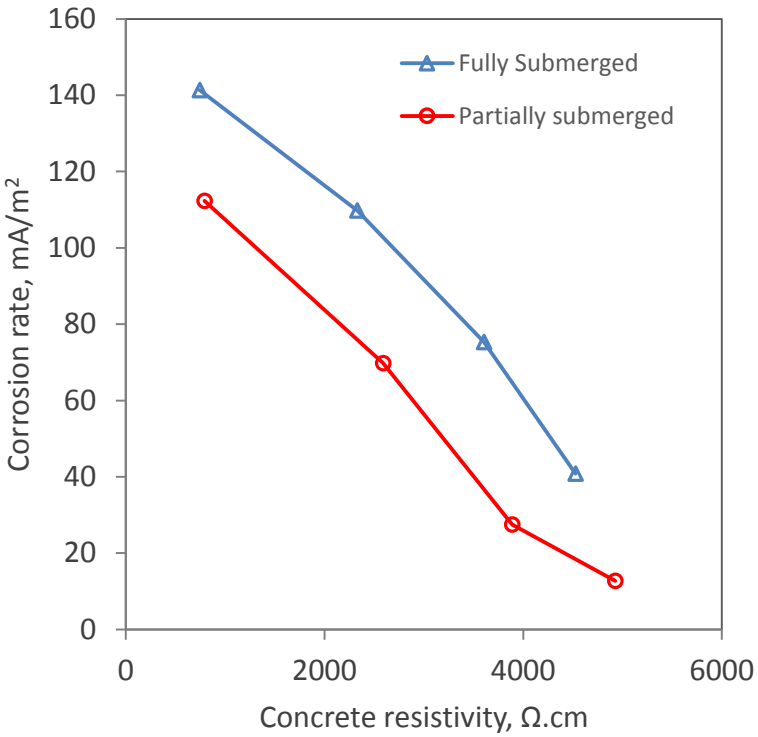

Figure 6.4: Relationship between corrosion rate and electrical resistivity of fully and partially submerged concrete specimens

The measured rebars corrosion potential (E_{corr}) and corrosion rate (i_{corr}) at the three different exposure conditions (i.e., fully submerged, partially submerged and air exposed concrete specimens) can be quantified in terms of water content as illustrated in Figures 6.5 and 6.6. Figure 6.5 shows a general tendency that at a specific chloride content, corrosion potential decreases (becomes more negative) with an increase of the water content. Also, lower corrosion potential is associated with high chloride content under a certain water content. But this fact is only applicable for the specimens that are not fully saturated (water content is less than 6.5%). In case of fully saturated specimens (water content is greater than 7%), values of corrosion potential are quite close varying in the range of -550 to -600 mV at the four different chloride contents. They are independent of chloride concentration. This could be due to insufficient oxygen supply under water which supressed the active influence of chloride on corrosion (Hussain and Ishida, 2012; M. Montemor et al., 2000).

However, Figure 6.6 shows that corrosion rate increases with the increase of water and chloride content. At low water content, the chloride effect on corrosion rate becomes small.

With the water content increases, the chloride effect becomes more significant. This may be attributed to the free chloride increases in pore water.

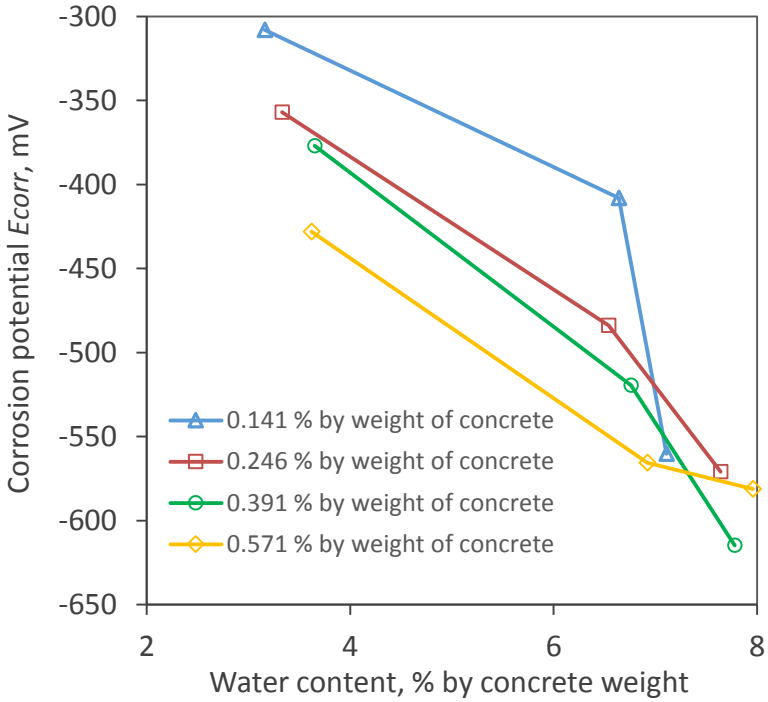

Figure 6.5: Relation of corrosion potential and water content at different chloride concentrations

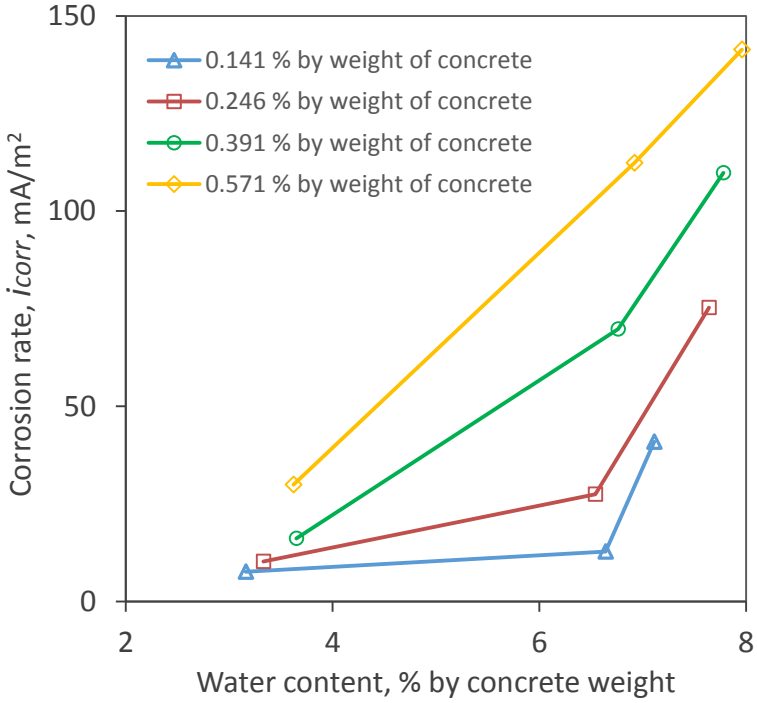

Figure 6.6: Relation of corrosion rate and water content at different chloride concentrations

From the results and discussion above, it can be concluded that corrosion potential may be used to indicate a probability of corrosion for a general guidance but not to be used as a stand-alone single rule to establish the state of real activity of corrosion in saturated concrete. In this case, the evaluation of other measurements such as corrosion rate, concrete resistivity and chloride analysis could be useful for more information in such ambiguous conditions.

6.2 Fully Submerged Specimens under Constant CP Current Density

Figure 6.7 shows the shifted rebars potential from the start of the application of CP with different current densities for 5 days followed by a depolarization for other 24 hours. It can clearly be noticed that the rebar potential steadily decreases with time. In addition, the rate of potential shift with time (the slope of these curves) is proportional to the density of the applied current.

This trend has been noticed for all the specimens of different chloride contents under various applied levels of CP current densities, as shown in Figure 6.7 (a, b, c and d), and does not tend to stabilize in the 5 days of CP operation period. Such steadily decrease of the rebar potential likely leads to overprotection and the hydrogen evolution at the reinforcement surface when the potential exceeds the specified limit of -1100 mV in standards (BS EN ISO 12696, 2012).

Figure 6.7 also shows the recorded 24 hours potential decay after CP interrupted. The characterisation of potential decay is considering as one of the major consideration for the evaluation of protection efficiency. It can be seen that the potential moves at a very slow rate towards the original potential before applying CP. Also, the 4 hours and 24 hours potential decay in all the cases are less than 100 mV. For all the fully submerged specimens, the instant-off potential is about the same as the on-potential.

From the results, it may be concluded that the depolarization rate is less dependent on the chloride and CP current density for fully submerged samples where the availability of oxygen is low.

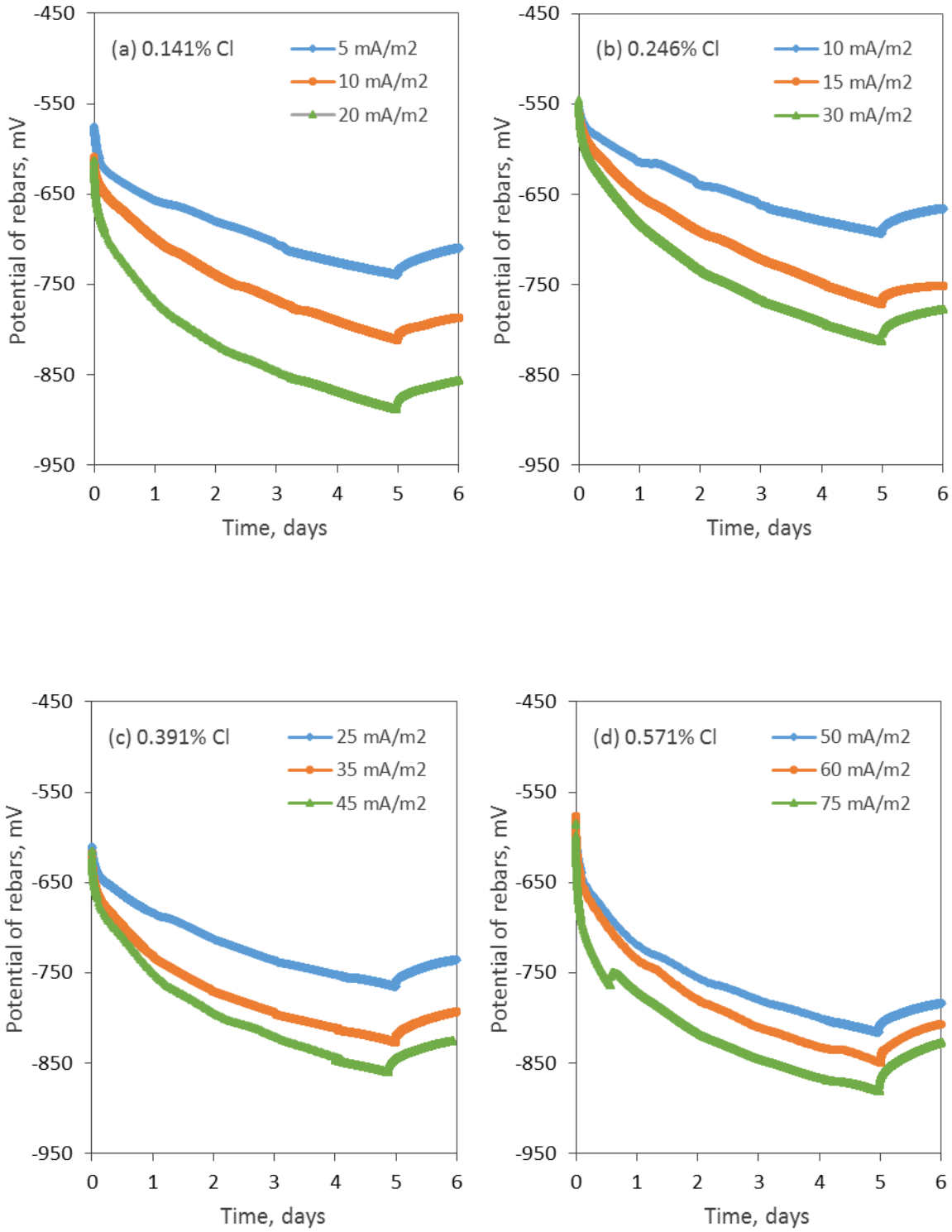

Figure 6.7: Potential variation with time of fully submerged specimens under various chloride contents and CP current densities, and the corresponding potential decay curves.

6.3 Constant Potential Technique

In order to avoid overprotection in the application of constant current technique, using constant potential protection could be an alternative for submerged concrete reinforcements. In the study, concrete specimens were fully and partially submerged in salty. The potential of rebars was forced and maintained using potentiostatically controlled potential technique at a certain level (-800 and -900 mV vs Ag/AgCl/0.5KCl, respectively in the study) for 5 days. Specimens with four chloride concentrations were examined. The variation of passing current density has been monitored and recorded as shown in Figure 6.8. It shows that the current decreases with time. The rate of decreasing was particularly high at early stage of operation. After that, it was gradually decreased with time. All the specimens with different chloride contents show the same trend. Similar observation in which the initial current density is higher by several times of magnitude than the later stabilised current density was reported before (Chess and Broomfield, 2013). It also can be noticed that the higher the applied potential, the higher the current density and the shorter the time to achieve a stable current condition. All of these can be attributed to the re-alkalisation and chloride removal in concrete, which change the concrete resistivity.

Figure 6.9 replots the data in Figure 6.8 to illustrate the influence of chloride on the current density under the application of -800 mV and -900 mV for the fully and partially submerged, respectively. It can be seen that in general the required current density under certain potential increases with the increase of chloride content because of the low resistivities of concrete of high chloride content. However, the chloride content looks have little influence on the time to achieve a stable condition.

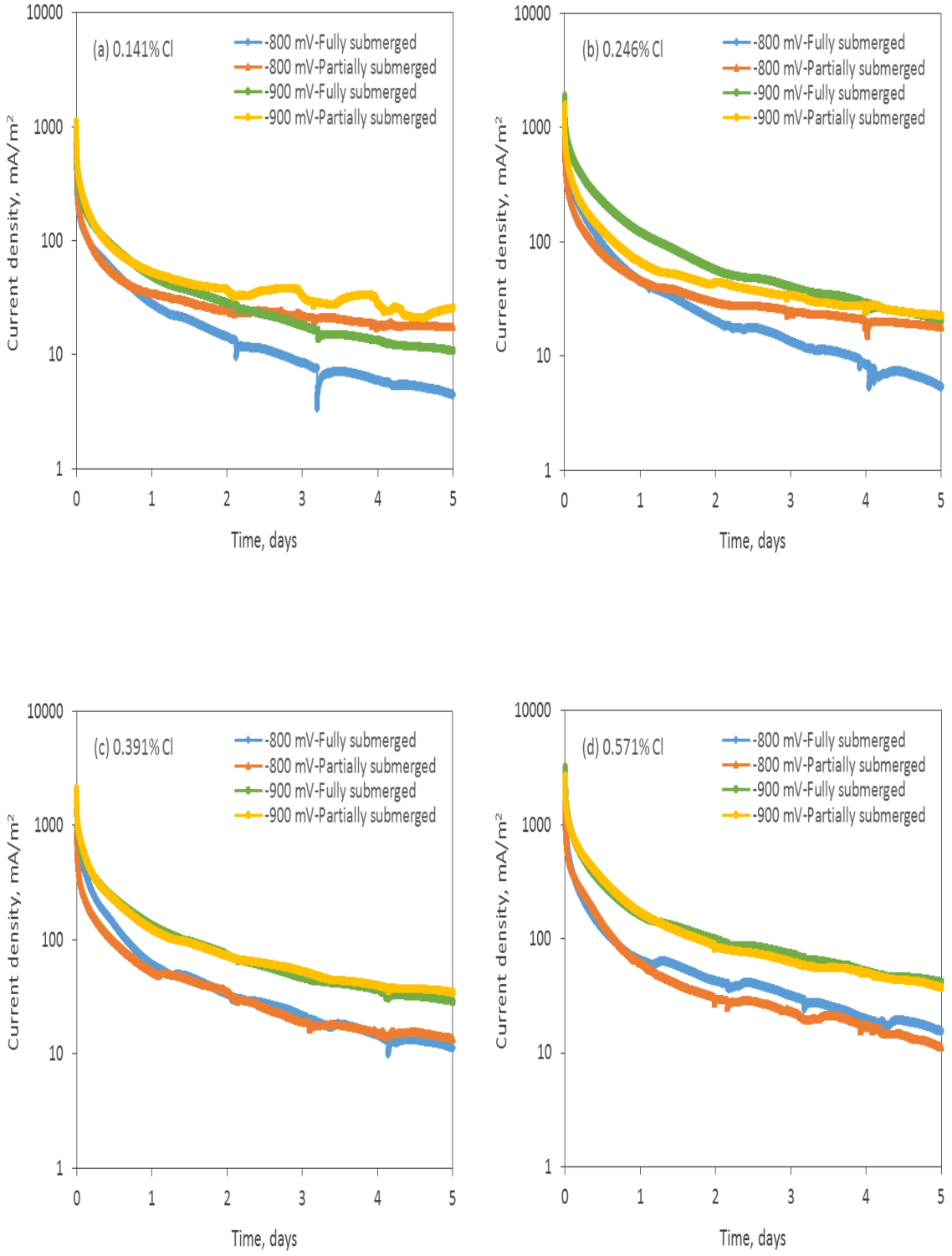

Figure 6.8: Variation of flowing current with time for the potential demand of CP for fully and partially submerged specimens with various concentration of total chloride.

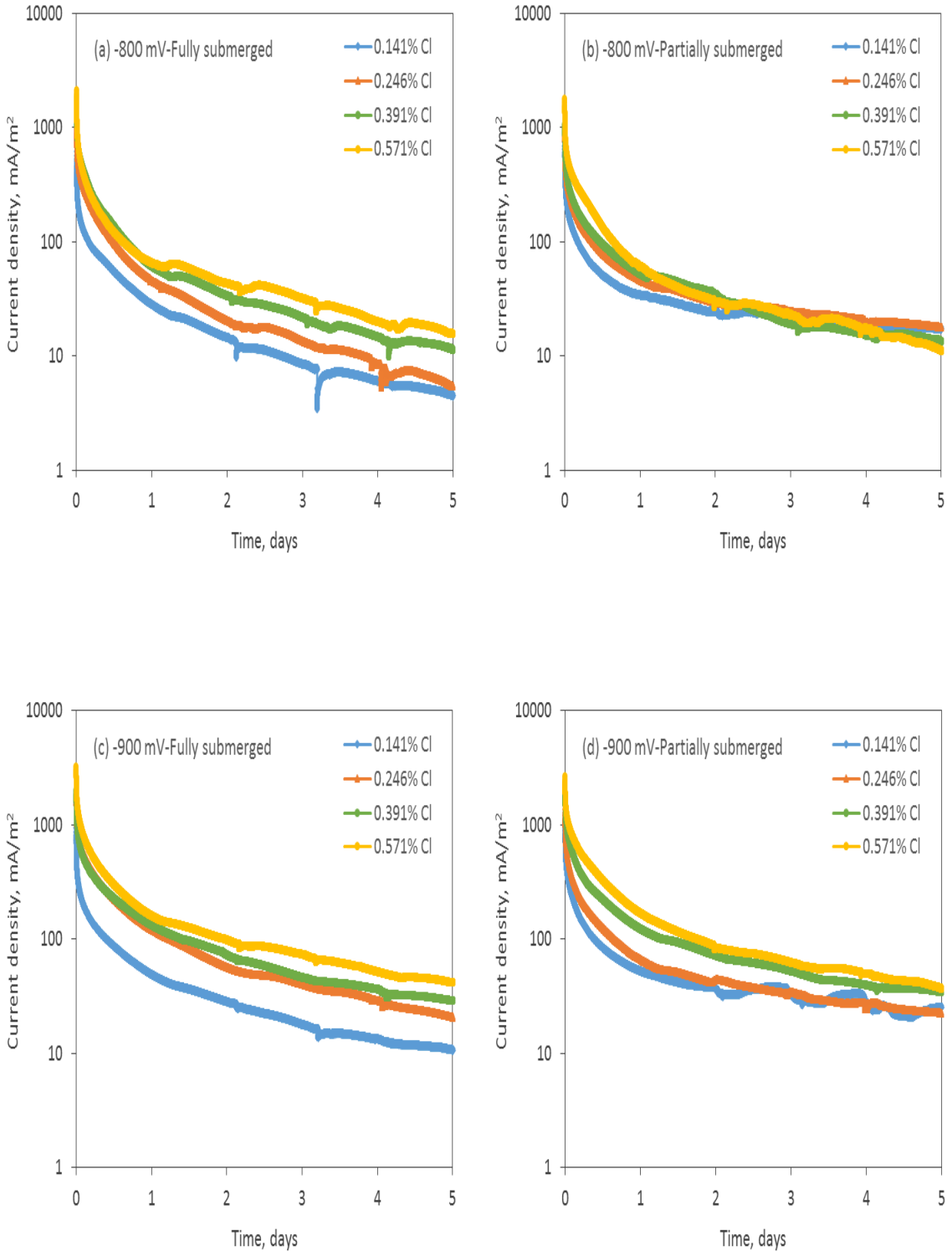

Figure 6.9: Effect of chloride contents on the required current of CP under various potential demands and exposure conditions.

A depolarization test, as shown in Figure 6.10, was also performed to evaluate the effectiveness of the protection based on 100 mV depolarization criteria recommended by standards (BS EN ISO 12696, 2012). The potential decay was recorded for 24 hours after CP has been stopped using data logger. A similar behavior was observed as that obtained for using constant current technique in the case of the fully submerged specimens. The depolarization of all the specimens at 4 and 24 hours were in the range of (5-15) mV and (10-25) mV, respectively regardless the magnitude of the applied potential or the concentration of the total chloride, and it is much less than the value 100 mV stated in standards for the efficiency of protection.

However, in the case of partially submerged specimens, the observed 24 hours depolarization was higher and reached up to about 80 mV for the specimens with 0.141% total chloride when protection potential of -800 mV was applied. But, the depolarization decreased with the increase of chloride content. For example, it is about 15 mV for the specimens with 0.571% total chloride. When the applied protection potential increased to -900 mV, the depolarization increased to just over 100 mV for the specimens with 0.141% total chloride. All other specimens with higher chloride contents showed a depolarization less than 100 mV. Specimens with 0.391% and 0.571% total chloride showed same depolarization regardless the applied potential or exposure condition. The lower depolarization for the specimens of higher chloride contents may be attributed to the less chloride redistributed under the same applied protective potential.

In conclusion, the 100 mV depolarization criterion in 4 or 24 hours is not applicable for the evaluation of CP of fully submerged specimens. On the other hand, in the case of partially submerged specimens, the magnitude of the applied protection potential, chloride concentration, oxygen existence and time of depolarization have significance influences on the value of depolarization. The obtained results in this work produced useful information, but the data was inconclusive to characterize the required CP protection for those two situations and further investigation of this approach is needed.

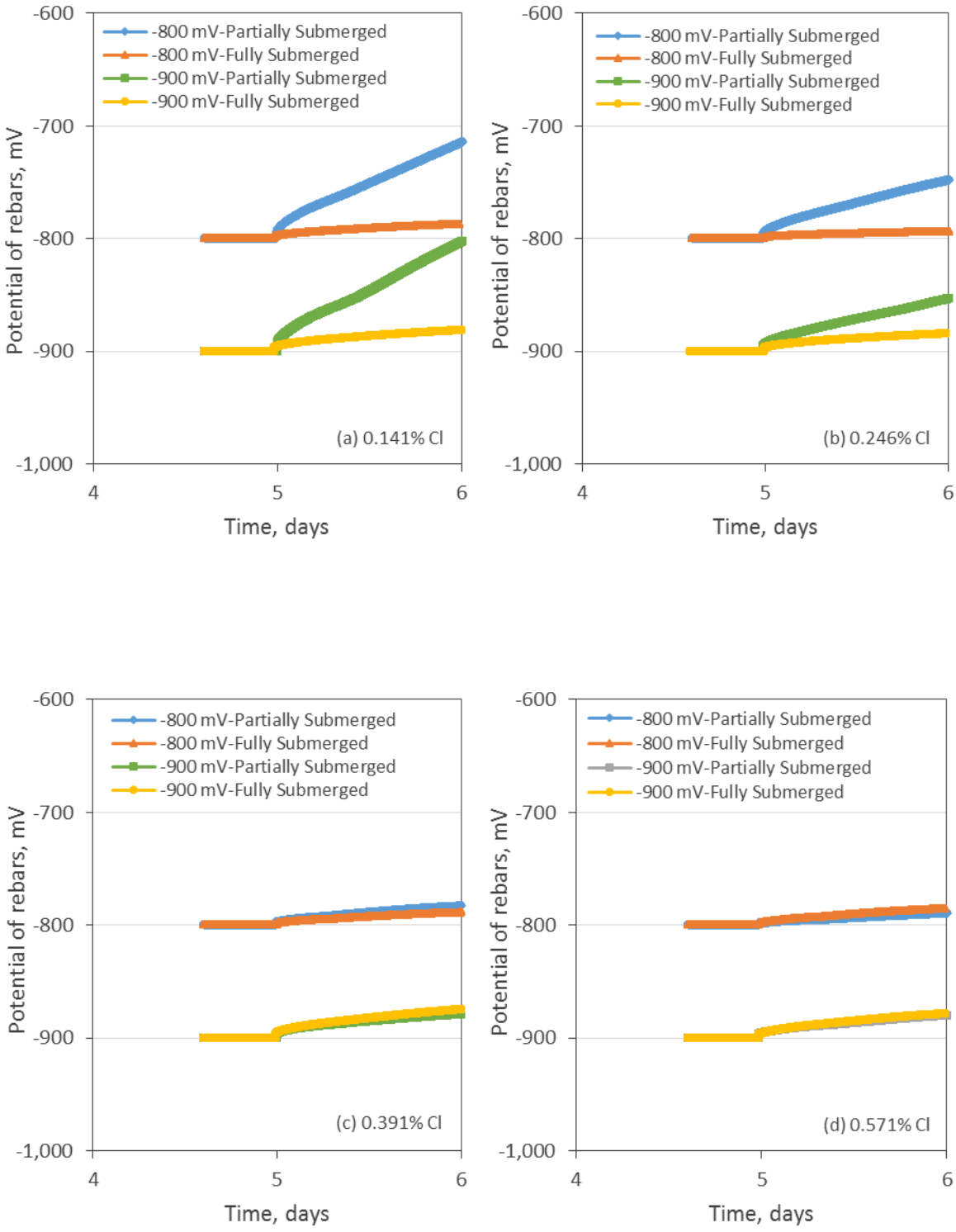

Figure 6.10: Potential decay with time for fully and partially submerged specimens under different applied protection potentials and chloride contents

6.4 Anode Potential under CP with Constant Potential

Figure 6.11 shows the variation of the anode potential (Ea), the cathode potential (Ec) and their difference (Ec-Ea) in relation with the applied feeding voltage during the application of CP system. The applied feeding voltage represents the voltage difference between the rebars cathode and the anode during CP operation. The data in Figure 6.11 were collected during the application of -900 mV protection potential on the rebars of the partially submerged specimens at three different chloride contents.

It can be seen from Figure 6.11 that potential of the anode is not a constant at the start, but becomes stable after 1 ~ 2 days. Also, it is clearly that, as expected, the applied feeding voltage is equal to the cathode potential minus the anode potential. However, the behaviour where the feeding voltage is equal to the potential difference between the cathode and the anode depends on the water and chloride distribution in concrete. In an evenly distributed conditions, the feeding voltage is equal to the potential difference between the cathode and the anode. Otherwise, they will be different. For example, the increase of resistivity will result to increase the difference between the applied potential and the actual one, which means higher feeding voltage is required to apply a certain value of steel polarization to anodic areas with high resistivity. So, this test can reflect the effect of concrete resistance on the polarization efficiency.

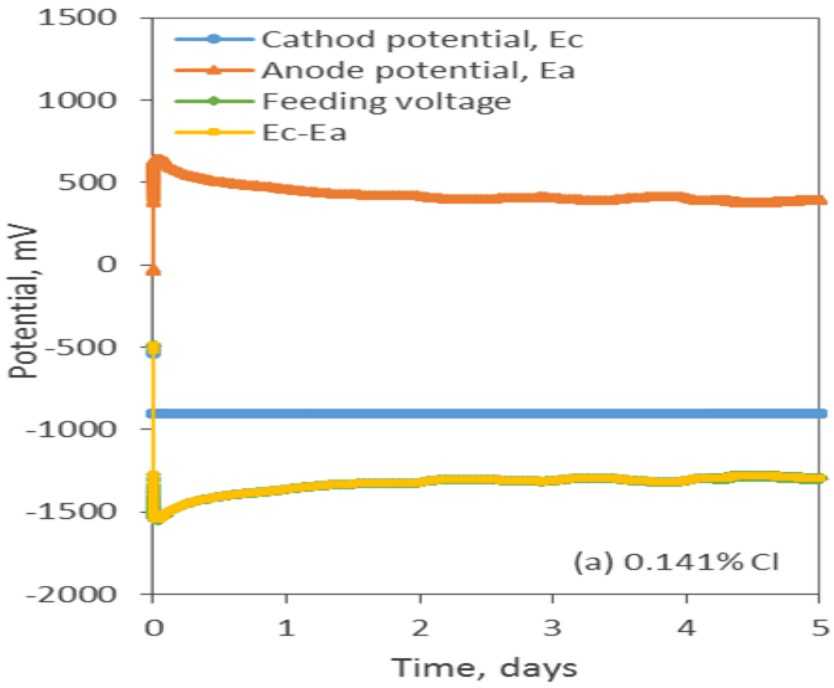

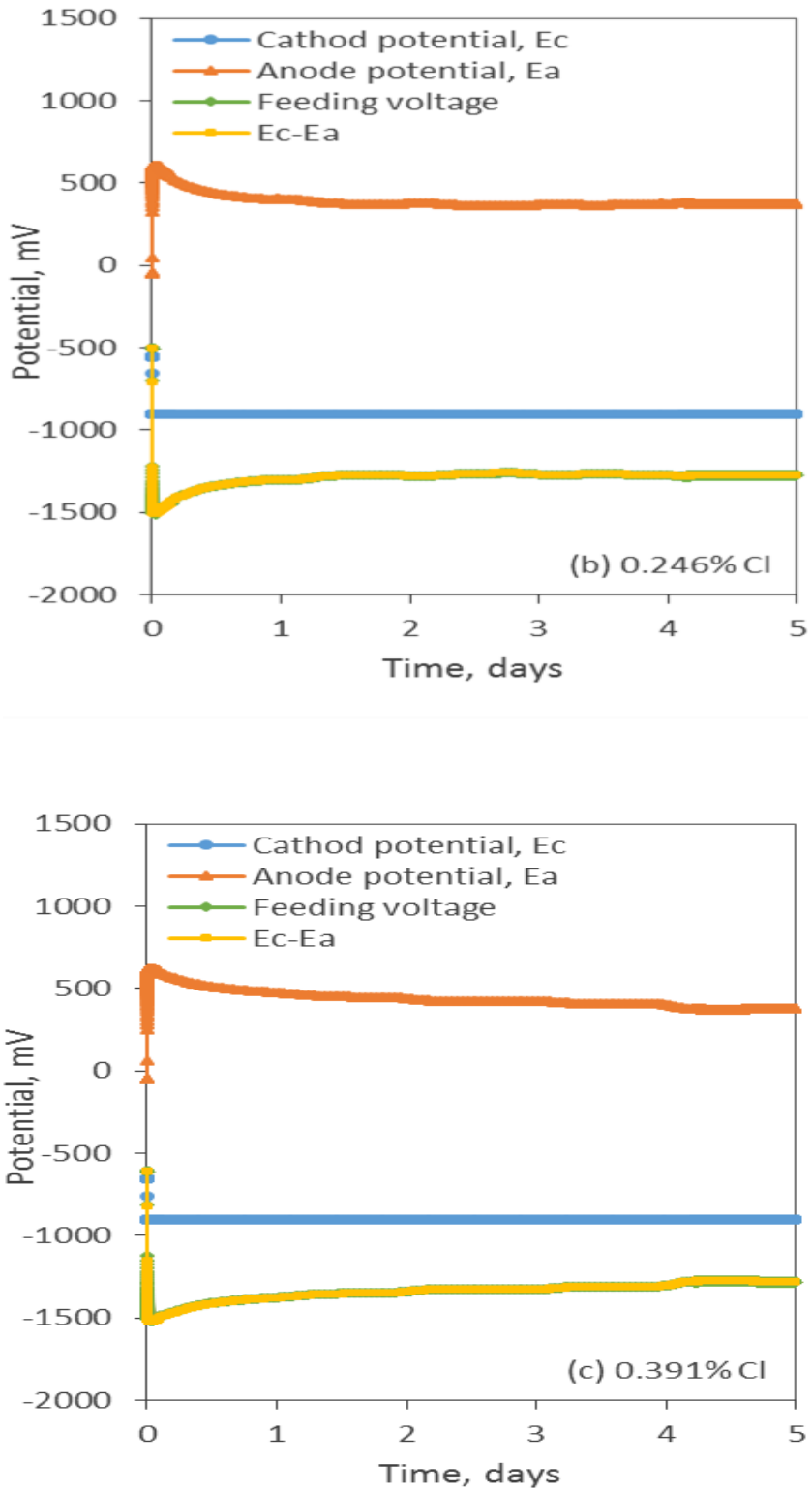

Figure 6.11: Rebars and anode potential and potential difference in relation with feeding voltage for partially submerged specimens at different chloride contents.

CHAPTER SEVEN

SUMMARY, CONCLUSIONS AND FUTURE WORK

CHAPTER 7 SUMMARY, CONCLUSIONS AND FUTURE WORK

7.1 Summary

The research undertaken has been concerned with concrete resistivity, rebars corrosion and CP of reinforced concrete at different chloride contents and exposure conditions. The research programme was designed to provide an insight into some significant interactive factors which are directly related to the measurement of concrete resistivity and design process of the CP system.

The main aims of the present work were to investigate the effect of chloride concentration, water content, exposure conditions, concrete resistivity and applied current density on the efficiency of CP in terms of the existing design criteria, and outline the information in order to obtain an optimal design parameters for corrosion protection. Reinforced concrete specimens had varied chloride and water contents have been examined. They were subjected to three different exposure conditions (air-exposure, fully and partially submerged in salty solutions). Constant current mode was used for the application of CP for the specimens of the air dried condition as it the most popular approach in practice for the structures exposed to atmospheric conditions. However, for submerged structures, the situation of the reinforcement is quite different. To understand if the constant current mode is efficient to provide adequate protection, a question still not very clear to date. An experimental investigation has been conducted to compare the two modes using constant CP current and constant CP potential for their effects referring to the existing CP design criteria.

The research was also planned to investigate the key influencing factors on electrical resistivity of concrete, a key parameter in the design of CP. The optimal frequency and electrode configuration have been investigated for their effects on the measurement results. Specimens with internal CF electrodes and external electrodes made of CF and copper were compared under different alternative electrical current of frequencies. The key influencing factors include water to cement ratio, chloride contents and water saturation.

7.2 Conclusions

Based on the results obtained in this work, the following conclusions can be drawn:

Electrical Resistivity of Concrete

1. To obtain a reliable measurement, low frequencies should be avoided as they give overestimation particularly in the case of using external electrodes. High frequency of 10,000 Hz is recommended.

2. Using internal electrodes of CF sheets is a more reliable, which improve the accuracy of the measurement of both saturated and unsaturated concrete specimens.

3. A corrosion factor of 1.14 on average and can reach up to 1.22 in some cases could be applied for the resistivity values of unsaturated specimens measured at 60% RH using external electrodes.

4. External CF sheets could be an alternative choice for copper plates to measure the resistivity of concrete particularly when inert, and flexible for better contact material is required.

5. Amount of chloride and w/c ratio have an important influence on the resistivity of concrete. For the specimens with 0% Cl at saturated condition, increasing w/c ratio from 0.4 to 0.5 and from 0.4 to 0.6 led to 35 and 43% reduction in the resistivity value, respectively. While increasing total chloride content from 0 to 0.5% (by weight of dry concrete) for the specimens of w/c ratio of 0.4 at saturated condition, the resistivity decreased by 73%.

6. RH which reflects the water content has a significant effect on the resistivity much more than chloride and w/c ratio. For the specimens of 0% Cl and 0.4 w/c, decreasing RH from 100 to 80% and from 100 to 60%, the resistivity increased from 6 to 113 kΩ.cm and from 6 to 805 kΩ.cm, respectively. The electrical resistivity decreases sharply and nonlinearly with the increase of the water content. The higher the water content, the lower the electrical resistivity of the concrete.

7. Under the conditions of a certain chloride and relatively low water contents, the effect of the pore porosity evaluated in terms of the w/c in practical range on the electrical resistivity of the concrete can be neglected. However, at high water saturation, resistivity presents an approximately linear decrease with the increase of w/c.

Cathodic Protection for Air Exposure Specimens

1. The reinforcement in chloride free concrete is safe from corrosion. A total chloride content equivalent to 0.141% by concrete weight is sufficent to activate a severe corrosion of reinforcement, and severity of corrosion increases with the increase of chloride content. An approximately linear relationship exists between the resistivity of concrete and chloride content, while the relation between cholride content or the concrete resistivity with the reinforcement corrosion potentail can be represented using power function.

2. A total chloride content of 0.055% by weight of concrete (equivalent to 0.32% by cement weight) or 17 kΩ.cm concrete electrical resisitivity, which showed to initiate corrosion, may be set as a threshold for CP implementation to protect the reinforcements in Portland concrete from corrosion.

3. Running CP for 24 hrs is long enough to make assessment for the performance of CP.

4. The recommended instant-off potential (-720 mV vs Ag/AgCl/0.5KCl) by the British standard as a criterion for the evaluation of CP system has not been achieved for the specimens with the selected chloride contents in this work even under the application of high CP current densities (i.e., 75 mA/m^2).

5. An instant-off potential of -500 mV with respect to Ag/AgCl/0.5KCl reference electrode can provide adequate protection for the reinforced concrete of up to 0.59 % chloride contamination by concrete weight (3.4% by weight of cement) , or with concrete resistivity of not less than 6.7 kΩ.cm. The adequacy of CP depends on the chloride content if the instant-off potential is less negative than -500 mV.

6. The conventional 100 mV depolarization criterion for CP operation gives an over estimated protection that increases with the increase of the protection current

requirement. For the chloride contaminated reinforced concrete under atmospheric condition, half of the depolarization criterion, i.e., 50 mV, may be used for CP assessment.

7. In term of the 100 mV depolarization criterion, the minimum current density required for sufficient protection is linearly proportional to the degree of chloride contamination with a slope of 136 mA/m^2/total chloride percentage minus 7.5, or inversely proportional to the concrete resistivity with a slope of -6.5 and interception of 113.

8. No sign of cracks or deterioration was observed at the concrete-embedded CF interface when CP current densities of 20 and 200 mA/m^2 were applied, respectively, for 28 days between the rebars and CF anode that embedded in concrete specimens. This reflects that using embedded CF as anode improves debonding issues that occur when contact materials (commercial conductive carbon aluminosilicate paste, carbon fibre reinforced mortar and carbon reinforced epoxy) that reported in previous publications were used as adhesives for external CF anode.

Cathodic Protection for Submerged Specimens

1. Corrosion potential can not be used as a stand –alone technique to indicate the real severity of corrosion for the fully submerged specimens as there was no clear relationship observed between the corrosion potential and chloride contents.

2. Measurements of chloride, concrete resistivity and corrosion rate are highly recommended to obtain a clear vision of the corrosion activity in structures exposed to high moisture.

3. The water content and chloride content should be explicitly related to the corrosion state rather than through a single parameter of the concrete resistivity for the saturated specimens because the water content will affect the oxygen transportation in concrete, and the oxygen availability at the rebar surface will play an important role in the corrosion process, and this is unassessable by concrete resistivity

4. Adopting a constant current mode for CP operation of the fully submerged specimens is likely lead to overprotection and causing hydrogen evolution at the reinforcement surface. Using constant potential mode is more convenient than applying constant current mode and it is highly recommended for submerged structures.

5. In terms of 100 mV depolarisation criterion, 4 or 24 hours is not applicable for assessing the performance CP where concrete structures are fully submerged due to the low availability of oxygen and the depolarization rate is less dependent on the chloride and CP current density. However, it can be adopted for the partially submerged specimens. Different parameters affect the depolarization value such as the magnitude of the applied protection current or potential, chloride concentration, exposure condition and oxygen existence and time of depolarization.

6. The passing current which reflect the current demand to provide the required potential for a CP system increases with the increase of chloride content.

7.3 Future Work

An experimental investigation was carried out in this research and generated a significant laboratory and practical findings which expand the knowledge and understating when considering concrete resistivity measurement and designing cathodic protection for different site conditions. However, based on previous research and the present study, the following research areas would be very interesting.

1. Using internal electrodes made of carbon fibre improved the accuracy of the electrical resistivity measurement for saturated and unsaturated concrete specimens. This was limited to laboratory investigation. Therefore, it is suggested to correlate this data with the obtained using 4-probe Wenner method, which is the most commonly technique used in practice.

2. High corrosion rates reached up to 140 mA/m^2 were measured for the submerged concrete specimens using linear polarization method. A research program may be carried out to determine corrosion rate for specimens with high moisture content using different test methodologies for comparison.

3. A research program to observe the microstructure of the contact zone between embedded carbon fibre anode and concrete surface. Scanning Electron Microscope (SEM) technique can be performed for the seek if there is any degradation. This needs to be undertaken before and after the application of cathodic protection.

4. A research plan is suggested to study the influence of water level of the partially submerged laboratory columns under different chloride concentrations on the 100 mV depolarization design criteria. This study can also observe the variation of corrosion rate, corrosion potential, concrete resistivity and CP current distribution along the specimens.

5. Unsaturated reinforced concrete specimens with different chloride and water contents can be investigated for corrosion potential, corrosion rate and CP under different temperatures.

6. The benefit of rebars coating on the requirement of cathodic protection under various environmental condition can be investigated.

7. The outcomes of this work are very useful to provide a design tool for the resistivity of concrete and calculation of cathodic protection current requirement in relation with the design criteria.

8. In this study, only Portland cement was investigated. A research program is required to investigate the influence of different types of cement and additives on the threshold value of chloride, reinforcement corrosion resistance and cathodic protection requirements.

9. Further work is also needed to compare carbon fibre sheet with the most widely used titanium mesh as anode in impressed current cathodic protection system. The comparison could include electrical and mechanical properties and service life.

REFERENCES

Ahmad, S. (2003). Reinforcement corrosion in concrete structures, its monitoring and service life prediction—a review. *Cement and Concrete Composites, 25*(4–5), 459-471. doi:http://dx.doi.org/10.1016/S0958-9465(02)00086-0

Ahmad, S., Jibran, M. A. A., Azad, A. K., and Maslehuddin, M. (2014). A simple and reliable setup for monitoring corrosion rate of steel rebars in concrete. *The scientific world journal, 2014*.

Al-Sulaimani, G., Kaleemullah, M., and Basunbul, I. (1990). Influence of corrosion and cracking on bond behavior and strength of reinforced concrete members. *ACI Structural Journal, 87*(2).

Ali, M. G., and Alsulaimani, G. J. (1993). Degradation of bond between reinforcing steel and concrete due to cathodic protection current. *Materials Journal, 90*(1), 8-15.

Alonso, C., Andrade, C., Castellote, M., and Castro, P. (2000). Chloride threshold values to depassivate reinforcing bars embedded in a standardized OPC mortar. *Cement and Concrete Research, 30*(7), 1047-1055.

Alonso, C., Andrade, C., and Gonzalez, J. (1988). Relation between resistivity and corrosion rate of reinforcements in carbonated mortar made with several cement types. *Cement and Concrete Research, 18*(5), 687-698.

Andrade, C., and Alonso, C. (1996). Corrosion rate monitoring in the laboratory and on-site. *Construction and Building Materials, 10*(5), 315-328.

Andrade, C., and Alonso, C. (2004). Test methods for on-site corrosion rate measurement of steel reinforcement in concrete by means of the polarization resistance method. *Materials and Structures, 37*(9), 623-643.

Andrade, C., and Gonzalez, J. (1978). Quantitative measurements of corrosion rate of reinforcing steels embedded in concrete using polarization resistance measurements. *Materials and Corrosion, 29*(8), 515-519.

Angst, U., Elsener, B., Larsen, C. K., and Vennesland, Ø. (2009). Critical chloride content in reinforced concrete—a review. *Cement and Concrete Research, 39*(12), 1122-1138.

Angst, U. M., Elsener, B., Larsen, C. K., and Vennesland, Ø. (2011). Chloride induced reinforcement corrosion: electrochemical monitoring of initiation stage and chloride threshold values. *Corrosion Science, 53*(4), 1451-1464.

Ann, K. Y., and Song, H.-W. (2007). Chloride threshold level for corrosion of steel in concrete. *Corrosion Science, 49*(11), 4113-4133.

Araujo, A., Panossian, Z., and Lourenço, Z. (2013). Cathodic protection for concrete structures. *Revista IBRACON de Estruturas e Materiais, 6*(2), 178-193.

Arya, C., Bioubakhsh, S., and Vassie, P. (2014). Chloride penetration in concrete subject to wet/dry cycling: influence of moisture content. *Proceedings of the ICE - Structures and Buildings, 167*(2), 94-107. doi:10.1680/stbu.12.00027

Ashworth, V. (2010). Principles of Cathodic Protection. *Shreir's Corros.*, 2747-2762.

ASTM C876. (2015). Standard test method for corrosion potentials of uncoated reinforcing steel in concrete: ASTM International, West Conshohocken, PA, USA.

ASTM C1152/C1152M. (2012). Standard test method for acid-soluble chloride in mortar and concrete: ASTM International, West Conshohocken, PA, USA.

ASTM C1218/C1218M. (2015). Standard test method for water-soluble chloride in mortar and concrete. ASTM International, West Conshohocken, PA, USA.

ASTM C1760. (2012). Standard Test Method for Bulk Electrical Conductivity of Hardened Concrete ASTM International, West Conshohocken, PA, USA.

ASTM G5. (2014). Standard reference test method for making potentiodynamic anodic polarization measurements: ASTM International, West Conshohocken, PA, USA.

Austin, S. A., Lyons, R., and Ing, M. (2004). Electrochemical behavior of steel-reinforced concrete during accelerated corrosion testing. *Corrosion, 60*(2), 203-212.

Azarsa, P., and Gupta, R. (2017). Electrical Resistivity of Concrete for Durability Evaluation: A Review. *Advances in Materials Science and Engineering, 2017*.

Badea, G., Caraban, A., Sebesan, M., Dzitac, S., Cret, P., and Setel, A. (2010). Polarisation measurements used for corrosion rates determination. *Journal of sustenable energy, 1*.

Banea, P. (2015). *The study of electrical resistivity of mature concrete.* TU Delft, Delft University of Technology.

Banthia, N., Djeridane, S., and Pigeon, M. (1992). Electrical resistivity of carbon and steel micro-fiber reinforced cements. *Cement and Concrete Research, 22*(5), 804-814.

Barnhart, R. (1982). FHWA position on cathodic protection systems. *Memorandum of FHWA, FHWA, Washington, DC*.

Bastidas, D., Cobo, A., Otero, E., and González, J. (2008). Electrochemical rehabilitation methods for reinforced concrete structures: advantages and pitfalls. *Corrosion Engineering, Science and Technology, 43*(3), 248-255.

Basu, B. (2016). *Biomaterials for Musculoskeletal Regeneration: Concepts*: Springer.

Bentur, A., Berke, N., and Diamond, S. (1997). *Steel corrosion in concrete: fundamentals and civil engineering practice*: CRC Press.

Berkeley, K., and Pathmanaban, S. (1990). *Cathodic protection of reinforcement steel in concrete*. london: Butterworth.

Bertolini, L., Bolzoni, F., Cigada, A., Pastore, T., and Pedeferri, P. (1993). Cathodic protection of new and old reinforced concrete structures. *Corrosion Science, 35*(5–8), 1633-1639. doi:http://dx.doi.org/10.1016/0010-938X(93)90393-U

Bertolini, L., Bolzoni, F., Gastaldi, M., Pastore, T., Pedeferri, P., and Redaelli, E. (2009). Effects of cathodic prevention on the chloride threshold for steel corrosion in concrete. *Electrochimica Acta, 54*(5), 1452-1463. doi:10.1016/j.electacta.2008.09.033

Bertolini, L., Bolzoni, F., Pedeferri, P., and Pastore, T. (1998). *Cathodic protection of reinforcement in carbonated concrete*. Retrieved from

Bertolini, L., Carsana, M., and Redaelli, E. (2008). Conservation of historical reinforced concrete structures damaged by carbonation induced corrosion by means of electrochemical realkalisation. *Journal of Cultural Heritage, 9*(4), 376-385.

Bertolini, L., Elsener, B., Pedeferri, P., Redaelli, E., and Polder, R. B. (2013). *Corrosion of steel in concrete: prevention, diagnosis, repair* (Second ed.). Germany: John Wiley & Sons.

Bertolini, L., Yu, S., and Page, C. (1996). Effects of electrochemical chloride extraction on chemical and mechanical properties of hydrated cement paste. *Advances in Cement Research, 8*(31), 93-100.

Bhargava, J., and Rehnstrom, A. (1978). Electrochemical aspects of electrical resistance gages for concrete. *NASA STI/Recon Technical Report N, 79*.

Bird, J. O., and Chivers, P. (2014). *Newnes engineering and physical science pocket book*: Newnes.

Bolzoni, F., Goidanich, S., Lazzari, L., and Ormellese, M. (2006). Corrosion inhibitors in reinforced concrete structures Part 2–Repair system. *Corrosion Engineering, Science and Technology, 41*(3), 212-220.

Bremner, T., Hover, K., Poston, R., Broomfield, J., Joseph, T., Price, R., . . . Clifton, J. (2001). *Protection of metals in concrete against corrosion*. Retrieved from

Broomfield, J. P. (2000). The principles and practice of galvanic cathodic protection for reinforced concrete structures. *CPA Monograph*(6).

Broomfield, J. P. (2007). *Corrosion of steel in concrete: understanding, investigation and repair* (Second ed.). UK: Taylor & Francis.

Browner, R. (1982). Design prediction of the life for reinforced concrete in marine and other chloride environments. *Durability of building materials, 1*(2), 113-125.

BS EN 206. (2016). Concrete — Specification, performance, production and conformity: British Standards Institution, London.

BS EN 14038-1. (2016). Electrochemical realkalization and chloride extraction treatments for reinforced concrete - Part 1: Realkalization: British Standards Institution, London.

BS EN 14629. (2007). Determination of chloride content in hardened concrete: British Standards Institution, London.

BS EN ISO 8044. (2015). Corrosion of metals and alloys — Basic terms and definitions: British Standards Institution, London.

BS EN ISO 12696. (2012). Cathodic protection of steel in concrete: British Standards Institution.

Buenfeld, N. R., Glass, G. K., Hassanein, A. M., and Zhang, J.-Z. (1998). Chloride transport in concrete subjected to electric field. *Journal of Materials in Civil Engineering, 10*(4), 220-228.

Byrne, A., Holmes, N., and Norton, B. (2016). State-of-the-art review of cathodic protection for reinforced concrete structures. *Magazine of Concrete Research, 68*(13), 664-677.

Cairns, J., and Melville, C. (2003). The effect of concrete surface treatments on electrical measurements of corrosion activity. *Construction and Building Materials, 17*(5), 301-309.

Calleja, J. (1953). *Determination of setting and hardening time of high-alumina cements by electrical resistance techniques.* Paper presented at the Journal Proceedings.

Carmona, J., Climent, M., and Garcés, P. (2016). Influence of different ways of chloride contamination on the efficiency of cathodic protection applied on structural reinforced concrete elements. *Journal of Electroanalytical Chemistry*.

Carmona, J., Garcés, P., and Climent, M. (2015). Efficiency of a conductive cement-based anodic system for the application of cathodic protection, cathodic prevention and electrochemical chloride extraction to control corrosion in reinforced concrete structures. *Corrosion Science, 96*, 102-111.

Cavalier, P., and Vassie, P. (1981). *Investigation and repair of reinforcement corrosion in a bridge deck.* Paper presented at the Institution of Civil Engineers, Proceedings, Pt 1.

Chacko, R. M., Banthia, N., and Mufti, A. A. (2007). Carbon-fiber-reinforced cement-based sensors. *Canadian Journal of Civil Engineering*, *34*(3), 284-290.

Chang, C., Song, G., Gao, D., and Mo, Y. L. (2013). Temperature and mixing effects on electrical resistivity of carbon fiber enhanced concrete. *Smart Materials and Structures, 22*(3), 035021. doi:10.1088/0964-1726/22/3/035021

Chang, J.-J., Yeih, W., and Huang, R. (1999). Degradation of the bond strength between rebar and concrete due to the impressed cathodic current. *Journal of marine science and technology, 7*(2), 89-93.

Chaussadent, T., Nobel-Pujol, V., Farcas, F., Mabille, I., and Fiaud, C. (2006). Effectiveness conditions of sodium monofluorophosphate as a corrosion inhibitor for concrete reinforcements. *Cement and Concrete Research, 36*(3), 556-561.

Checchetti, A., and Lanzo, J. (2015). Qualitative Measurement of pH and Mathematical Methods for the Determination of the Equivalence Point in Volumetric Analysis. *World Journal of Chemical Education, 3*(3), 64-69.

Chemrouk, M. (2015). The deteriorations of reinforced concrete and the option of high performances reinforced concrete. *Procedia Engineering, 125*, 713-724.

Chen, C.-T., Chang, J.-J., and Yeih, W.-c. (2014). The effects of specimen parameters on the resistivity of concrete. *Construction and Building Materials, 71*, 35-43. doi:10.1016/j.conbuildmat.2014.08.009

Chess, P. M., and Broomfield, J. P. (2013). *Cathodic protection of steel in concrete and masonry* (Second ed.). USA: CRC Press.

Cheung, M. M. S., and Cao, C. (2013). Application of cathodic protection for controlling macrocell corrosion in chloride contaminated RC structures. *Construction & Building Materials, 45*, 199-207. doi:10.1016/j.conbuildmat.2013.04.010

Chynoweth, G., Stankie, R. R., Allen, W. L., Anderson, R. R., Babcock, W. N., Barlow, P., . . . Constantino, F. J. (1996). Concrete repair guide. *ACI committee, concrete repair manual, 546*, 287-327.

Committee, A. C. I. (1985). Corrosion of Metals in Concrete. *Journal Proceedings, 82*(1). doi:10.14359/10311

COST Action 509. (1997). *Corrosion and Protection of Metals in Contact with Concrete, Final report (eds R.N. Cox, R. Cigna, O. Vennesland, and T. Valente), European Commission, Directorate General Science, Research and Development, Brussels, EUR 17608 EN.* Retrieved from

COST Action 521. (2003). *Corrosion of Steel in Reinforced Concrete Structures, Final Report, (eds R. Cigna, C. Andrade, U. Nürnberger, R. Polder, R. Weydert, and E. Seitz) European Commission, Directorate General for Research, EUR20599*. Retrieved from

Covino Jr, B. S., Cramer, S. D., Bullard, S. J., Holcomb, G. R., Russell, J. H., Collins, W. K., . . . Cryer, C. B. (2002). *Performance of zinc anodes for cathodic protection of reinforced concrete bridges*. Retrieved from

Daily, S. F. (1999). *Understanding corrosion and cathodic protection of reinforced concrete structures*: Corrpro Companies, Incorporated.

Davis, J. R. (2000). *Corrosion: Understanding the basics*: ASM International.

DD CEN/TS 14038-2. (2011). Electrochemical realkalisation and chloride extraction for reinforced concrete. Part 2: Chloride extraction, European technical specification.: British Standards Institution, London.

De Schutter, G. (2012). *Damage to concrete structures*: Crc Press.

Dhir, R., Jones, M., and Ahmed, H. (1990). Determination of total and soluble chlorides in concrete. *Cement and Concrete Research, 20*(4), 579-590.

Dugarte, M., and Sag, A. A. (2009). *Galvanic point anodes for extending the service life of patched areas upon reinforced concrete bridge members*. Retrieved from

Elkey, W., and Sellevold, E. J. (1995). Electrical resistivity of concrete.

Elsener, B. (2001). *Corrosion inhibitors for steel in concrete: state of the art report* (Vol. 773): Maney Pub.

Elsener, B., Andrade, C., Gulikers, J., Polder, R., and Raupach, M. (2003). Hall-cell potential measurements—Potential mapping on reinforced concrete structures. *Materials and Structures, 36*(7), 461-471.

Evans, U. R. (1960). *The corrosion and oxidation of metals: scientific principles and practical application*: Edward Arnold.

Farnam, Y., Todak, H., Spragg, R., and Weiss, J. (2015). Electrical response of mortar with different degrees of saturation and deicing salt solutions during freezing and thawing. *Cement and Concrete Composites, 59*, 49-59.

Feliu, S., Gonzalez, J. A., and Andrade, C. (1996). Electrochemical methods for on-site determinations of corrosion rates of rebars *Techniques to assess the corrosion activity of steel reinforced concrete structures*: ASTM International.

Fontana, M. G. (2005). *Corrosion engineering*: Tata McGraw-Hill Education.

Ghods, P., Chini, M., Hoseini, M., and Alizadeh, R. (2005). *Evaluating the chloride diffusion of concrete by measuring electrical resistivity.* Paper presented at the International Congress-Global Construction: Ultimate Concrete Opportunities, Proceedings of the International Conference on Young Researchers' Forum.

Ghods, P., Isgor, O., Brown, J., Bensebaa, F., and Kingston, D. (2011). XPS depth profiling study on the passive oxide film of carbon steel in saturated calcium hydroxide solution and the effect of chloride on the film properties. *Applied Surface Science, 257*(10), 4669-4677.

Gjørv, O. E., Vennesland, Ø. E., and El-Busaidy, A. (1977). *Electrical resistivity of concrete in the oceans.* Paper presented at the Offshore Technology Conference.

Glass, G., and Buenfeld, N. (1997). The presentation of the chloride threshold level for corrosion of steel in concrete. *Corrosion Science, 39*(5), 1001-1013.

Glasser, F., and Sagoe-Crentsil, K. (1989). Steel in concrete: Part II Electron microscopy analysis. *Magazine of Concrete Research, 41*(149), 213-220.

González, F., Fajardo, G., Arliguie, G., Juárez, C., and Escadeillas, G. (2011). Electrochemical realkalisation of carbonated concrete: An alternative approach to

prevention of reinforcing steel corrosion. *International Journal of Electrochemical Science, 6*(12), 6332-6349.

Gonzalez, J., and Andrade, C. (1982). Effect of carbonation, chlorides and relative ambient humidity on the corrosion of galvanized rebars embedded in concrete. *British Corrosion Journal, 17*(1), 21-28.

Gonzalez, J., Miranda, J., and Feliu, S. (2004). Considerations on reproducibility of potential and corrosion rate measurements in reinforced concrete. *Corrosion Science, 46*(10), 2467-2485.

Gower, M., and Windsor, D. (2000). Cathodic protection and condition monitoring: residential tower block, N. Lanarkshire. *Structural Engineer*.

Gowers, K., and Millard, S. (1999). Electrochemical techniques for corrosion assessment of reinforced concrete structures. *Proceedings of the Institution of Civil Engineers. Structures and buildings, 134*(2), 129-137.

Gu, P., and Beaudoin, J. J. (1998). *Obtaining effective half-cell potential measurements in reinforced concrete structures*: Institute for Research in Construction, National Research Council of Canada Ottawa.

Gummow, R. (1993). Cathodic protection potential criterion for underground steel structures. *Materials Performance, 32*(11).

Hammond, E., and Robson, T. (1955). Comparison of electrical properties of various cements and concretes. *The Engineer, 199*(5165), 78-80.

Hansson, C. (1984). Comments on electrochemical measurements of the rate of corrosion of steel in concrete. *Cement and Concrete Research, 14*(4), 574-584.

Hansson, C., Poursaee, A., and Laurent, A. (2006). Macrocell and microcell corrosion of steel in ordinary Portland cement and high performance concretes. *Cement and Concrete Research, 36*(11), 2098-2102.

Hansson, C. M., Poursaee, A., and Jaffer, S. J. (2012). Corrosion of reinforcing bars in concrete. *Portland Cement Association (PCA), PCA R&D Serial*(3013).

Hansson, I., and Hansson, C. (1983). Electrical resistivity measurements of Portland cement based materials. *Cement and Concrete Research, 13*(5), 675-683.

Haque, M., and Kayyali, O. (1993). Aspects of chloride ion determination in concrete. *Aci Materials Journal, 92*(5).

Hassanein, A. M., Glass, G. K., and Buenfeld, N. R. (2002). Protection current distribution in reinforced concrete cathodic protection systems. *Cement and Concrete Composites, 24*(1), 159-167. doi:http://dx.doi.org/10.1016/S0958-9465(01)00036-1

Haupt, S., and Strehblow, H. (1987). Corrosion, layer formation, and oxide reduction of passive iron in alkaline solution: a combined electrochemical and surface analytical study. *Langmuir, 3*(6), 873-885.

Hausmann, D. (1967). Steel corrosion in concrete--How does it occur? *Materials protection*.

Henry, R. L. (1964). *Water Vapor Transmission and Electrical Resistivity of Concrete*. Retrieved from

Hong, D., Fan, W., Luo, D., Ge, Y., and Zhu, Y. (1993). Study and application of impressed current cathodic protection technique for atmospherically exposed salt-contaminated reinforced concrete structures. *Aci Materials Journal, 90*(1).

Hope, B. B., Ip, A. K., and Manning, D. G. (1985). Corrosion and electrical impedance in concrete. *Cement and Concrete Research, 15*(3), 525-534. doi:http://dx.doi.org/10.1016/0008-8846(85)90127-9

Hope, B. B., Page, J. A., and Poland, J. S. (1985). The determination of the chloride content of concrete. *Cement and Concrete Research, 15*(5), 863-870.

Hornbostel, K., Larsen, C. K., and Geiker, M. R. (2013). Relationship between concrete resistivity and corrosion rate–a literature review. *Cement and Concrete Composites, 39*, 60-72.

Hoseini, M., Cumming, N., Fussell, J., and Cook, S. (2016). *Rehabilitation and Maintenance of Reinforced Concrete Bridge Decks using Cathodic Protection System-A 30-year old Case*

Study. Paper presented at the TAC 2016: Efficient Transportation-Managing the Demand-2016 Conference and Exhibition of the Transportation Association of Canada.

Hou, Z., Li, Z., and Wang, J. (2010). Electrically conductive concrete for heating using steel bars as electrodes. *Journal of Wuhan University of Technology-Mater. Sci. Ed., 25*(3), 523-526. doi:10.1007/s11595-010-0035-x

Huang, R., Chang, J.-J., and Wu, J.-K. (1996). Correlation between corrosion potential and polarization resistance of rebar in concrete. *Materials Letters, 28*(4), 445-450.

Hughes, B., Soleit, A., and Brierley, R. (1985). New technique for determining the electrical resistivity of concrete. *Magazine of Concrete Research, 37*(133), 243-248.

Hunkeler, F. (1996). The resistivity of pore water solution—a decisive parameter of rebar corrosion and repair methods. *Construction and Building Materials, 10*(5), 381-389.

Hussain, R. R., and Ishida, T. (2012). Multivariable Empirical Analysis of Coupled Oxygen and Moisture for Potential and Rate of Quantitative Corrosion in Concrete. *Journal of Materials in Civil Engineering, 24*(7), 950-958. doi:10.1061/(asce)mt.1943-5533.0000474

Jeong, J.-A., Jin, C.-K., and Chung, W.-S. (2012). Tidal water effect on the hybrid cathodic protection systems for marine concrete structures. *Journal of Advanced Concrete Technology, 10*(12), 389-394.

Joiret, S., Keddam, M., Nóvoa, X., Pérez, M., Rangel, C., and Takenouti, H. (2002). Use of EIS, ring-disk electrode, EQCM and Raman spectroscopy to study the film of oxides formed on iron in 1 M NaOH. *Cement and Concrete Composites, 24*(1), 7-15.

Katwan, M. (1999). *Corrosion of steel reinforcement in concrete.* Paper presented at the Proceeding of the fourth conference for corrosion and corrosion prevention in industry, Iraq.

Katwan, M., and Al-Sofi, G. (1999). *TECHNICAL ASPECTS OF CONCRETE RESISTANCE MEASUREMENT.* Paper presented at the Controlling Concrete Degradation: Proceedings of the International Seminar Held at the University of Dundee, Scotland, UK on 7 September 1999.

Katwan, M. J. (1988). Corrosion fatique of reinforced concrete, PhD thesis. *University of Glasgow, Glasgow, UK*, , http://theses.gla.ac.uk/5327/.

Katwan, M. J. (2000). *Corrosion of stell reinforcement in concrete, durabilty problem No.1*. Iraq: Ministry of housing and construction, national centre for construction labs

Kendell, K. (1995). *A five year review of the application of cathodic protection to various industrial concrete structures in the arabian gulf*. Paper presented at the second regional concrete durability in the Arabian Gulf, Bahrain.

Kepler, J. L., Darwin, D., and Locke, C. E. (2000). Evaluation of corrosion protection methods for reinforced concrete highway structures. *Kansas department of transportation K-tran project No. Ku-99-6, University of Kansas centre for research, Inc. Lawrence, Kansas*, , http://www2.ku.edu/~iri/projects/corrosion/SM58.PDF.

Kerkhoff, B. (2007). *Effects of substances on concrete and guide to protective treatments*: Portland Cement Association Skokie.

Koch, G. H., Koch, G. H., Brongers, M. P. H., Thompson, N. G., Virmani, Y. P., and Payer, J. H. (2002). *HISTORIC CONGRESSIONAL STUDY: CORROSION COSTS AND PREVENTIVE STRATEGIES IN THE UNITED STATES*. Retrieved from

Kranc, S., Sagues, A. A., and Presuel-Moreno, F. J. (1997). *Computational and experimental investigation of cathodic protection distribution in reinforced concrete marine piling.* Paper presented at the CORROSION-NATIONAL ASSOCIATION OF CORROSION ENGINEERS ANNUAL CONFERENCE-.

Kupwade-Patil, K., and Allouche, E. N. (2012). Examination of chloride-induced corrosion in reinforced geopolymer concretes. *Journal of Materials in Civil Engineering, 25*(10), 1465-1476.

Küter, A. (2009). *Management of Reinforcement Corrosion: A Thermodynamic Approach.* Technical University of Denmark (DTU).

Lambert, P., Van Nguyen, C., Mangat, P. S., O'Flaherty, F. J., and Jones, G. (2015). Dual function carbon fibre fabric strengthening and impressed current cathodic protection (ICCP) anode for reinforced concrete structures. *Materials and Structures, 48*(7), 2157-2167.

Langford, P., and Broomfield, J. (1987). Monitoring the corrosion of reinforcing steel. *Construction Repair, 1*(2).

Layssi, H., Ghods, P., Alizadeh, A. R., and Salehi, M. (2015). Electrical Resistivity of Concrete: Concepts, applications, and measurement techniques. *Concrete international, 37*(5), 41-46.

Lian, C., Zhuge, Y., and Beecham, S. (2011). The relationship between porosity and strength for porous concrete. *Construction and Building Materials*, *25*(11), 4294-4298. doi:10.1016/j.conbuildmat.2011.05.005

Liu, Y., and Shi, X. (2009a). Cathodic protection technologies for reinforced concrete: introduction and recent developments. *Reviews in Chemical Engineering, 25*(5-6), 339-388.

Liu, Y., and Shi, X. (2009b). Electrochemical chloride extraction and electrochemical injection of corrosion inhibitor in concrete: state of the knowledge. *Corrosion reviews, 27*(1-2), 53-82.

Lorenz, W., and Mansfeld, F. (1981). Determination of corrosion rates by electrochemical DC and AC methods. *Corrosion Science, 21*(9-10), 647-672.

Lübeck, A., Gastaldini, A., Barin, D., and Siqueira, H. (2012). Compressive strength and electrical properties of concrete with white Portland cement and blast-furnace slag. *Cement and Concrete Composites, 34*(3), 392-399.

Mailvaganam, N. P., and Rixom, M. (2002). *Chemical admixtures for concrete*: CRC Press.

Mansfeld, F. (1981). *Electrochemical corrosion testing* (Vol. 727): ASTM International.

Marcotte, T., Hansson, C., and Hope, B. (1999). The effect of the electrochemical chloride extraction treatment on steel-reinforced mortar Part II: Microstructural characterization. *Cement and Concrete Research, 29*(10), 1561-1568.

Martínez, I., and Andrade, C. (2008). Application of EIS to cathodically protected steel: Tests in sodium chloride solution and in chloride contaminated concrete. *Corrosion Science, 50*(10), 2948-2958. doi:10.1016/j.corsci.2008.07.012

McCafferty, E. (2010). *Introduction to Corrosion Science*: Springer Science & Business Media.

McCarter, W., Taha, H., Suryanto, B., and Starrs, G. (2015). Two-point concrete resistivity measurements: interfacial phenomena at the electrode–concrete contact zone. *Measurement Science and Technology, 26*(8), 085007.

Medeiros-Junior, R. A., and Lima, M. G. (2016). Electrical resistivity of unsaturated concrete using different types of cement. *Construction and Building Materials, 107,* 11-16.

Medeiros, M., Rocha, F., Medeiros-JUNIOR, R., and Helene, P. (2017). Corrosion potential: influence of moisture, water-cement ratio, chloride content and concrete cover. *Revista IBRACON de Estruturas e Materiais, 10*(4), 864-885.

Mietz, J. (1998). *Electrochemical Rehabilitation Methods for Reinforced Concrete Structures – A State of the Art Report, European Federation of Corrosion Publication number 24, IOM Communications, London.* Retrieved from

MILLER, J. B. (1994). Structural Aspect of High Powered Electrochemical Treatment of Reinforced Concrete'. Corrosion and Corrosion Protection of Steel in Concrete, ed. By Prof. R.N. Swamy, Academic Press, Sheffield, ISBN 1 85075 723 2.

Miranda, J., González, J., Cobo, A., and Otero, E. (2006). Several questions about electrochemical rehabilitation methods for reinforced concrete structures. *Corrosion Science, 48*(8), 2172-2188.

Mohammed, T., and Hamada, H. (2003). Relationship between free chloride and total chloride contents in concrete. *Cement and Concrete Research, 33*(9), 1487-1490.

Monfore, G. (1968). The electrical resistivity of concrete. *Journal of the PCA Research andDevelopment Laboratories, 10*(2), 35-48.

Montemor, M., Simoes, A., and Salta, M. (2000). Effect of fly ash on concrete reinforcement corrosion studied by EIS. *Cement and Concrete Composites, 22*(3), 175-185.

Montemor, M. F., Simões, A. M. P., and Ferreira, M. G. S. (2003). Chloride-induced corrosion on reinforcing steel: from the fundamentals to the monitoring techniques. *Cement and Concrete Composites, 25*(4–5), 491-502. doi:http://dx.doi.org/10.1016/S0958-9465(02)00089-6

Montenegro, I., Queirós, M. A., and Daschbach, J. L. (2012). *Microelectrodes: theory and applications* (Vol. 197): Springer Science & Business Media.

Moore, W. J. (1975). A Comparison of Corrosion Rates Determined by Polarization Resistance Measurements for Zinc and Cadmium Metal Immersed in Nonstirred Aqueous Portland Cement Solution.

Morris, W., Moreno, E., and Sagüés, A. (1996). Practical evaluation of resistivity of concrete in test cylinders using a Wenner array probe. *Cement and Concrete Research, 26*(12), 1779-1787.

Morris, W., Vico, A., and Vázquez, M. (2004). Chloride induced corrosion of reinforcing steel evaluated by concrete resistivity measurements. *Electrochimica Acta, 49*(25), 4447-4453. doi:10.1016/j.electacta.2004.05.001

Morris, W., Vico, A., Vazquez, M., and de Sanchez, S. R. (2002). Corrosion of reinforcing steel evaluated by means of concrete resistivity measurements. *Corrosion Science, 44*(1), 81-99. doi:http://dx.doi.org/10.1016/S0010-938X(01)00033-6

Mundra, S., Criado, M., Bernal, S. A., and Provis, J. L. (2017). Chloride-induced corrosion of steel rebars in simulated pore solutions of alkali-activated concretes. *Cement and Concrete Research, 100*, 385-397.

NACE SP0290. (2007). Impressed current cathodic protection of reinforcing steel in atmospherically exposed concrete structures: NACE International, Houston, TX, USA.

Naish, C., Harker, A., and Carney, R. (1990). *Concrete Inspection-Interpretation of Potential and Resistivity Measurements*.

Nawy, E. G. (2008). *Concrete construction engineering handbook*: CRC press.

Neville, A. (1995). Chloride attack of reinforced concrete: an overview. *Materials and Structures, 28*(2), 63-70.

Neville, A. M. (1995). *Properties of concrete* (Vol. 4): Longman London.

Newlands, M. D., Jones, M. R., Kandasami, S., and Harrison, T. A. (2008). Sensitivity of electrode contact solutions and contact pressure in assessing electrical resistivity of concrete. *Materials and Structures, 41*(4), 621.

Ngala, V., Page, C., and Page, M. (2003). Corrosion inhibitor systems for remedial treatment of reinforced concrete. Part 2: sodium monofluorophosphate. *Corrosion Science, 45*(7), 1523-1537.

Novokshchenov, V. (1997). Corrosion surveys of prestressed bridge members using a half-cell potential technique. *Corrosion, 53*(6), 489-498.

Oelssner, W., Berthold, F., and Guth, U. (2006). The iR drop–well-known but often underestimated in electrochemical polarization measurements and corrosion testing. *Materials and Corrosion, 57*(6), 455-466.

Oh, B. H., Jang, S. Y., and Shin, Y. (2003). Experimental investigation of the threshold chloride concentration for corrosion initiation in reinforced concrete structures. *Magazine of Concrete Research, 55*(2), 117-124.

Ohtsuka, T., Nishikata, A., Sakairi, M., and Fushimi, K. (2017). Electrochemistry for Corrosion Fundamentals: Springer.

Orellan, J., Escadeillas, G., and Arliguie, G. (2004). Electrochemical chloride extraction: efficiency and side effects. *Cement and Concrete Research, 34*(2), 227-234.

Osterminski, K., Polder, R. B., and Schießl, P. (2012). Long term behaviour of the resistivity of concrete. *Heron, 57 (2012) 3*.

Page, C., and Havdahl, J. (1985). Electrochemical monitoring of corrosion of steel in microsilica cement pastes. *Materials and Structures, 18*(1), 41-47.

Page, C., and Lambert, P. (1986). *Analytical and electrochemical investigations of reinforcement corrosion* (0266-7045). Retrieved from

Page, C. L., and Page, M. M. (2007). *Durability of concrete and cement composites*: Elsevier.

Page, C. L., and Sergi, G. (2000). Developments in cathodic protection applied to reinforced concrete. *Journal of Materials in Civil Engineering, 12*(1), 8-15.

Papadakis, V., Fardis, M., and Vayenas, C. (1992). Effect of composition, environmental factors and cement-lime mortar coating on concrete carbonation. *Materials and Structures, 25*(5), 293-304.

Pargar, F., Koleva, D. A., and van Breugel, K. (2017). Determination of Chloride Content in Cementitious Materials: From Fundamental Aspects to Application of Ag/AgCl Chloride Sensors. *Sensors, 17*(11), 2482.

Parthiban, G. T., Parthiban, T., Ravi, R., Saraswathy, V., Palaniswamy, N., and Sivan, V. (2008). Cathodic protection of steel in concrete using magnesium alloy anode. *Corrosion Science, 50*(12), 3329-3335. doi:10.1016/j.corsci.2008.08.040

Pastore, T., Pedeferri, P., Bertolini, L., and Bolzoni, F. (1991). Current distribution in cathodically protected concrete slabs. *GTE Rendezveny Iroda gondozasaban(Hungary)*, 676-681.

Pedeferri, P. (1996). Cathodic protection and cathodic prevention. *Construction and Building Materials, 10*(5), 391-402. doi:http://dx.doi.org/10.1016/0950-0618(95)00017-8

Pei, H., Li, Z., Zhang, J., and Wang, Q. (2015). Performance investigations of reinforced magnesium phosphate concrete beams under accelerated corrosion conditions by multi techniques. *Construction and Building Materials, 93*, 989-994.

Perez, N. (2004). *Electrochemistry and corrosion science* (Vol. 412): Springer.

Pithouse, K. B. (1986). The cathodic protection of steel reinforcement in concrete. *CORROSION PREVENTION & CONTROL*(October), 113-119.

Polder, R. B. (1998). Cathodic protection of reinforced concrete structures in The Netherlands-experience and developments. *Book-Institute of Materials, 710*, 172-183.

Polder, R. B. (2001). Test methods for on site measurement of resistivity of concrete—a RILEM TC-154 technical recommendation. *Construction and Building Materials, 15*(2), 125-131.

Polder, R. B. (2009). Critical chloride content for reinforced concrete and its relationship to concrete resistivity. *Materials and Corrosion, 60*(8), 623-630. doi:10.1002/maco.200905302

Polder, R. B., Leegwater, G., Worm, D., and Courage, W. (2014). Service life and life cycle cost modelling of cathodic protection systems for concrete structures. *Cement and Concrete Composites, 47*, 69-74. doi:10.1016/j.cemconcomp.2013.05.004

Popoola, A., Olorunniwo, O., and Ige, O. (2014). Corrosion resistance through the application of anti-corrosion coatings. In M. Aliofkhazraei (Ed.), Developments in Corrosion Protection (pp. 241-270): InTech, DOI: 10.5772/57420.

Popov, B. N. (2015). *Corrosion engineering: principles and solved problems*: Elsevier.

Poulsen, E. (1995). Chloride profiles–Analysis and interpretation of observations. *AEClaboratory, Vadbaek*.

Poursaee, A. (2016). *Corrosion of Steel in Concrete Structures*: Woodhead Publishing.

Poursaee, A., and Hansson, C. (2009). Potential pitfalls in assessing chloride-induced corrosion of steel in concrete. *Cement and Concrete Research, 39*(5), 391-400.

Pradhan, B. (2014). Corrosion behavior of steel reinforcement in concrete exposed to composite chloride–sulfate environment. *Construction and Building Materials, 72*, 398-410.

Princigallo, A., van Breugel, K., and Levita, G. (2003). Influence of the aggregate on the electrical conductivity of Portland cement concretes. *Cement and Concrete Research, 33*(11), 1755-1763.

Qian, S., Zhang, J., and Qu, D. (2006). Theoretical and experimental study of microcell and macrocell corrosion in patch repairs of concrete structures. *Cement and Concrete Composites, 28*(8), 685-695.

Qiao, G., Guo, B., Ou, J., Xu, F., and Li, Z. (2016). Numerical optimization of an impressed current cathodic protection system for reinforced concrete structures. *Construction and Building Materials, 119*, 260-267.

Raj, M., and Muthupriya, P. (2016). Determination of concrete carbonation depth by experimental investigation. *International Journal of Engineering Science Invention Research & Development, II*(VIII February).

Rasheeduzzafar, F. H. D., Bader, M. A., and Khan, M. M. (1992). Performance of Corrosion-Resisting Steels in Chloride-Bearing Concrete. *Aci Materials Journal, 89*(5).

Redaelli, E., and Bertolini, L. (2011). Electrochemical repair techniques in carbonated concrete. Part I: electrochemical realkalisation. *Journal of Applied Electrochemistry, 41*(7), 817-827.

Ribeiro, P., Meira, G., Ferreira, P., and Perazzo, N. (2013). Electrochemical realkalisation of carbonated concretes–Influence of material characteristics and thickness of concrete reinforcement cover. *Construction and Building Materials, 40*, 280-290.

Robinson, R. (1975). Cathodic protection of steel in concrete. *ACI Special Publication, 49*.

Rosenberg, A., Hansson, C., and Andrade, C. (1989). Mechanisms of corrosion of steel in concrete. *Materials science of concrete, 1*, 285-314.

Roy, S., Poh, K., and Northwood, D. (1999). Durability of concrete—accelerated carbonation and weathering studies. *Building and environment, 34*(5), 597-606.

Sadowski, L. (2013). Methodology for assessing the probability of corrosion in concrete structures on the basis of half-cell potential and concrete resistivity measurements. *The scientific world journal*.

Sadowski, L., and Nikoo, M. (2014). Corrosion current density prediction in reinforced concrete by imperialist competitive algorithm. *Neural Computing and Applications, 25*(7-8), 1627-1638.

Saleem, M., Shameem, M., Hussain, S., and Maslehuddin, M. (1996). Effect of moisture, chloride and sulphate contamination on the electrical resistivity of Portland cement concrete. *Construction and Building Materials, 10*(3), 209-214.

Saremi, M., and Mahallati, E. (2002). A study on chloride-induced depassivation of mild steel in simulated concrete pore solution. *Cement and Concrete Research, 32*(12), 1915-1921.

Sathiyanarayanan, S., Natarajan, P., Saravanan, K., Srinivasan, S., and Venkatachari, G. (2006). Corrosion monitoring of steel in concrete by galvanostatic pulse technique. *Cement and Concrete Composites, 28*(7), 630-637.

Schweitzer, P. A. (2009). *Fundamentals of corrosion: mechanisms, causes, and preventative methods*: CRC Press.

Sellevold, E., Larsen, C., and Blankvoll, A. (1997). Moisture state of concrete in a coastal ridge. *Special Publication, 170*, 823-834.

Sengul, O. (2014). Use of electrical resistivity as an indicator for durability. *Construction and Building Materials, 73*, 434-441.

Sergi, G., Page, C., and Thompson, D. (1991). Electrochemical induction of alkali-silica reaction in concrete. *Materials and Structures, 24*(5), 359-361.

Shakouri, M., Trejo, D., and Gardoni, P. (2017). A probabilistic framework to justify allowable admixed chloride limits in concrete. *Construction and Building Materials, 139*, 490-500.

Shi, X., Cross, J. D., Ewan, L., Liu, Y., and Fortune, K. (2011). Replacing thermal sprayed zinc anodes on cathodically protected steel reinforced concrete bridges. *Oregon Department of Transportation Research Section and Federal Highway Administration, Washington*, , http://www.trb.org/BridgesOtherStructures/Blurbs/166080.aspx.

Siddiqi, Z. A. (2012). *Concrete Structures Part-II* (Vol. 2): Zahid Ahmad Siddiqi.

Sims, I. (1994). The assessment of concrete for carbonation. *Concrete, 28*(6).

Smith, J., and Virmani, Y. P. (2000). *Materials and methods for corrosion control of reinforced and prestressed concrete structures in new construction*. Retrieved from

Soleymani, H. R., and Ismail, M. E. (2004). Comparing corrosion measurement methods to assess the corrosion activity of laboratory OPC and HPC concrete specimens. *Cement and Concrete Research, 34*(11), 2037-2044.

Solomon, I., Bird, M. F., and Phang, B. (1993). An economic solution for the cathodic protection of concrete columns using a conductive tape system. *Corrosion Science, 35*(5), 1649-1660.

Song, H.-W., and Saraswathy, V. (2007a). Corrosion Monitoring of Reinforced Concrete Structures-A. *Int. J. Electrochem. Sci, 2*, 1-28.

Song, H.-W., and Saraswathy, V. (2007b). Corrosion Monitoring of Reinforced Concrete Structures-A Review. *Int. J. Electrochem. Sci, 2*, 1-28.

Söylev, T. A., and Richardson, M. (2008). Corrosion inhibitors for steel in concrete: State-of-the-art report. *Construction and Building Materials, 22*(4), 609-622.

Stanish, K., Hooton, R., and Thomas, M. (1997). Testing the chloride penetration resistance of concrete: a literature review. *Dep. Of Civil Eng., University of Toronto*.

Stern, M., and Geary, A. L. (1957). Electrochemical polarization I. A theoretical analysis of the shape of polarization curves. *Journal of the electrochemical society, 104*(1), 56-63.

Su, J. K., Yang, C. C., Wu, W. B., and Huang, R. (2002). Effect of moisture content on concrete resistivity measurement. *Journal of the Chinese Institute of Engineers, 25*(1), 117-122.

Sulapha, P., Wong, S., Wee, T., and Swaddiwudhipong, S. (2003). Carbonation of concrete containing mineral admixtures. *Journal of Materials in Civil Engineering, 15*(2), 134-143.

Takewaka, K. (1993). Cathodic protection for reinforced-concrete and prestressed-concrete structures. *Corrosion Science, 35*(5-8), 1617-1626.

Tilly, G., and Jacobs, J. (2007). *Concrete repairs: Performance in service and current practice*: IHS BRE Press.

Torres-Acosta, A. A., Sen, R., and Martínez-Madrid, M. (2004). Cathodic Protection of Reinforcing Steel in Concrete Using Conductive-Polymer System. *Journal of Materials in Civil Engineering, 16*(4), 315-321. doi:10.1061/(ASCE)0899-1561(2004)16:4(315)

Tremper, B., Beaton, J. L., and Stratfull, R. (1958). Causes and repair of deterioration to a california bridge due to corrosion of reinforcing steel in a marine environment. Part ii: fundamental factors causing corrosion. *Highway Research Board Bulletin*(182).

Trethewey, K. R., and Chamberlain, J. (1995). *Corrosion for science and engineering*. England: longman.

Teychenné, D. C., Franklin, R. E., and Erntroy, H. C. (1997). *Design of normal concrete mixes* (Second ed.). UK: Construction Research Communications Ltd.

Tuutti, K. (1980). Service life of structures with regard to corrosion of embedded steel. *Special Publication, 65*, 223-236.

Tuutti, K. (1982). *Corrosion of steel in concrete.* Swedish Cement and Concrete Research Institute.

Van Nguyen, C., Lambert, P., Mangat, P., O'Flaherty, F., and Jones, G. (2012). The performance of carbon fibre composites as iccp anodes for reinforced concrete structures. *ISRN Corrosion, 2012*, 1-9. doi:10.5402/2012/814923

Van Noort, R., Hunger, M., and Spiesz, P. (2016). Long-term chloride migration coefficient in slag cement-based concrete and resistivity as an alternative test method. *Construction and Building Materials, 115*, 746-759.

Verma, S. K., Bhadauria, S. S., and Akhtar, S. (2014). Monitoring corrosion of steel bars in reinforced concrete structures. *The scientific world journal*.

Villagrán Zaccardi, Y. A., and Di Maio, Á. A. (2014). Electrical resistivity measurement of unsaturated concrete samples. *Magazine of Concrete Research, 66*(10), 484-491. doi:10.1680/macr.13.00207

Virmani, Y. P., and Clemena, G. G. (1998). *Corrosion Protection-Concrete Bridges*. Retrieved from

Walter, G. (1978). The effect of IR-drop on corrosion rates calculated from low polarization data. *Corrosion Science, 18*(10), 927-945.

Wang, Y., Wang, X., Scholz, M., and Ross, D. (2012). A physico-chemical model for the water vapour sorption isotherm of hardened cementitious materials. *Construction and Building Materials, 35*, 941-946.

Wenner, F. (1915). A method for measuring earth resistivity. *Journal of the Washington Academy of Sciences, 5*(16), 561-563.

Whiting, D. A., and Nagi, M. A. (2003). Electrical resistivity of concrete-a literature review. *R&D Serial*(2457).

Whittington, H., McCarter, J., and Forde, M. (1981). The conduction of electricity through concrete. *Magazine of Concrete Research, 33*(114), 48-60.

Wilson, K., Jawed, M., and Ngala, V. (2013). The selection and use of cathodic protection systems for the repair of reinforced concrete structures. *Construction & Building Materials, 39*, 19-25. doi:10.1016/j.conbuildmat.2012.05.037

Wyatt, B. S. (1993). Cathodic protection of steel in concrete. *Corrosion Science, 35*(5–8), 1601-1615. doi:http://dx.doi.org/10.1016/0010-938X(93)90390-3

Wyatt, B. S. (1995). *Cathodic protection of steel in concrete.* Paper presented at the second regional concrete durability in the Arabian Gulf Bahrain.

Xi, Y., and Bažant, Z. P. (1999). Modeling chloride penetration in saturated concrete. *Journal of Materials in Civil Engineering, 11*(1), 58-65.

Xu, J., and Yao, W. (2009). Current distribution in reinforced concrete cathodic protection system with conductive mortar overlay anode. *Construction and Building Materials, 23*(6), 2220-2226.

Yang, L. (2008). *Techniques for corrosion monitoring*: Elsevier.

Yeih, W., and Chang, J. J. (2005). A study on the efficiency of electrochemical realkalisation of carbonated concrete. *Construction and Building Materials, 19*(7), 516-524.

Yodsudjai, W., and Pattarakittam, T. (2017). Factors influencing half-cell potential measurement and its relationship with corrosion level. *Measurement, 104*, 159-168.

Yoon, I.-S., Çopuroğlu, O., and Park, K.-B. (2007). Effect of global climatic change on carbonation progress of concrete. *Atmospheric Environment, 41*(34), 7274-7285.

Zafeiropoulou, T., Rakanta, E., and Batis, G. (2013). Carbonation resistance and anticorrosive properties of organic coatings for concrete structures. *Journal of Surface Engineered Materials and Advanced Technology, 3*(01), 67.

Zakroczymski, T., Fan, C. J., and Szklarska-Smialowska, Z. (1985). Kinetics and mechanism of passive film formation on iron in 0.05 M NaOH. *Journal of the electrochemical society, 132*(12), 2862-2867.

Zayed, A. M., and Sagues, A. A. (1990). Corrosion at surface damage on an epoxy-coated reinforcing steel. *Corrosion Science, 30*(10), 1025-1044.

Zhang, J., Liu, C., Sun, M., and Li, Z. (2017). An innovative corrosion evaluation technique for reinforced concrete structures using magnetic sensors. *Construction and Building Materials, 135*, 68-75.

Zhao, X., Gong, P., Qiao, G., Lu, J., Lv, X., and Ou, J. (2011). Brillouin corrosion expansion sensors for steel reinforced concrete structures using a fiber optic coil winding method. *Sensors, 11*(11), 10798-10819.

Zhou, Y., Gencturk, B., Willam, K., and Attar, A. (2014). Carbonation-Induced and Chloride-Induced Corrosion in Reinforced Concrete Structures. *Journal of Materials in Civil Engineering*.

Zhu, J.-H., Miaochang, Z., Ningxu, H., Wei, L., and Feng, X. (2014). Electrical and mechanical performance of carbon fiber-reinforced polymer used as the impressed current anode material. *Materials (1996-1944), 7*(8), 5438-5453. doi:10.3390/ma7085438

Zhu, J.-H., Wei, L., Zhu, M., Sun, H., Tang, L., and Xing, F. (2015). Polarization Induced Deterioration of Reinforced Concrete with CFRP Anode. *Materials, 8*(7), 4316-4331.

APPENDIXES

APPENDIX A

Potentiometric Titration Data of Chloride Determination

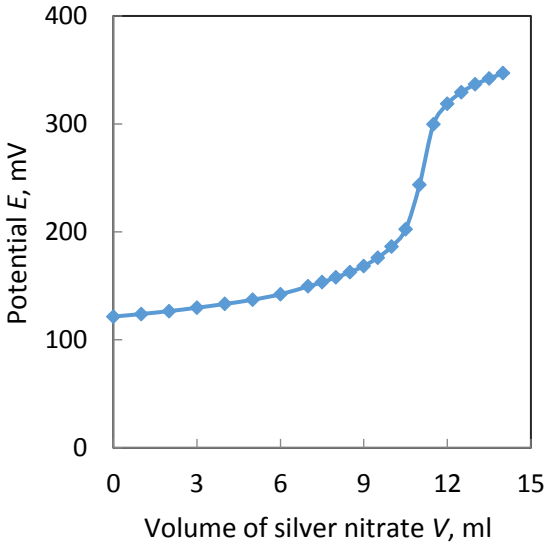

(a) Titration curve for the total chloride determination

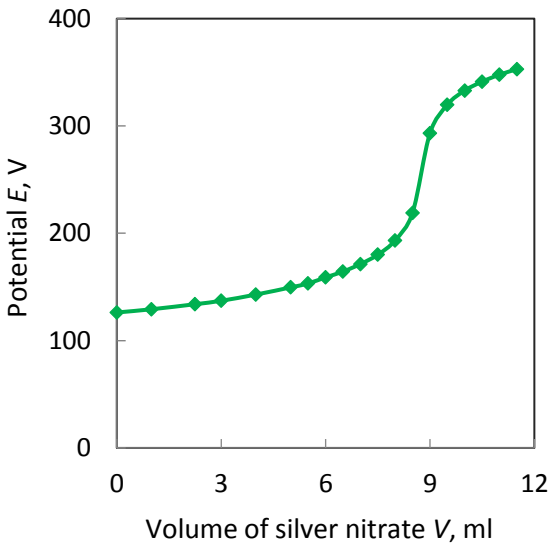

(c) Titration curve for the free chloride determination

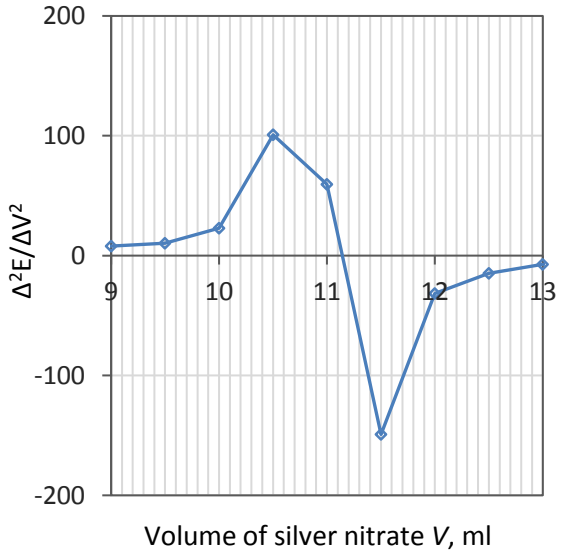

(b) Second derivative curve for the total chloride determination

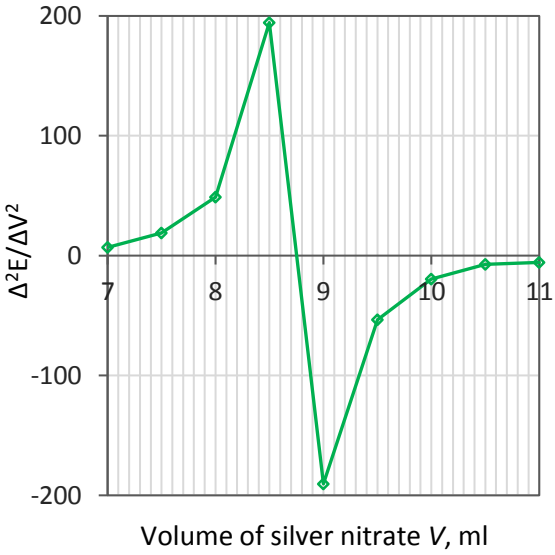

(d) Second derivative curve for the free chloride determination

Figure A.1: Potentiometric titration data of the samples at w/c of 0.4 and added NaCl of 1.5%

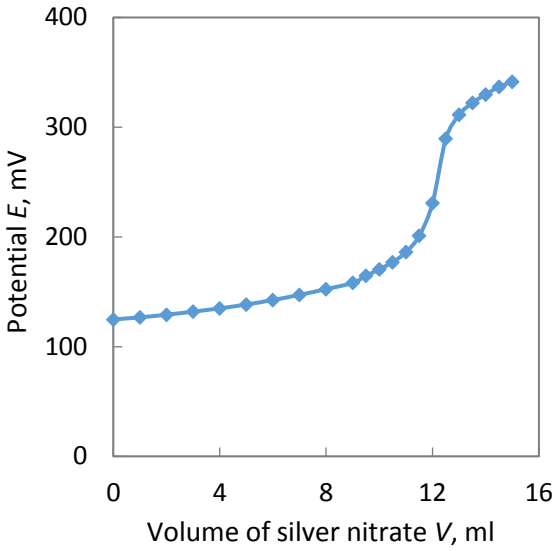

(a) Titration curve for the total chloride determination

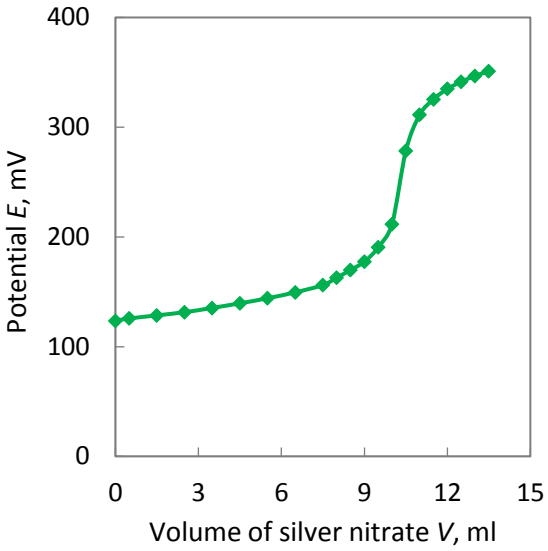

(c) Titration curve for the free chloride determination

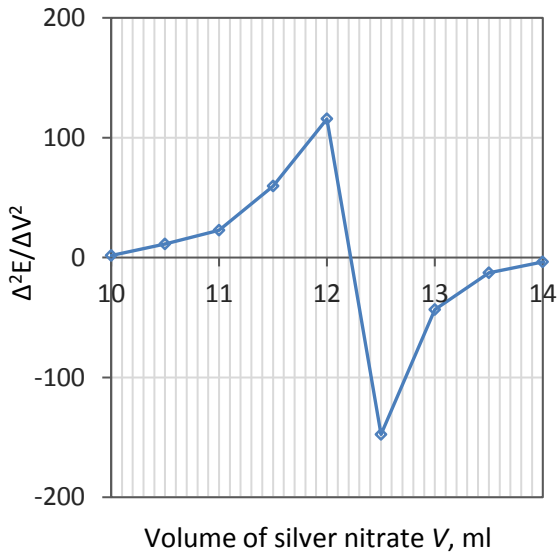

(b) Second derivative curve for the total chloride determination

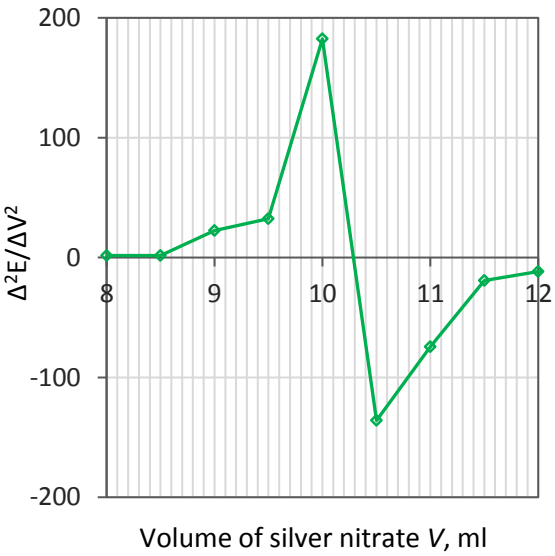

(d) Second derivative curve for the free chloride determination

Figure A.2: Potentiometric titration data of the samples at w/c of 0.5 and added NaCl of 1.5%

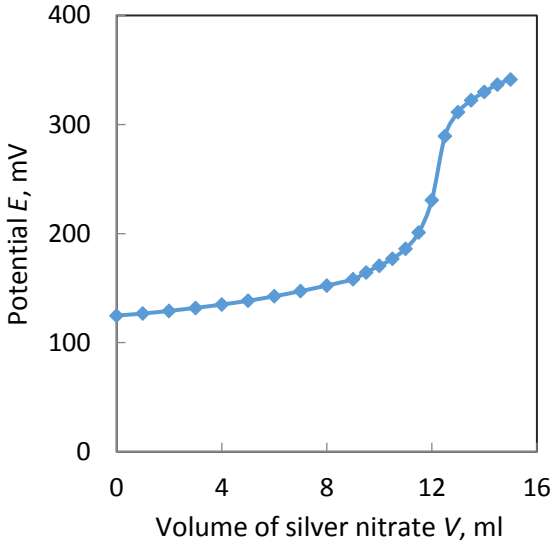

(a) Titration curve for the total chloride determination

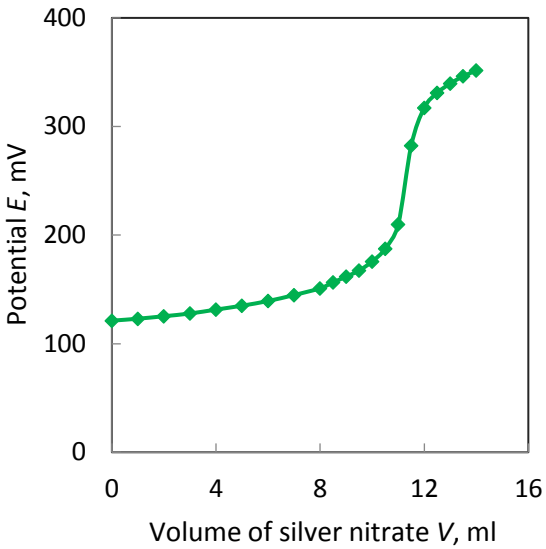

(c) Titration curve for the free chloride determination

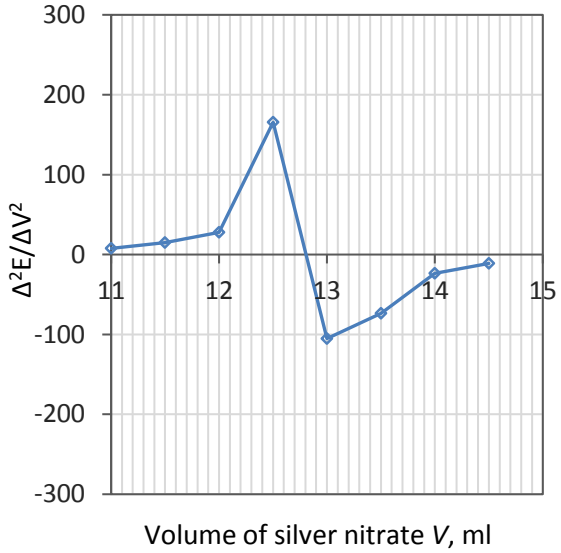

(b) Second derivative curve for the total chloride determination

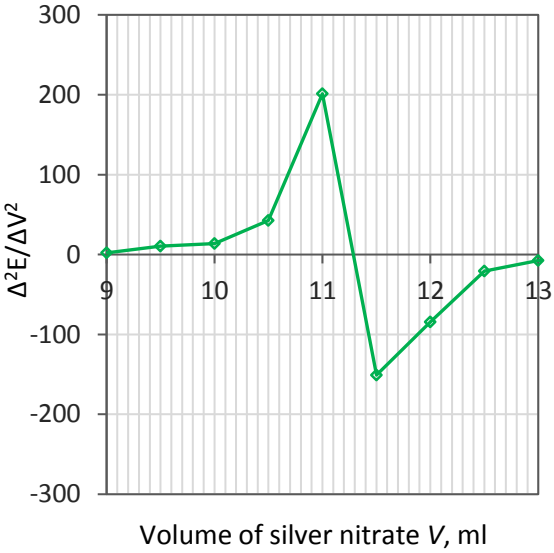

(d) Second derivative curve for the free chloride determination

Figure A.3: Potentiometric titration data of the samples at w/c of 0.6 and added NaCl of 1.5%

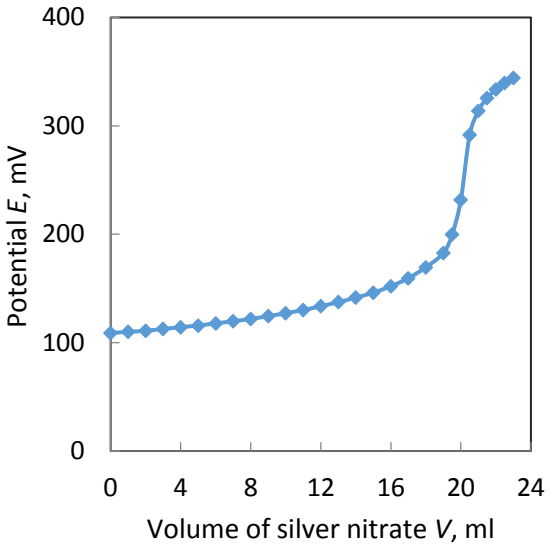

(a) Titration curve for the total chloride determination

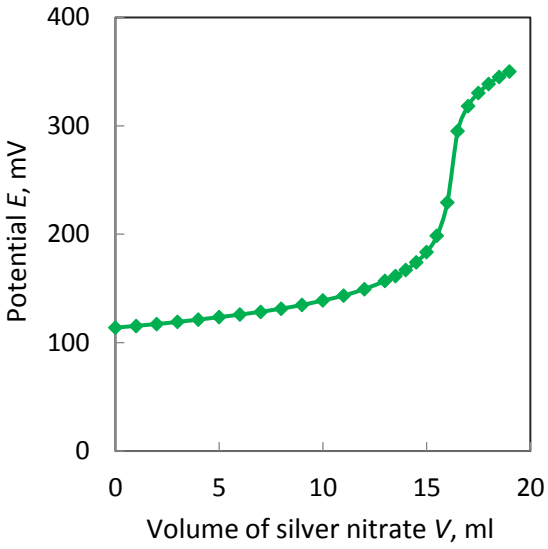

(c) Titration curve for the free chloride determination

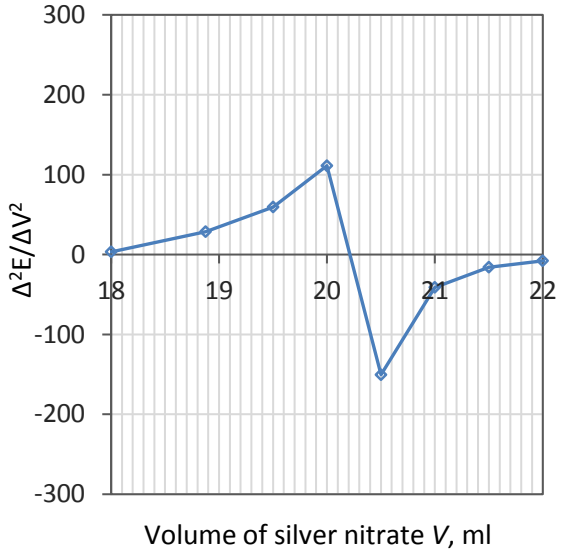

(b) Second derivative curve for the total chloride determination

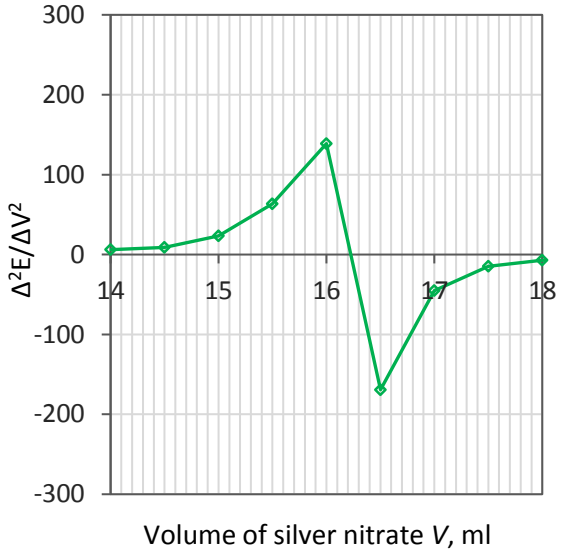

(d) Second derivative curve for the free chloride determination

Figure A.4: Potentiometric titration data of the samples at w/c of 0.4 and added NaCl of 3%

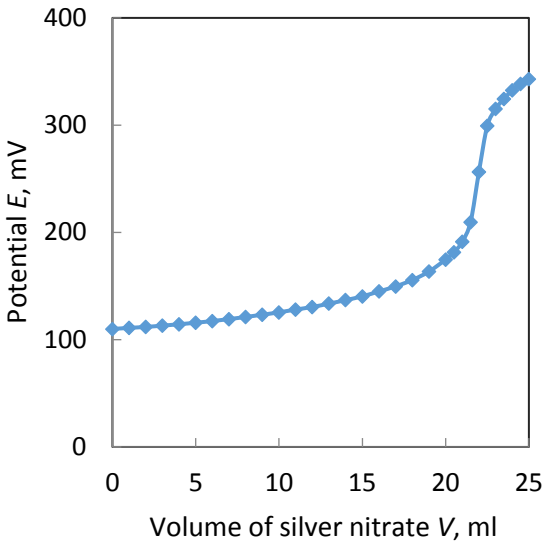

(a) Titration curve for the total chloride determination

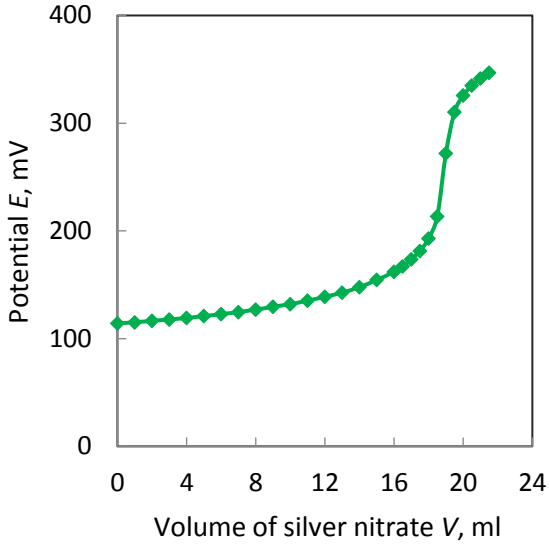

(c) Titration curve for the free chloride determination

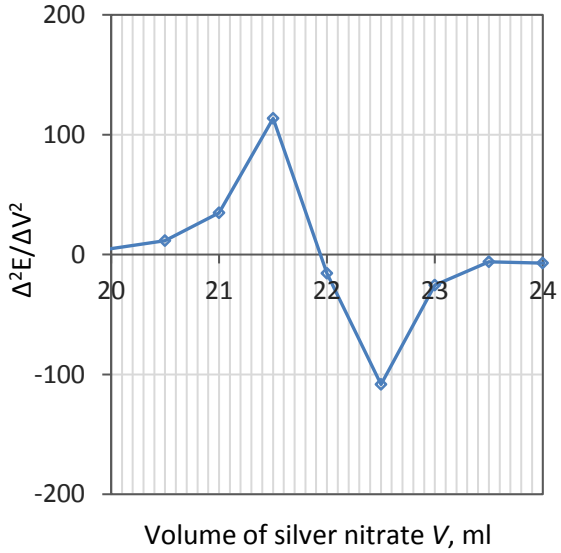

(b) Second derivative curve for the total chloride determination

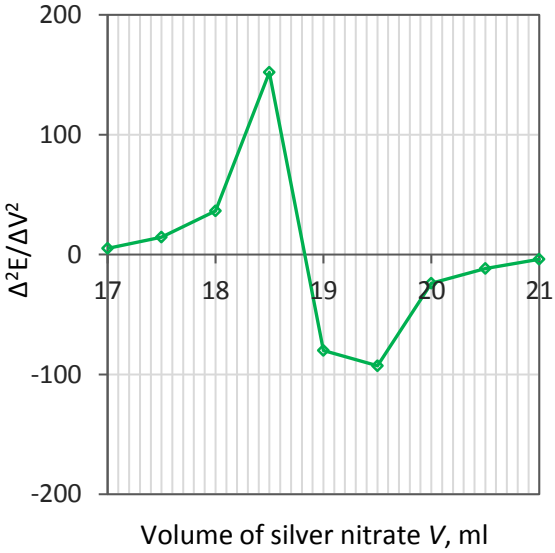

(d) Second derivative curve for the free chloride determination

Figure A.5: Potentiometric titration data of the samples at w/c of 0.5 and added NaCl of 3%

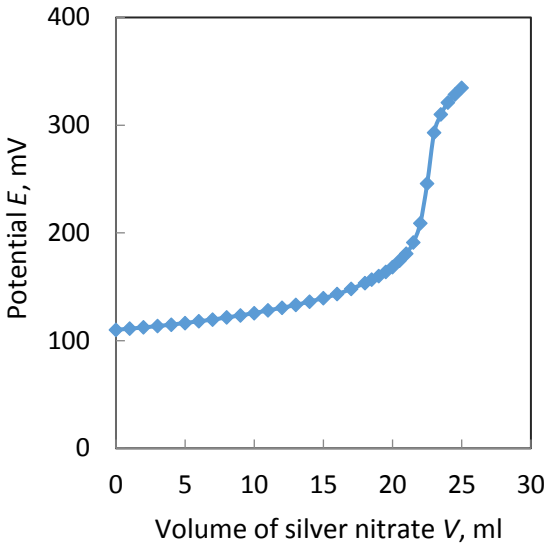

(a) Titration curve for the total chloride determination

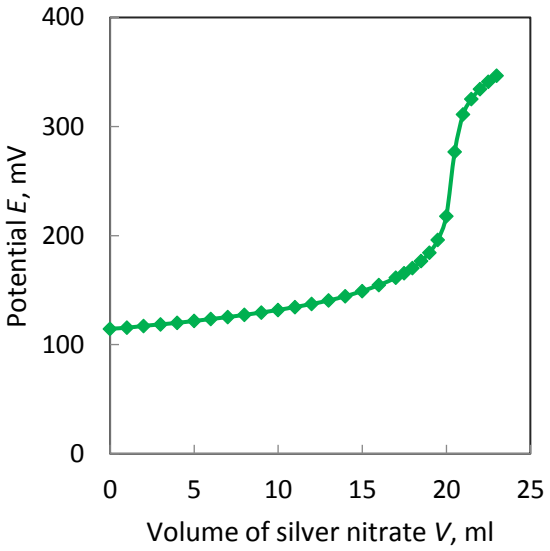

(c) Titration curve for the free chloride determination

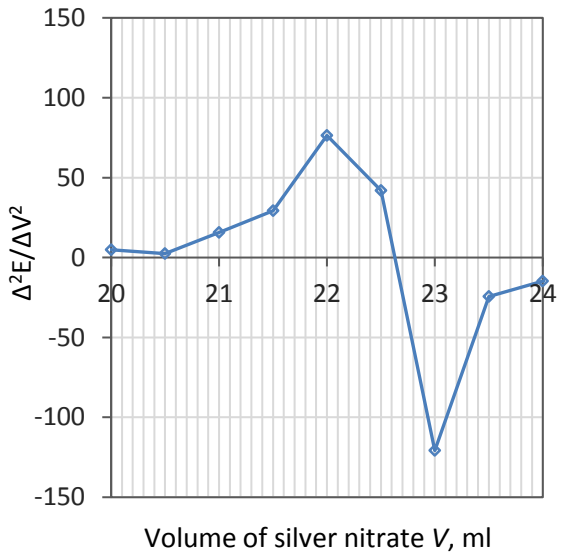

(b) Second derivative curve for the total chloride determination

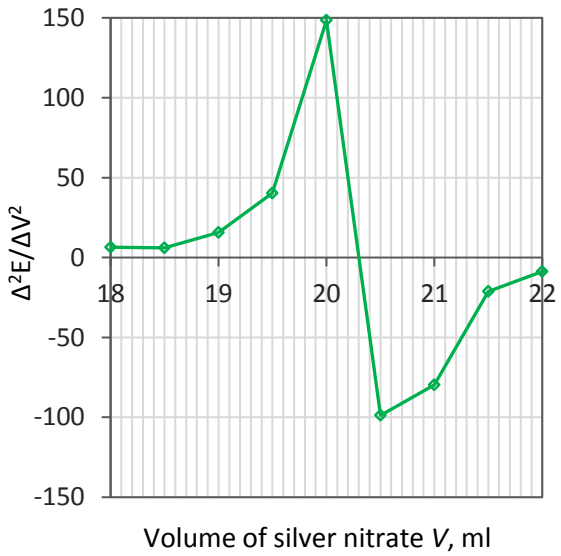

(d) Second derivative curve for the free chloride determination

Figure A.6: Potentiometric titration data of the samples at w/c of 0.6 and added NaCl of 3%

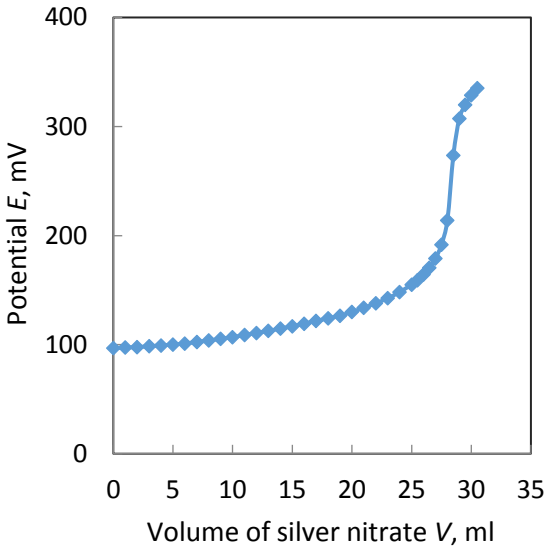

(a) Titration curve for the total chloride determination

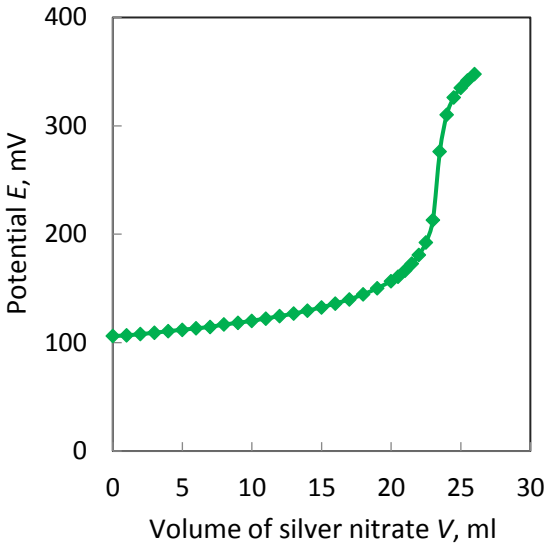

(c) Titration curve for the free chloride determination

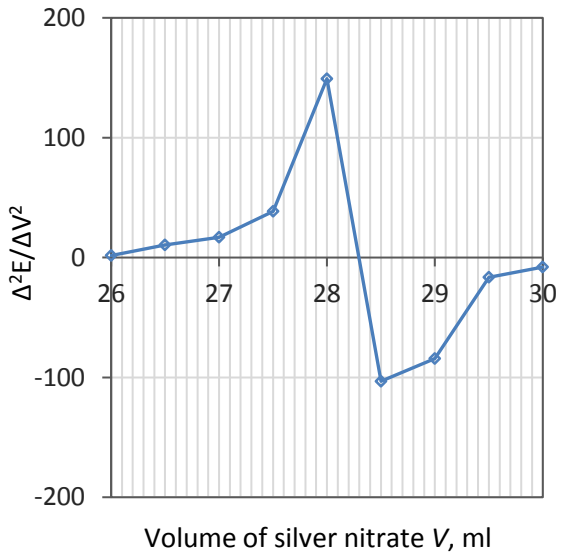

(b) Second derivative curve for the total chloride determination

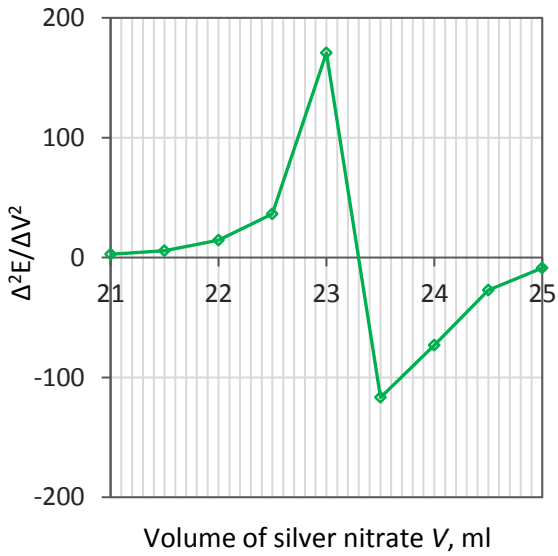

(d) Second derivative curve for the free chloride determination

Figure A.7: Potentiometric titration data of the samples at w/c of 0.4 and added NaCl of 4.5%

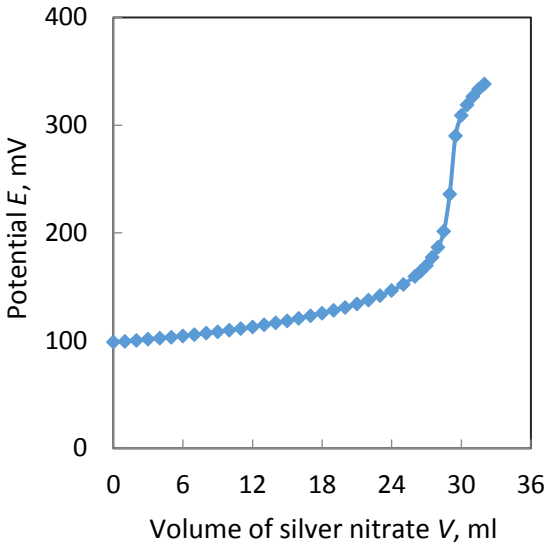

(a) Titration curve for the total chloride determination

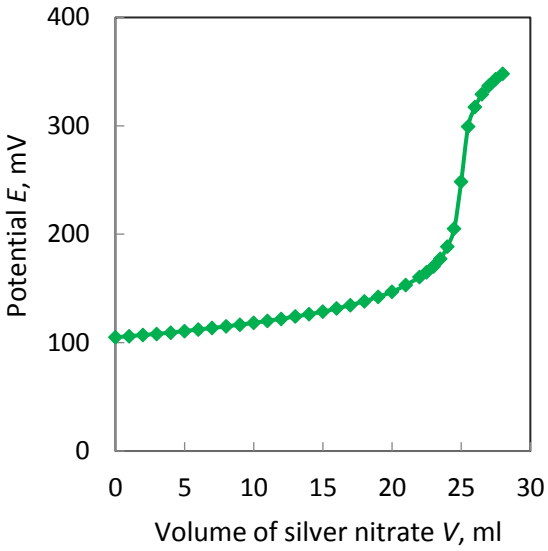

(c) Titration curve for the free chloride determination

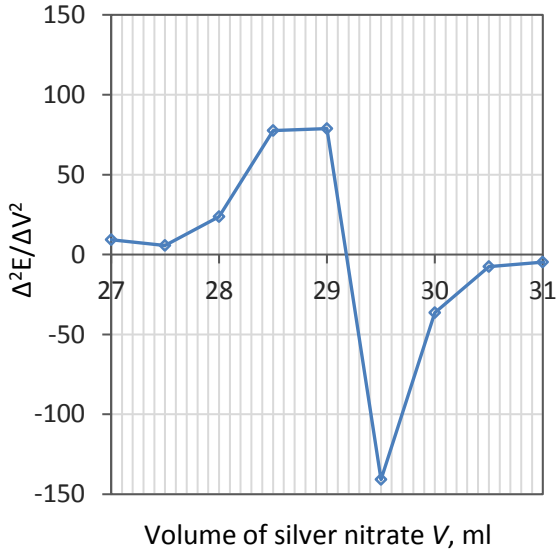

(b) Second derivative curve for the total chloride determination

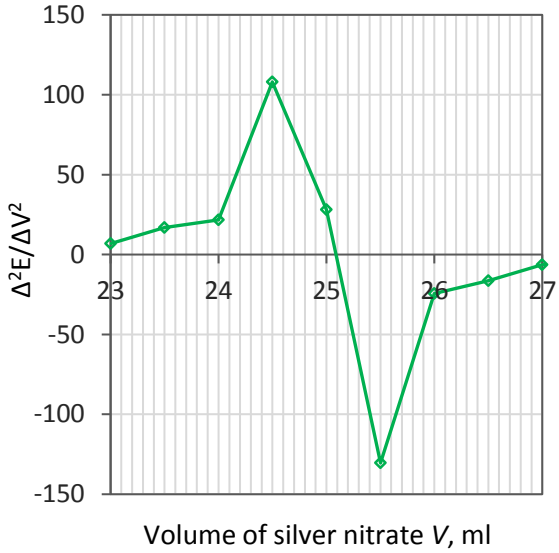

(d) Second derivative curve for the free chloride determination

Figure A.8: Potentiometric titration data of the samples at w/c of 0.5 and added NaCl of 4.5%

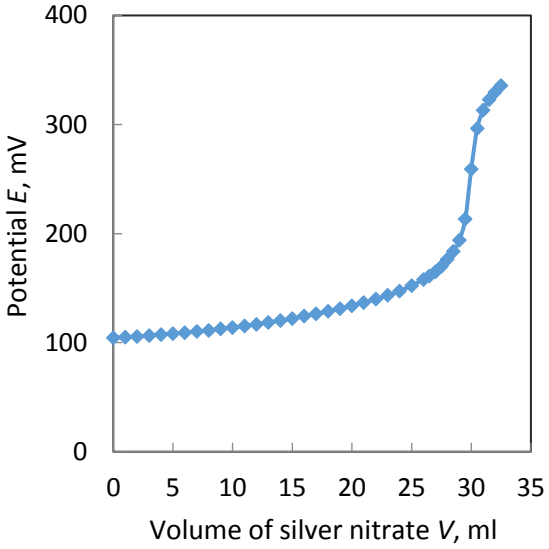

(a) Titration curve for the total chloride determination

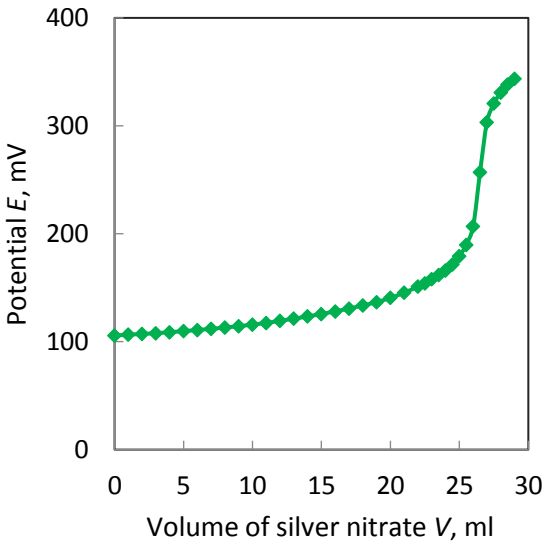

(c) Titration curve for the free chloride determination

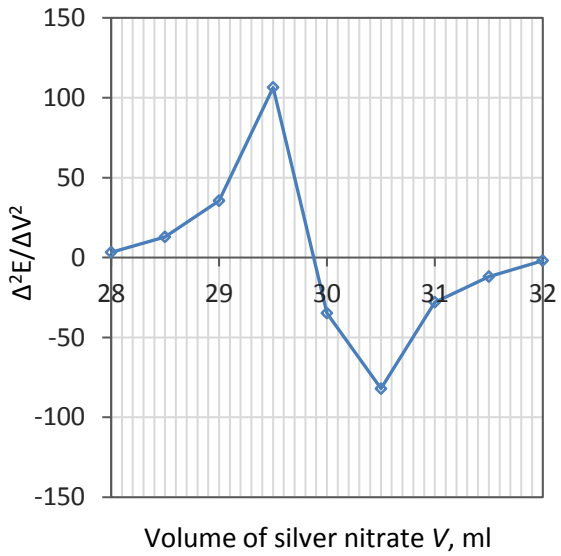

(b) Second derivative curve for the total chloride determination

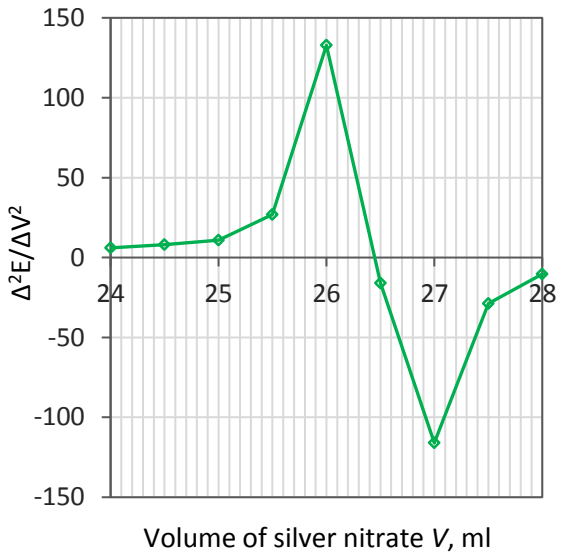

(d) Second derivative curve for the free chloride determination

Figure A.9: Potentiometric titration data of the samples at w/c of 0.6 and added NaCl of 4.5%

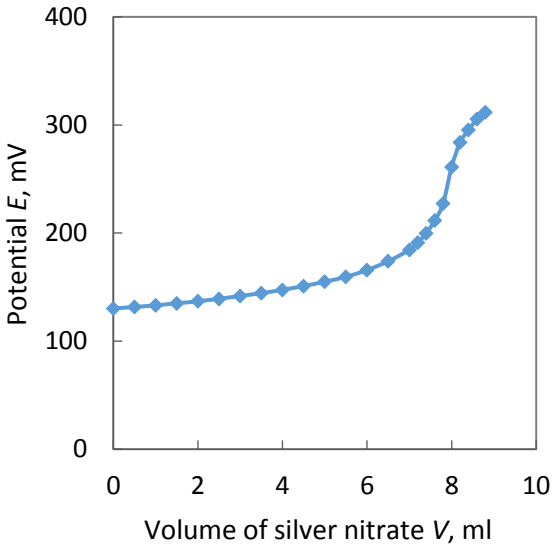

(a) Titration curve for the total chloride determination

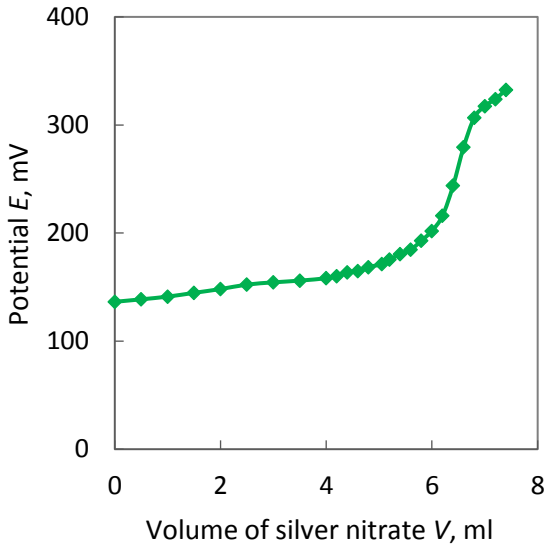

(c) Titration curve for the free chloride determination

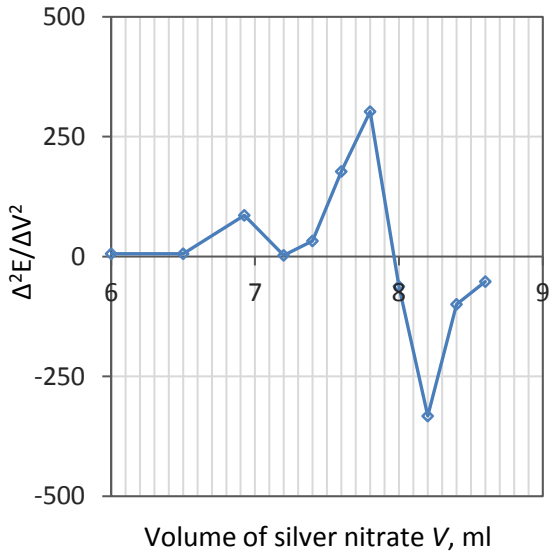

(b) Second derivative curve for the total chloride determination

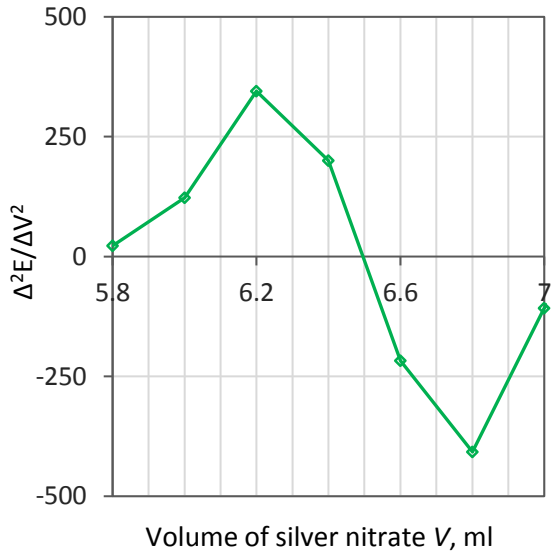

(d) Second derivative curve for the free chloride determination

Figure A.10: Potentiometric titration data of the samples at w/c of 0.4 and added NaCl of 1%

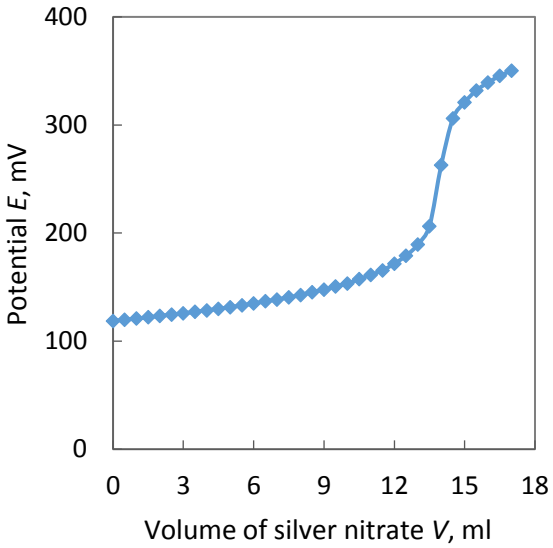

(a) Titration curve for the total chloride determination

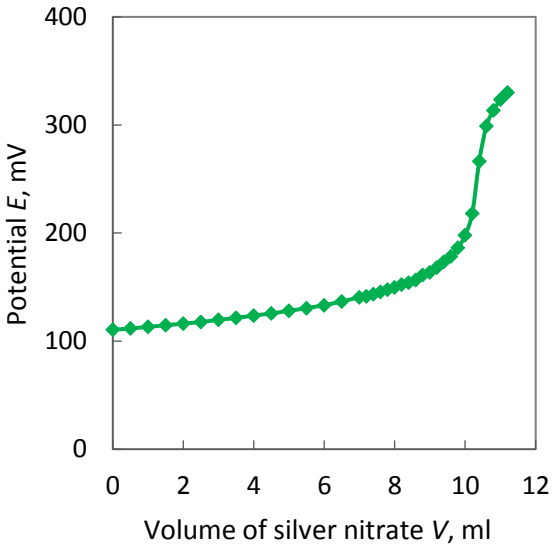

(c) Titration curve for the free chloride determination

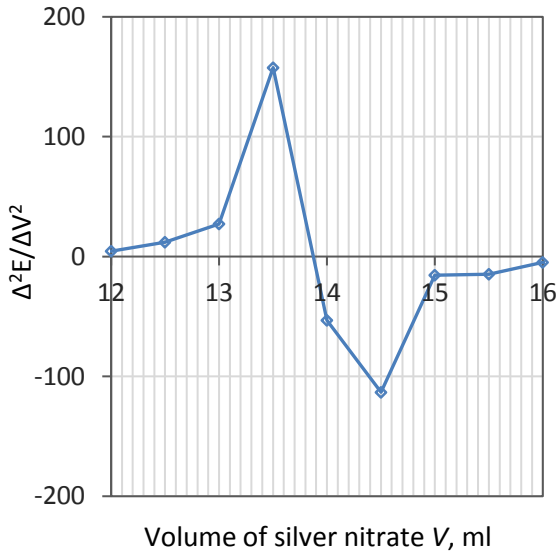

(b) Second derivative curve for the total chloride determination

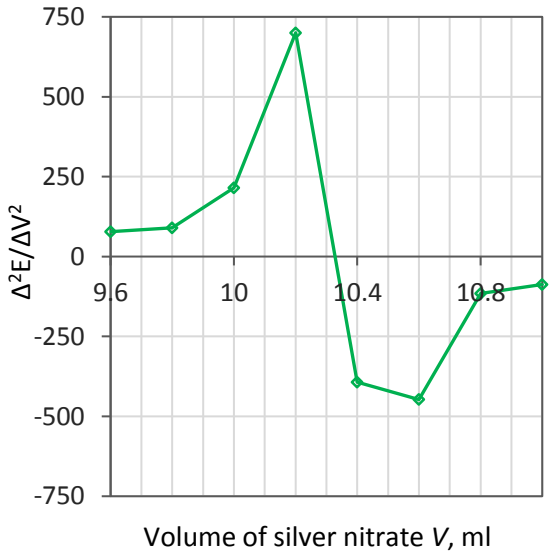

(d) Second derivative curve for the free chloride determination

Figure A.11: Potentiometric titration data of the samples at w/c of 0.4 and added NaCl of 2%

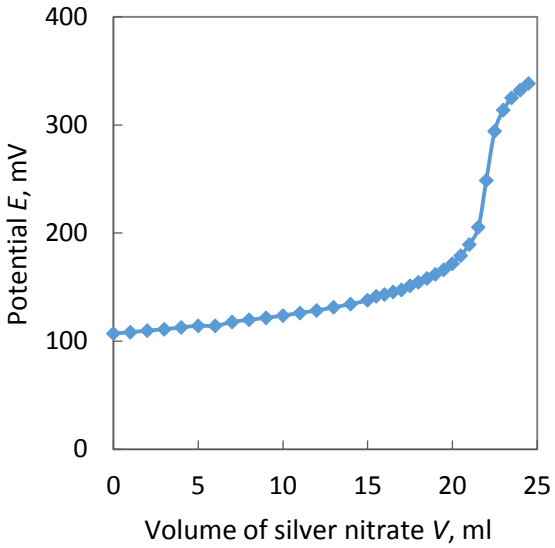

(a) Titration curve for the total chloride determination

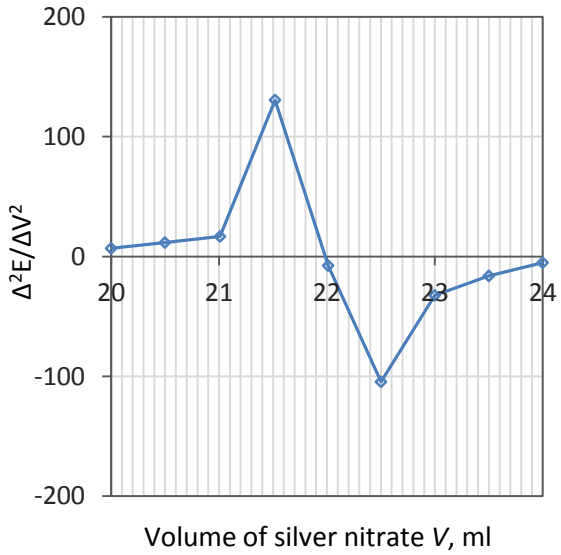

(b) Second derivative curve for the total chloride determination

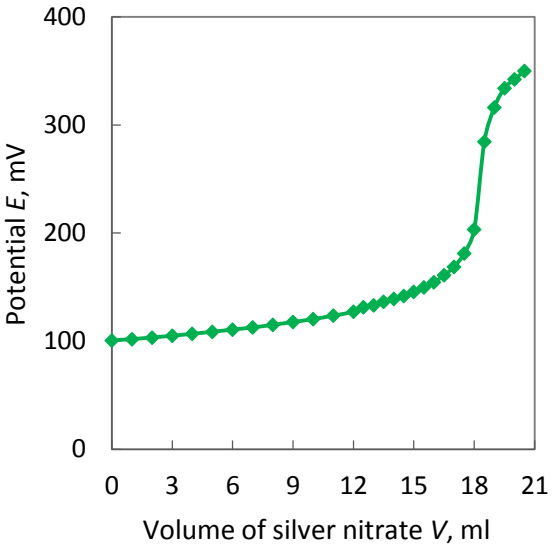

(c) Titration curve for the free chloride determination

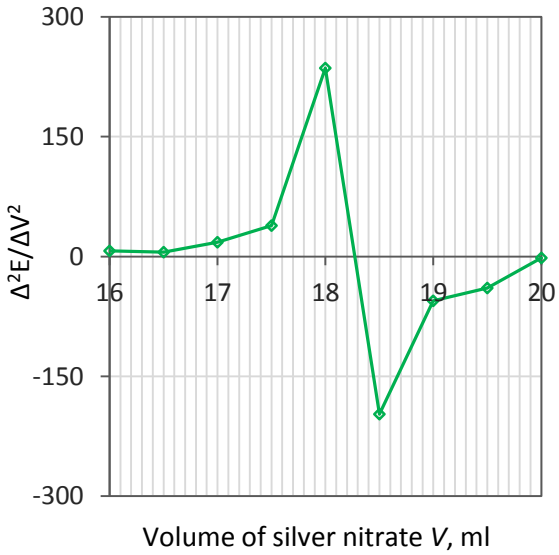

(d) Second derivative curve for the free chloride determination

Figure A.12: Potentiometric titration data of the samples at w/c of 0.4 and added NaCl of 3.5%

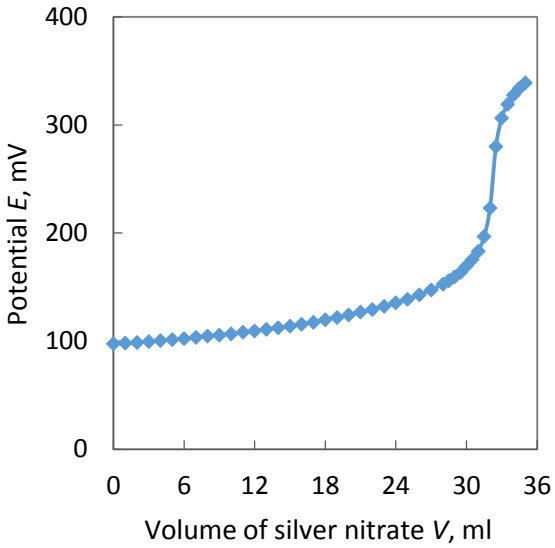

(a) Titration curve for the total chloride determination

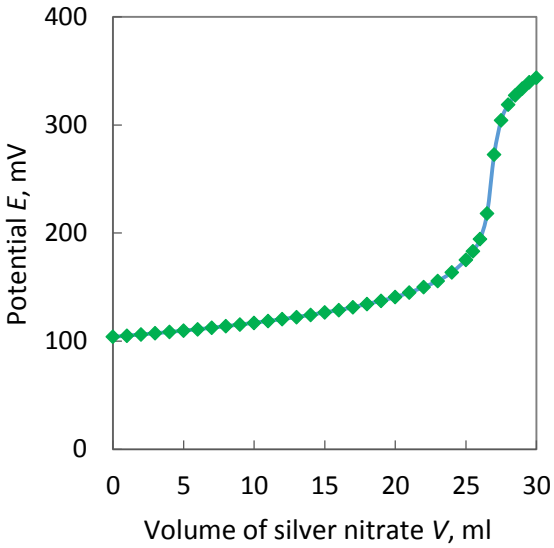

(c) Titration curve for the free chloride determination

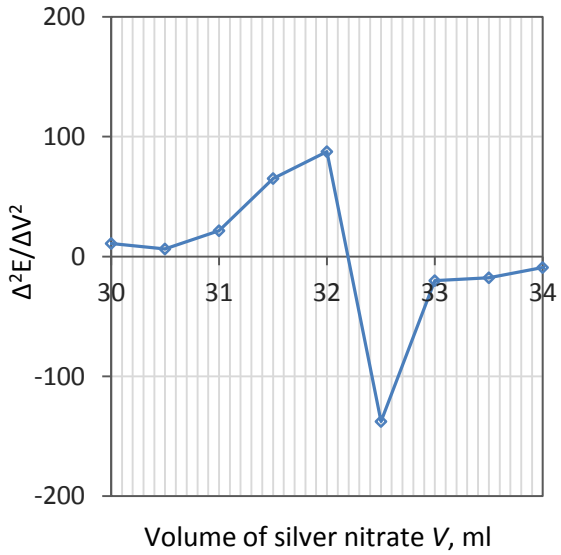

(b) Second derivative curve for the total chloride determination

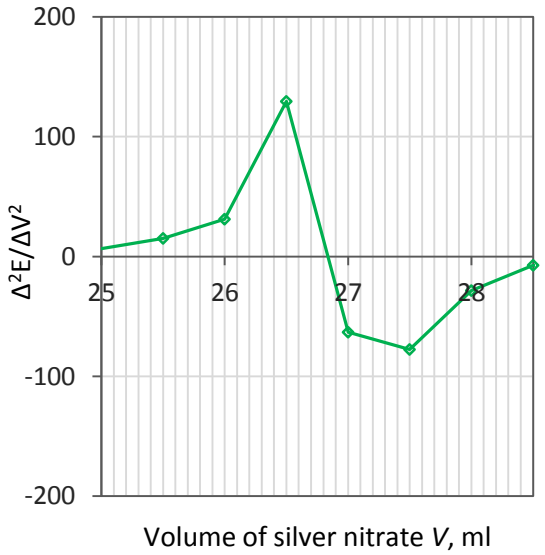

(d) Second derivative curve for the free chloride determination

Figure A.13: Potentiometric titration data of the samples at w/c of 0.4 and added NaCl of 5%

APPENDIX B

Variation of Rebars Potential with Time under the Application of Different CP Current Densities

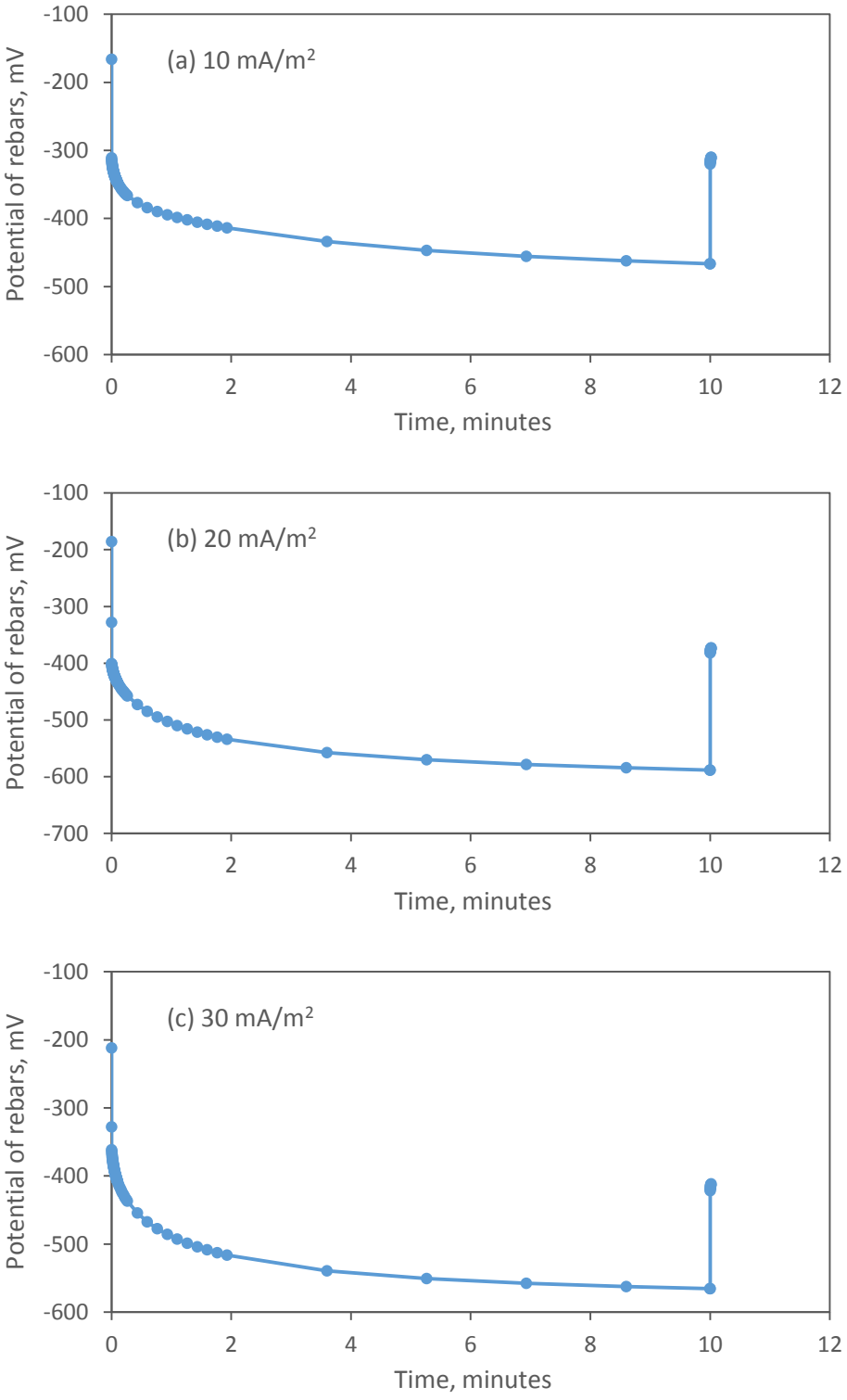

Figure B.1: Variation of rebars potential under the application of different CP current densities for 10 minutes.

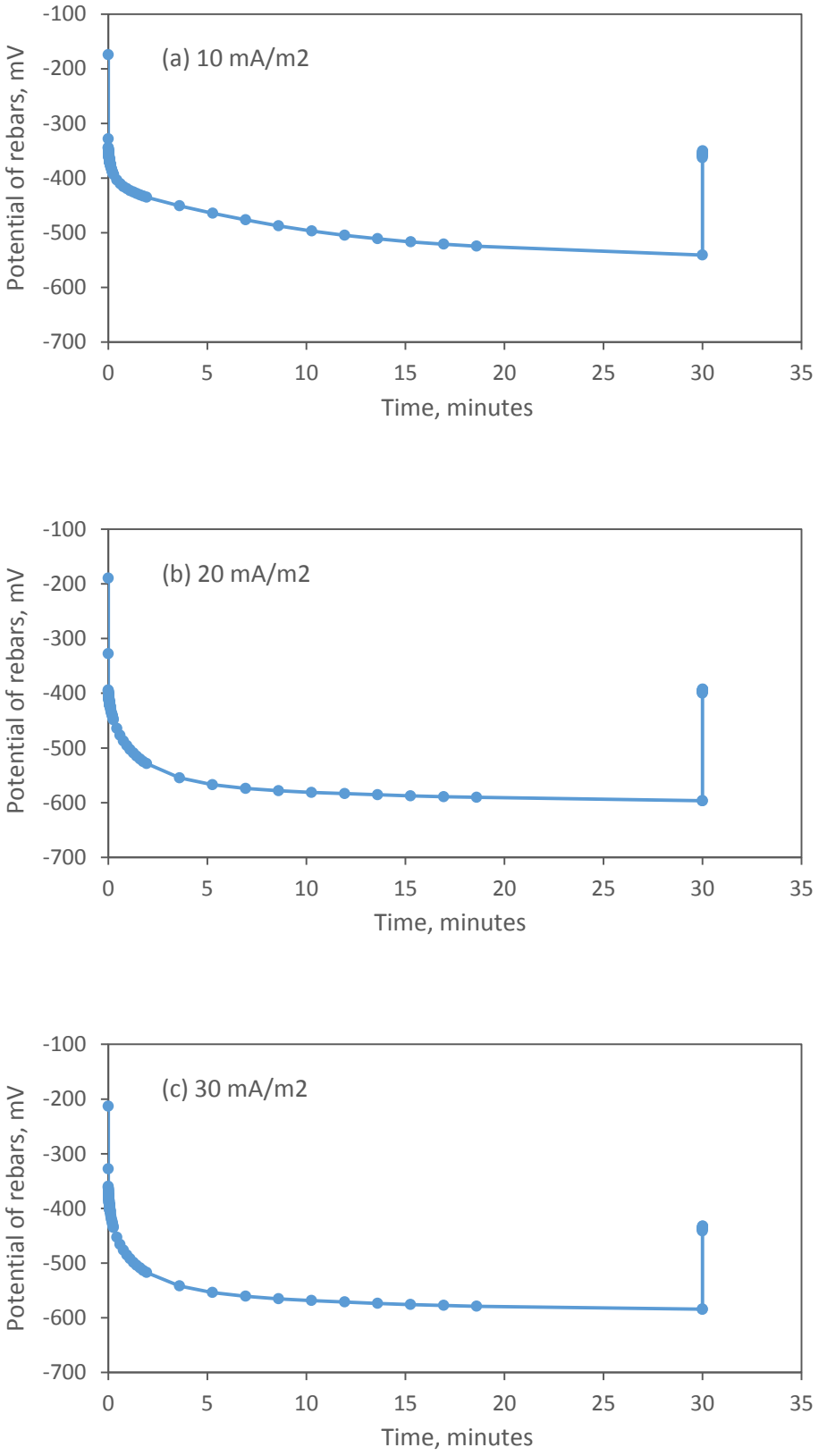

Figure B.2: Variation of rebars potential under the application of different CP current densities for 30 minutes.

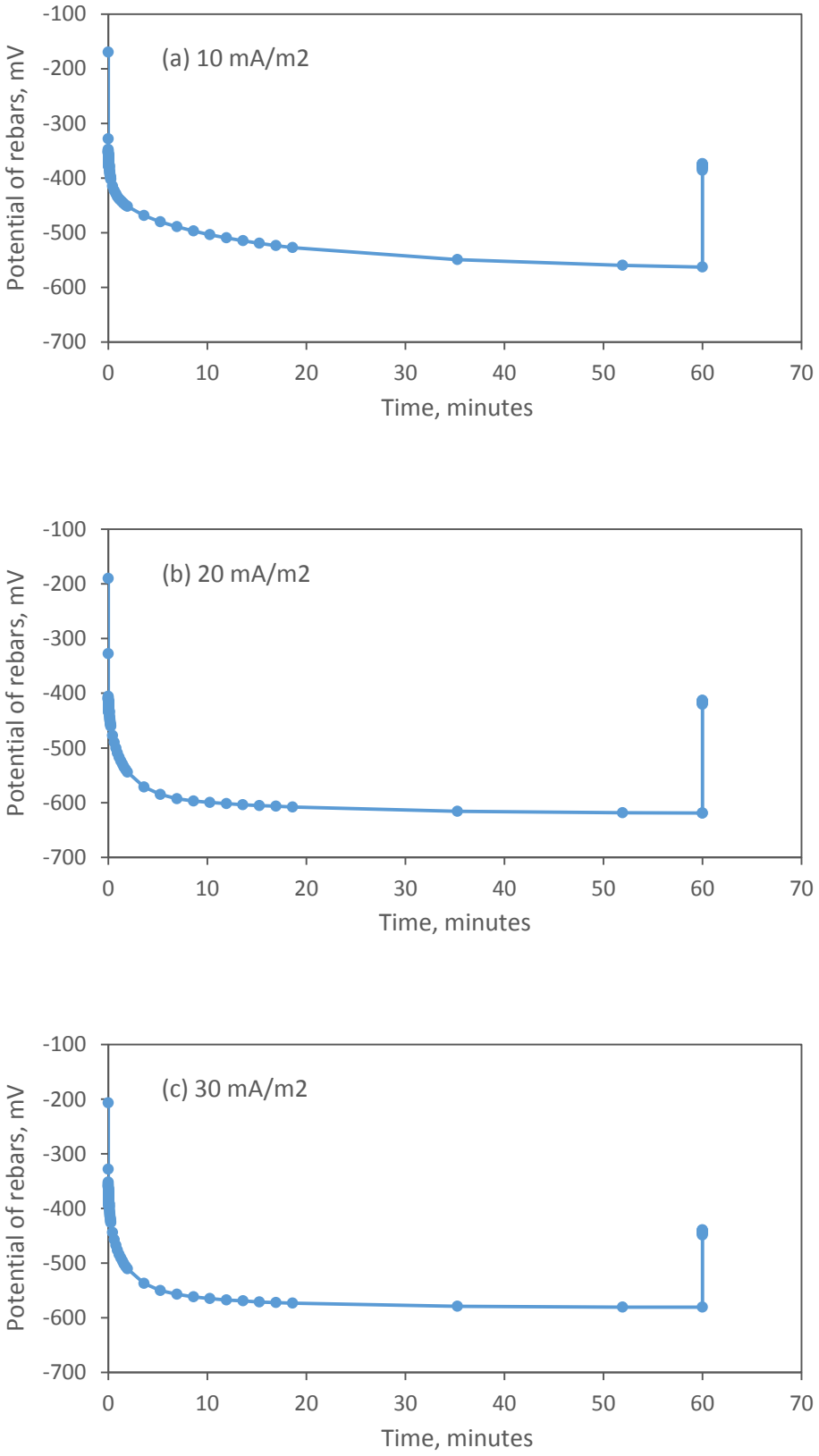

Figure B.3: Variation of rebars potential under the application of different CP current densities for 1 hour.

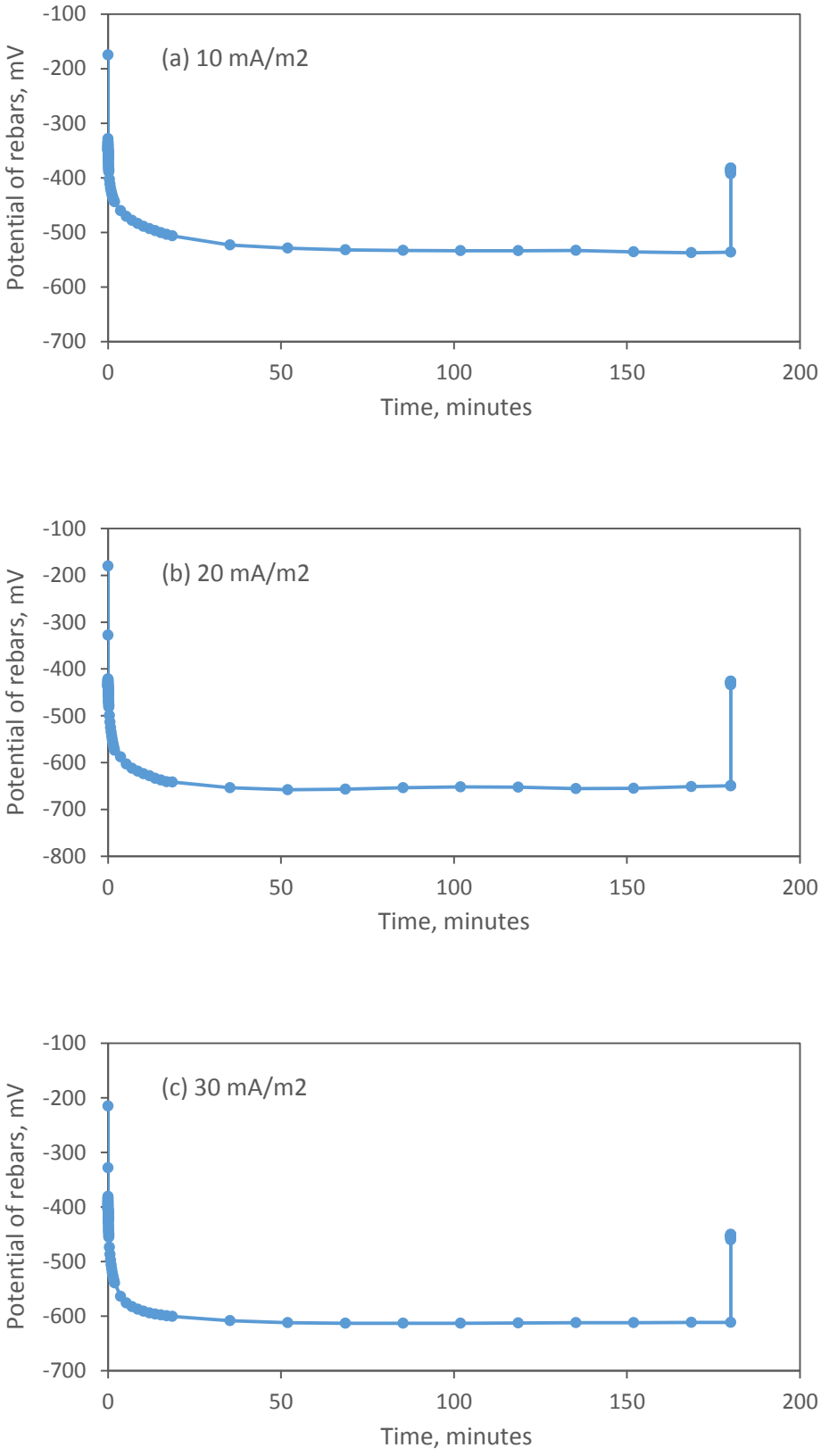

Figure B.4: Variation of rebars potential under the application of different CP current densities for 3 hours.

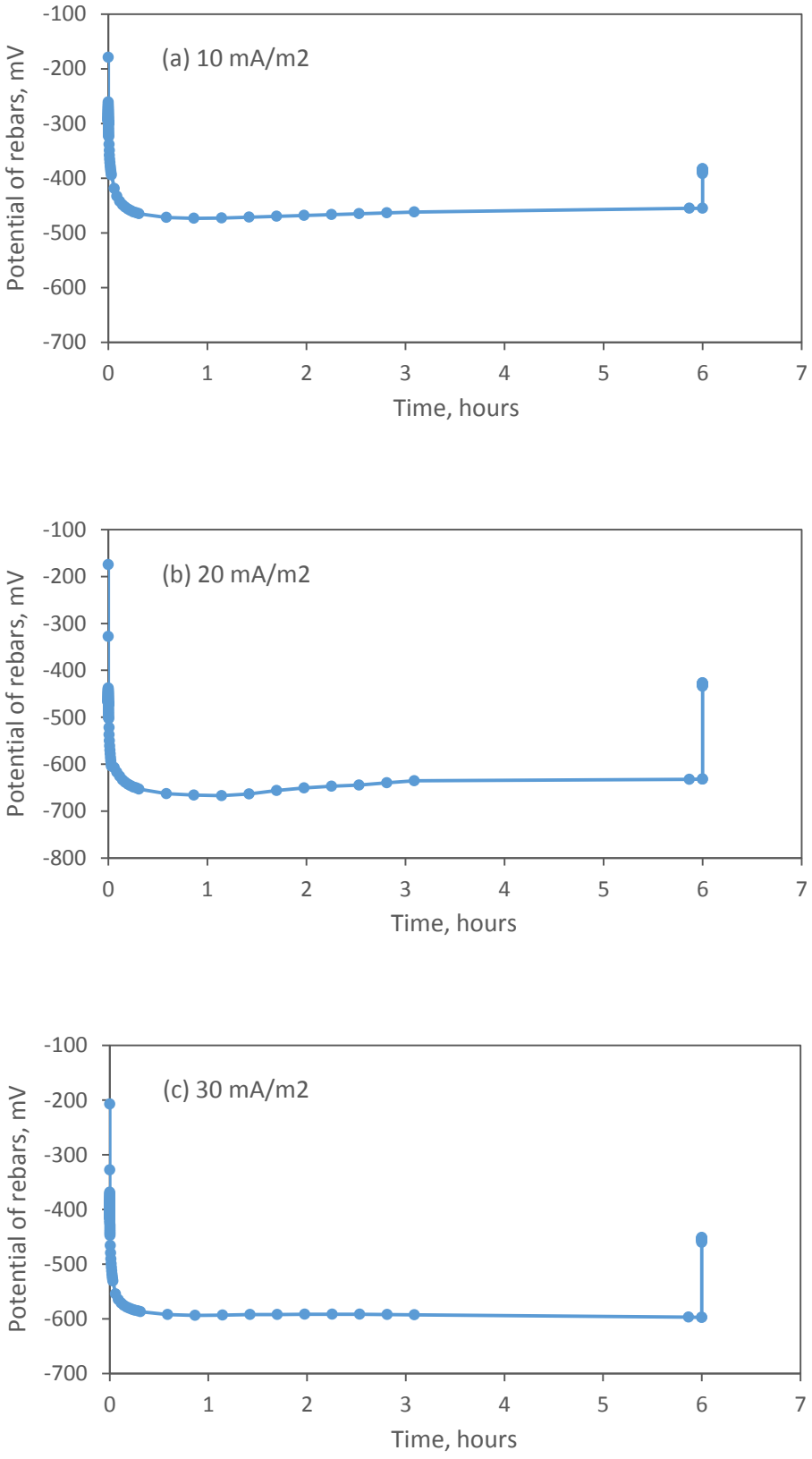

Figure B.5: Variation of rebars potential under the application of different CP current densities for 6 hours.

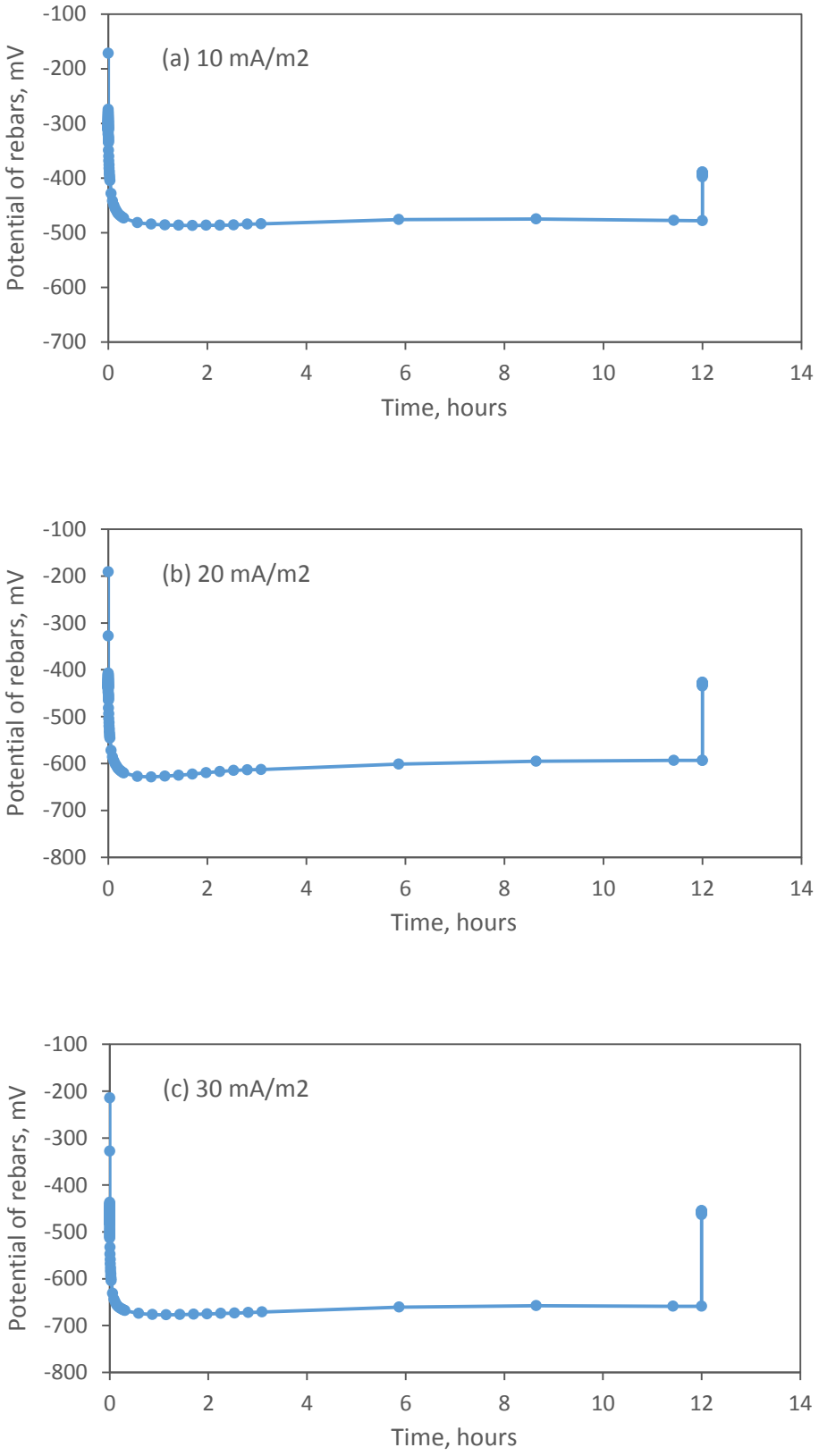

Figure B.6: Variation of rebars potential under the application of different CP current densities for 12 hours.

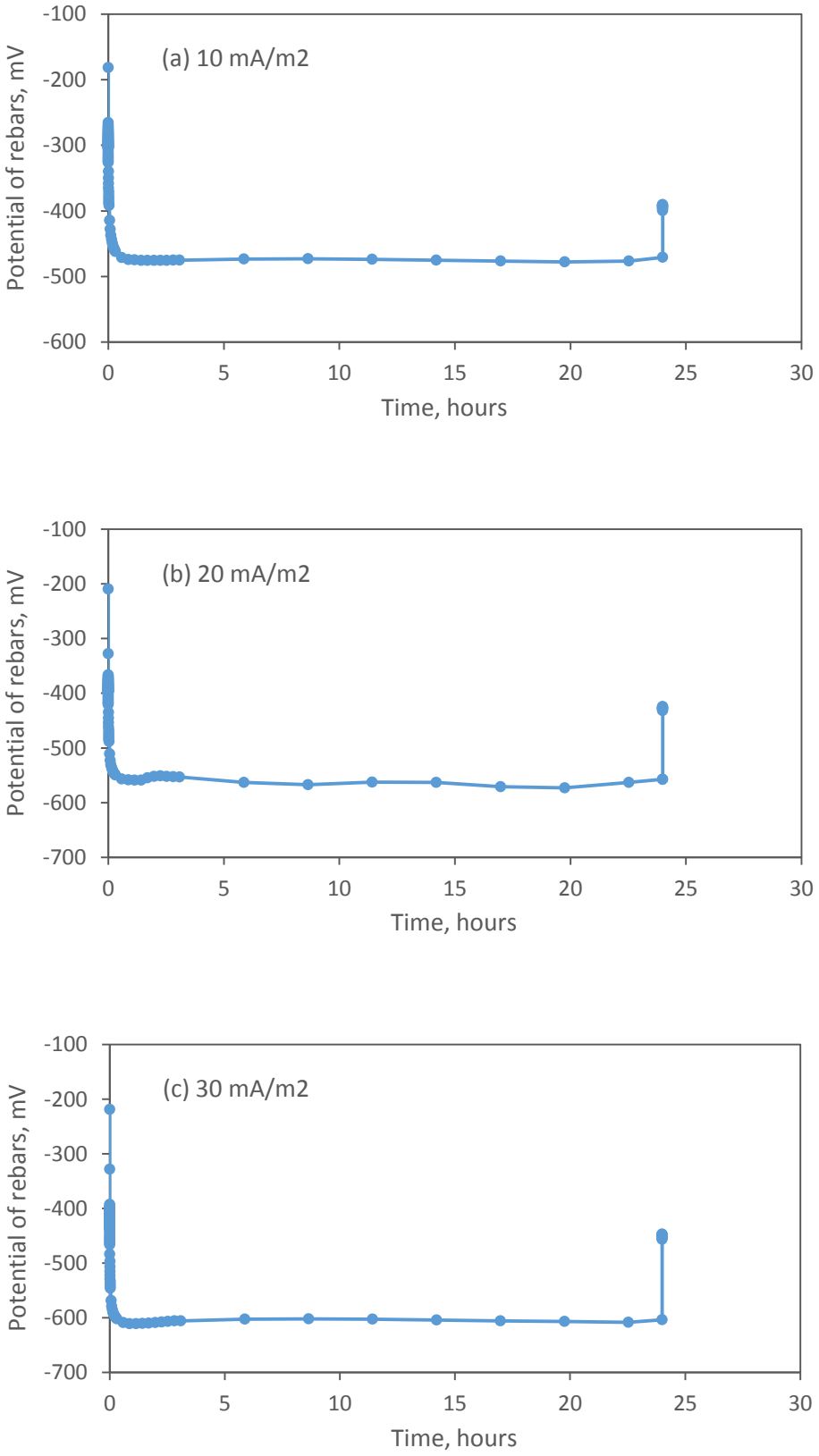

Figure B.7: Variation of rebars potential under the application of different CP current densities for 24 hours.

APPENDIX C

Potential Decay Curves for the Air Exposure Specimens

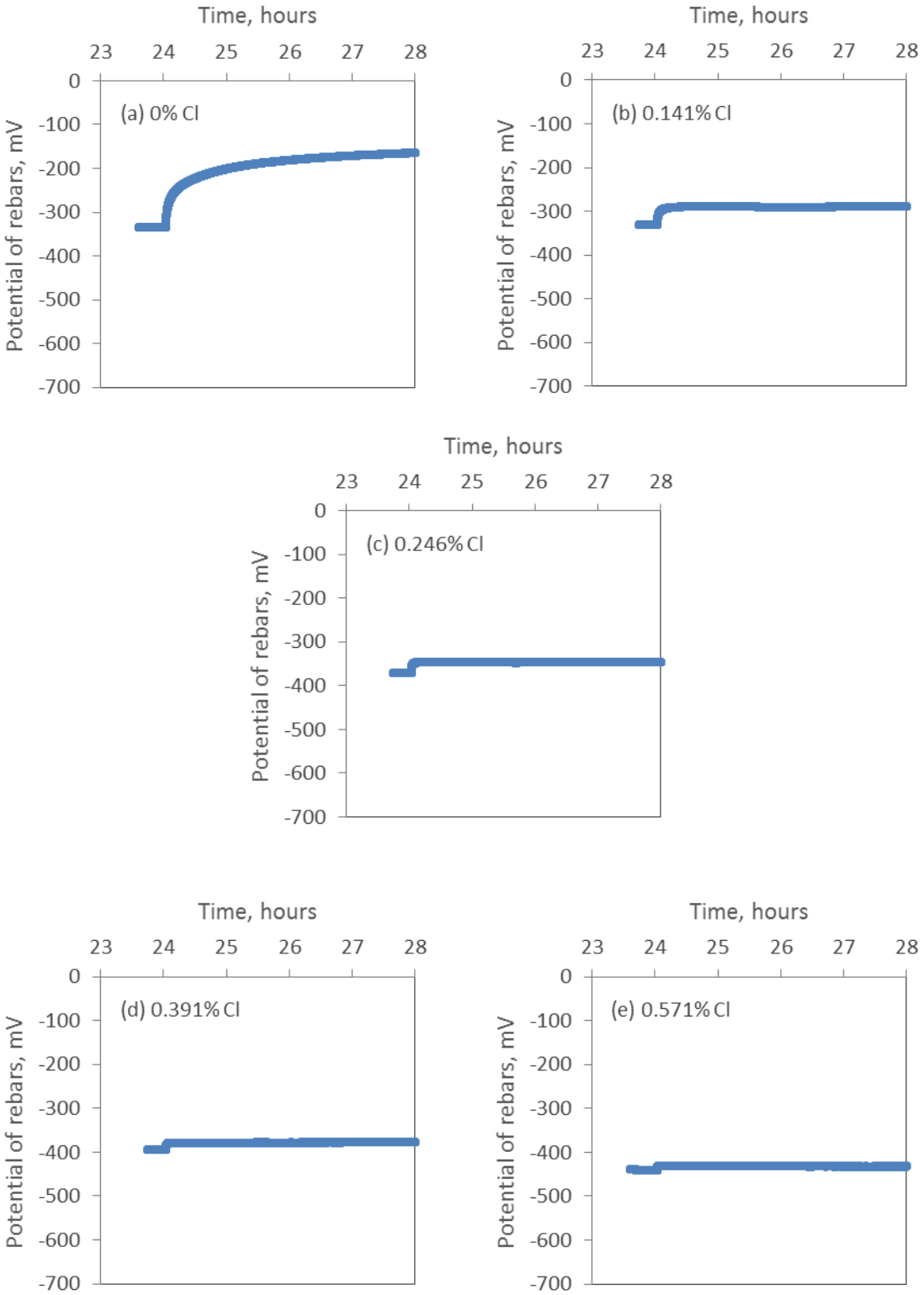

Figure C.1: Potential decay curves for specimens at various chloride contents after application of CP current density of 5 mA/m^2

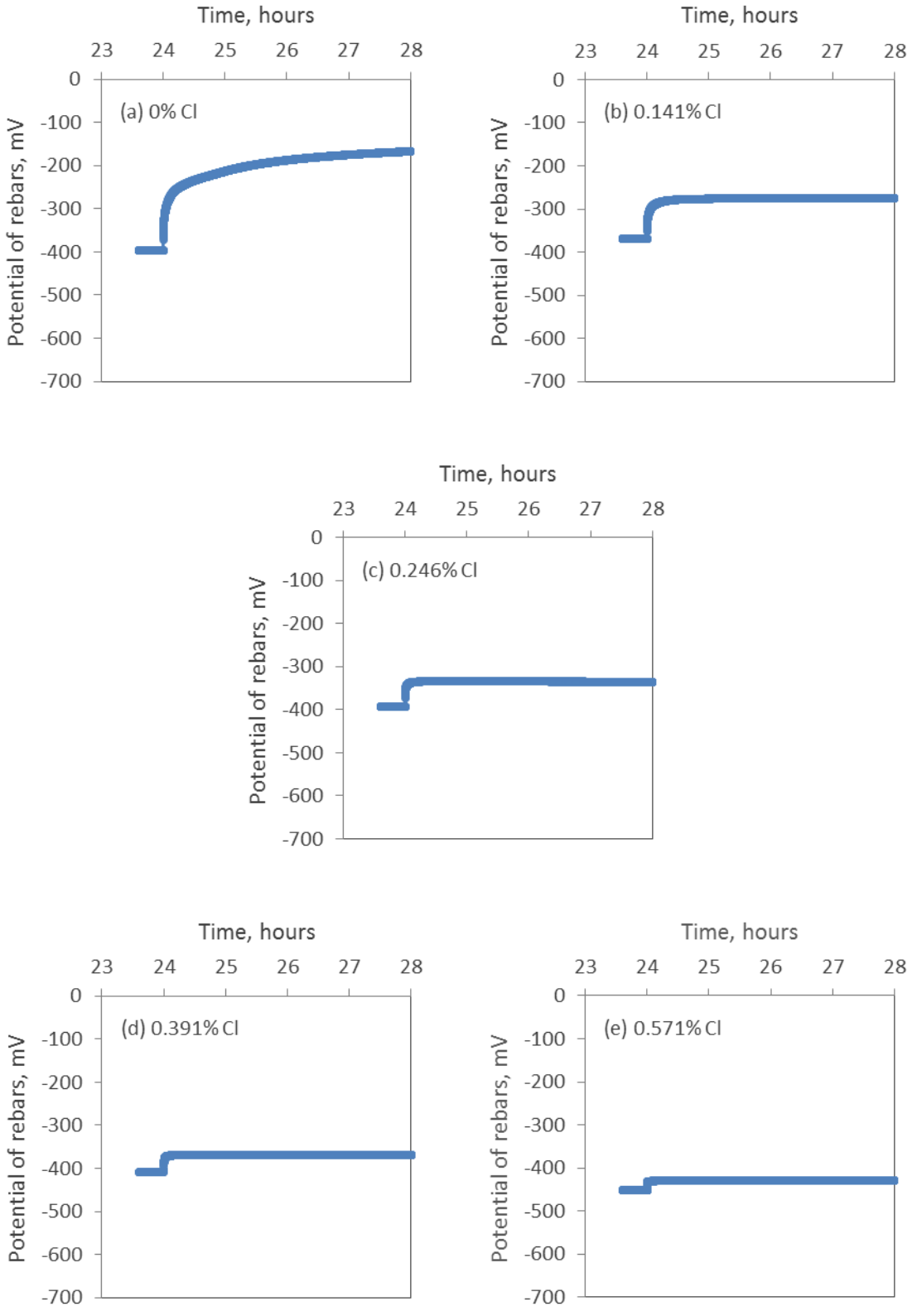

Figure C.2: Potential decay curves for specimens at various chloride contents after application of CP current density of 10 mA/m^2

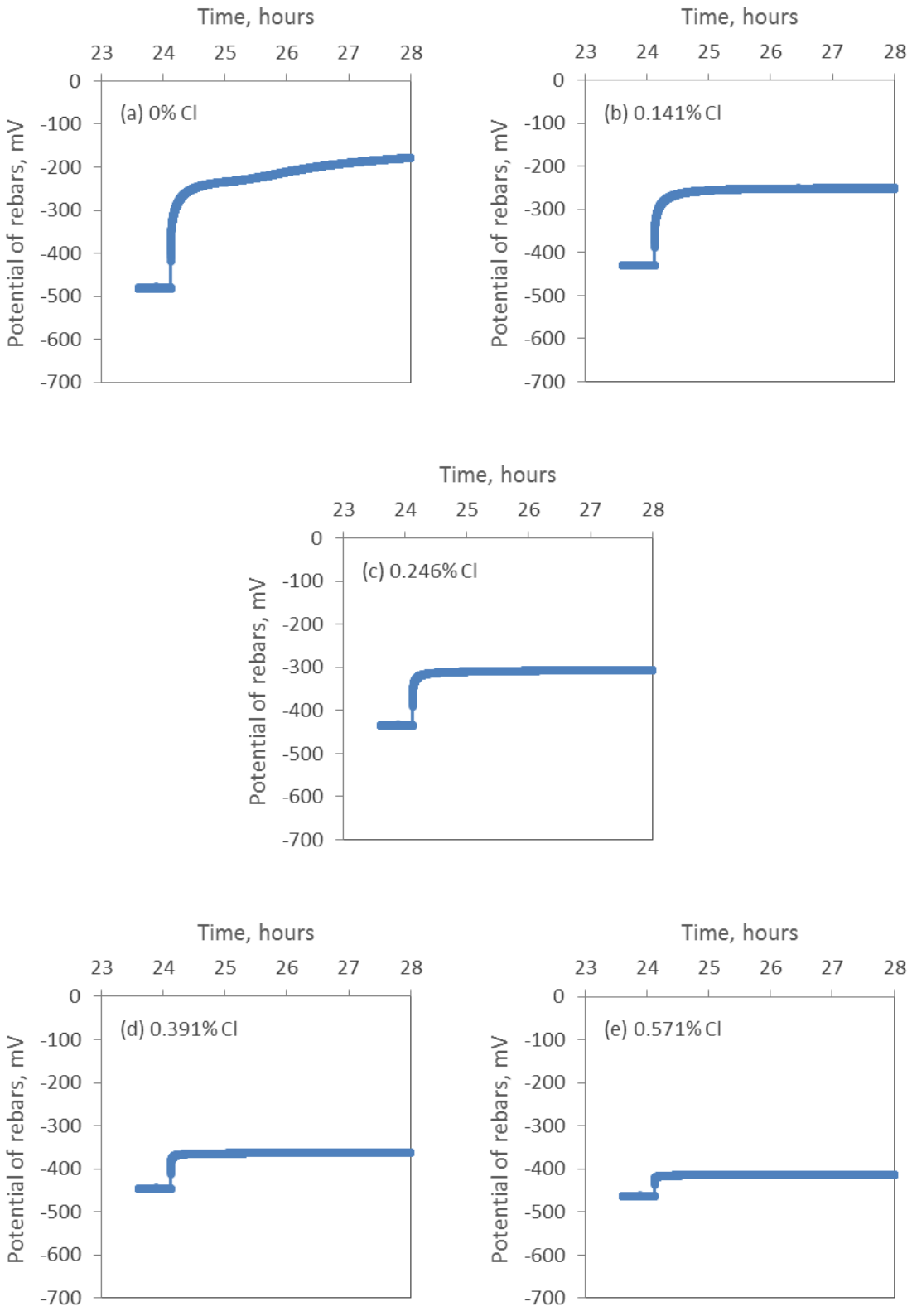

Figure C.3: Potential decay curves for specimens at various chloride contents after application of CP current density of 20 mA/m^2

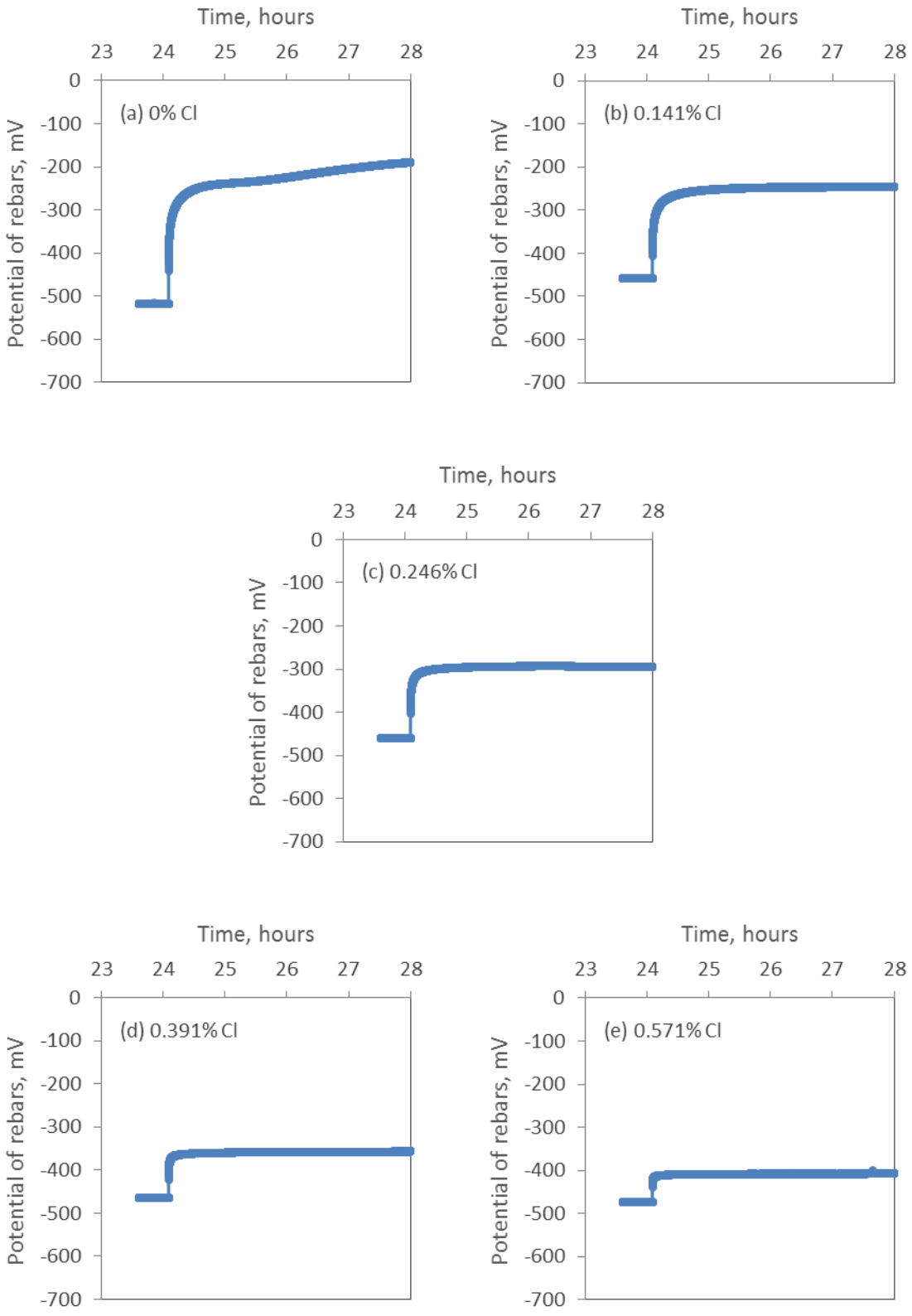

Figure C.4: Potential decay curves for specimens at various chloride contents after application of CP current density of 25 mA/m^2

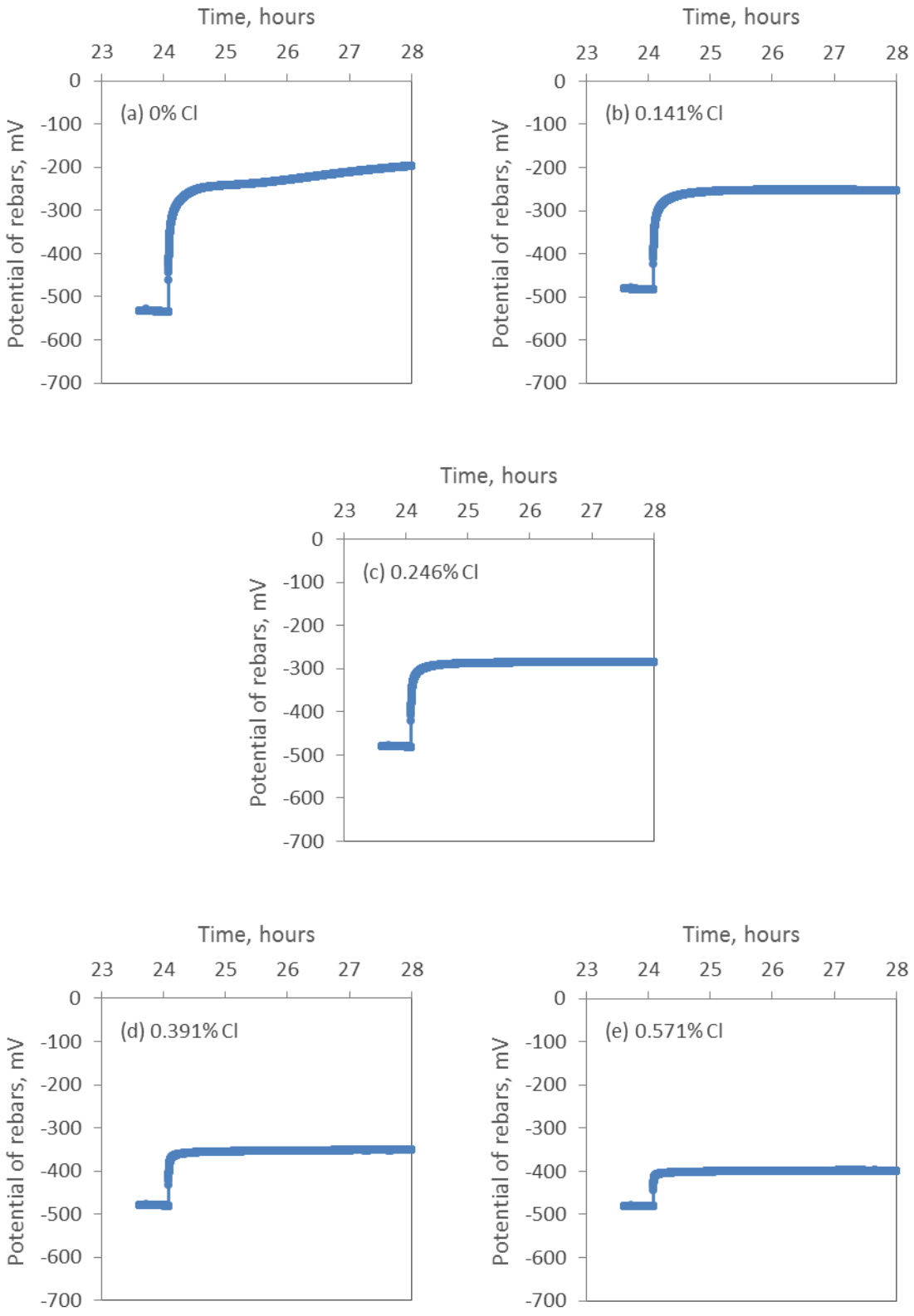

Figure C.5: Potential decay curves for specimens at various chloride contents after application of CP current density of 35 mA/m^2

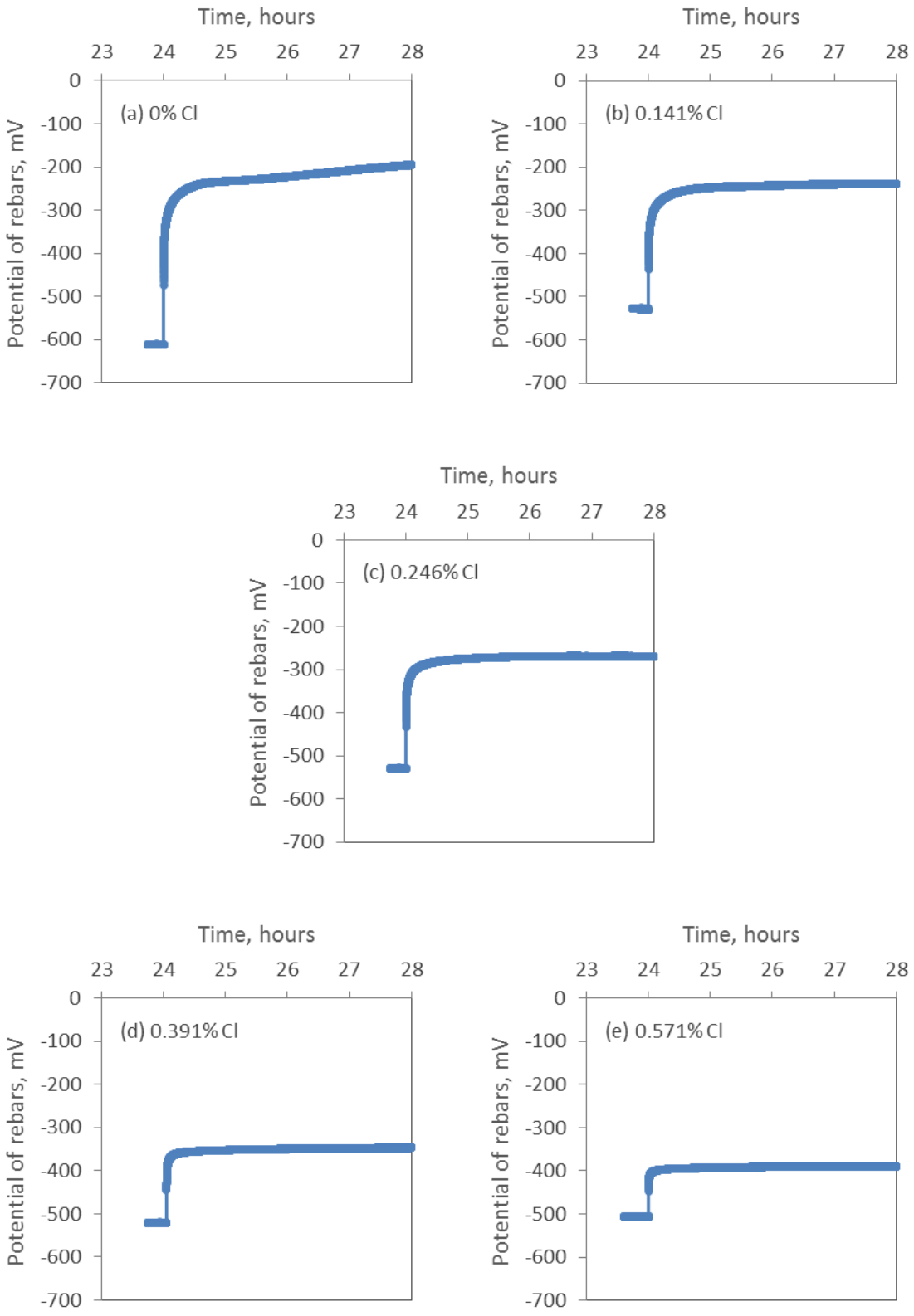

Figure C.6: Potential decay curves for specimens at various chloride contents after application of CP current density of 45 mA/m^2

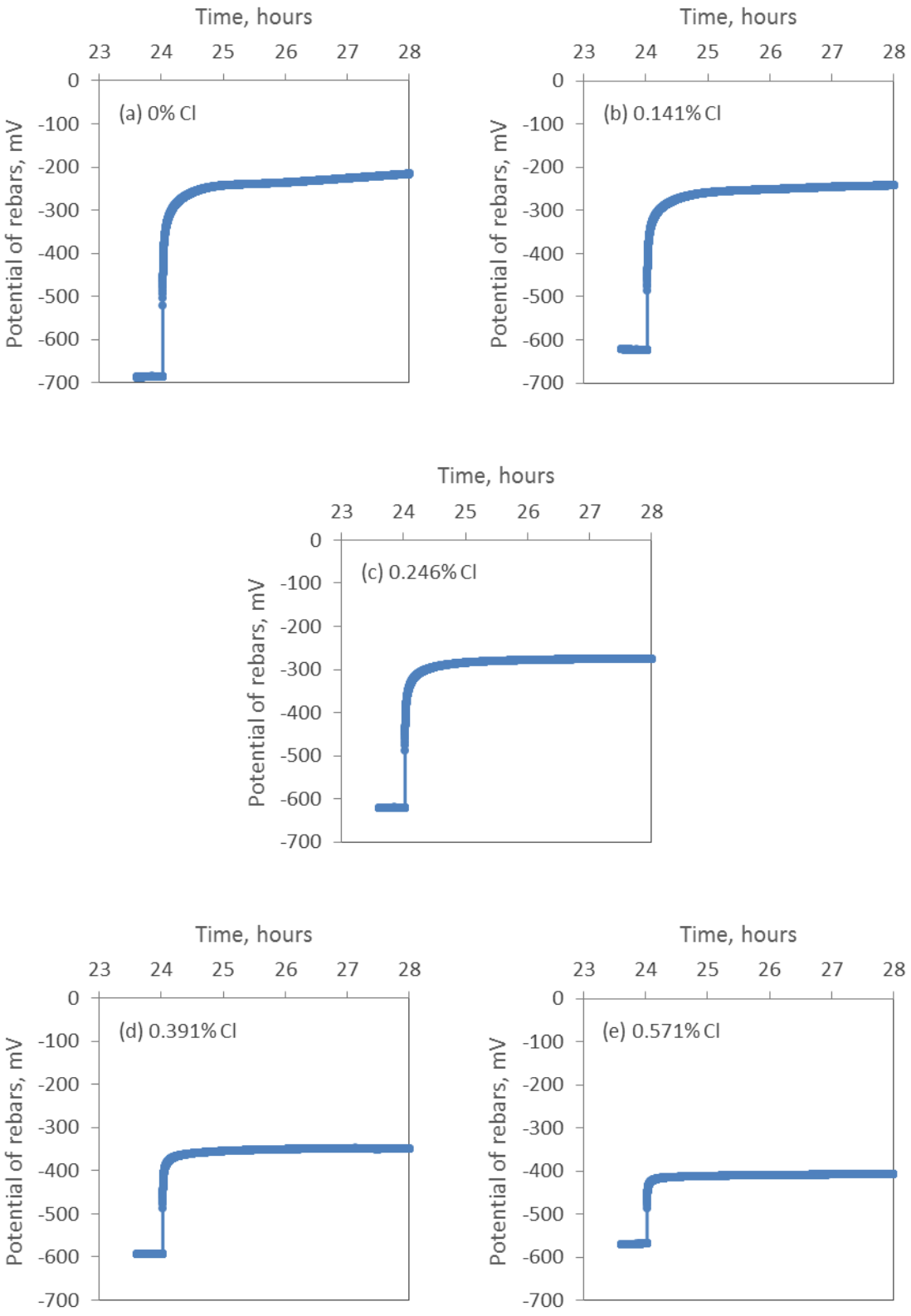

Figure C.7: Potential decay curves for specimens at various chloride contents after application of CP current density of 55 mA/m^2

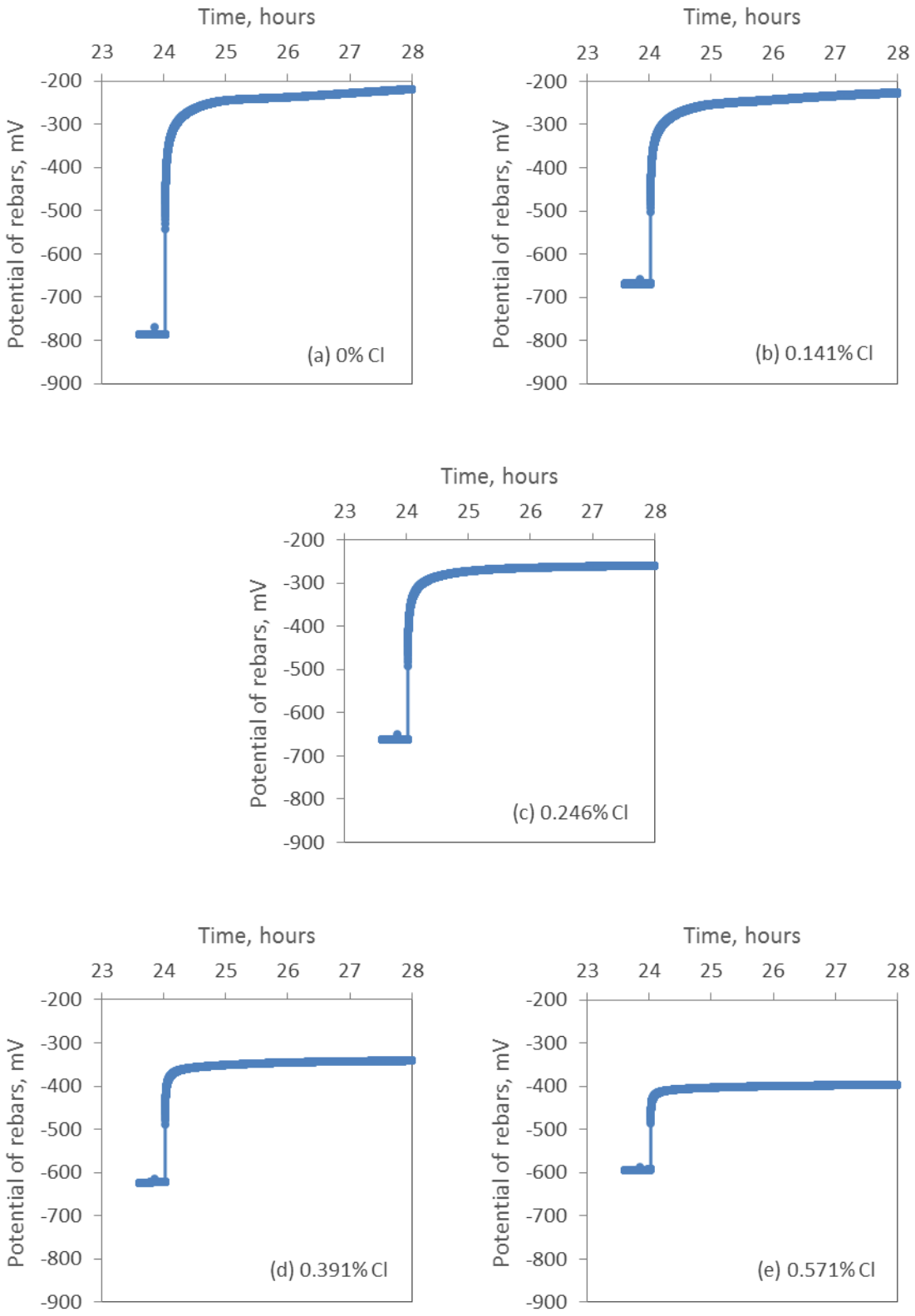

Figure C.8: Potential decay curves for specimens at various chloride contents after application of CP current density of 65 mA/m^2

APPENDIX D

Practical Aspects in the Design of CP for Reinforced Concrete Structures

In order to design a satisfactory cathodic protection for new reinforced concrete structures or existing structures as an optimum repair option, the designer should considered many influencing factors, such as exposure classifications (buried, immersed, tidal, splash, atmospheric, sheltered, exposed, etc.), chloride content, concrete resistivity, degree of saturation/water content, potential variations (BS EN ISO 12696, 2012). The design should also consider the type and location of anodes, the power source and possible transformer-rectifier location and other electrical parts, and the monitoring system.

The two most important parameters for the design of CP systems for the rebars in concrete are the current density required on the rebar surfaces and the current distribution provided (Chess and Broomfield, 2013).

In the present study, explicit characterisation obtained for the correlations between corrosion potential and concrete resistivity together with chloride content, degree of saturation and corrosion rate. A relationship between the required cathodic protection current density based on the concrete resistivity, chloride content and corrosion rate were then provided for the air exposed concrete structures. It should be noted that the results obtained in this work has led to useful information for the submerged concrete structures, but the data was inconclusive to characterise the required CP protection for such exposure condition and further investigation of this approach is needed. In such situations, a combination of engineering judgement, experience, and trial applications or with numerical modelling, is needed in order to estimate the optimum current density required (Bertolini et al., 2013; Chess and Broomfield, 2013).

Different CP current densities are required to be provided for effective protection system in the cases where a structure have different local chloride contents, degree of saturation, and hence the concrete resistivity. This requires to divide the structure into different electrically separated CP zones. Each zone has a particular part of the anode with its own power source, current and monitoring devices. Marine structures with tidal/splash/atmospheric zones are examples of structures with different resistivities as illustrated in Figure D.1. It should be

taken into account that the steel reinforcement of the individual zones can be electrically continuous over more than one zone. The reinforcement for each individual zone must be connected to the negative terminal of the zone power source and the anode of this zone in connected to the positive terminal of the power source (Bertolini et al., 2013; Chess and Broomfield, 2013).

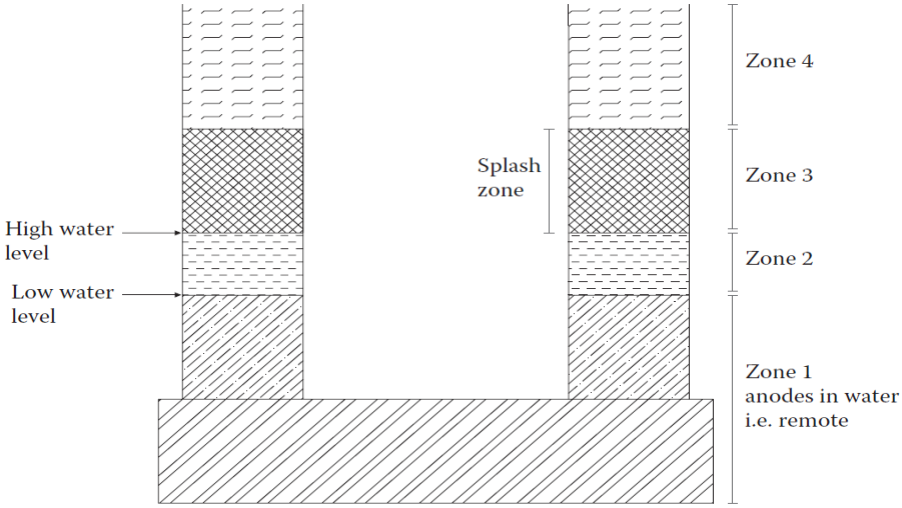

Figure D.1: Zoning of a marine structure (Chess and Broomfield, 2013).

For the new structures where cathodic prevention is required, anodes will be placed inside the structure during construction and the current will be switched on from the beginning. While in general, anodes are placed on the concrete surface or inside the structure in such a way for the existing structures to achieve a uniform current distribution (Bertolini et al., 2013; COST Action 521, 2003). A number of examples are given in Figures D.2 and D.3.

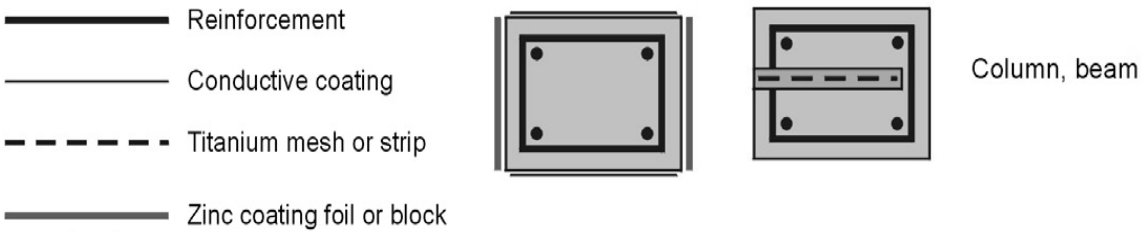

Figure D.2: Examples of anode layouts with respect to a concrete cross section (Bertolini et al., 2013)

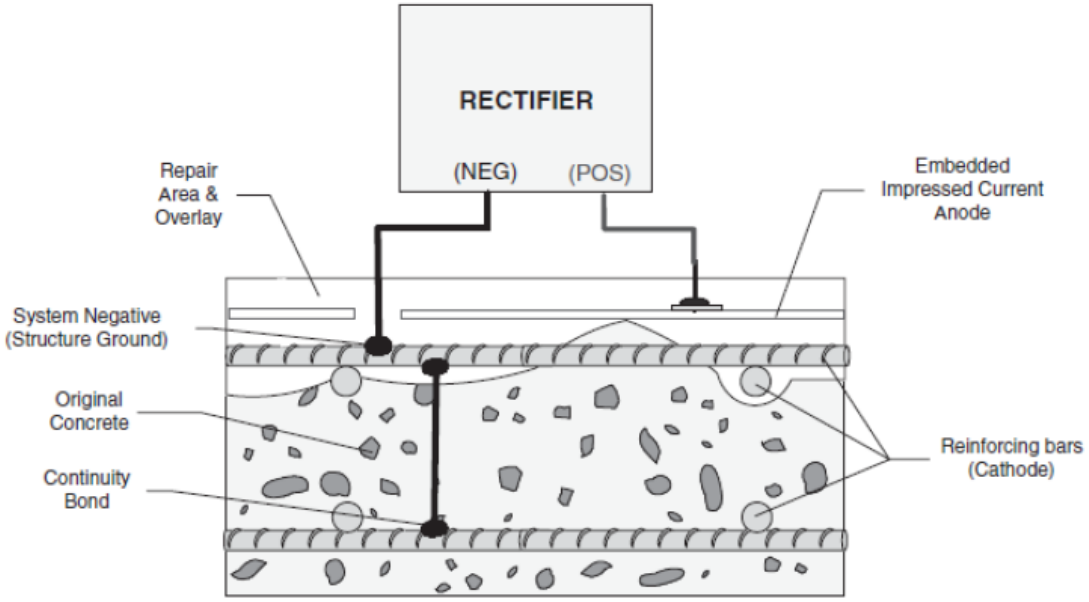

Figure D.3: Schematic layout of cathodic protection for reinforced concrete bridge deck (Hoseini et al., 2016)

Before the installation of CP for the existing structures, all the delaminated, cracked and spalled areas are removed and repaired. The reference electrodes and other monitoring probes are embedded. Then the anode is applied, with an overlay or top coat as designed (Bertolini et al., 2013)

In addition, when appraising a structure, an assessment of which steel is considered most at risk and the area is most desired to protect should be made. For example, on beams close to the sea, the worst damage was on the outer areas exposed to the prevailing wind, and the areas that the structural engineers were most worried about ongoing corrosion were the bottom outer layers of steel, so the biggest concentration of CP current was made in the bottom outer area (Chess and Broomfield, 2013).